FINAL REPORT - June 2005

# Please Pass the Salt: Using Oil Fields for the Disposal of Concentrate from Desalination Plants

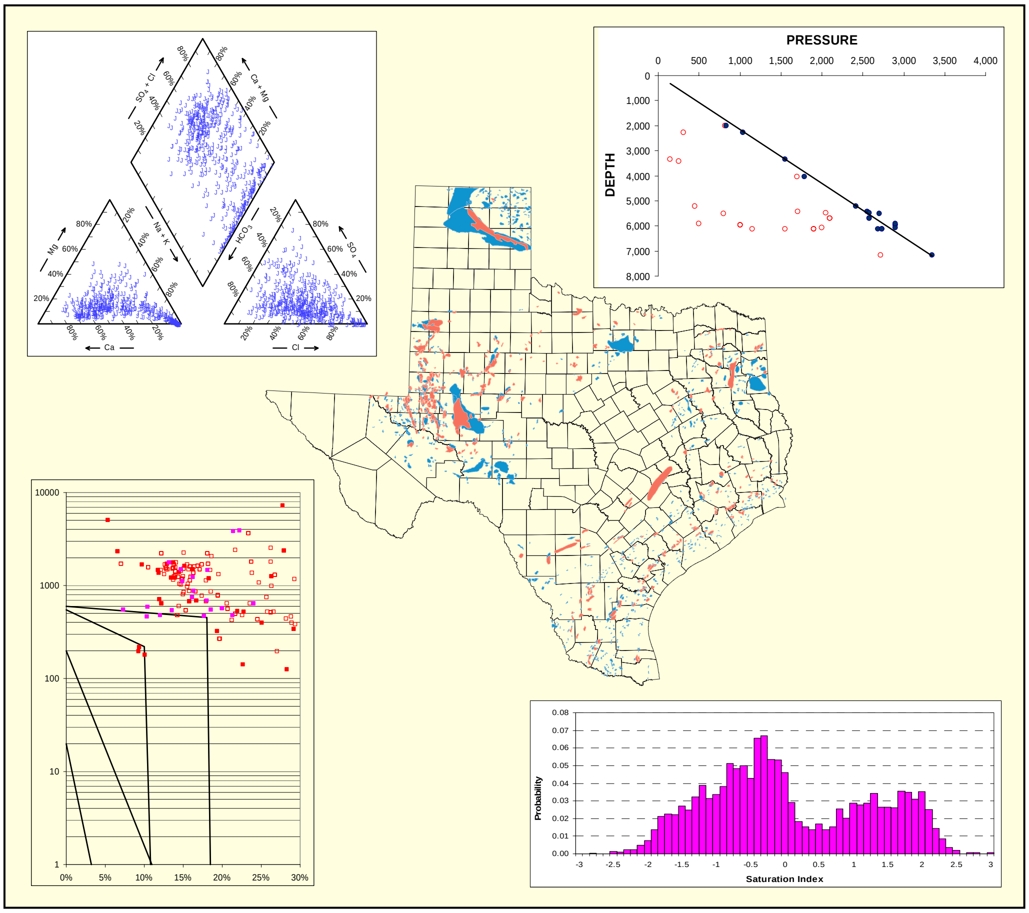

Prepared for

**Texas Water Development Board**

**Bureau of Economic Geology**
**Scott W. Tinker Director**
John A. and Katherine G. Jackson School of Geosciences
The University of Texas at Austin
Austin, Texas 78713-8924

FINAL REPORT – June 2005

# Please Pass the Salt: Using Oil Fields for the Disposal of Concentrate from Desalination Plants

Prepared for
**Texas Water Development Board**

under
Contract No. IA 2004-0001-012

**by Jean-Philippe Nicot, Ali H. Chowdhury[1], and Alan R. Dutton**

**Bureau of Economic Geology**
**Scott W. Tinker Director**
John A. and Katherine G. Jackson School of Geosciences
The University of Texas at Austin
Austin, Texas 78713-8924

[1] Texas Water Development Board, Austin, TX

# Table of contents

# List of Figures

# List of Tables

# Glossary and Abbreviations

| | |
|---|---|
| 3D | 3-Dimensional |
| Al | Aluminum |
| AOR | Area of Review |
| ASR | Aquifer Storage and Recovery |
| Ba | Barium |
| bbl | Barrel |
| Bcf | Billion cubic feet |
| BEG | Bureau of Economic Geology |
| BUQW | Base of Usable Quality Water |
| Ca | Calcium |
| CEC | Cation Exchange Capacity |
| Cu | Copper |
| ED | Electrodialysis |
| EDR | Electrodialysis Reversal |
| EOR | Enhanced Oil Recovery |
| EPA | Environmental Protection Agency |
| Fe | Iron |
| Fm. | Formation |
| GAM | Groundwater Availability Model |
| K | Potassium |
| LSI | Langelier Saturation Index |
| MAR | Mass Action Ratio |
| MF | Microfiltration |
| Mg | Magnesium |
| mg/L | Milligrams per liter |
| Na | Sodium |
| NF | Nanofiltration |
| MGD | Million Gallons a Day |
| ppm | Parts per million |
| PTTC | Petroleum Technology Transfer Council |
| RO | Reverse Osmosis |
| RRC | Railroad Commission of Texas |

| | |
|---|---|
| RWPG | Regional Water Planning Groups |
| | |
| SDWA | Safe Drinking Water Act |
| Si | Silicon |
| SI | Saturation Index |
| SR | Saturation Ratio |
| Sr | Strontium |
| | |
| TCEQ | Texas Commission on Environmental Quality |
| TDS | Total Dissolved Solids |
| TIPRO | Texas Independent Producers and Royalty Owners |
| TOF | Top of Fluids |
| TSS | Total Suspended Solids |
| TWDB | Texas Water Development Board |
| TX | Texas |
| | |
| UIC | Underground Injection Control (Regulations) |
| UF | Ultrafiltration |
| | |
| VRF | Volcanic Rock Fragments |

# 1 Executive Summary

The demand for fresh water in Texas will increase in the future owing to population growth and because conventional sources such as surface water and groundwater will not be sufficient to cover needs. Desalination of brackish water and seawater is an alternative being actively pursued by the State, whose technology of choice includes reverse osmosis (RO) and electrodialysis (ED/EDR). These are proven technologies widely used in desalination plants. Feed water is processed to produce a permeate that typically augments other water sources in the potable water system. In the process, however, a concentrate is created that collects all salts rejected from the permeate. The concentrate’s salinity ranges from 2 to 5 times that of the feed water. Several options are available for disposing of desalination concentrates, such as discharge to the ocean in coastal communities or discharge to a sewer system if the salinity can be handled by local water treatment plants. Another promising possibility is deep-well injection. In Florida, desalination concentrates are commonly disposed of by deep-well injection and, in Texas, the oil and gas industry has been reinjecting saline produced waters into the subsurface for years. A combination of deep-well injection and reinjection is attractive for Texas, where oil and gas fields are plentiful. Formation pressures in oil and gas reservoirs have been greatly lowered because of past oil and gas production, after all, creating an opportunity for injecting foreign fluids at a lower cost.

However, legal, and to a much lesser degree, technical issues can arise. Injection of desalination concentrates and produced waters from oil and gas fields is under the jurisdiction of Underground Injection Control regulations (UIC) promulgated in Part C of the Safe Drinking Water Act under Class I (injection of hazardous and nonhazardous wastes beneath the base of usable-quality water) and Class II (disposal of saltwater and other fluids co-produced with oil and gas), respectively. This document deals mainly with the technical issues that may arise owing to mixing of desalination concentrates and formation waters in the deep subsurface.

For a more realistic analysis, we selected six analysis areas across Texas from geologically defined sedimentary basins. From north to south and west to east they are: the Anadarko Basin in the Texas Panhandle, the Permian Basin, the East Texas Basin, the

Fort Worth Basin, the Maverick Basin at the Mexico-US border, and the south part of the Gulf Coast Basin. In each basin, the analysis area covers a few counties that were selected by a set of criteria: (1) depleted oil and gas fields; (2) counties with water needs, according to the State Water Plan; (3) areas with sufficient overlying brackish groundwater resources; and (4) areas where injection wells are not too deep. We collected information from different sources on formation geochemical attributes and formation flow parameters, such as permeability and porosity. Current pressure information was gathered from Railroad Commission of Texas (RRC) files. The hypothetical concentrate chemical composition was computed from that of the likely brackish-water source overlying the pressure-depleted formation. The brackish-water composition was then modified using standard water-treatment additives and applying a generic concentration factor of 4. This concentration factor of 4 is actually observed in desalination concentrates of many plants.

Technical issues examined were (1) pressure-related matters and (2) chemical changes during injection of concentrate into the deep formation, which can potentially lead to formation damage such as scaling and clay mobilization. Pressure data were evaluated relative to the possibility of requesting a variance of the UIC-required area of review studies. We also analyzed the distribution of injection flow rates computed in accordance with RRC rules or collected from RRC H1 forms. When concentrate is injected into the subsurface, it is subject to a change in environmental conditions, including an increase in temperature and pressure. It mixes with the resident formation water as well. To analyze the impact of these changes, we used a batch geochemical code in combination with a Monte Carlo approach. We sampled the formation water and brackish-water data sets multiple times and mixed the selected samples in different proportions. We then analyzed distribution of saturation indices that most likely determines development of scales, one important aspect of formation damage. Another highly relevant concern is clay sensitivity to fresher-water injection. Clayey material and fines can be mobilized when they come in contact with a water of smaller ionic strength and/or different ionic makeup.

Despite some differences, the six analysis areas show a consistent picture when desalination concentrate is injected into depleted oil and gas reservoirs. They all have a history of fresh-waterflooding, especially in their early production periods in the first half of the 20th century. Except for the Maverick Basin, more than half of the wells in each basin are potentially eligible for a variance of the area of review study. Achievable injection rates are not on average historically high, which is confirmed by the low-permeability values of the Paleozoic formations. The East Texas and Gulf Coast reservoirs have higher permeability and subsequent maximum potential injection rates. Multiple wells will be needed to accommodate the desalination concentrate stream of a typical plant. Lack of detailed chemical analyses did not allow for a thorough study of all bothersome scale-building minerals, barite in particular. However, the scaling tendency by calcite and gypsum is not outside of that typically encountered and dealt with by the oil and gas industry (antiscalant additives for sulfates and acid for carbonates are used). Water sensitivity of the clayey material can be accommodated similarly using operational solutions such as pretreatments with appropriate chemicals or buffer solutions. Overall, this study found no technical drawback to allowing injection of desalination concentrates into depleted oil or gas fields using existing wells.

# 2 Background

## 2.1 Introduction

The population in Texas is expected to nearly double over the next 50 years (from 21 million people in 2000 to almost 40 million in 2050). This growth will put extreme stress on current water resources, which will not be sufficient to cover the demand if no additional resources are added. This shortage in water supply will be especially severe during drought periods. Current estimates show an increase in demand from 17 million acre-ft ($21x10^9$ $m^3$) in 2000 to 20 million acre-ft ($25x10^9$ $m^3$) in 2050 (TWDB, 2002) (Appendix 1 shows a unit conversion table). Growth in demand is tempered because conservation measures are assumed to be applied at a large scale. They are already in place in many cities, and they often times make good economic sense. Nevertheless, even if the total demand is projected to grow only slightly, municipal demand is anticipated to almost double from 4.3 million acre-ft ($5.3x10^9$ $m^3$) to 7.1 million acre-ft ($8.8x10^9$ $m^3$) per year (Figure 2.1). Many towns and cities especially in the eastern part of the state rely on surface water from rivers or dams, but some cities such as San Antonio or El Paso rely heavily on groundwater to meet their municipal needs. To anticipate population growth and higher water demand, municipalities are trying to expand their water resource base by conventional methods such as buying land and developing well fields but also trying new approaches such as reuse of waste water or desalination.

Desalination, also called desalting or desalinization, is a process by which solutes are removed from brackish or saline water to produce fresh water. In coastal areas, the source of water can be seawater, but for inland locations it is more likely to be brackish water from either an aquifer or surface water. Water is considered fresh if it has less than 1,000 mg/L of solutes (or Total Dissolved Solids – TDS). The Safe Drinking Water Act, passed in 1974, established minimum primary drinking water standards. Those standards set limits on various substances, mainly contaminants, the so-called MCL's (Maximum Contaminant Levels). Secondary drinking water standards were also adopted. Their purpose is the less stringent goal of protecting public welfare as opposed to public health. The secondary standard for drinking water TDS is 1,000 mg/L in Texas. However, people prefer to use water with a salinity of less than 500 mg/L TDS for drinking purposes.

Livestock and irrigation water salinity can reach a TDS up to 3,000 mg/L. Other standards are also shown on Table 2.1. By definition, brackish water contains between 1,000 and 10,000 mg/L. Several cities already use desalination as a major means to meet water needs: Fort Stockton in West Texas and Sherman in North Texas use groundwater and surface water as feed water, respectively. Other examples are El Paso and Brownsville. In the desalination process, a small fraction of the water becomes even more enriched in solutes typically by a factor of between 2 and 5 and needs to be disposed of. Several options are possible and include disposal into a surface water body, stream or lake; into an evaporation pond; to the sewer system; and injection in the subsurface. However, environmental concerns and cost remain critical issues. Environmentally sound disposal is important to prevent the discharge of concentrate to environmentally sensitive streams, rivers, bays, and estuaries. The desalination waste stream could also overwhelm the local water-treatment plant if discharged into municipal sewers. Cost is also an issue especially for inland concentrate disposal because it can account for 10 to 25 percent of the total project cost. Offshore discharge to the Gulf of Mexico might be cost-prohibitive, even for coastal communities, because of environmental concerns.

The major problem facing desalination is the fate of the concentrate. Most of the world production from desalination plants is in the Middle East along the coast, and a common way to dispose of the concentrate is to discharge it back to the ocean. This is also the plan for the few desalination plants scheduled for construction along the Texas Gulf coast. This is probably the most economical way to dispose of the waste. However, in Texas, pipelines would possibly have to be built to the open ocean to keep the waste from entering streams and environmentally sensitive areas (Laguna Madre). Another popular way of disposing of the waste, as currently done in the Fort Stockton desalination plant, is to use evaporation ponds. However, the ultimate fate of the sludge/residue still has to be dealt with. Current disposal methods include direct ocean or surface water discharge, “co-disposal” in public sewer lines, disposal through “non-reclaimable” sewer lines, lined evaporation ponds, spray irrigation, and zero liquid discharge. Another solution is to inject the waste into the subsurface through deep well injection. This issue of concentrate disposal is hampering small communities from considering desalination as an option.

In order to help those communities, big and small, in developing desalination, this study investigates the technically sound possibility of injecting the waste in a special kind of injection: Class II injection wells. Class II injection wells are typically dedicated to injection of produced waters linked to oil and gas production. The possibly lower cost for underground injection of desalination concentrate through existing Class II wells is important for the viability of desalination for public water supply. Regulated classes of injection wells identified in Federal Law (CFR 40 parts 144 and 146) under the Underground Injection Control Regulations (UIC) promulgated under Part C of the Safe Drinking Water Act include:

- Class I—injection of hazardous and nonhazardous wastes beneath the base of usable quality water.
- Class II—disposal of saltwater and other fluids co-produced with oil and gas.
- Class III—injection of super-heated steam, water, or other mining fluids.
- Class IV—injection of hazardous or radioactive wastes into or above underground sources of drinking water, banned under the UIC program.
- Class V—not included in the other classes.

In Texas, U.S. EPA delegates the UIC duties to State agencies. The Railroad Commission of Texas (RRC) regulates Class II wells; Texas Commission on Environmental Quality (TCEQ) has jurisdiction over classes I and III to V.

Oil and gas fields, as recipients to desalination concentrates, are a promising avenue to follow for Texas because (1) they occur in many parts of Texas including most of the Gulf Coast and much of the interior of the state (Figure 2.2), (2) oil-field operators already have considerable experience injecting co-produced saltwater in these fields, (3) costs are lower than for offshore disposal or injection in Class I nonhazardous wells, and (4) potential impact to the environment is negligible from properly sited, installed, and operated injection wells. As will be described later, oil and gas fields in Texas are usually located near sources of brackish groundwater. These fields are also near many small- to large-sized communities across Texas, including areas that are currently using desalination for industrial purposes and areas that propose to use desalination in the future for public-water supply.

Texas has a long history of injecting various fluids into the subsurface. Current water injection operations in Texas include secondary and tertiary oil recovery (all over Texas), hazardous waste disposal (mainly along the Gulf Coast), and aquifer storage and recovery (ASR) (at Kerrville for the Upper Guadalupe River Authority and at El Paso). The oil and gas industry in Texas has a great deal of experience in injecting fluids because a substantial amount of co-produced saltwater is already being reinjected. It is also relevant to this project that makeup water for pressure maintenance has been often historically either fresh or brackish. In the U.S., more than 92 percent of produced water was reinjected in 1995, with 71 percent used for enhanced oil recovery (EOR) and 21 percent disposed of in Class II injection wells. When oil is produced, as much as 10 times more formation water may be produced than oil. Formation water salinity can range from 35,000 to more than 250,000 mg/L. Producers need to dispose of this formation water. Most (about 75 percent in Texas) of the co-produced saltwater is injected back through Class II wells into producing horizons as part of secondary recovery (waterflooding) operations in an oil field. The remainder is reinjected in saltwater disposal wells into either productive or nonproductive horizons. In Texas, there are over 31,000 active permitted Class II injection wells in oil and gas fields; more than 7,000 are saltwater disposal wells (Figure 2.3). More than 700,000 acre-ft of liquids per year is being injected through these wells. Figure 2.4 presents a map of the different RRC districts. RRC statistics are often tabulated by district, and we will discuss some of them in this document.

## 2.2 Current Status of Desalination in Texas

There is a growing interest in desalination in Texas as demonstrated by having 6 out of the 16 Regional Water Planning Groups (RWPG) list desalination as an alternative to meet future water demand (Figure 2.5). At the world-scale, a medium-sized desalination plant would produce about 25 to 30 million gallons per day (95 to $114 \times 10^6$ $m^3$) of fresh water, enough to cover water needs of more than 100,000 people. To estimate the approximate size needed for a city, one can use typical consumption rates in dry years, about 200 gallons per day per capita. The population of a typical county seat of 5,000 inhabitants would need a desalination facility generating 1 million gallons per day of fresh water, exclusive of other needs. Such a facility may produce on the order of 200,000 gallons per day of waste (~130 gpm).

A map of the current desalination plants in Texas with a capacity larger thab 0.025 50 millions gallons per day shows that they are present across the state (Figure 2.6). Nearly 83 percent of the desalination plants in Texas use brackish groundwater whi1e 17 percent use surface water. Their total production capacity is approximately 50 millions gallons per day spread over about 100 plants of which approximately 40 have a capacity larger than 0.025 MGD (Nicot et al., 2005). Municipal use accounts for more than half of this total. Most of the plants are small. For the most part, these facilities produce small volumes in the tens to hundreds of thousands of gallons per day, except for a few pioneers such as the City of Fort Stockton in West Texas (where maximum production of 3.8 million gallons per day is subsequently blended with water from another source) and recent facilities such as the Southmost Regional Water Authority plant in South Texas. Texas desalination facilities produce a waste stream of about 5 to 10 million gallons per day. Desalination facilities can be described according to their capacity, the source of their feed water, the treatment process, and the fate of the waste. Mickley (2001) presented information on a few of Texas desalination facilities (Table 2.2).

## *2.3 Current Legislative Environment*

Although several states are considering injection of desalination concentrates using Class II wells (Burnett and Veil, 2004), only Class I injection wells can be used in compliance with current regulations. The City of El Paso is currently seeking approval for a Class I injection well to dispose of future desalination concentrates. In Texas, a community is currently required to file for a Class I permit to inject concentrate from a desalination plant into the subsurface. Attaining a Class I permit can take more than a year and may cost as much as $5,750 in fees. Assembling a Class I permit requires the collection and processing of a substantial amount of technical information and posting of public notices. It is a much shorter process to attain a Class II than a Class I permit; a Class II permit application takes about 45 days with fees of $300 with no requested exemptions. Construction cost of a Class I well can also run into millions of dollars, while Class II wells are already available that just need to be retrofitted.

## 2.4 Goals

Possible concerns from interested operators stem from legal and technical issues. To understand those concerns a survey was carried out (Appendix 2) to find out whether there is an interest in the oil community to accept desalination concentrates (assuming it can be done legally through Class II injection wells). A larger goal of the study, mainly handled by the Texas Water Development Board (TWDB), was to meet with EPA and other regulating agencies to better understand the legal issues. This technical document is in support of the larger goal of providing a framework for allowing injection wells for disposal of desalination concentrates. The technical goals of the project are to:

- Identify locations of oil/gas fields that may be potential sites for concentrate injection wells (by superimposing maps of those areas in Texas with a potential future deficit in fresh water, of brackish water sources, and of oil/gas fields with the appropriate attributes).
- Through examination of the analysis areas, show that the target formations can support additional pressure and still be candidates for a variance of Area Of Review (AOR) (see Section 5.3). Injection of fluids in a production or disposal zone will result in an increase in formation pressure. AOR analyses may be of considerable use to determine how many of the existing injection wells in the analyses areas meet the AOR requirements.
- Show that the target formations can receive concentrate with no chemical problems, such as pore plugging with scale-forming minerals or reduction in permeability due to water-sensitive clays.

An additional goal, in which the BEG had only a supporting role, is to make recommendations on ways to best streamline the permitting process. It should be noted that this study does not deal with the treatment of produced waters and their potential use for irrigation or other uses typically covered by fresh water but rather explores the concept of adding desalination concentrates to the produced water stream loop.

To address the technical issues, a few analysis areas matching selected criteria were chosen. The present document first describes the criteria used to delineate the analysis areas (Section 3), followed by an overview of desalting (especially reverse osmosis and electrodialysis) and deep-well injection operations (Sections 4 and 5). Section 6 introduces the analysis areas in terms of geology, nature of the fluids present, and flow parameters, while Section 7 presents the final results of the study.

In the study, we use a statistical approach for two reasons. Its scope is very general in nature, and, if we are using a few particular potential sites, they were chosen as being representative of Texas as a whole. Secondly, brackish water quality may change with time as pumping brings water from farther and farther away and/or from areas of lower permeability typically of lesser quality. Variations in water quality during the life of a facility are assumed to be approximated by current variations in space. An increase in feed-water total dissolved solids (TDS) would create higher pressure requirements and higher energy costs, whereas a change in the chemical makeup of the feed water may transform an initially optimal membrane into an only marginally optimal one with a smaller rejection rate. In this study, we are, however, concerned only with the ability of depleted reservoirs to receive concentrates of variable chemical composition.

Table 2.1. Secondary standards for potable water

| | National Secondary Drinking Water Standards | Texas Secondary Drinking Water Standards |
|---|---|---|
| Chloride (mg/L) | 250 | 300 |
| Sulfate (mg/L) | 250 | 300 |
| Iron (mg/L) | 0.3 | |
| Copper (mg/L) | 1.0 | |
| Aluminum (mg/L) | 0.05 to 0.2 | |
| TDS (mg/L) | 500 | 1,000 |
| pH | 6.5-8.5 | >7.0 |

Table 2.2. Representative sample of Texas desalination facilities operating in 1999 and with a design capacity greater than 0.05 MGD (from Mickley, 2001).

| Plant Name | Disposal | Type | Category | Design Capacity |
|---|---|---|---|---|
| Big Bend Motor Inn, Terlingua, TX | Evaporation pond | Brackish Reverse Osmosis | DW | 0.05 |
| Dell City, Texas | Holding tank then irrigation | Electrodialysis Reversal | DW | 0.10 |
| Esperanza, TX | Small evaporation pond | Brackish Reverse Osmosis | DW | 0.06 |
| Ft. Stockton, TX, City of | City wastewater effluent lagoon | Brackish Reverse Osmosis | DW | 3.00 |
| Granbury, TX, City of | Into Lake Granbury | Electrodialysis Reversal | DW | 0.62 |
| Haciendas Del Norte | Evap. pond | Brackish Reverse Osmosis | DW | 0.08 |
| Harlingen Waterworks System | Receiving stream, tidal-affected | Brackish Reverse Osmosis | WW | 4.00 |
| Lake Granbury, TX | Lake Granbury | Electrodialysis Reversal | DW | 7.50 |
| Oak Trail Shores, TX | 100 ft pipe into Lake Granbury | Electrodialysis Reversal | DW | 0.14 |
| River Oaks Ranch, TX | Open pond | Brackish Reverse Osmosis | DW | 0.08 |
| Sherman, TX, City of | Sewer | Electrodialysis Reversal | DW | 6.00 |
| Sportsmans World, TX | Back to Possum Kingdom Lake | Brackish Reverse Osmosis | DW | 0.14 |

Design capacity is in millions gallons a day (MGD)
DW=Drinking Water; WW=Waste Water

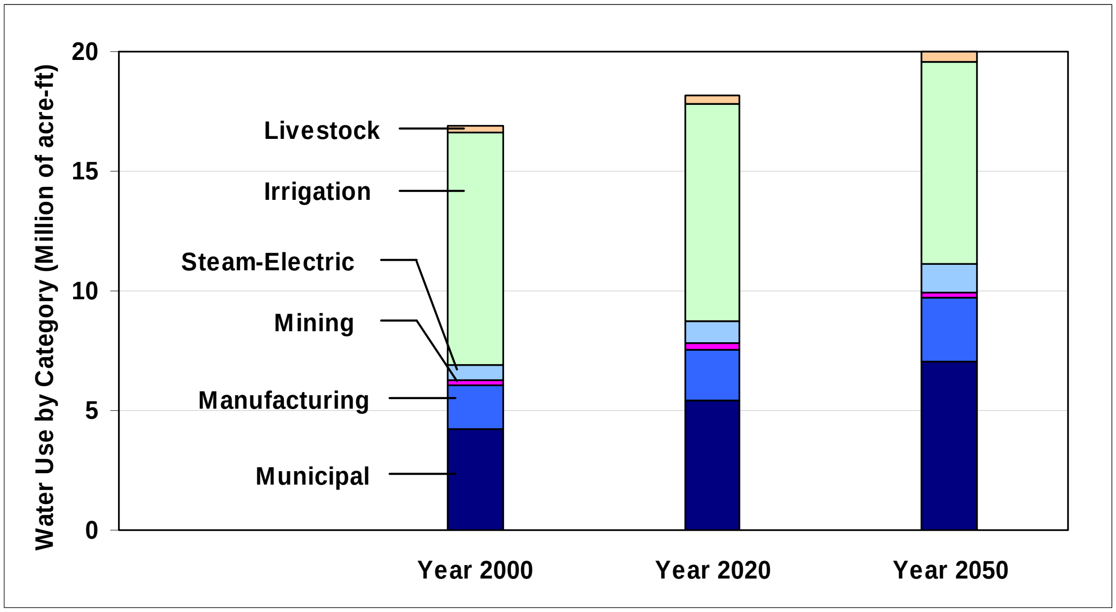

Figure 2.1. Current water use in Texas and predictions (data from TWDB, 2002)

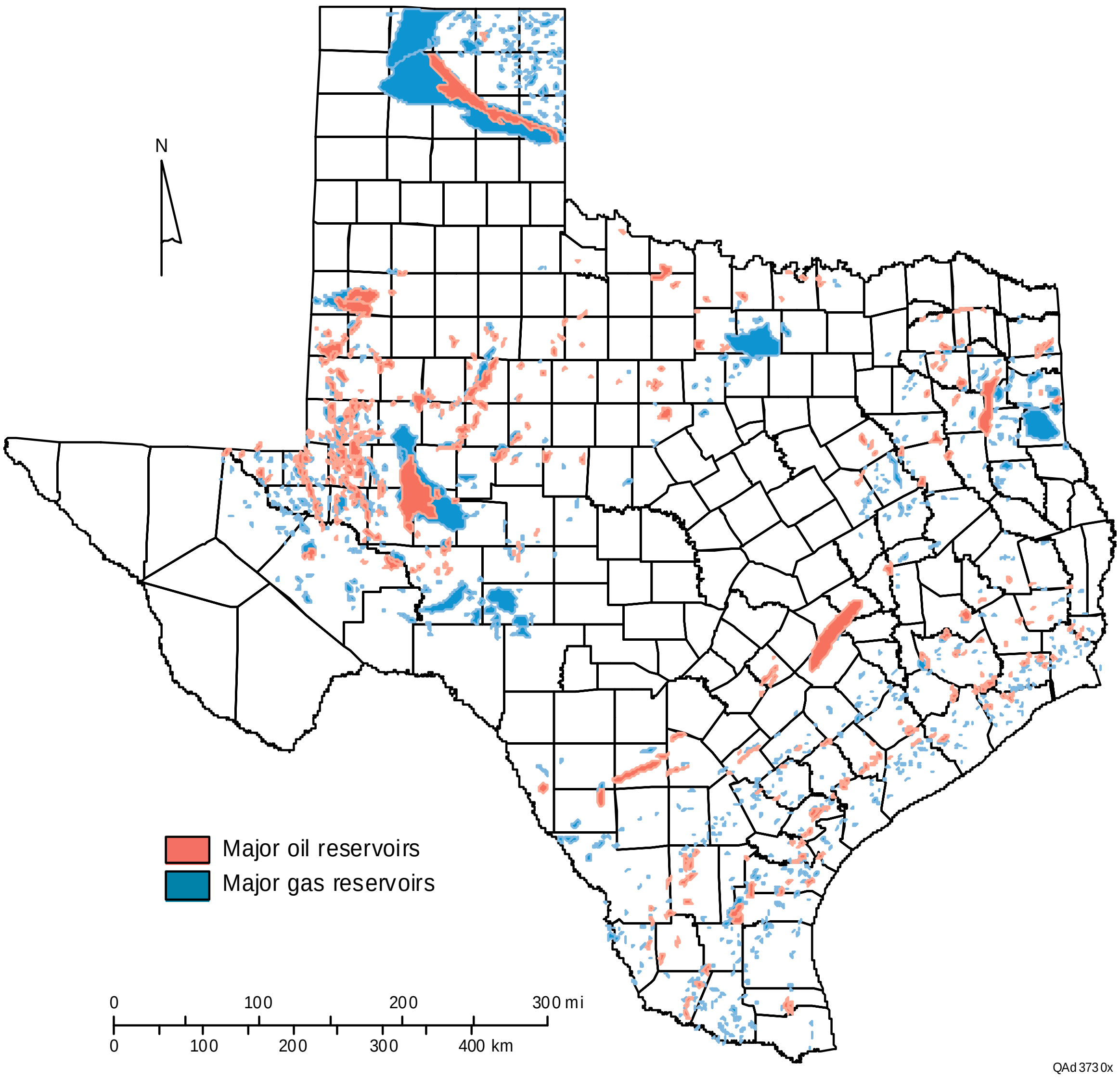

Figure 2.2. Map of major oil and gas fields in Texas

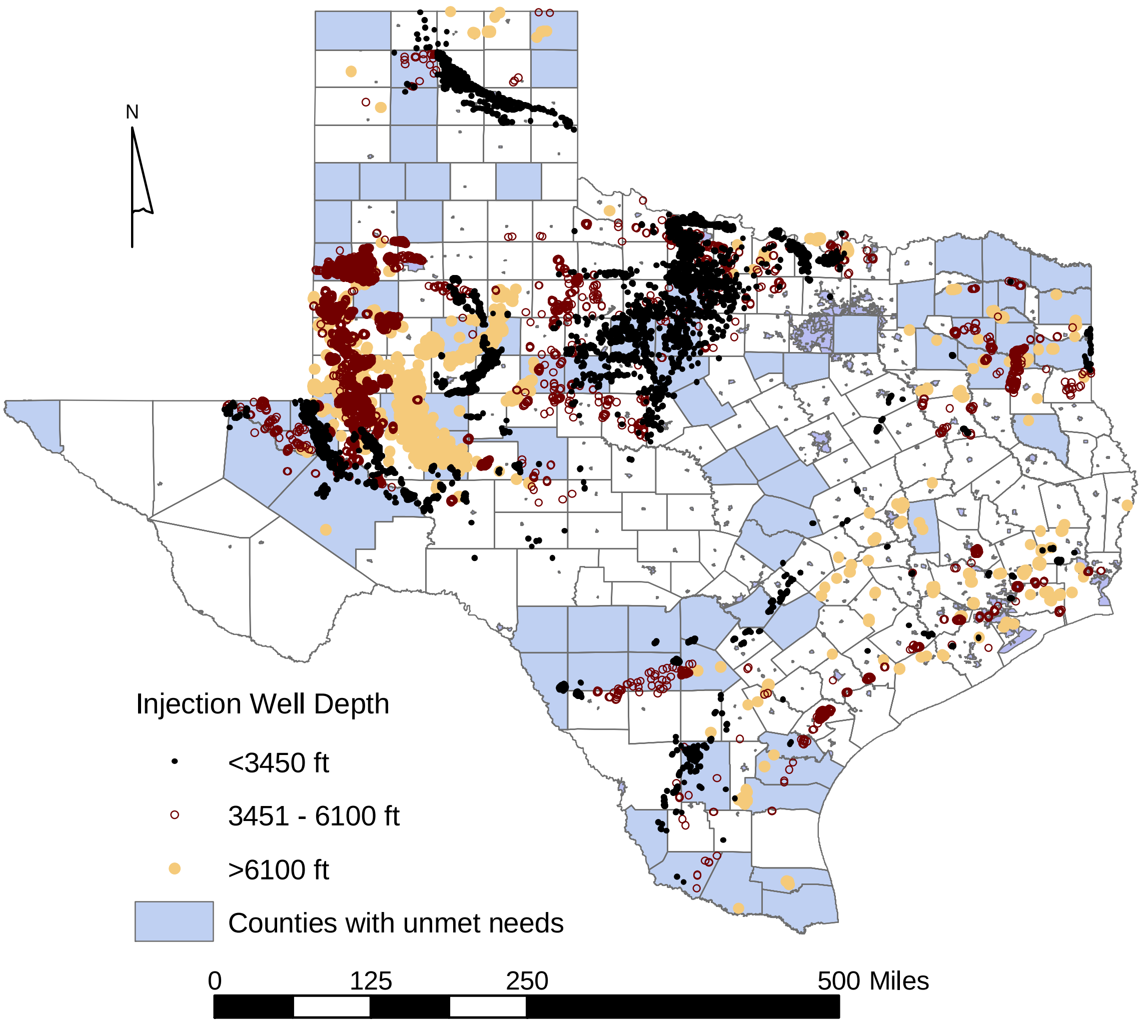

Note: Class II injection wells split in 3 depth groups of equivalent size (~25,000 points with depth information out of ~30,000 active injection wells).

Figure 2.3. Map showing distribution of Class II injection wells in Texas

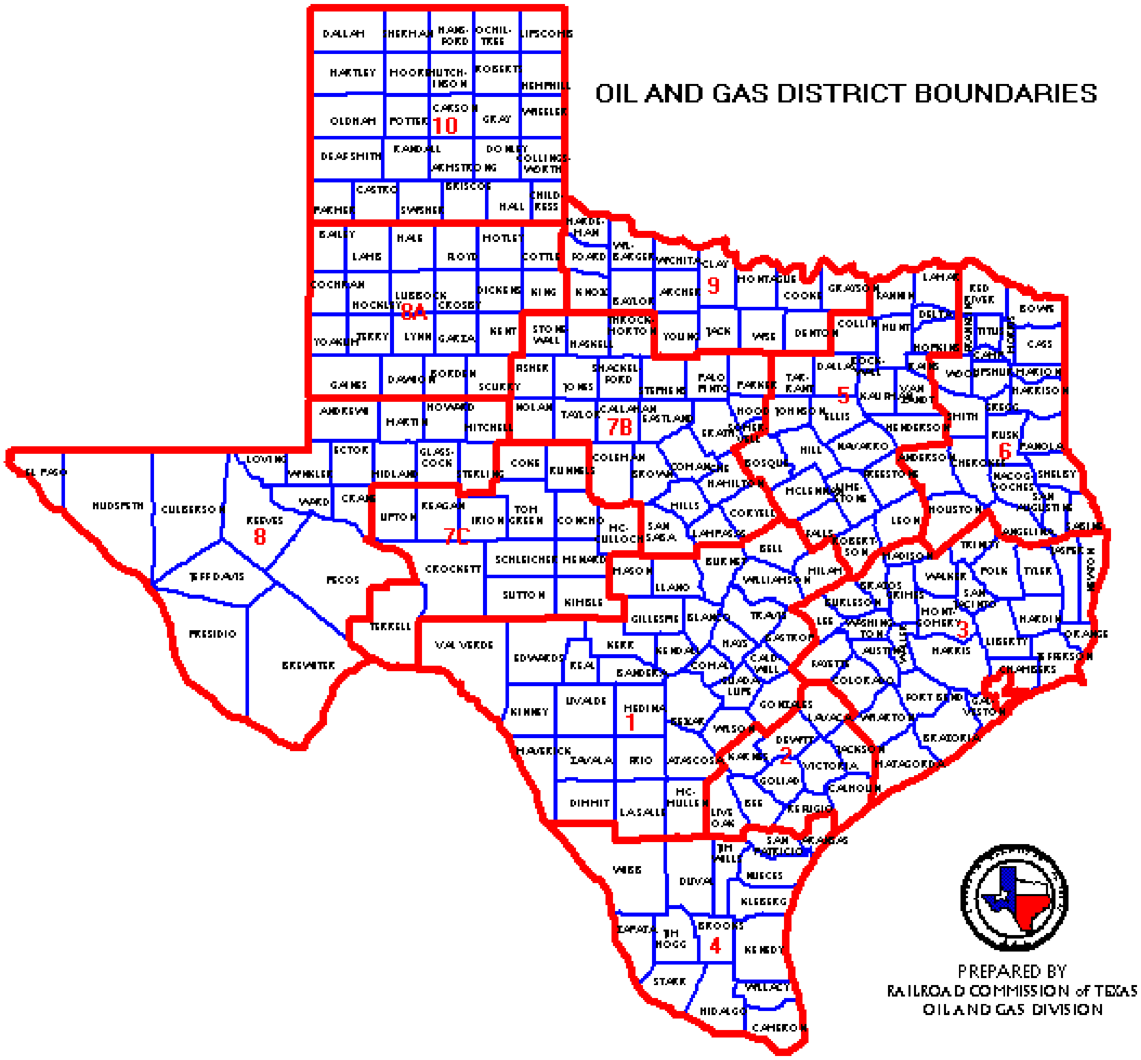

Source: RRC Website

Figure 2.4. RRC district map also showing county lines

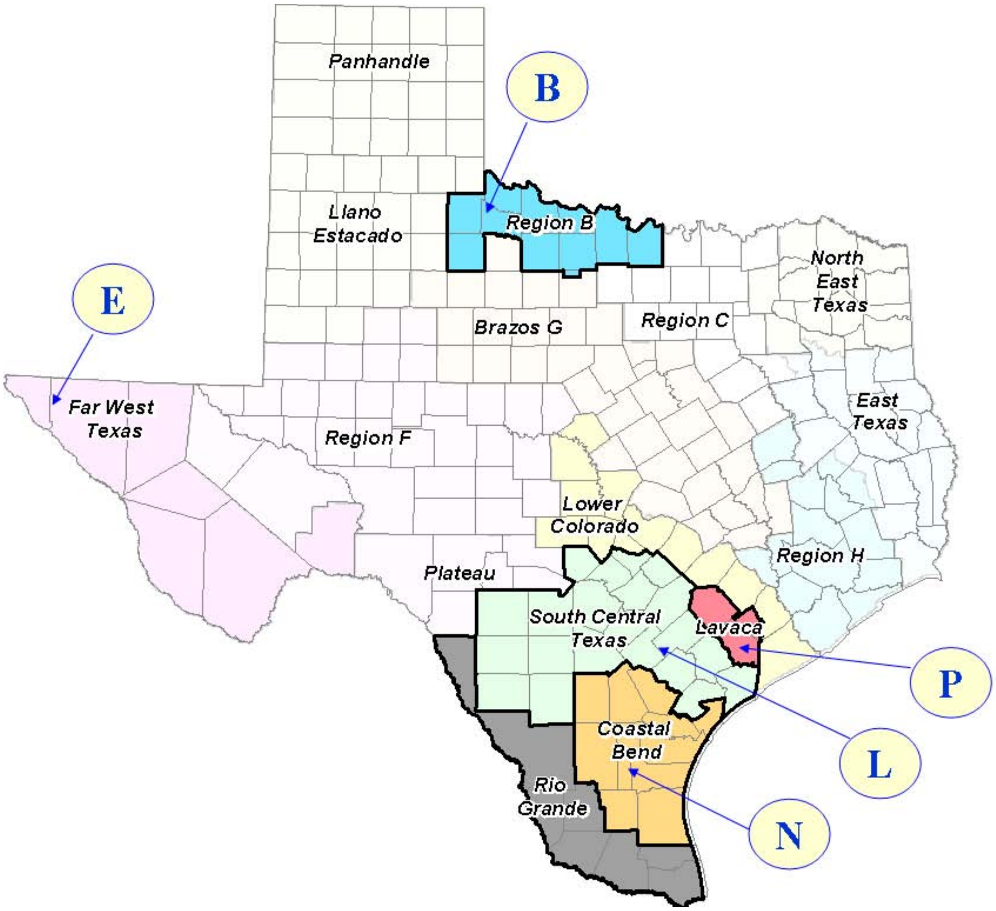

Source: TWDB (2002)

Figure 2.5. Water planning regions with desalination water management strategies

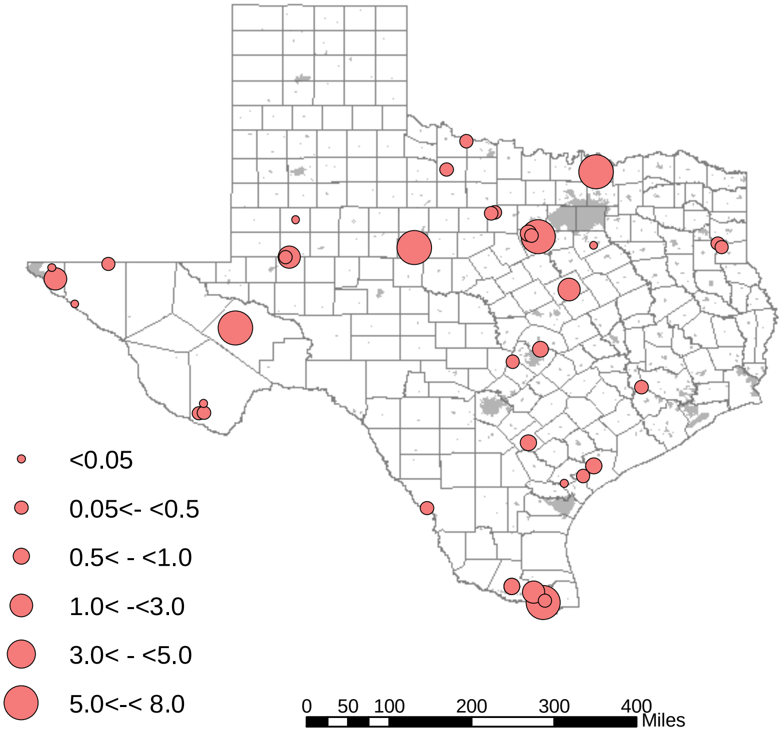

(a)

NOTE: Capacity in MGD (millions gallons a day)

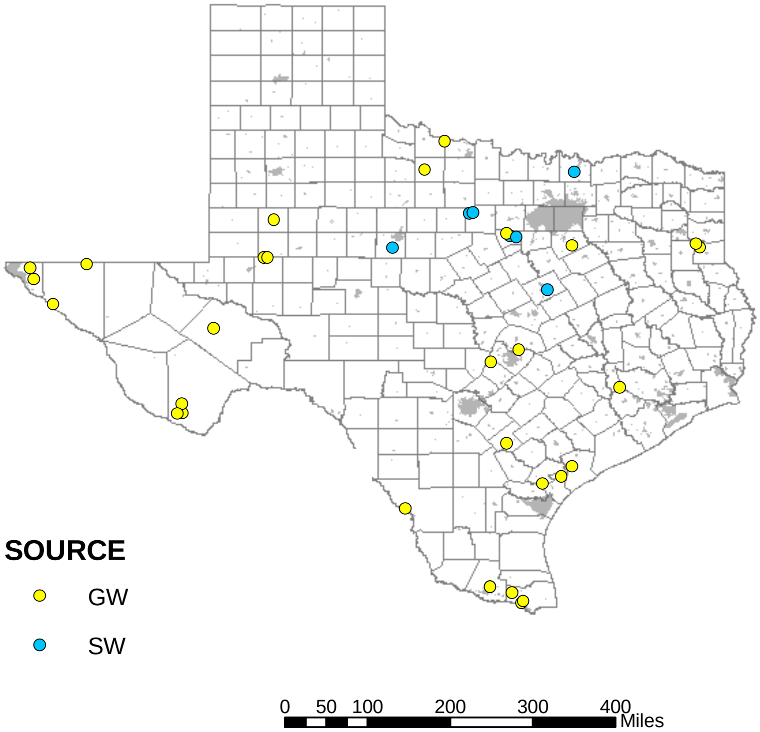

(b)

Figure 2.6. Map of current desalination facilities in Texas with capacity >0.025 MGD (from Nicot et al., 2005) (a); their feedwater source (b)

# 3 Approach

## 3.1 Communication with Stakeholders

Stakeholders for this study fall into two groups: communities and public or private entities that have a need to dispose of their concentrate on one side and, on the other side, oil and gas operators who may have a need for that water. For this study, BEG focused on the latter group by using its contacts within the oil industry to evaluate whether operators can accept large volumes of concentrate to dispose along with their produced waters into Class II wells. To gauge the interest of the operators as opposed to that of the produced water hauling industry, a presentation was made to a group of potentially interested parties at a TIPRO (Texas Independent Producers and Royalty Owners) meeting in January 2004 (see Appendix 2). A questionnaire was also made available through the Worldwide Web and posted with background information, as well as through email to hundreds of members of the Texas PTTC (Petroleum Technology Transfer Council) and included in a PTTC newsletter. The success of the survey was limited in terms of number of replies received, but it is clear that legal issues carry more weight than technical issues. The details and the history of this task are described in Appendix 2.

## 3.2 Method to Target Selected Depleted Oil/Gas Fields

Given the multiplicity of potential targets for this study, the following approach was used to determine the six analysis areas examined in more detail. They were selected to have both a geographic spread and variability in lithologic composition. ArcGIS software was used to help in the decision process. The first step was to digitize current paper atlases of major oil and gas fields in Texas (Figure 2.2) (Galloway et al., 1983 and Kosters et al., 1989). Many more oil and gas fields exist in Texas, but those selected have been in production for decades or have been historically producing large amounts of oil and/or gas. Because they have had large production, they are pressure depleted and most likely able to receive large amounts of fluids. The threshold value for a reservoir to be described in the relevant atlas is 10 million bbl ($15.9\text{x}10^6$ $\text{m}^3$) of cumulative production of oil or 30 billions cubic ft ($850\text{x}10^6$ $\text{m}^3$) of gas. With some overlap, a total of 450 and

868 reservoirs, for oil and gas, respectively, are described in the atlases. The cumulative production of these reservoirs is large enough to take up desalination concentrate produced in the 20+ years of the plant's life. A quick computation shows that 4 MGD of drinking-quality water translates into at most 1 MGD of concentrate (see Section 1), that is, 695 gpm or ~8.7 million bbl per year. Shallower reservoirs were selected because start-up and operating injection costs increase with depth, although deep-seated injection wells may be cheaper in the long run because concentrate can be injected by gravity only. A secondary criterion was to consider fields in terms of a variety of geological settings (carbonates, arkosic sands, clean sands), which represented the different hydrocarbon-bearing formations in Texas.

The other elements required to locate potential analysis areas are the existence of brackish water in sufficient quantity, a potential need from local communities, and the presence of injection wells, possibly with a chance to obtain an Area of Review (AOR) variance (see Section 5.3). Brackish water aquifers occur across most of the state (LBG-Guyton Associates, 2003). Several counties across the state would need additional water supply to meet the projected demand in 2050 (Figure 3.1). All or only part of the county may show a water deficit in 2050.

Six analysis areas (Figure 3.1), delimited by grouping neighboring counties, within six oil- and gas-producing basins (Anadarko, Permian, East Texas, Fort Worth, Maverick, and Gulf Coast Basins) were selected according to the intersection of the following criteria:

- Shortfall of water supply over the next 50 years planning time frame (TWDB, 2002) (Figure 3.1).
- Overlying brackish groundwater resources (LBG-Guyton Associates, 2003) (Figure 3.2).
- Depleted oil/gas fields with large oil productions (scanned maps from Galloway et al., 1983, and Kosters et al., 1989) (Figure 2.2). Figure 3.3 illustrates the amount of pressure depletion in some of these reservoirs. At a given depth (any horizontal line), current reservoir pressure is much lower than initial (hydrostatic) pressure.
- Injection wells that are not too deep (shallower formation) (Figure 2.3).

## ***3.3 Identification of the Analysis areas***

The first step in the identification of the analysis areas was to scan oil and gas maps (*Atlas of Major Texas Oil Reservoirs*, Galloway et al., 1983, and *Atlas of Major Texas Gas Reservoirs*, Kosters et al., 1989) and convert them into GIS formats. In addition, complementary information (production, depth, net pay, average permeability, and porosity) already in digital form (Holtz et al., 1991; Garrett et al., 1991) was linked to the scanned map data to be used in the later phases of the study. We then overlaid shallow groundwater TDS, including brackish water, and injection well maps on top of the oil and gas field maps. Because much of the information came from different sources, sometimes with unknown geographic projection, discrepancies existed between data sets. They are not apparent on a large scale (Figure 2.2) but obvious at the basin scale. These maps of hydrocarbon fields were repositioned on analysis area maps and anchored relative to counties lines whose traces are well defined.

Stratigraphic columns and relative oil and gas productions are depicted in Figure 3.4 (oil production in East Texas and Gulf Coast Basins), Figure 3.5 (gas production in East Texas and Gulf Coast Basins), Figure 3.6 (oil production in paleozoic basins), and Figure 3.7 (gas production in paleozoic basins). These figures illustrate that the selected formations are indeed the most prolific in their respective areas and thus the most likely to have the highest pressure depletion. Because these formations have also heavily produced, they are most likely to have a dense surface infrastructure able to carry fluids. The Granite Wash Formation is the most important oil producing unit of the Anadarko Basin and also yielded significant amounts of gas (Figure 3.6 and Figure 3.7). The San Andres-Grayburg of the Permian Basin is the shallowest major oil producing unit of the basin (Figure 3.6) with still nonnegligible amounts of gas (Figure 3.7). Similarly the Woodbine Formation in the East Texas Basin produced huge amounts of oil (Figure 3.4). The Fort Worth Basin in the analysis area has a relatively minor oil production from the Bend Conglomerate/Atoka Formations (Figure 3.6), while the Maverick Basin yielded relatively large amounts of oil from the San Miguel/Olmos Formations (Figure 3.4). The Frio Formation in the southern Gulf Coast is also a prolific gas and oil producer (Figure 3.4 and Figure 3.5).

Table 3.1 presents a summary of the brackish water availability in the water planning regions encompassing the six analysis areas according to LBG-Guyton Associates (2003). Definitions of availability, productivity, and production cost are identical to those in the report by LBG-Guyton Associates (2003). Availability is a measure of the amount of water available. A low availability may be sufficient for a relatively modest desalination facility (a feed water stream of 5 MGD). Productivity is a function of transmissivity and other aquifer parameters, while production cost is mainly a function of depth to the water table and depth to the top of the formation. These three characterization parameters are variable across the six analysis areas, as they are for the brackish aquifers of Texas.

Table 3.2 displays the resulting selection and associates the likely brackish water source with the likely injection formation. Names of major oil and gas fields are also given. Numerous smaller oil and gas fields exist in addition to the major fields displayed in the maps described next, and some of the numerical information used in the report do come from these minor fields. In the remainder of the document, the different areas will be presented from north to south and west to east starting with the Anadarko Basin in the north (Figure 3.8), moving to the Permian (Figure 3.9) and East Texas Basins (Figure 3.10), then to the Fort Worth Basin (Figure 3.11), and finally to the Maverick (Figure 3.12) and southern Gulf Coast Basins (Figure 3.13). More details about the basins are given in Section 6.1.

Table 3.1. Brackish water availability in the six analysis areas, according to LBG-Guyton Associates (2003)

| Water Panning Region | Aquifer | Availability | Productivity | Production Cost |
|---|---|---|---|---|
| **Anadarko** | | | | |
| A - Panhandle | Ogallala | Low | High | Low to Moderate |
| | Dockum | Low | Low | Low |
| **Permian** | | | | |
| F | Ogallala | Moderate | High | Low to Moderate |
| | Dockum | High | Low to Moderate | High |
| | Rustler | Moderate | Low | High |
| **East Texas** | | | | |
| D - Northeast Texas | Carrizo-Wilcox | High | Moderate | Moderate to High |
| **Fort Worth** | | | | |
| G - Brazos | Trinity | Low | Low | Low |
| **Maverick** | | | | |
| L – South Central Texas | Carrizo-Wilcox | Low | Low | Moderate to High |
| **Gulf Coast** | | | | |
| N | Gulf Coast | Moderate | Moderate to High | Low |

Adapted from Table 9 of LBG Guyton Associates (2003)

Table 3.2. Selected feed water source, injection formation, counties, and major oil and gas fields

| Basin | Brackish Water Source | Formation | Counties | Major Fields |
|---|---|---|---|---|
| Anadarko | Ogallala and Dockum Aquifers | Panhandle (granite wash /dolomite) | Carson<br>Armstrong<br>Moore<br>Potter | Panhandle |
| Permian | Ogallala, Dockum, and Rustler Aquifers | San Andres Fm (carbonates) | Ector<br>Midland<br>Andrews | Cowden North<br>Cowden South<br>Goldsmith<br>Means<br>McElroy |
| East Texas | Carrizo-Wilcox Aquifer | Woodbine Fm (sandstone) | VanZandt,<br>Wood<br>Smith<br>Gregg<br>Upshur | East Texas<br>Van<br>Hawkins<br>New Diana |
| Fort Worth | Trinity Aquifer | Bend Conglomerate (sandstone) and Glen Rose Fm (carbonates) | Shackelford<br>Young,<br>Stephens<br>Eastland | Boonsville<br>Breckenridge<br>Kildare Rodessa |
| Maverick | Carrizo-Wilcox Aquifer | San Miguel and Olmos Delta Fms (sandstone) | Maverick<br>Zavala<br>Frio<br>Dimmit<br>Atascosa | Sacatosa<br>Big Wells Chittim<br>Big foot<br>Catarina |
| Southern Gulf Coast | Gulf Coast Aquifers | Frio Fm (Sandstone) | Nueces,<br>Jim Well,<br>Kleberg | TCB<br>Seelington<br>Borregos<br>Stratton<br>Brayton |

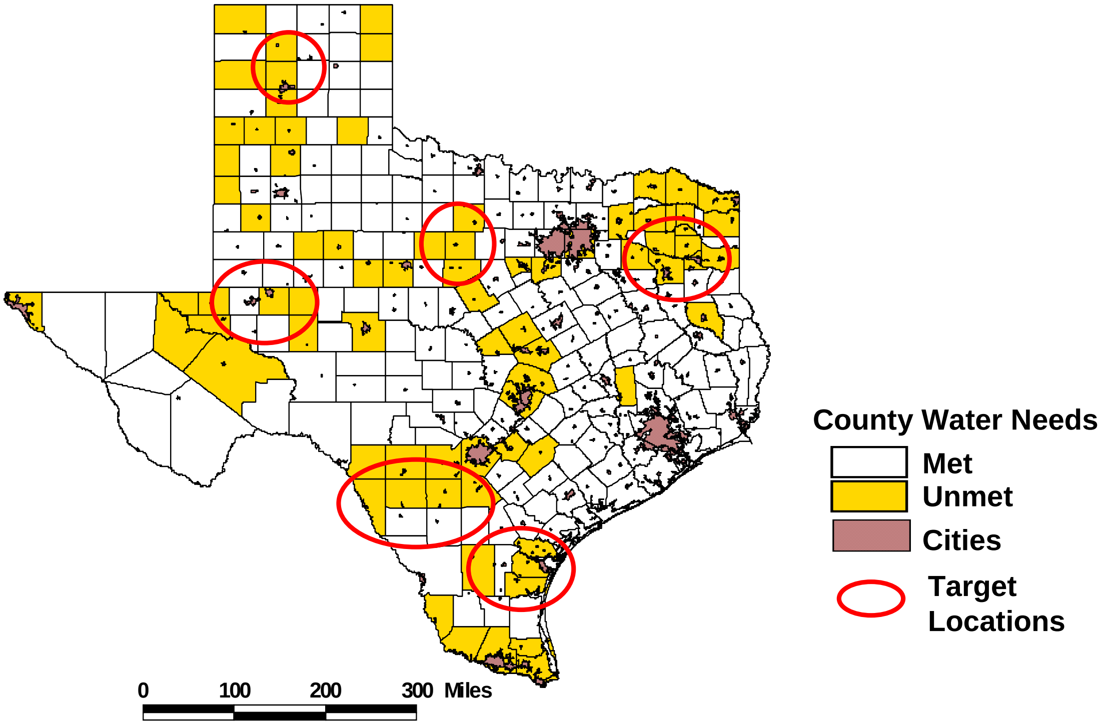

Figure 3.1. Map of Texas counties with water needs to meet demand in 2050. The map also shows areas analyzed by this study

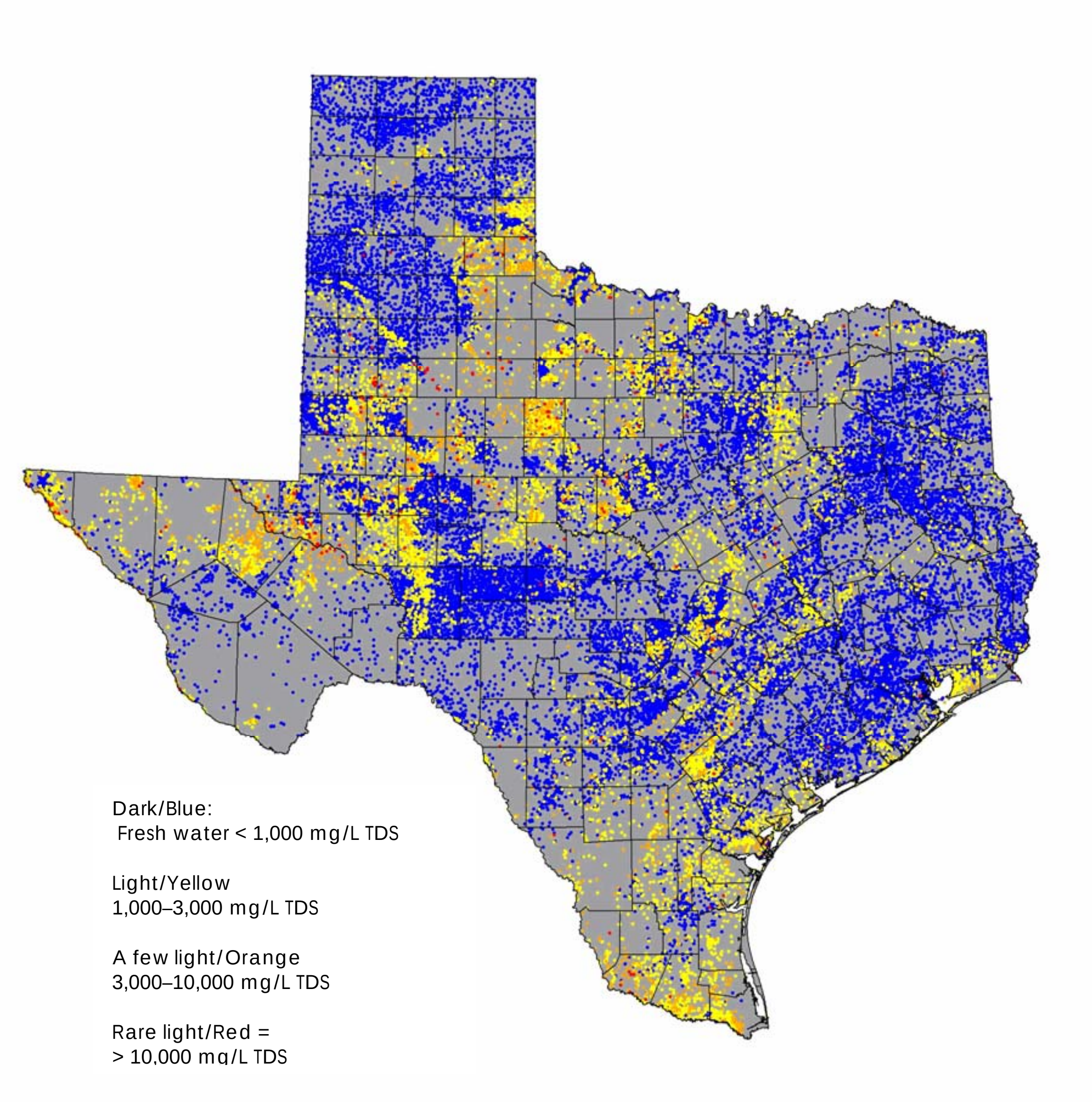

Source: LBJ Guyton Associates (2003)

Figure 3.2. Map of water quality of shallow waters in Texas

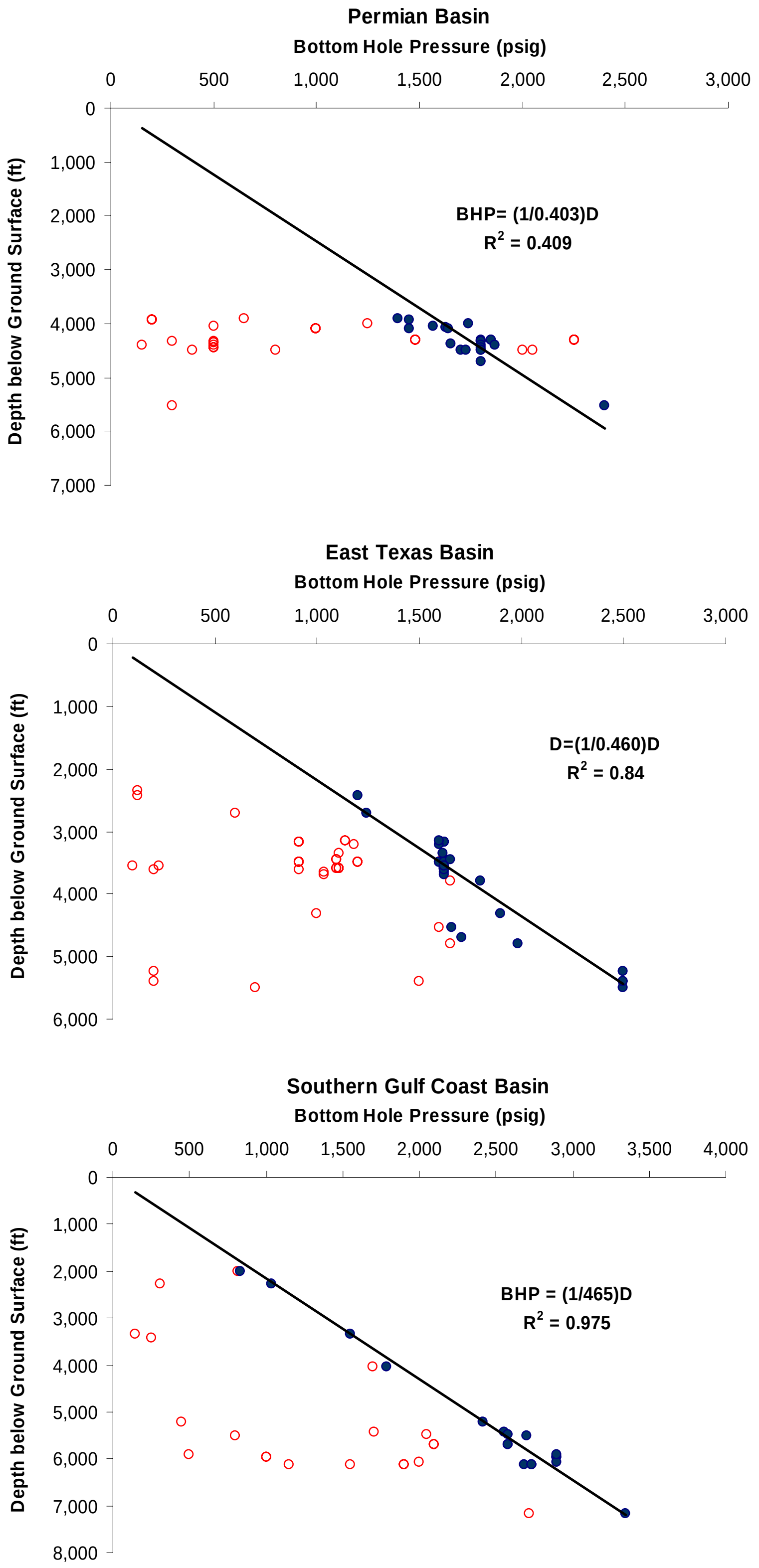

NOTE: Open circles represent current depleted pressures while colored-in circles represent initial pressures.

Figure 3.3. Reservoir pressure as a function of depth (from RRC H1 forms)

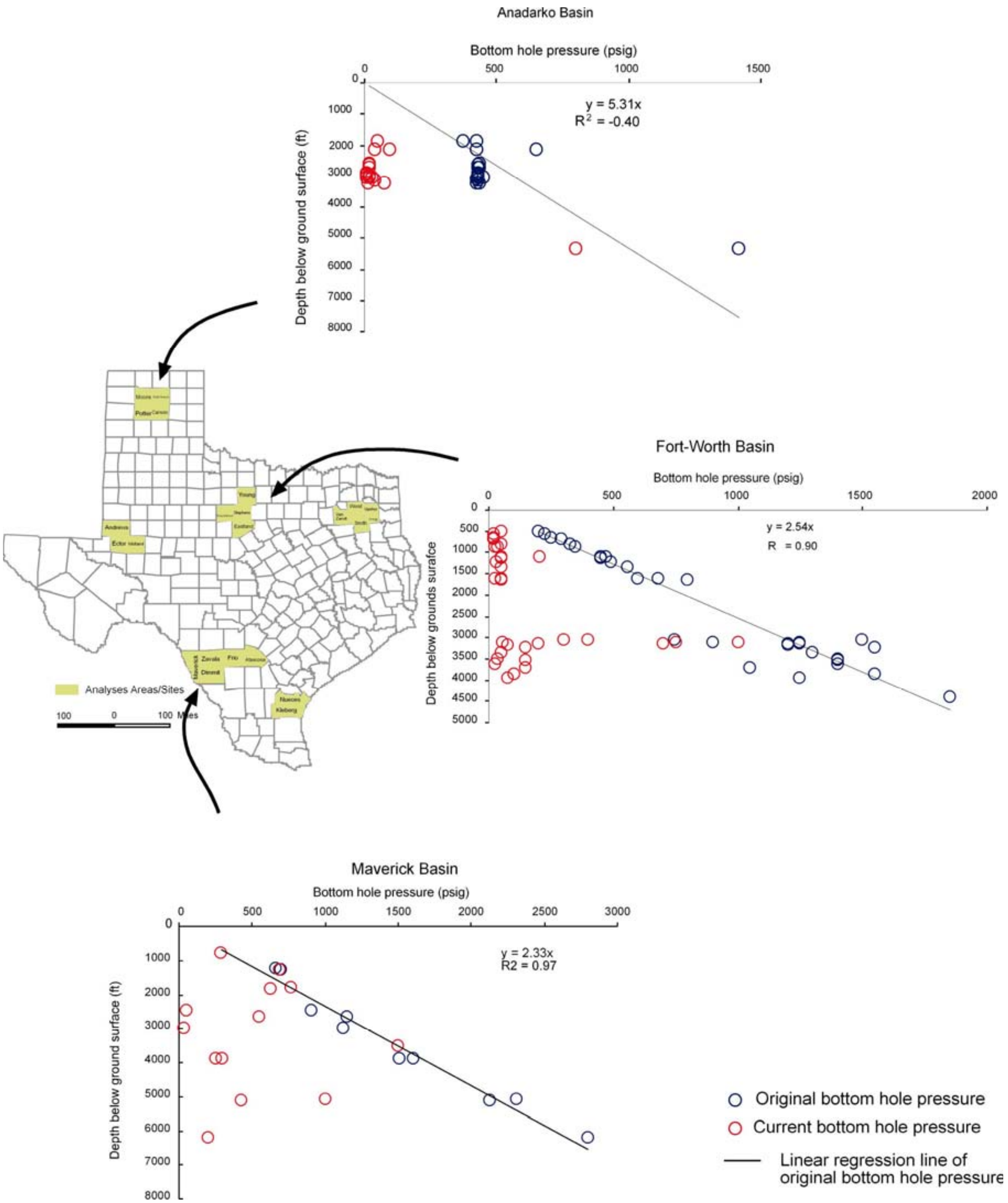

Figure 3.3 (continued). Reservoir pressure as a function of depth (from RRC H1 forms)

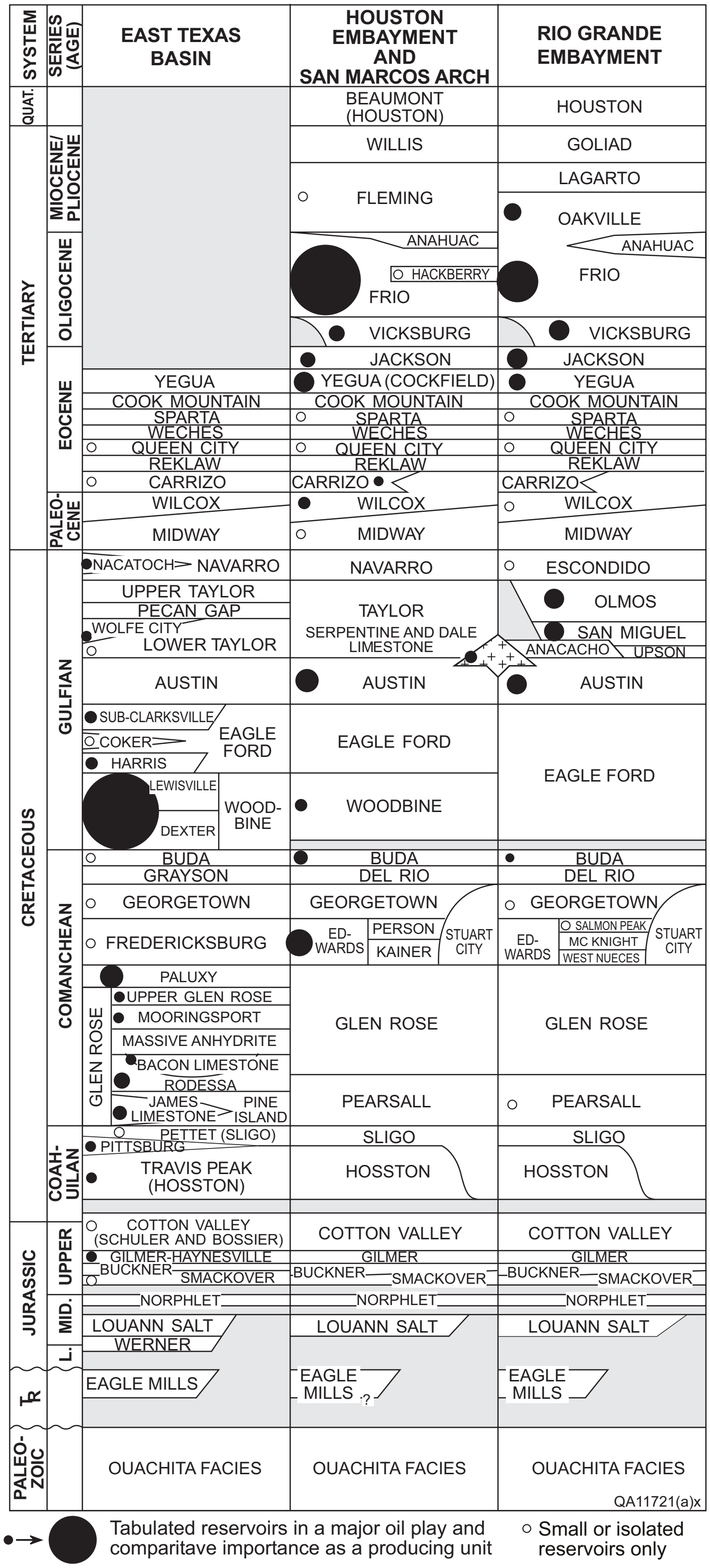

Figure 3.4. Stratigraphic column and relative oil production for the Gulf Coast and East Texas Basins (after Galloway et al., 1983)

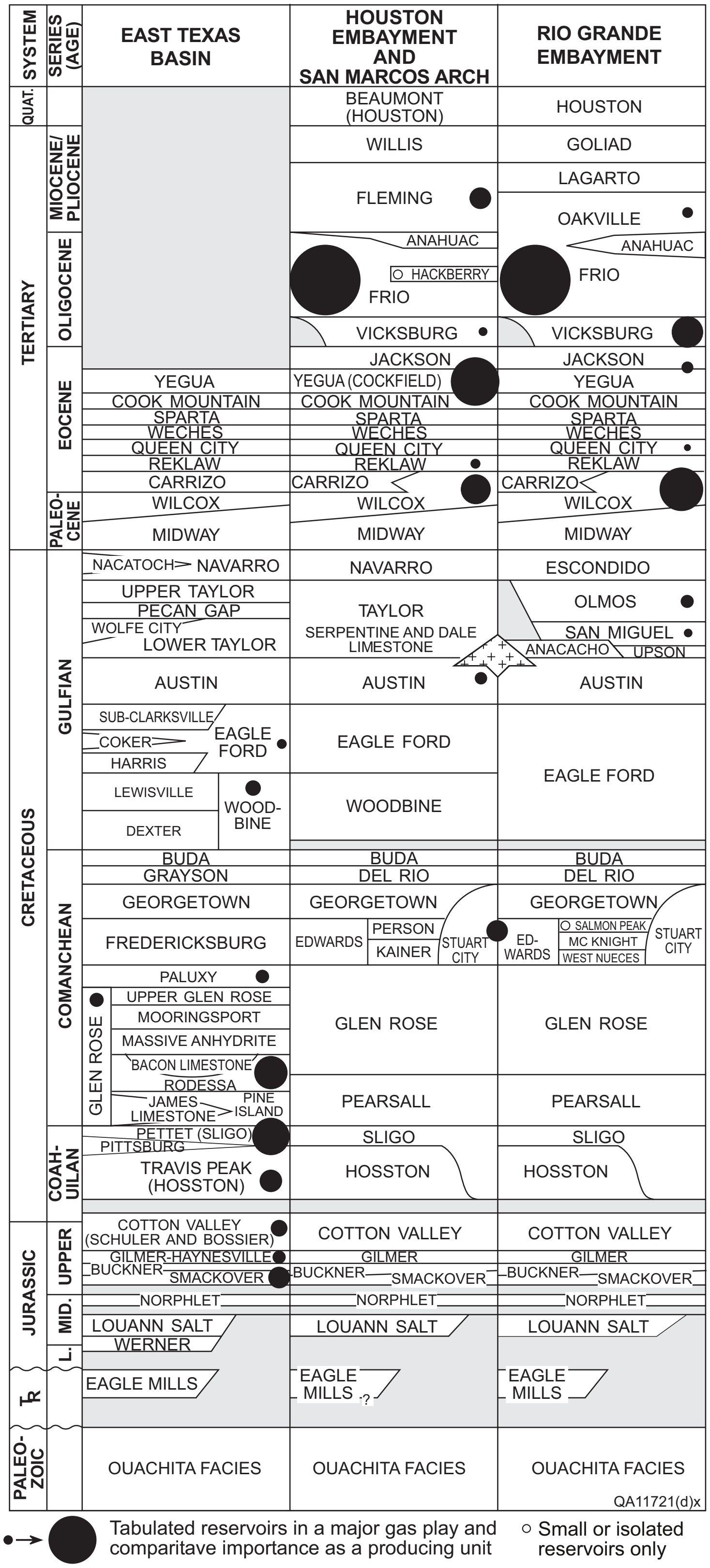

Figure 3.5. Stratigraphic column and relative gas production for the Gulf Coast and East Texas Basins (after Kosters et al., 1989)

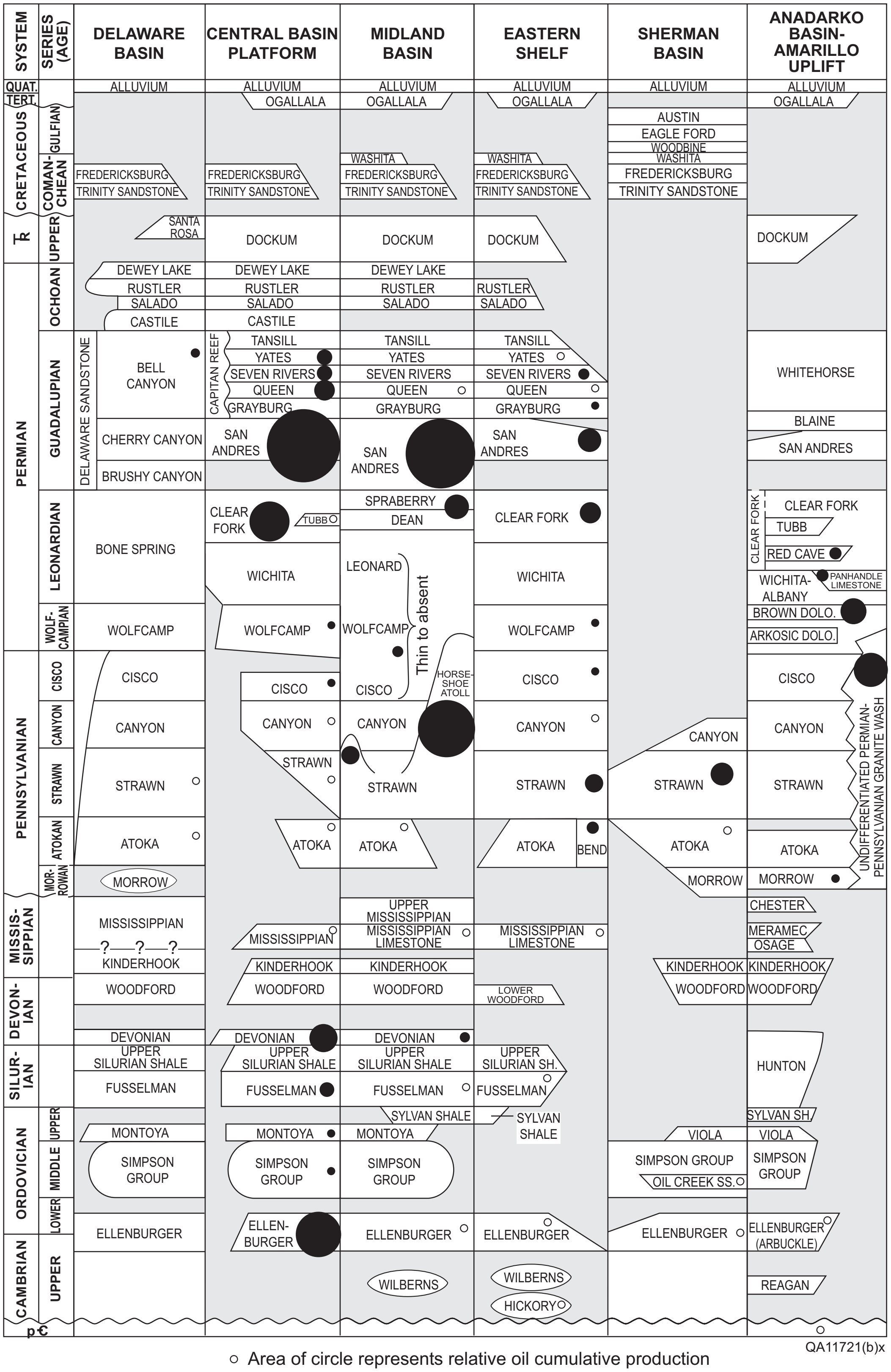

Figure 3.6. Stratigraphic column and relative oil production for the North-Central and West Texas Basins (after Galloway et al., 1983)

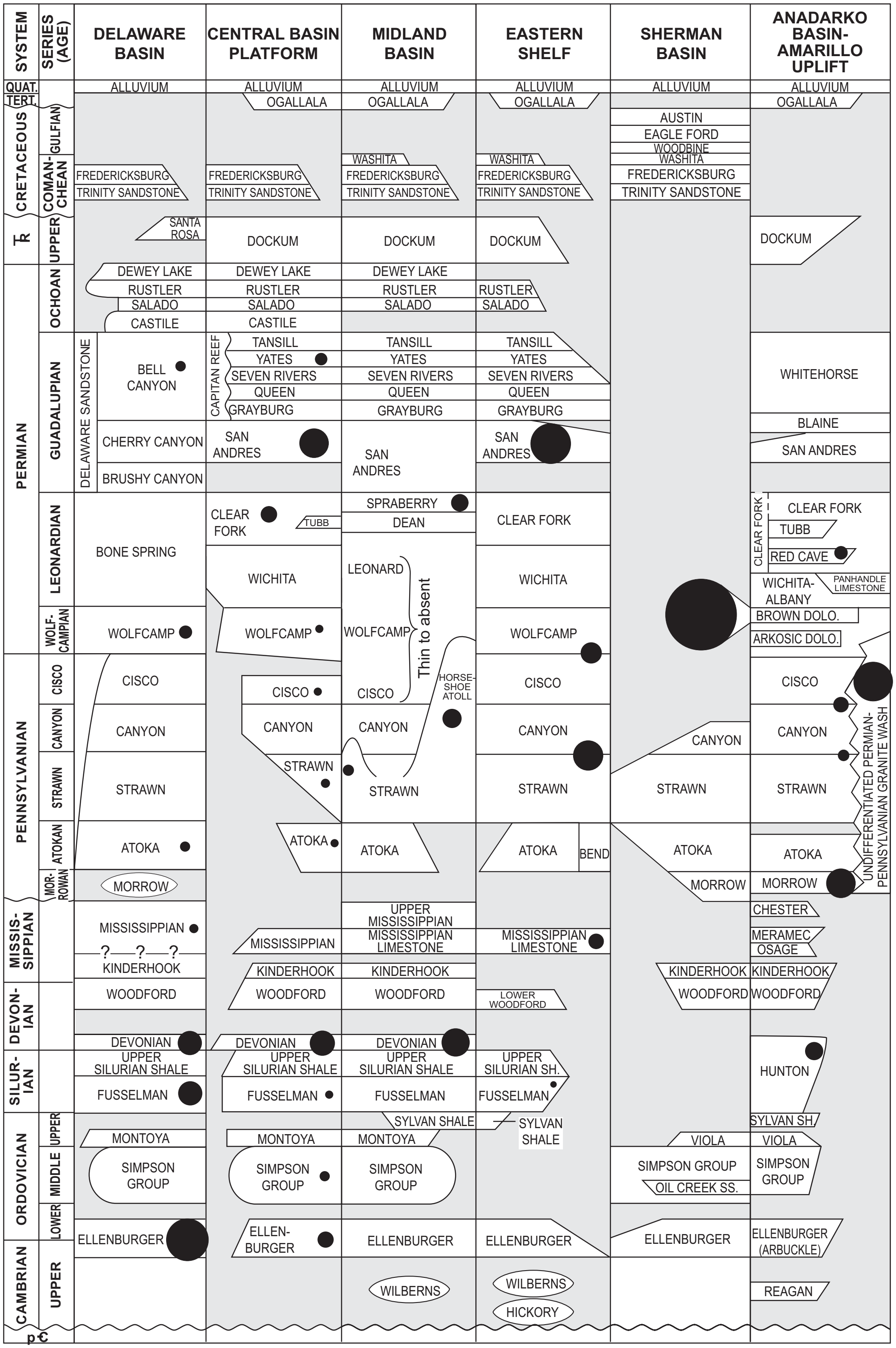

Area of circle represents relative gas cumulative production

QA11721(e)x

Figure 3.7. Stratigraphic column and relative gas production for the North-Central and West Texas Basins (after Kosters et al., 1989)

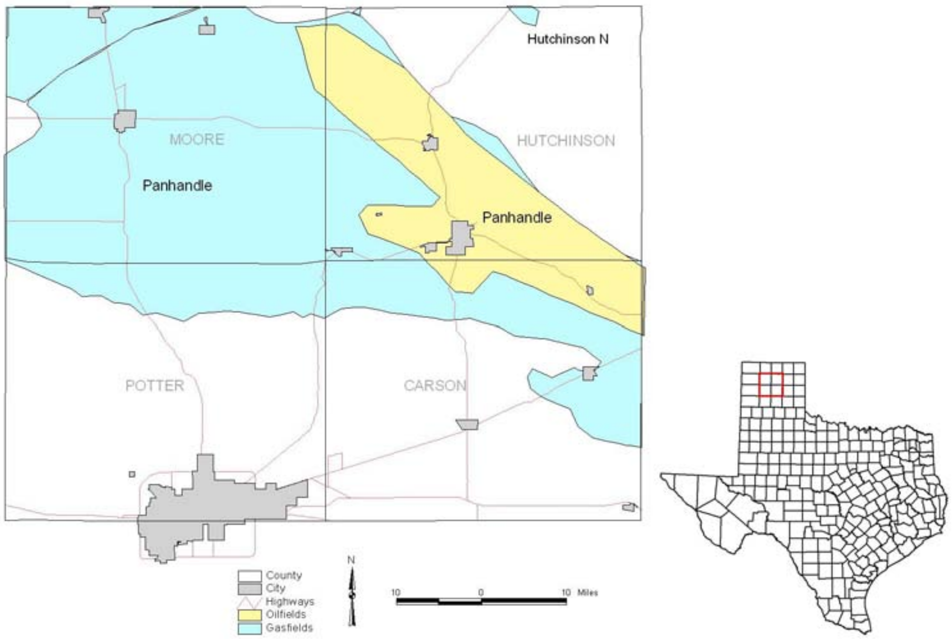

Figure 3.8. Major oil and gas fields in the Anadarko Basin analysis area.

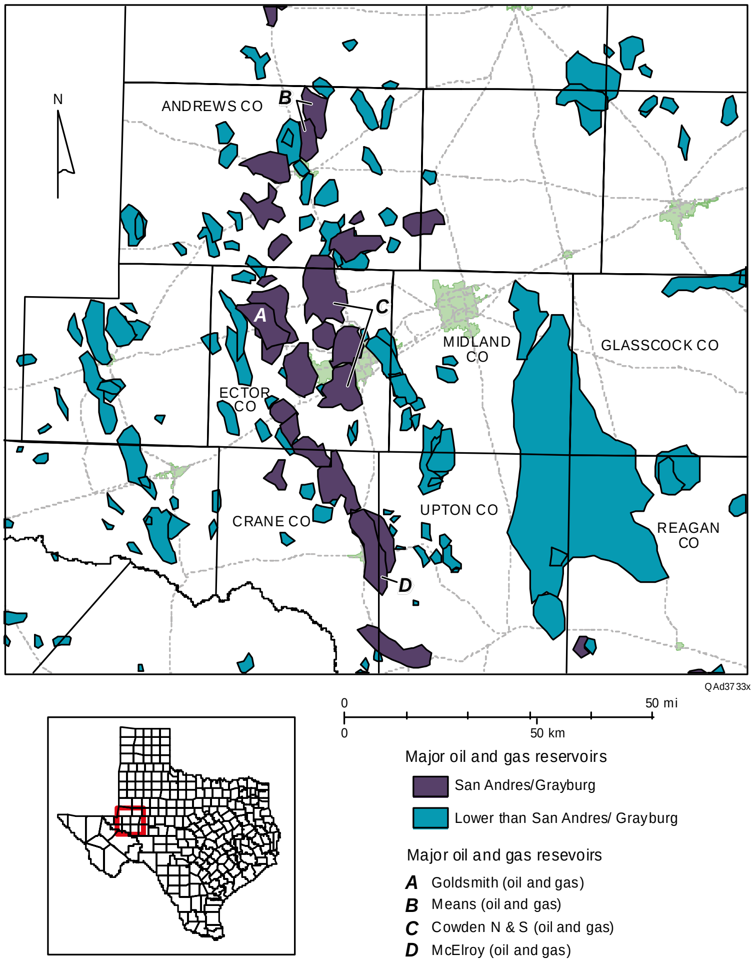

Figure 3.9. Major oil and gas fields in the Permian Basin analysis area

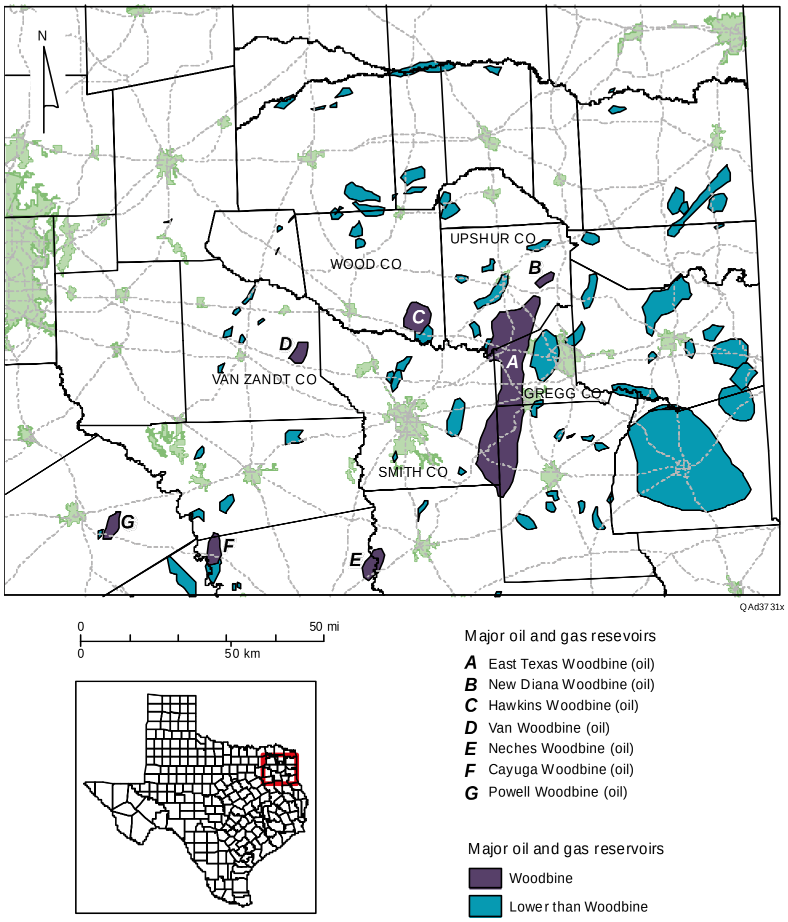

Figure 3.10. Major oil and gas fields in the East Texas Basin analysis area

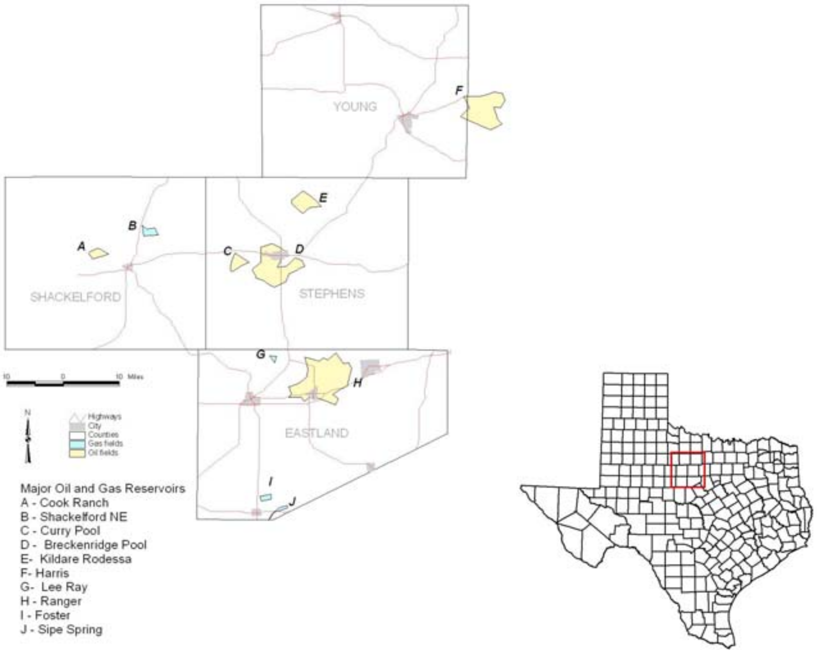

Figure 3.11. Major oil and gas fields in the Fort Worth Basin analysis area

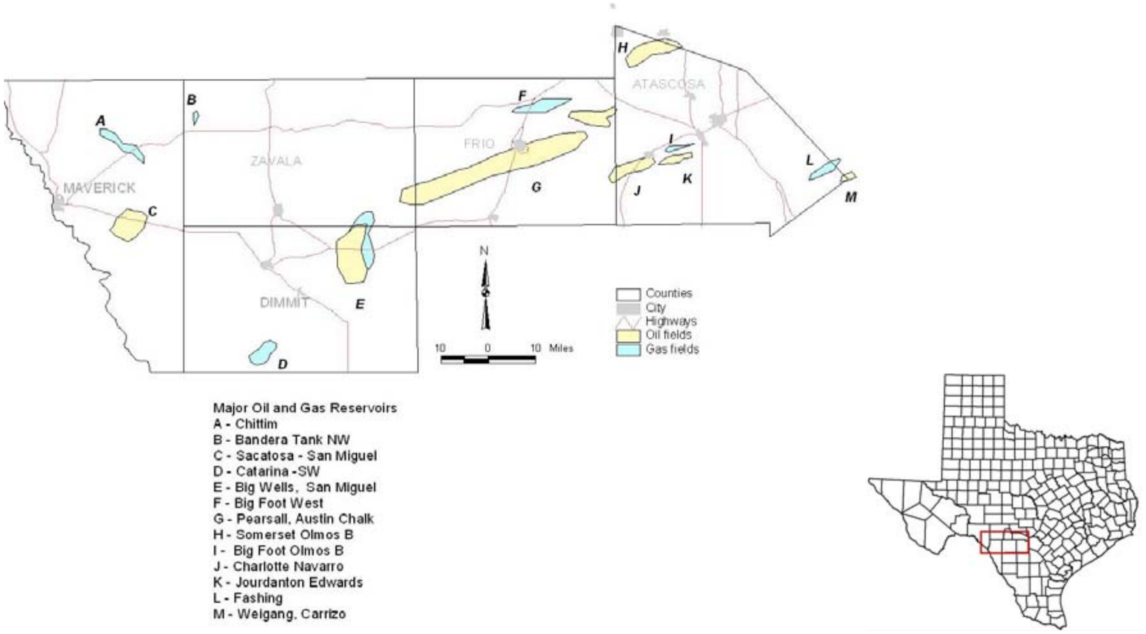

Figure 3.12. Major oil and gas fields in the Maverick Basin analysis area

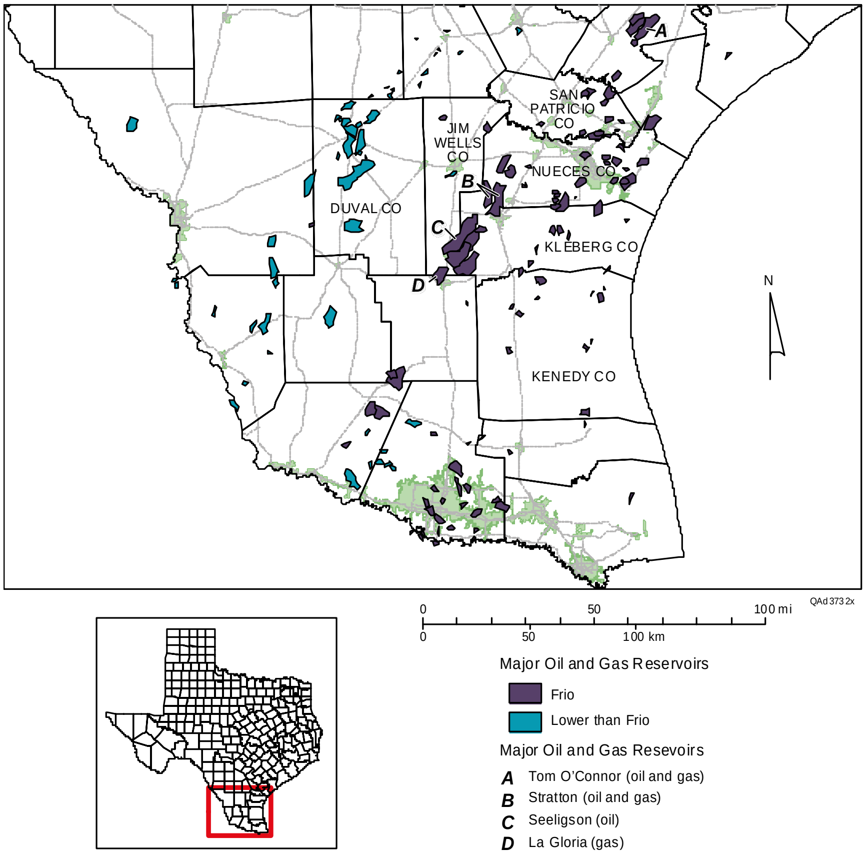

Figure 3.13. Major oil and gas fields in the Southern Gulf Coast Basin analysis area

# 4 Desalination Technologies and Concentrate

## 4.1 Introduction

There are two main types of technology available to desalinate water: membrane-based and evaporation-based technologies. As described in Table 4.1, evaporation-based technologies such as multistage flash or multiple-effect distillation are more suited to seawater desalination and/or larger plants because energy requirements are almost independent of the source water salinity. They also have a small recovery translating into a large waste stream, which may be hard to dispose of short of sending it to a large body of water. Membrane-based technologies are more widely used in smaller plants and/or for the treatment of brackish water. In this study we focus on the membrane-based technologies because they form the overwhelming majority of the plants in the continental U.S. These membranes are also called semipermeable because they are selective in what can flow through them.

Membrane processes can be described according to the mechanisms involved and the size of the particles they allow through. The two mechanisms, described in more detail later, are pressure-driven and electro-potential-driven processes. Pressure-driven, membrane processes are further described as microfiltration (MF), ultrafiltration (UF), nanofiltration (NF), and reverse osmosis (RO). MF and UF act only mechanically, blocking bacteria and suspended particles (10 – 0.1 μm) because they cannot flow through the membrane pores. UF also blocks colloids and macromolecules (0.05 – 0.005 μm). In contrast NF (0.005 – 0.0005 μm), blocking solutes down in size to small organic molecules and divalent ions, and RO (0.001 – 0.0001 μm), blocking them down to monovalent ions, operate mainly through diffusion and chemical interaction between the membrane and the solutes. NF is also called low-pressure RO, or water softening. NF removes more Ca-Mg than Cl, resulting in softer waters. NF also removes more $SO_4$ and $HCO_3$ than Cl. The two electro-potential-driven processes are electrodialysis (ED) and electrodialysis reversal (EDR). RO plants are the most widely used in the nation for desalination, with 72 percent of plants using brackish water RO, 2 percent seawater RO, 15 percent ED/EDR, and 11 percent nanofiltration (Mickley, 2001). Of the 102 desalination plants operating in Texas, over 95 percent of the plants use RO with the remaining 5 percent using ED/EDR plants. As such, we discuss only RO and ED/EDR processes below. Nearly 83 percent of the desalination plants in Texas use brackish groundwater, while 17 percent use surface water (Figure 2.6). Below about 3,000-3,500 mg/L salinity, both RO and ED/EDR processes can be competitive and can produce low salinity water at low cost.

## *4.2 Summary of Technologies*

### 4.2.1 RO Technology

A solute in water tends to migrate until it reaches chemical equilibrium with its surroundings. Water flows from lower to higher chemical concentrations to achieve chemical equilibrium. *Osmosis* is defined as the flow of a solute through a semipermeable membrane in response to a concentration gradient across the membrane. The flow will stop when the concentrations on both sides of the membrane are equal (or more accurately activities). Increasing the pressure on the receiving side of the membrane will progressively limit the solute migration. Increasing the pressure even more will generate solute flow against the concentration gradient; hence the name *reverse osmosis*. In the case of desalination, the solute is water. RO is a pressure-driven process, and the pressure requirements increase as the salinity of the feed water increases. High pressures are needed to overcome the high osmotic pressure of seawater (375 to 500 psi) compared with the low pressures (less than 100 psi) needed for desalination of brackish water. The source water is also termed feed water, while the resulting fresh water is called the *permeate* and the waste is called the *concentrate*.

The first RO membranes were made of cellulose acetate. Limitations due to the stability of cellulose restrict the use of this membrane to a pH between 3 and 6 and a temperature around 30$^{o}$C (HDR, 2000, p. A3.1). They are also subject to biodegradation but they tolerate chlorine, which is routinely added to the feed water for disinfection purposes. Numerous polymeric membranes are now on the market (polyamide, polysulfone, polyhydrazide, polyurea, etc). They are not tolerant of chlorine, but neither are they subject to biodegradation. In addition, they can operate in a wider range of temperature and pH conditions.

### 4.2.2 EDR Technology

Both ED and EDR processes differ from the pressure-driven membrane processes. The processes employ both cation and anion selective membranes developing electrical potential that allows cations to migrate toward one electrode and anions toward the other. Owing to this migration, the ions pass through either the cation or anion membranes leaving the central feed stream relatively depleted in ions and the other two streams more concentrated. To inhibit fouling and scale growth on the membranes, membrane polarity are periodically reversed in the EDR process; hence the name *electrodialysis reversal*. ED and EDR systems are used to treat brackish water for potable use or to desalt and concentrate effluents for reuse (Mickley et al., 1993). Most ED plants are truly EDR plants. They are typically used for feed water on the low end of the brackish water range (<2,000 mg/L). ED/EDR plants are also typically considered when RO membrane could be subject to silica fouling. Because silica is a neutral compound unaffected by the electric fields, it stays in the ED/EDR concentrate stream.

In the ED/EDR processes, there is less behavior difference between monovalent and divalent ions. Thus, the concentrate in the EDR process generally contains higher proportion of sodium chloride than the concentrate from an equivalent RO system. Recoveries in the ED/EDR processes can reach up to 90 percent. It is important to note that, unlike in the RO process, the ED/EDR water does not pass through the membrane. Thus, if colloids, viruses, or organics are present in the feed water, they must be removed during pretreatment. On the other hand, the concentrate stream does not contain as many particulates as in RO systems. Consequently, turbidity criteria for the ED/EDR processes are more stringent than for that of the RO membranes. Higher concentration of calcium and carbonate species is also acceptable in the ED/EDR systems compared with the RO processes. If a high concentration of hydrogen sulfide is present in the water, the ED/EDR systems may be designed for its removal prior to the process unlike, RO systems (Mickley et al., 1993).

## *4.3 Concentrates*

As discussed earlier, desalination concentrates are produced during removal of salts from low quality water in RO and ED/EDR plants. This study is too generic to take into account various concentrate compositions that may arise when the same feed water is processed by different types of membrane technology. The amount of concentrate as a percentage of feed water varies depending on the desalination method used, percent recovery, and the chemical additives used. In RO systems that produce drinking water, a typical pretreatment consists of acidification and addition of antiscalant chemicals (see next section). Membrane concentrate is essentially a concentrate of the feed water plus the chemical added for pretreatment purposes. However, complication arises owing to variation in ion rejection rates. Watson (1990) made the following observation from desalination of brackish groundwater in Fort Meyers, Fl: (1) heavy metals (Ag, Hg, etc.) are rejected at the same ratio as Ca and Mg, (2) if an anaerobic condition and $H_2S$ occur in groundwater then the concentrate will also be equally anaerobic and contain $H_2S$, and (3) concentrate pH is generally higher than the feed water pH owing to the concentration of bicarbonate ions.

The degree of concentration, also called the *concentration factor* (CF), is defined as:

$$CF = 1/(1-R_w) * [1-R_w(1-R_s)] \qquad \text{Equation 4-1}$$

where $R_s$ is the fractional salt rejection, and $R_w$ is the fraction product water recovery (Glater and Cohen, 2003). Thus, the concentration factor can be readily calculated knowing the compositions of the feed water and expected recovery rate. Assuming a 100 percent salt rejection, a recovery of 75, 85, and 95 percent would yield a concentration factor of 4, 6.67, and 20, respectively. In general divalent ions are rejected at a higher rate than monovalent ions. However, the error introduced by considering that they have the same rejection rate of 100 percent is minimal, as illustrated in Mickley et al. (1993, Chapter 5). There is no more than a few percent difference between monovalent and divalent ion rejection for high rejection values (90-100 percent).

An examination of the major ion ratios of the desalination concentrates and the feed water from Texas and elsewhere (Table 4.2 and Table 4.3) indicates that the ion ratios largely depend on the feed water composition (Ahmed, 2000). Feed water and concentrate compositions that we collected from four desalination facilities in Texas do not have a complete list of chemical parameters (Table 4.2). Some of the chemical parameters were measured for the feed water but not for the corresponding concentrate.

Most of the chemical parameters in the concentrate have more elevated values than the feed water composition, as would be expected during concentration of dissolved salts in the reverse osmosis process. Overall, salt concentration ratios (concentrate/feed water) for brackish water vary from 1.55 to 3.62 for TDS, 1.6 to 3 for $SO_4$, and 1.26 to 3.77 for Cl. These variations in the salt concentration values are due to differences in pretreatment and initial compositions of feed water. When the TDS in the feed water approaches that of seawater, salt concentration ratios for all chemical parameters are considerably reduced (Table 4.3). An examination of the major ion ratios of the desalination concentrates and the feed water from Texas and elsewhere indicates that the ion ratios largely depend on the feed water composition.

A cross plot of the total dissolved solids (TDS) of the feed water and the desalination concentrates that include Texas samples shows a good correlation ($R^2 = 0.98$) (Figure 4.1a). At lower TDS (<10,000 mg/L), desalination concentrates are approximately 4 times more enriched than the feed water composition. Nearly all Texas samples with TDS value of less than 10,000 mg/L fall into this category. At TDS values approaching that of seawater salinity, recovery rate is significantly reduced, as reflected in the lower concentrate/feed water ratios. Cross plots of Na and Mg compositions of the desalination concentrates and the feed water show good correlation ($R^2 > 0.96$) (Figure 4.1b and c). Cross plots of Ca and $SO_4$ compositions of the desalination concentrates and feed waters show poor correlation ($R^2 = 0.57$ and 0.5, respectively) probably because acidification during pretreatment perhaps unevenly affects these ions at varying salinities (Figure 4.1d and e). Membrane desalting technologies allow the dissolved gases, typically $O_2$, $CO_2$ and $H_2S$, to go through the membrane (RO) or not go through the membrane (ED/EDR) and be mostly depleted in the concentrate.

As mentioned above, concentrate composition is a strong function of the feed water composition and pretreatment. It is also a function of the membrane type and of the operational details. Almost every membrane vendor has proprietary software valid for their membranes that would compute permeate and concentrate concentrations as a function of the feed water composition and operating parameters. It is beyond the scope of this study to determine the range of feed water composition that could result from the large variety of membranes available on the market. Instead, on the basis of on our analyses of brackish water samples from Texas and elsewhere and information from the literature (Mickley et al., 1993), we applied a uniform concentration factor of 4 to all samples.

## 4.4 Changes Due to Pretreatment

Because the feed water undergoes numerous transformations during the desalination process, it is important to understand and describe those changes. As mentioned above, for operational reasons, the feed water needs to be treated (e.g., Wilbert et al., 1998, Chapter 6). It generally entails (1) acidification to reduce the alkalinity of the raw water and prevent scaling by calcite and (2) addition of antiscalant(s) to prevent scaling by other minerals, particularly sulfates. If the source water is groundwater, the pretreatment is in general limited to that chemical conditioning of pH adjustment and scale control. Surface waters and some groundwaters may require a more complex process that would also include filters and cartridge filtration to remove suspended solids and bacteria. A typical biocide pretreatment could also involve chlorination and subsequent dechlorination with activated carbon or maybe addition of sodium bisulfite because of the low tolerance of most modern membranes to chlorine. Bisulfite will react with chlorine to generate chloride and sulfate. Because of the possible detrimental effect of sulfate during the injection, care must be taken to ensure that no alternative treatment to bisulfite can be used. A biocide such as ozone may be preferred. However, this would also entail, as for chlorine, an extra degasification treatment of the feed stream before reaching the membrane.

Acidification is generally done using sulfuric acid (dosage <300 mg/L) and sometimes hydrochloric acid. Among the 33 drinking water RO/EDR/NF facilities described in Mickley (2001) that adjust pH, all but 5 use sulfuric acid. Three use hydrochloric acid and two use sodium hydroxide. Sulfuric acid is cheaper but might generate sulfate scaling problems in feed water already high in sulfate while the addition of the chloride ion in hydrochloric acid enhances corrosion. However, decreasing pH to less than 7.0 will also decrease solubility of silica, encouraging its precipitation onto the membrane. The 18 MGD Hollywood, FL membrane softening and reverse osmosis plant injects a scale inhibitor and sulfuric acid into the feed stock before the pretreatment cartridge filter. The design pHs for the membrane softening and reverse osmosis are 6.0

and 6.5 respectively (Bloetscher and Ortiz., 1999). The raw water supply comes from the Biscayne and Floridan aquifers. Another surficial calcium carbonate water with a high iron concentration (4 to 6 mg/L) is brought to a pH of 5.2 to 5.6 by addition of sulfuric acid before a nanofiltration or membrane softening process (Messner et al., 1999). Acid addition increases solubility of calcium carbonate and prevents scaling. Both acid addition and water softening processes do not, however, control sulfate-based scaling that requires use of antiscalants. Hydrochloric acid is added to the feed water to the Port Hueneme, CA, EDR brackish water facility (AWWA, 2004, Case Study 2). The facility also operates in parallel NF and RO modules, which do not require acid addition. Mickley et al. (1993, Chapter 3) reported a study of 12 Florida brackish water desalination plants where the amounts of acid added ranged from 40 to 300 ppm.

Antiscalant treatment involves the addition of a small amount of chemical (<10 mg/L) that does not modify the chemical characteristics of the concentrate. The antiscalants typically delay the scale formation process, but some can thermodynamically prevent the scale precipitation. Antiscalants are often made up of polyphosphates, phosphonates, or polycarboxylates (Cowan and Weintritt, 1976). There are many antiscalant manufacturers, each with an assortment of products more or less efficient according to the facility needs, and the panoply of products increases every day. Makers of some antiscalants claim that their product can inhibit the precipitation of $CaCO_3$ at a Langelier Saturation Index up to +2.3 and of $CaSO_4$ up to 1.8 times supersaturation. Experiments have in general proven those claims to be accurate (He et al., 1994; Matty and Tomson, 1988). He et al. (1994) reported that the effectiveness of antiscalants (for $CaSO_4$ and $BaSO_4$) is a function of temperature, pH, and ionic strength, as well as the nature of other divalents ions. They reported that $CaSO_4$ and $BaSO_4$ in NaCl solutions can be inhibited at least to a saturation index of 0.7 and 2.9 (if $T<50^oC$), respectively. Matty et al. (1985) reported a probable value of 2.3 for $CaCO_3$ saturation index for the inhibitor action in in situ conditions. King (2003) reported that current antiscalants are effective up to an *LSI* of 3.2 for calcite, a *SI* of 2.6 for gypsum, 1.7 for barite, and 1.6 for strontium sulfate. He also suggested that silica concentration can be as high as 280 ppm with the appropriate antiscalant.

More involved pretreatment techniques can also be used as in any water treatment plant for water softening, Fe/Mn removal, and silica removal, although at an added cost. They have the advantage of targeting one troublesome element or compound. These less-common feed water alterations were not explored in this document. Scale-forming material could be removed or their concentration decreased by ion-exchange techniques on special resins or ultrafiltration. Some form of chemical precipitation used in conventional water treatment plants can also be used, although they are typically costly. For example, alum coagulation/flocculation and filtration could also be a possibility to prevent the fouling and clogging of membranes by suspended solids. Adding lime to the feed water stream will raise the pH and precipitate calcium carbonate and magnesium hydroxide, softening the water. Alum also reacts with alkalinity and softens the feed water. NF and cation exchange columns will also have a softening effect. Iron and manganese can be taken out of solution by flowing through a "greensand" system (actually, mainly glauconite clay). All this will decrease the feed water TDS and consequently the concentrate TDS.

A related issue is the open or closed nature of the flow system to the atmosphere. $O_2$ and $CO_2$ increase the corrosiveness of water and may need to be removed before they reach the membranes. Because gases go through RO membranes and are unaffected by ED/EDR, they are not present in the concentrate if the system operates in a closed loop. We assumed that the desalination process operates in a closed loop with no contact with the atmosphere between the time the water is retrieved from the brackish water aquifer and the time the concentrate is injected in the subsurface.

## 4.5 Posttreatment of Concentrate

The permeate needs to be treated before it is suitable for human consumption, typically by adding lime and increasing its pH. Depending on the disposal method, the concentrate also needs to be treated. Only 1 of the 10 desalination facilities described in Mickley (2001) which disposed of the concentrate through deep-well injection, does some kind of pretreatment before injection. The Mabry Carlton EDR Facility (design capacity of 12 MGD) adds an antiscalant for gypsum (that would work for $SI<1.5$). Sometimes cartridge filtration has to be performed to remove TSS added when backwash from UF pretreatment and other cleanup residues are added to the concentrate stream. An upper limit of 1 ppm TSS is generally accepted before injection. As a guide, a typical TSS value in seawater is 50 mg/L. Anticorrosion products are also typically added to the waste stream. A more thorough description of possible preinjection treatment is given in the next section.

Table 4.1. Summary of characteristics of major desalination technologies

| | **Reverse Osmosis (RO)** | **Electrodialysis Reversal (ED/EDR)** | **Multistage Flash (MSF)** | **Multiple-Effect Distillation (MED)** |
|---|---|---|---|---|
| Energy cost | Moderate | High | High | Very high |
| Energy/Salinity | Increases with salinity | Increases fast with salinity | Independent of salinity | Independent of salinity |
| Applicable to | All water types | Brackish | Seawater - brine | Seawater - brine |
| Plant size | Modules | Modules | Large | Large |
| Bacterial contamination | Possible | Posttreatment always needed | Unlikely | Unlikely |
| Final product salinity | On demand | On demand | Can be <10 mg/L TDS | Can be <10 mg/L TDS |
| Complexity | Easy to operate<br>Small footprint | Easy to operate<br>Small footprint | Only large complex plants | Only large complex plants |
| Susceptibility to scaling | High | Low | Low | Low |
| Recovery | Typically 30-50% for seawater and up to 90% for brackish water | | Poor (10-25%) | Low but better than MSF |

Table 4.2. Comparison of feed water and concentrate compositions from desalination facilities in Texas

| Facility | As | Al | Ba | Fe | Mn | Ca | Mg | Na | Cl | F | Nitrate as N | $SO_4$ | TDS | TSS | pH |
|---|---|---|---|---|---|---|---|---|---|---|---|---|---|---|---|
| **El Paso ( groundwater)** | | | | | | | | | | | | | | | |
| FW | 0.01 | ND | 0.02 | 1.05 | 0.04 | | | | 374 | 0.85 | 0.92 | 592 | 1540 | | 7.70 |
| Conc | 1.38 | <0.08 | 0.03 | | | | | | 1410 | | | | 5101 | 10 | 8.11 |
| C/FW | 98.21 | | 1.30 | | | | | | 3.77 | | | | 3.31 | | |
| **City of Sherman (surface water)** | | | | | | | | | | | | | | | |
| FW | | 32.00 | 120.00 | 0.04 | 31.00 | | | 220 | 280 | | <0.5 | 220 | 980 | | |
| Conc | 0.09 | 0.09 | 0.22 | | | | | 609 | 1005 | | | 668 | 3548 | 6 | |
| C/FW | | 0.0028 | 0.0018 | | | | | 2.77 | 3.59 | | | 3.04 | 3.62 | | |
| **Dell City ( groundwater)** | | | | | | | | | | | | | | | |
| FW | <0.02 | <0.05 | 0.01 | <0.010 | <0.008 | 205 | 61 | 16.50 | 19 | | | 588 | 753 | | |
| Conc | | | | | | | | | 24 | | | 968 | 1170 | | |
| C/FW | | | | | | | | | 1.26 | | | 1.65 | 1.55 | | |
| **City of Seadrift ( groundwater)** | | | | | | | | | | | | | | | |
| FW | | | | | | 115 | 48 | 468 | 875 | | | 34 | 1699 | | 8.20 |
| Conc | | | | | | | | | | | | | 4710 | | |
| C/FW | | | | | | | | | | | | | 3 | | |

Units are mg/L; FW=Feed Water; Conc=Concentrate; C/FW=Ratio Concentrate / Feed Water

Table 4.3. Comparison of feed water and concentrate compositions from desalination facilities in the United Arab Emirates

| Facility | Ca | Mg | Na | Cl | K | $SO_4$ | Sr | Alkalinity | Hardness | Bicarbonate | pH | TDS |
|---|---|---|---|---|---|---|---|---|---|---|---|---|
| **Adam** | | | | | | | | | | | | |
| FW | 103 | 70 | 410 | 506 | 12 | 773 | 3 | 195 | 548 | 230 | 8 | 2,000 |
| Conc | 417 | 280 | 1,670 | 1,964 | 43 | 4,336 | 13 | 30 | 2,211 | 37 | 6 | 8,747 |
| C/FW | 4.05 | 4.00 | 4.07 | 3.88 | 3.72 | 5.61 | 3.95 | 0.15 | 4.03 | 0.16 | | 4.37 |
| **Haima** | | | | | | | | | | | | |
| FW | 652 | 267 | 3,340 | 1,697 | 125 | 2,037 | 16 | 62 | 2,748 | | 7 | 8,217 |
| Conc | 1,020 | 406 | 406 | 9,090 | 174 | 3,881 | 24 | | | | 3 | |
| C/FW | 1.56 | 1.52 | 0.12 | 5.36 | 1.39 | 1.91 | 1.54 | | | | | |
| **Esherja** | | | | | | | | | | | | |
| FW | 496 | 1,100 | 8,630 | 15,868 | 355 | 4,104 | 11 | 114 | 5,785 | 139 | 7 | 30,638 |
| Conc | 841 | 1,900 | 14,800 | 24,062 | 631 | 6,139 | 18 | 181 | 9,951 | 221 | 7 | 48,510 |
| C/FW | 1.70 | 1.73 | 1.71 | 1.52 | 1.78 | 1.50 | 1.63 | 1.59 | 1.72 | 1.59 | | 1.58 |
| **Sowqrah** | | | | | | | | | | | | |
| FW | 404 | 1,170 | 9,360 | 16,193 | 415 | 3,310 | 8 | 136 | 5,845 | 153 | 8 | 30,955 |
| Conc | 625 | 1,830 | 14,600 | | 668 | 4,824 | 12 | 203 | | 173 | 7 | |
| C/FW | 1.55 | 1.56 | 1.56 | | 1.61 | 1.46 | 1.52 | 1.49 | 0.00 | 1.13 | | |
| **Hitam** | | | | | | | | | | | | |
| FW | 563 | 382 | 3,400 | 7,483 | 124 | 2,366 | 13 | 125 | 2,996 | 135 | 8 | 14,451 |
| Conc | 665 | 448 | 4,250 | 8,118 | 145 | 2,466 | 15 | 142 | 3,526 | 125 | 8 | 16,142 |
| C/FW | 1.18 | 1.17 | 1.25 | 1.08 | 1.17 | 1.04 | 1.20 | 1.14 | 1.18 | 0.93 | | 1.12 |
| **Madrakh** | | | | | | | | | | | | |
| FW | 429 | 1,390 | 11,200 | 17,999 | 483 | 3,161 | 8 | 111 | 6,809 | | 8 | 34,744 |
| Conc | 611 | 1,980 | 15,300 | 24,802 | 685 | 3,846 | 1 | 102 | 9,698 | | 7 | 47,305 |
| C/FW | 1.42 | 1.42 | 1.37 | 1.38 | 1.42 | 1.22 | 0.17 | 0.92 | 1.42 | | | 1.36 |
| | | | | | | | | | | | | |

| Facility | Ca | Mg | Na | Cl | K | $SO_4$ | Sr | Alkalinity | Hardness | Bicarbonate | pH | TDS |
|---|---|---|---|---|---|---|---|---|---|---|---|---|
| | | | | | | | | | | | | |
| **Zahar** | | | | | | | | | | | | |
| FW | 179 | 95 | 746 | 1,408 | 28 | | 5 | 244 | | | 7 | |
| Conc | 612 | 315 | 1,980 | 4,367 | 95 | 1,143 | 16 | 704 | 2,846 | | 7 | 8,990 |
| C/FW | 3.42 | 3.32 | 2.65 | 3.10 | 3.36 | | 3.47 | 2.89 | | | | |
| **Assadanat** | | | | | | | | | | | | |
| FW | 367 | 174 | 1,290 | 2,160 | 12 | | 30 | 196 | | | 8 | |
| Conc | 923 | 413 | 2,780 | 4,532 | 82 | 1,552 | 28 | 380 | 4,041 | | 7 | 10,553 |
| C/FW | 2.51 | 2.37 | 2.16 | 2.10 | 7.03 | | 0.93 | 1.94 | | | | |
| **Abu-Mudhaibi** | | | | | | | | | | | | |
| FW | 294 | 137 | 1,360 | 2,151 | 29 | 515 | 8 | 200 | 1,309 | 245 | 7 | 4,651 |
| Conc | 962 | 448 | 4,630 | 7,335 | 101 | 3,296 | 27 | 168 | 4,281 | 205 | 7 | 16,960 |
| C/FW | 3.27 | 3.27 | 3.40 | 3.41 | 3.47 | 6.40 | 3.34 | 0.84 | 3.27 | 0.84 | | 3.65 |
| **Qidfa I** | | | | | | | | | | | | |
| FW | 464 | 1,640 | 11,900 | 23,149 | 574 | 2,787 | 5 | 111 | 7,922 | 136 | 8 | 40,592 |
| Conc | 617 | 2,150 | 15,100 | 30,540 | 767 | 3,931 | 7 | 96 | 10,409 | 117 | 7 | 53,177 |
| C/FW | 1.33 | 1.31 | 1.27 | 1.32 | 1.34 | 1.41 | 1.58 | 0.86 | 1.31 | 0.86 | | 1.31 |
| **Qidfa II** | | | | | | | | | | | | |
| FW | 533 | 1,620 | 12,200 | 23,484 | 581 | 3,181 | 7 | 82 | 8,015 | 100 | 7 | 41,661 |
| Conc | 730 | 2,240 | 15,800 | 32,004 | 805 | 4,500 | 7 | 102 | 11,067 | 125 | 7 | 56,158 |
| C/FW | 1.37 | 1.38 | 1.30 | 1.36 | 1.39 | 1.41 | 0.99 | 1.24 | 1.38 | 1.25 | | 1.35 |
| **Kalba** | | | | | | | | | | | | |
| FW | 446 | 245 | 536 | 2,103 | 11 | 265 | 5 | 109 | 2,130 | 133 | 7 | 3,700 |
| Conc | 1,180 | 644 | 1,170 | 5,413 | 34 | 756 | 11 | 285 | 5,615 | 347 | 8 | 9,432 |
| C/FW | 2.65 | 2.63 | 2.18 | 2.57 | 3.09 | 2.85 | 2.12 | 2.61 | 2.64 | 2.61 | | 2.55 |
| | | | | | | | | | | | | |

| Facility | Ca | Mg | Na | Cl | K | $SO_4$ | Sr | Alkalinity | Hardness | Bicarbonate | pH | TDS |
|---|---|---|---|---|---|---|---|---|---|---|---|---|
| **Umm-Al-Qwain** | | | | | | | | | | | | |
| FW | 49 | 110 | 775 | 1,182 | 19 | 562 | 5 | 226 | 581 | 275 | 8 | 2,851 |
| Conc | 202 | 510 | 3,190 | 4,108 | 85 | 2,444 | 21 | 538 | 2,630 | 656 | 8 | 10,923 |
| C/FW | 4.12 | 4.64 | 4.12 | 3.48 | 4.36 | 4.35 | 4.23 | 2.38 | 4.53 | 2.39 | | 3.83 |
| | | | | | | | | | | | | |
| **Jabal al-Dhana** | | | | | | | | | | | | |
| FW | 636 | 2,140 | 14,200 | 27,098 | 661 | 3,121 | 10 | 113 | 474 | 138 | 8 | 47,941 |
| Conc | 760 | 2,660 | 17,700 | 34,839 | 950 | 4,602 | 10 | 96 | 10,418 | 117 | 6 | 61,587 |
| C/FW | 1.19 | 1.24 | 1.25 | 1.29 | 1.44 | 1.47 | 1.04 | 0.85 | 21.98 | 0.85 | | 1.28 |
| **Hamriyah** | | | | | | | | | | | | |
| FW | 48 | 85 | 498 | 779 | 13 | 407 | 4 | 177 | 474 | | 7 | 1,949 |
| Conc | 173 | 311 | 1,930 | 2,933 | 51 | 1,537 | 14 | 617 | 1,730 | | 8 | 7,350 |
| C/FW | 3.60 | 3.66 | 3.88 | 3.77 | 3.84 | 3.78 | 3.81 | 3.49 | 3.65 | | | 3.77 |

Units are mg/L; FW=Feed Water; Conc=Concentrate; C/FW=Ratio Concentrate / Feed Water
Source: Ahmed (2000)

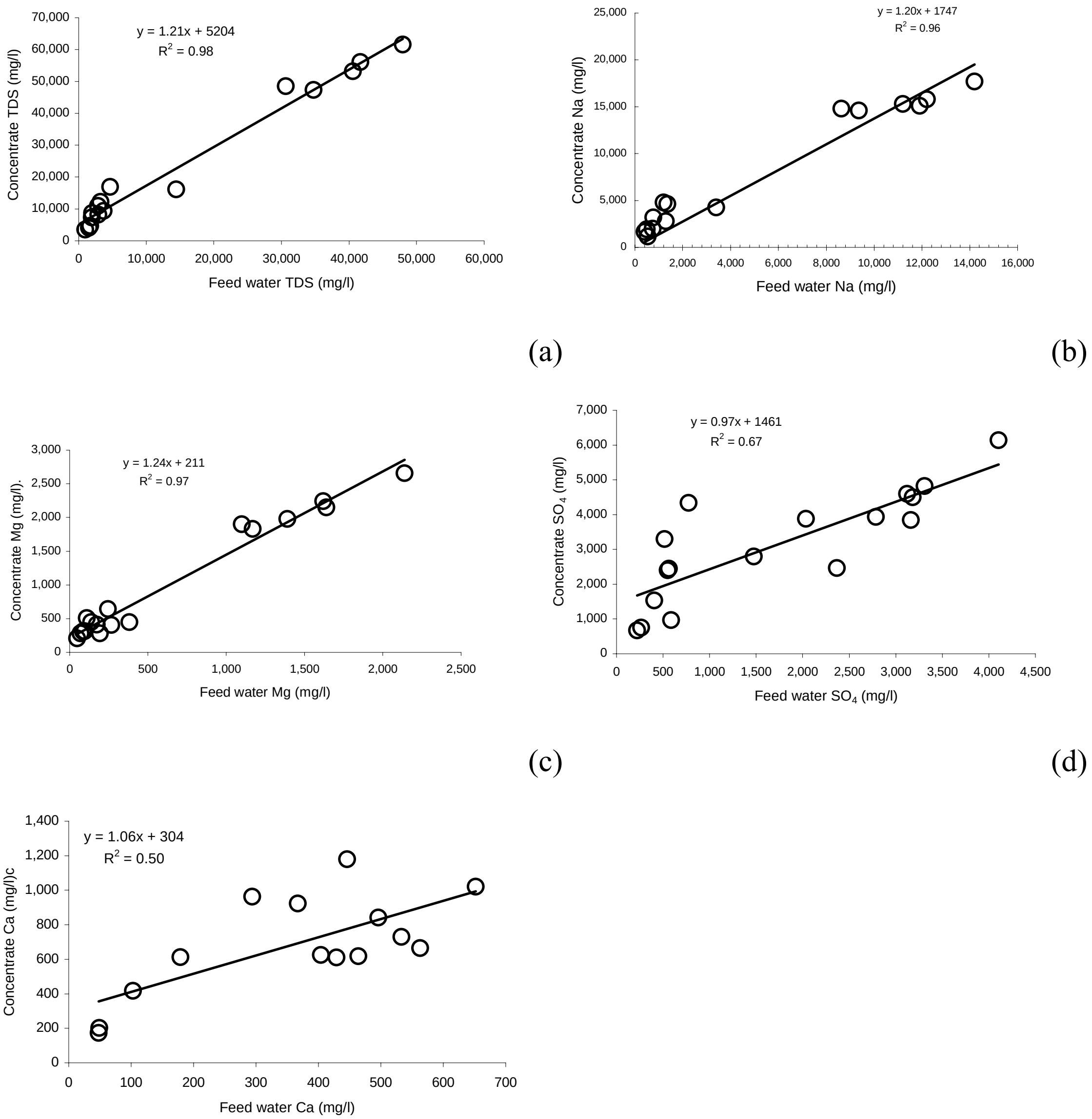

(a)

(b)

(c)

(d)

(e)

Figure 4.1. Crossplots of some of the chemical parameters for the feed water and desalination concentrates

# 5 Class I and Class II Injection Wells

Currently, deep injection wells are used to dispose of municipal wastes (e.g., Florida), hazardous wastes (e.g., Texas and Louisiana), and produced waters (oil-producing regions). Deep-well injection disposal of RO and EDR concentrates is currently done in Florida (Table 5.1). However, the analogy with Texas is limited because the concentrate is injected in the often cavernous Lower Floridan aquifer (e.g., Mickley, 2001, Chapter 9). There is no recorded instance of injection of desalination concentrate into oil-bearing formations to the authors' knowledge. Injection wells of all types share the same potential problems of formation damage when a foreign fluid is injected into a deep formation and also, possibly, of well fouling and tubing corrosion.

## *5.1 Deep-Well Waste Injection*

In 1985, in Texas, about 5.1 billion gallons of Class I waste was injected through about 100 disposal wells (Capuano et al., 1989, p.5); that is, at a rate of 100 gpm or 3,400 bbl/day per well on average. The injection rate can be seven times as high for the most efficient wells (Capuano et al., 1989, Table 1). Most operators inject in the sandy aquifers along the Gulf Coast, namely the Wilcox, Yegua, Frio, Catahoula, Oakville, and other Miocene sandstones (Capuano et al., 1989, p. 53). Injection depth ranges from 2,000 to 8,500 ft but mostly from 4,000 to 7,000 ft (Capuano et al., 1989, p. 53) against a formation pressure that is mainly hydrostatic. Any facility must have at least two wells because of unexpected downtimes or regular maintenance. It must be noted that desalination concentrates are not hazardous in most instances, unless contaminants and radioactive elements are concentrated beyond their MCL.

To ensure an optimal injection process and avoid corrosion, preliminary steps need to be taken. Injection of fines, compatibility issues, and corrosion concerns need to be addressed. Surface filtration and injectate conditioning are paramount to keeping the injection well in good condition. Pretreatment processes include all or some of the following: addition of anticorrosion additives to limit corrosion, filtering of suspended solids (to 1 µm and sometimes to 0.2 µm), pH adjustment to assure compatibility with formation fluids, and, possibly, flocculation additives to limit clay migration and swelling. Pretreatment could also include degasification of the injectate (by addition of chemical scavengers, vacuum deaeration, or counterflow gas stripping). The target gas is $O_2$ because lowering pH will make the water more aggressive; hence the necessity to deoxygenate the water before injection. Other gases that need to be stripped from the injection stream are $CO_2$ and $H_2S$. Records show that in Texas typical pretreatment of Class I waste before injection consists of addition of scale inhibitor and/or of pH adjustment by addition of acid or base (Capuano et al., 1989, p. 4). Those preinjection treatment steps are very similar to those taken before undergoing membrane desalination, suggesting that any pretreatment of the concentrate before injection may not be warranted.

As in the pretreatment of desalination feed water, economic benefits of addition of chemicals must be seriously weighted. For example, counter-flow gas stripping columns are more expensive than sodium bisulfite addition (~10 mg for each ppm of $O_2$). However, bisulfite reacts with oxygen to produce sulfate, which might be detrimental to injection if barium is present in the formation waters because of the very low solubility of barium sulfate.

## *5.2 Operational Characteristics of Oil and Gas Reservoirs*

Early after the initial production of an oil reservoir, water is injected for pressure maintenance if the reservoir does not have a natural water drive (note that gas reservoirs are usually not waterflooded). A natural water drive occurs when the hydrocarbon volume removed by the oil production is occupied by water moving in, keeping the reservoir under pressure and the production going with minimal assistance. Other common types of production drive are solution gas drive and gas cap drive. The former happens when light hydrocarbons in solution in the oil outgas to maintain pressure while the latter occurs when a free gas cap is present on top of the oil. Waterfloods often occur later in the life of a field. For example, most of the West Texas fields were under solution gas drive (Galloway et al., 1983, Plate 5) and have been good candidates for waterfloods. The Permian Basin area is still being heavily waterflooded.

Most fields were under natural water drive in East Texas. Consequently, waterflooding has not been as widespread. However, East Texas fields have extensive reinjection programs where the produced waters are disposed of typically in the same formation but farther downdip. The southern Gulf Coast Frio fields have seen little waterflooding, although saltwater disposal wells are frequent. Solution gas and gas cap expansion drives are common in this basin. Relevant knowledge about water injection can be gained by looking at the injection history of the fields.

Depressurization resulting from hydrocarbon production is common in long-producing formations such as the San Andres in the Permian Basin, the Woodbine in the East Texas Basin, and the Frio in the Gulf Coast Basin. Natural recovery of original pressure can be a long process. Senger et al. (1987) estimated that it would take 10,000 years for a hypothetical field in the Palo Duro Basin in the Texas Panhandle to return to 90 percent of the original pressure. The recovery rate is dependant upon permeability and storativity, but the order of magnitude of the recovery time interval suggests that the fields will stay underpressured for a long time.

The RRC delivers injection permits through H1 forms and tracks the injection history. Recent completed H1 forms are available on the RRC website while forms filled before 2000 can be consulted at the RRC in Austin, TX. The latest compilation of injection operations in Texas dates back from 1982 (RRC, 1982). Form H1 provides information into the type of fluid to be injected (saltwater, brackish, fresh water, air, gas, $CO_2$, polymer, etc.) and the purpose of the injection (disposal, secondary recovery), as well as well and formation characteristics such as depth, perforated interval, porosity, and permeability. Volume of water needed is in general 150 to 170 percent of the targeted pore volume (Thomas et al., 1987, p. 44-41). The largest demand for external water is at the beginning of the waterflood before breakthrough at the producing wells. Return water will progressively be reinjected unless precluded by the treatment cost of the produced water. It is common in the industry to convert a production well into an injection well as the waterflood front passes by. The external water source could be surface waters (rivers and lake), fresh-water aquifer, brackish water aquifer, and produced water possibly from the same formation. Typically, when water of different sources must be mixed, the mixing is done at the surface rather than downhole. The injection system can be closed or open to the atmosphere. The former limits pretreatment and, for example, allows ferrous iron to stay in solution. Ferric iron is insoluble except at low pH, and exposing a solution with ferrous iron to oxygen would mean certain iron oxide precipitation somewhere in the system. On the other hand, water with a content too high in corrosive dissolved gases, such as $H_2S$ or $CO_2$, may have to be thoroughly treated before injection. However, $O_2$ itself introduced by opening the system to the atmosphere may have a deleterious effect, and it is costly to remove from water.

From a review of the H1 forms, we observe that most of the fields have significant potential to accept considerable volumes of water. Forms H1/H1A are required when proposed injection will take place within 2 miles of a past or current productive reservoir (RRC Rule 46). Attached to the application, the operators need to provide Area of Review (AOR) data. Injection of fresh water as makeup fluid is now restricted to cases where there is no technically or economically viable alternative. In such a case, Form H7 must be provided. Selected H1 and H1A forms were analyzed. We extracted the relevant parameters (e.g., pressure as a function of depth, well geometry parameters, and distribution of porosity and permeability). We noted that currently the oil industry is using various sources of water that include saltwater (produced water), brackish water, fresh water from lakes, commercially available fresh water, and gas plant waste water for waterflooding the reservoirs. In essence, convenience, economics, and availability of water determine the type of water being used in waterflooding operations. Estimated maximum daily rate of injection per well in the analysis areas could considerably vary and ranges from less than 100 bbl/d to more than 5,000 bbl/d (3 gpm to more than 150 gpm). A rule of thumb generally applied in the industry is to limit injection pressure at the sandface to 1 to 1.5 psi/ft of depth. Higher pressure tends to open fractures possibly detrimental to production and safety.

## 5.3 Area of Review Principles

The UIC regulations of the U.S. EPA require an Area of Review (AOR) for newly drilled or converted Class II saltwater injection well. The permitting process requires operators to file an AOR study with the RRC. Applicants are required to submit a map showing all wells within a 0.25-mile radius of a proposed well as well, as the well characteristics for those wells penetrating the formation of interest (drilling date, well status, among other parameters). The purpose of an AOR study is to identify unplugged wells that may allow injected fluids to migrate upward and endanger the overlying underground sources of drinking water. RRC states that a variance of AOR request can be granted by demonstrating either that reservoir pressure is insufficient to raise fluids to groundwater or that geological conditions preclude upward movement of fluids or if any other compelling evidence is available.

If wells of unknown conditions are encountered, corrective action may be necessary to meet UIC requirements. Performing this study can be a hindrance to small operators because of the administrative search and field work it entails. However, it is permissible to ask for a variance to the AOR permitting process on the following bases (Warner et al., 1997):

- Variance based on absence of aquifer with water of good quality (<10,000 mg/L or <3,000 mg/L). The UIC program defines an Underground Source of Drinking Water (USDW) as an aquifer that contains less than 10,000mg/L of total dissolved solids.
- Variance based on negative flow potential between injection-zone fluid levels and base of drinking water. If the injection zone pressure head is sufficiently below the stratigraphic base of usable quality drinking water (BUQW), there is little potential for the injection fluids to migrate upward and contaminate the drinking water, even if some unplugged wells were left unnoticed. A separation of 500 ft between the injection zone fluid level and BUQW is recognized as acceptable (Smyth et al., 1998) (Figure 5.1).
- Variance based on lack of intersection. No adjacent well is drilled to the depth of the injection zone.
- Variance based on mitigating geological factors. There could be the presence of a thief zone that would divert most upward flowing fluid or of an incompetent formation that tends to cave into the wellbore. Warner et al. (1997) suggested that 100 ft of continuous shale/mudstone or 250 ft of cumulative thickness may be enough to justify a variance.
- Variance based on well construction and abandonment methods, for example, for an oil or gas field developed after adequate regulations were promulgated (i.e., after 1982 according to Warner et al. (1996)).
- Variance based on other compelling evidence.

A previous statewide BEG study (Smyth et al., 1998) co-funded by the U.S. DOE and the Texas RRC provided a field-level basis for operators to request a variance from the AOR permitting requirement. The RRC has adopted a procedure in its review of injection permits to consider an AOR variance if fluid levels reported on H15 forms as measured in shut-in wells can be shown to be well beneath the level of the BUQW. Warner et al. (1996) did a study of selected fields in the Permian Basin while Warner et al. (1997) did a study of the Frio Formation in South Texas. Smyth et al. (1998) investigated 113 fields in 36 counties across Texas. Warner et al. (1996) used the second-to-last-described variance of AOR approach. Warner et al. (1997) studied the shale/mudstone abundance in the interval between injection formation and BUQW, while Smyth et al. (1998) quantified the separation between formation head and BUQW (second approach). The interest of focusing on depleted oil and gas fields is that the separation between formation head and BUQW has been potentially increased by removing hydrocarbons.

Warner et al. (1996) concluded that most wells abandoned after 1967, and even more so for those abandoned after 1982, were protective of usable quality water. They concluded that the 78 Permian Basin injection fields analyzed could qualify for a variance of AOR. Warner et al. (1997) also reported that sloughing shales are common along the Gulf Coast and that an open well bore will be quickly sealed. They concluded that most Texas Gulf Coast Frio Formation well fields can be considered for variance of AOR on the basis of either well completion or presence of shales. Smyth et al. (1998) concluded that 42 fields out of 113 could be recommended for variance of AOR.

In this study, we followed the methodology presented in Smyth et al. (1998). Oil wells no longer economically producing are commonly shut-in or temporarily abandoned. In Texas, shut-in wells that are at least 25 years old are required to submit an H15 Form to the RRC to prove the wells are not leaking (RRC Rule 14 (b) (2) (E)). To comply with instructions outlined on the Form H15, operators have the choice of either performing a mechanical integrity test every 5 years or measuring water level annually. In this study we used yearly data levels recorded during a period going from 1995 to 2003 as a surrogate for formation pressure. We used records of data compiled from RRC Form H15, which are maintained in an RRC database, to show that a significant fraction of the fields considered in this study qualify for a variance of AOR because of sufficient separation. It should be noted that the purpose of Form H15 is not to feed the variance of the AOR process. For example, operators could choose to install bridge plugs and load the casing with a fluid, whose level is monitored to detect a leak. In this case, the fluid level reported on Form H15 is not representative of the formation pressure. However, overall, Form H15 pressures are statistically accurate for the purpose of this study. The RRC database also includes depth to BUQW as provided by TCEQ. The BUQW is typically chosen on the basis of the 3,000 mg/L cutoff value but can include aquifers with higher TDS if they have been used historically. In this study, we did not try to validate the values provided by TCEQ. The database was queried to include only those counties and formations of interest. In the areas of interest, there are more than 1,300 data points for shut-in wells with both BUQW and top-of-fluid readings.

In order to analyze the separation between formation head and BUQW on an oil or gas field basis we rearranged data provided by the RRC. In addition to choosing county and formation, the data points from the H15 database were selected in such a way that both BUQW and Top of Fluids (TOF) were available. Because of their variability, it was not feasible to define a potentiometric surface for either parameter in either field. For each of the six analysis areas, the separation $Sep_w$ (Figure 5.1) was calculated and plotted as a histogram for individual wells:

$$Sep_w = TOF_w - BUQW_w \qquad \text{Equation 5-1}$$

Then the separation $Sep_f$ was computed on a field basis:

$$Sep_f = TOF_f - BUQW_f \qquad \text{Equation 5-2}$$

where $Sep_f$ is, for a given field, the separation between the 95th percentile TOF and 5th percentile BUQW of all TOF and BUQW recorded for that field. To avoid giving outliers an undeserved weight, we did not assume that the separation distribution follows a normal distribution, which it does not, but, instead, use the 95th and 5th percentile in lieu of the usual 2 standard deviations. Results of the variance of AOR study are presented in Section 7.1.

## *5.4 Pressure Studies and Deep-Well Injection*

### 5.4.1 Formation Pressures

Formation pressure is critical to our understanding of the economic disposal potential of a reservoir. Distribution of oil and gas is related to regional and local subsurface pressure and temperature environments. Knowledge of the expected pore pressure gradients helps (1) efficient drilling of wells, with correct mud densities; (2) proper engineering of casing programs, and (3) proper well completion without causing excessive formation damage. Normal or hydrostatic pressures have gradients in the range of 9.8 to 11 kPa/m (~0.433 psi/ft), depending on the water density. The hydrostatic pressure is the pressure executed by the weight of a column of fluid. Hydrostatic pressure varies with the density of the fluid and the height of the column. Normally pressured formations are considered "open systems" permitting hydraulic communication of interstitial fluids with the surface. Within a lithified formation there will be a number of pressures that individually tend to either lend support to, or attempt to further compact the formation. The main pressure types include the pore pressure, the rock grain pressure (matrix stress), the total overburden pressure which is supported by the pore and rock grain pressures.

When the gradients are outside the stated range, the reservoir is exhibiting abnormal pressures. Abnormally pressured formations are usually "closed systems", which have been geologically pressured. In such cases, a permeability barrier acts as a pressure seal. In a geopressured sequence of shales and sands, the shales composed primarily of platy clay minerals fill the role of the permeability barrier. Overpressures are developed and maintained by restriction of pore fluid movement in the reservoirs. In such a sequence, the ratio of shale to sand must be fairly high in order to increase the possibility of a sand unit being completely isolated and encapsulated by the surrounding shales. The creation of an overpressured formation is related to many physical, geochemical, and mechanical processes. For example, several kinds of stress changes can lead to abnormal pore fluid pressures: (1) rapid geologic loading or unloading creating compaction disequilibrium, (2) thermal expansion of fluids, (3) regional compressive or tensile tectonic stresses, and (4) generation of oil and gas from organic matter. However, this is a transient phenomenon at the geological scale and typically occurs at depth larger than those considered in this study. Some deep formations (~>10,000ft) of the Texas Gulf Coast are geopressured. Underpressured reservoirs are common in rocks that have been subjected to recent uplift and erosion. Most commonly, underpressure is subsequently developed when a reservoir is depleted of all its fluids. It may also result from surface exposure of the permeable bed at a depth greater than where it is penetrated by the bit.

The hydrostatic pressure $p_f$ at depth $D$ assuming water continuity from the surface is given by:

$$p_f = \int_0^D \rho_w(x) g dx \approx \rho_{w,aver} gD \qquad \text{Equation 5-3}$$

where $\rho_w$ is the water density varying with depth. Water density is given as function of the TDS by (Kharaka et al., 1988):

$$\rho_w = 1 + 0.000688 \text{x} TDS \text{ with } TDS \text{ in g/L} \qquad \text{Equation 5-4}$$

Seawater with a salinity of ~35 g/L would have a density of 1.024 kg/L at $20^0$C according to this formulation.

### 5.4.2 Deep-Well Injection Technology

The technology for deep-well injection is similar for both Class I and Class II wells. Injection wells are typically completed according to one of three following modes: open hole in competent formations, fully screened in incompetent sand and gravel formations, and fully cased and cemented with the casing perforated, valid for both competent and incompetent formations.

A statistical analysis of the Form H1 data set (heavily biased toward Permian Basin wells) shows that half of the currently operating Class II injection wells in the analysis areas are cased and perforated, with the remainder being open-hole well. Less than 10 percent of the injection systems are open. Most of them are closed to the atmosphere. More than half of the wells have a hole size of 7 7/8 inches and 85 percent of them are between 7.5 and 9.5 inches in diameter. The tubing size is in most cases between 2 3/8 and 2 7/8 inches (97 percent of wells in the data set). An analysis of the reported maximum injection pressure gradient (injection pressure/tubing depth) showed that all (except some outliers probably representing bad data) are less than or close to hydrostatic. The maximum injection pressure is a function of the tubing diameter: the smaller the diameter, the higher the head loss.

### 5.4.3 Injection Pressure and Flow Rates

Movement of the injectate into the formation requires a pressure high enough to overcome the resistance of the resident water. The response of an aquifer to the injection pressure is given, in a consistent system of units, by (Warner and Lehr, 1977, p. 104):

$$\Delta h = \frac{\Delta P}{\rho g} = \frac{Q}{4\pi T}\ln\left(\frac{2.25Tt}{r^2 S}\right) \qquad \text{Equation 5-5}$$

where $h$ is the head, $P$ is the pressure, $Q$ is the flow rate, $T$ is the transmissivity ($T=Kb$, where $K$ is the conductivity and $b$ is the aquifer thickness), $t$ is the time since injection began, $r$ is the radial distance from well to point of interest, and $S$ is the storativity or storage coefficient. The parameter $S$ is related to both the compressibility of water and of the rock by (Warner and Lehr, 1977, p. 41):

$$S = S_c b = \rho g(\phi\beta + \alpha)b \qquad \text{Equation 5-6}$$

where $S_c$ is the specific storage, $\beta$ is the compressibility of water, $\alpha$ is the compressibility of the rock skeleton, and $\phi$ is the rock porosity. Equation 5-5 is derived with the Theis assumptions (e.g., Domenico and Schwartz, 1990). In terms of pressure and using the relationship between conductivity $K$ and permeability $k$ ($K=k/\rho g\mu$ where $\mu$ is the water viscosity), Equation 5-5 becomes:

$$\Delta P = \frac{Q\mu}{4\pi k\mathrm{b}}\ln\left(\frac{2.25kt}{\phi c\mu r^2}\right) \qquad \text{Equation 5-7}$$

where $c$ is the compressibility of the aquifer. The parameter $c$ is typically unknown but its lower limit is the compressibility of water (~$3\text{x}10^{-6}$ $\text{psi}^{-1}$). That same equation is also written in customary oil-field units as:

$$\Delta P = \frac{162.6Q\mu}{k\mathrm{b}}\left[\log\left(\frac{kt}{\phi c\mu r^2}\right) - 3.23\right] \qquad \text{Equation 5-8}$$

where $Q$ is in bbl/day, $\mu$ in centipoises, $k$ in millidarcys, $t$ in hours, $c$ in $\text{psi}^{-1}$, and $r$ in feet. The equations is applied for the tubing radius $r=r_w$. Results are not very sensitive to this parameter because its range of value is small and it appears in a log term. The expressions do not take into account the skin factor, a parameter that measures variations from the theoretical formulation. Skin factors can vary from about -5 when there is less pressure drop than expected (e.g., when completion interval crosses a fracture or after a stimulation work) to more than 10 when the well or formation is damaged. Another parameter not explicitly taken into account is relative permeability. Those reservoirs used to contain oil. Even after a waterflood or tertiary recovery processes, there is still some residual saturation of oil and also, very likely, some flowing oil. We assumed that the opposite effects of a negative skin factor (leading to a pressure drop smaller than expected) and of a relative permeability smaller than 1 (generating a pressure drop higher than that when only water is present) cancel each other out on first approximation.

RRC requires that the injection pressure not exceed the formation fracture gradient. Generally, the maximum surface injection pressure is 1/2 psi/ft to the top of the injection interval unless the results of a fracture pressure step-rate support a higher pressure. The sandface pressure is the surface pressure added to the pressure due to the weight of the injected fluid minus head losses through the tubing. Because maximum $\Delta P$, pressure difference at the well sandface and in the formation, is imposed, the maximum flow rate $Q$ can be computed when the other parameters are known.

$$Q = \frac{4\pi k \mathrm{b} \Delta P}{\mu}\left[\ln\left(\frac{2.25kt}{\phi c \mu r^2}\right)\right]^{-1} \qquad \text{Equation 5-9}$$

with $\Delta P \approx 0.5D + 0.4D - P_f$ , where $D$ is the depth (ft) to the injection level and $P_f$ is the formation pressure (psi). A statistical distribution of permeability and porosity will be described later, as well as that of the pay thickness *b*. Another approach can be used that assumes a steady-state and not transient system. The equation in customary oil units is (Thomas et al., 1987):

$$Q = \frac{0.00708 k \mathrm{b} \Delta \mathrm{P}}{\mu}\left[\ln\left(\frac{5.61Qt}{\pi \phi b S_w r_w}\right)\right]^{-1/2} \qquad \text{Equation 5-10}$$

where $S_w$ is the water saturation (assumed at 0.7). Because $Q$ (in bbl/day) appears on both sides of the equation, an iterative solution is needed. The steady-state approach yields a flow rate 1.5 to 2 times higher than that of the transient approach. Given the approximations done during the computation and the use of average values possibly not representative of a given injection site, the flow rate obtained by this method cannot be known by less than a factor of 2.

## 5.5 Formation Damage

### 5.5.1 Definition

Formation damage can be defined as any process that leads to a reduction in production or injection rate. Formation damage can be generated by scaling, migration of fines or precipitated material, clay swelling, emulsion block, water flock, or other mechanisms. In the case of injection, one can define injectivity *I* as follows:

$$I = \frac{Q}{P_{wf} - P_r} \qquad \text{Equation 5-11}$$

where Q is the flow rate, and $P_{wf}$ and $P_r$ are the flowing and formation pressures, respectively. Injectivity decline can lead to economic problems. One of the most important processes leading to injectivity decline is the filtration of suspended solids. Formation damage can also be due to chemical processes, e.g., plugging of pores by minerals or precipitates, or to physical processes, in particular fine behavior. Fines are broadly defined as particles that can be put in motion by a flowing fluid. Suspended solids are a major factor in reduction in injectivity. They can originate from solids put in suspension but also from nuclei of precipitating minerals. As such, they can appear in a solution even after a filtration process designed to remove them. Formation damage is modeled by adding a “skin factor” to theoretical or ideal conditions. However, skin factor is truly a fudge factor that includes a lot of different processes, including formation damage, but also damage to the well. As discussed in the previous section, a positive skin indicates some damage while a negative skin indicates an enhancement in production typically due to well stimulation (e.g., fracturing, acidization).

There are several numerical codes able to help in predicting well behavior to injection of various fluids. UTWID (Pang and Sharma, 1994; Saripalli et al., 2000), developed by the Department of Petroleum and Geosystems Engineering at The University of Texas at Austin is one of them. The code requires facility-specific information about suspended solid concentration and size distribution. We were unable to collect the necessary information needed to use the software in a meaningful way.

### 5.5.2 Scaling

Scaling occurs either when a change in environmental conditions (temperature, pressure, pH, gas partial pressure) occurs or during mixing of incompatible solutions. Cations that frequently occur in formation waters and that can cause problems are calcium (Ca), strontium (Sr), barium (Ba), and iron (Fe). The most common scales are calcium carbonates (mainly calcite), and calcium sulfates (gypsum $CaSO_4.2H_2O$ and anhydrite $CaSO_4$) (Table 5.2). A particularly bothersome compound is barium sulfate ($BaSO_4$) because it is very insoluble. Strontium sulfate ($SrSO_4$) is also insoluble but to a lesser degree. Ba and Sr can also coprecipitate with Ca to form a mainly calcic solid solution carbonate. Silica, calcium fluoride, and phosphates could also hinder operations. In distilled water at 25°C, gypsum has a solubility of 2,080 mg/L, calcite 53 mg/L, $BaSO_4$ 2.3 mg/L, $SrSO_4$ 114 mg/L, and amorphous silica 110 mg/L (Heitman et al., 1990, Chapter 6). In distilled water at equilibrium with atmospheric gases and at 25°C, calcite solubility climbs to more than 100 mg/L, others are unaffected. Iron compounds (ferrous carbonate, ferrous sulfide, ferrous hydroxide, ferric hydroxide, and ferric oxide) (Patton, 1986; Cowan and Weintritt, 1976) can also cause problems even if they exist naturally at very low concentration in natural waters (<100µg/L) because corrosion of pipes and other devices can increase their concentration to much higher levels. The degree to which a chemical compound is close to saturation is given by the saturation index *SI*. *SI* is defined as the logarithm of the ratio of the ion activity product (*IAP*) to the solubility product ($K_{sp}$):

$$SI = \mathrm{Log}_{10}\left(\frac{IAP}{K_{SP}}\right)$$

A negative *SI* indicates that a mineral will not precipitate, but a positive index does not necessarily mean that a mineral will precipitate. The kinetics of the precipitation might be too slow for the considered time frame. Precipitation kinetics is influenced by a variety of factors (presence of particulates, total area and chemical and physical state of solid surfaces, chemistry of the solution, and environmental factors such as temperature and pressure). *SI* can become positive because of mixing of different solutions but also because of pressure or temperature changes. Scaling tendency may be different depending on the technology used. Lozier et al. (1992) reported that during pilot studies,

$CaSO_4$ scales were produced on the RO membranes, while $CaCO_3$ scales were produced on the EDR membranes.

*SI* value is not unique for a given mineral; it is a function of many parameters including, temperature, pressure, solution ionic strength, and pH. There are general rules such as solubility increasing with temperature. However, they are not valid for the most common scales; calcium sulfate and calcium carbonate are characterized by a reverse solubility. Their solubility decreases with temperature. Solubility also generally increases with pressure and is a more complex function of ionic strength or salinity. For example, gypsum is more soluble at high salinity but only at low pressure; the statement is not true at higher pressure. The solubility increase with pressure is a favorable parameter for injection. Ionic strength, a parameter related to salinity, has also, in general, a positive impact of solubility. However, noncharged species, such as silica, may be unaffected or negatively affected by an increase in salinity. Before the advent of computers and numerical geochemical models, many empirical relationships had been developed to estimate precipitation tendency from limited information. Those relationships cannot account for all the factors as well as geochemical models do (see Section 7.2), except in the simplest systems. An example of such an empirical index is the Langelier Saturation Index (*LSI*), widely used in the water treatment field. The Stiff and Davis index is another example that applies to oil-field brines. The Langelier index also helps in characterizing the corrosive character of a given water. As a general rule, scaling occurs more often in producing wells than in injection wells. Pressure increases with depth have a beneficial effect on solubility of most compounds. Temperature also increases with depth, but the effect is not as useful in typical cases because most carbonates have a retrograde solubility.

Calcium carbonate solubility is a strong function of $CO_2$ partial pressure. Its main mineralogical form is calcite. Calcium carbonate is very susceptible to precipitation during a pressure drop (which leads to a concomitant release of $CO_2$), whether it happens in an enclosed space for hydrodynamics reasons (such as at a valve or at a well screen) or in the open atmosphere. During an injection operation, the reverse might be true because solubility increases with $CO_2$ partial pressure and also because of the simple thermodynamic rule of solubility increasing with pressure increase (Patton, 1986). However, temperature increase has a negative impact on calcium carbonate solubility.

Most calcium sulfate scales are made of gypsum. Anhydrite or hemihydrate ($CaSO_4$:0.5$H_2O$) could form at higher temperatures, but they typically result from gypsum dehydration. Gypsum solubility increases slightly with temperature up to ~40°C then decreases (Patton, 1986). Both an increase in salinity, up to a value not reached in this study, and in pressure favor an increase in solubility of gypsum. Barium sulfate presents a "regular" behavior relative to solubility. The solubility increases with temperature, pressure, and salinity. However, barium sulfate solubility at surface temperature and pressure is low. If there is no scaling tendency of the concentrate at the surface, deep well injection should not present a problem until possibly the injectate meets the formation water.

Silica ($SiO_2$) exists under many mineralogical forms. A common crystallized form, quartz, has a solubility of ~10 mg/L, but amorphous silica solubility is more than 100 mg/L. Silica exists in water as a neutral $SiO_2$ ion or in colloidal form. Silica solubility increases with temperature, pressure, and dramatically with pH (from 110 mg/L at pH 5 to 300 mg/L at pH 9 in fresh water at 25°C). However, in contrast to other minerals resulting from the association of charged ions, an increase in salinity decreases silica solubility that decreases from 110 mg/L in fresh water to 85 mg/L in seawater.

Iron is another common element in water, albeit in low concentration. A high iron concentration generally suggests corrosion. In contrast to the other elements described so far, iron can commonly exist in two valence states, ferrous ($Fe^{2+}$) and ferric ($Fe^{3+}$). Iron oxides -goethite (FeOOH), hematite ($Fe_2O_3$), or their hydrated form -and iron sulfides -pyrite ($FeS_2$)- are common iron scales. Iron sulfides can appear in reducing environments when the formation contains large amount of $H_2S$ or when sulfate-reducing bacteria are present. Iron carbonate –siderite ($FeCO_3$)- has a limited solubility of ~70mg/L at 25°C and can be locally a problem on sites with a high concentrations of $CO_2$. In more typical cases, $Fe^{2+}$ would usually precipitate within the calcite structure.

Magnesium and strontium usually precipitate with calcium. Magnesium can also precipitate as hydroxide -brucite ($Mg(OH)_2$)- but it happens at a higher temperature than those considered in this study.

Physical form of the mineral precipitates varies. Precipitates of some minerals are colloids (iron oxides, silica) and can fast plug pores with flowing water. Others (calcite, gypsum, barite) are crystalline and feed already existing crystals. They may take a longer time to plug pores since the growth is spread over a larger surface area.

### 5.5.3 Fines

Fine particulates, called fines, could generate problems in injection and production wells. Three different origins for fines have been suggested. They could originate within the formation and be mobilized by physical or chemical processes. They could be injected with the water stream (suspended solids), and, finally, they could appear within the formation as free-floating particles resulting from material precipitated in the bulk water. The second and third categories can be dealt with using appropriate operational management. The first category, formation fines, is more problematic, although operational solutions to reduce their impact also exist. Numerous experiments and field studies have shown that a significant reduction in permeability can occur when a fluid of a nature different from that of the formation is injected. It is because formation fines are typically attached to walls of larger grains. A change in chemical environment can modify the binding between the fines and the larger grains or deflocculate them and have them move and then become immobilized in pore throats. Another way to plug pores is for fines of clayey nature to swell and obstruct pores on place. However, formation fines are not all of a clayey nature; their mineralogical nature is variable. Muecke (1978) presented results of X-ray analysis of formation fines in the Miocene section of five Gulf Coast wells. Clay minerals (montmorillonite, illite, and chlorite/kaolinite, in decreasing order of importance) represent ~12 percent weight on average. The most abundant mineralogical form of formation fine is quartz (~40 percent), followed by amorphous materials (~32 percent), and other minerals (~16 percent), such as feldspar, muscovite, sodium chloride, calcite, dolomite, and barite. Thomas and Crowe (1978) reported on two Texas Gulf Coast formations in Bee (Wilcox Fm.) and Milam ("Green Sand") Counties as having 9-29 and 11.2-15 percent clay range, respectively with 1.4-6 and 7.2-11.9 percent montmorillonite respectively. Sharma and Yortsos (1986) stated that fines can be detrital or diagenetic. Diagenetic clays are often present at the solid-fluid interface and are much more of a problem than the detrital clay often removed from the flowing fluid. It is thus important to determine, not only the overall composition of the formation, but also the spatial location of the mineral grains.

If nonclayey fines of diverse origin act mainly in a mechanical fashion by bridging pore throats when put in motion, clay movement in the formation results from more complex causes because it also involves chemical interactions between the clay mineral and the bulk water. Clay minerals, especially montmorillonites/smectites have the ability to exchange ions with the surrounding water. In a pristine formation at thermodynamic equilibrium, most clay particles are attached to larger particles and are bound together in clumps or sheets. They may also hold other particles in a loose network. A change in environmental conditions will throw clay minerals toward a new equilibrium, which may include deflocculation, also called dispersion, of the clay masses. A change in environmental conditions can also bring swelling of the clay sheets and subsequent closing of pore throats. This latter effect is, however, now recognized as secondary in most instances (Sharma and Yortsos, 1986; Scheuerman and Bergersen, 1990).

Minerals of the clay family can be categorized into five main groups (Table 5.3): smectites, vermiculites, chlorites, illites, and kaolinites (e.g., Brady, 1990). They all share a sheetlike crystallographic structure. An elementary layer of a clay mineral is made of either silicon tetrahedrons or aluminum octahedrons with oxygen atoms at the angles. Because of electrical imbalances, cations ($Ca^{2+}$, $Mg^{2+}$, $Na^{+}$, $K^{+}$, $H^{+}$) are attached to the silicon (Si) or aluminum (Al) elementary layers. Substitution of Si or Al by Mg or other cations is possible. The way Si-Al layers are organized, what substitutions are made and what cations charge-balance the elementary layers determine the clay group. The elementary pattern (called 1:1) of kaolinites is a stack of single Si and Al layers; there is no associated cation. Neither water nor cations can penetrate the interlayer space. In illite clays, two elementary Si layers sandwiches an elementary Al layer (pattern 2:1), some Al is substituted for Si, and K ions glue the multiple Si-Al-Si sheets together. Smectites also have a 2:1 pattern but with some substitution of $Mg^{++}$ for $Al^{3+}$. The stacked sheets are held together by weakly adsorbed $Ca^{2+}$, $Mg^{2+}$ or Na+ cations. The particularity of smectites (whose group includes montmorillonites as the most common member) is their ability to absorb water between the sheets, the molecular origin of the so-called swelling.

Vermiculites have a crystallographic structure similar to that of smectites, but it does not allow as much swelling. Chlorites have an extra sheet of Mg octahedrons (pattern 2:1:1) that, in essence locked the structure. Chlorites cannot undergo layer expansion. Mixed-layer clay minerals are materials in which different kinds of clay layers alternate with each other. The mixing in vertical stacking can be regular or random. Commonly described mixed-layer clays include illite-vermiculite, illite-smectite, chlorite-vermiculite, chlorite-smectite, and kaolinite-smectite. If not all clays can undergo swelling, all can be subject to deflocculation and put in motion. When solution salinity decreases, the exchange cations have a tendency to diffuse into the bulk solution. Below some salinity threshold, diffuse forces overcome attractive Van derWaals forces, and clay particles disperse (Scheuerman and Bergersen, 1990). At a given molar concentration, potassium cations are more effective than sodium cations at holding the clay particles together, and calcium cations even more so ($Ca^{2+}$>>$K^{+}$>$Na^{+}$).

Kaolinite is formed by the degradation of feldspars, especially K-feldspars, particularly at low pHs. Illite also results from the degradation of K-feldspar and other K-rich alumino-silicates, but at higher pHs. Glauconite, an iron-rich clay sometimes abundant in marine formations, can be considered part of the illite family. Smectites commonly result from the alteration of silicates rich in Ca and Mg. The geological occurrence of smectites is noteworthy. They are mainly connected to volcanic material (actually found in abundance in the Mesozoic and Cenozoic stratigraphic sections in Texas). They are converted to illite with depth. A limit of 10,000-15,000 ft for complete conversion is often cited. They rarely exist in rocks older than late Mississippian (Dunoyer de Segonzac, 1970). Thin section studies can help in understanding the spatial distribution of clays and, in particular, those in direct contact with flowing fluids.

Smectite and vermiculite clays can exchange those adsorbed cations with their environment, typically, $H^{+}$, $Na^{+}$, $K^{+}$, $Ca^{2+}$, and $Mg^{2+}$. Their ability to do so or *reactivity* is measured by the cation exchange capacity (CEC). Smectites have a CEC one order of magnitude higher than that of illites (~1 and 0.1-0.2 moles/kg, respectively), themselves about up to one order of magnitude higher than that of kaolinites (0.01-0.1 moles/kg). CEC is thus a measure of the possible disruption generated by the injected fluids. There are several general rules to determine the cation likely to be accepted in the interlayers:

the highest charge density wins but only if not overwhelmed by a higher concentration of an ion with a smaller charge density. For example, $Na^+$ will be the most frequent cation in the interlayers if the smectite is in equilibrium with a NaCl solution with minor $CaCl_2$. The percentage of exchange sites occupied by divalent ions increases with decreasing salinity. In general, Na concentration, both in relative and absolute terms, increases with depth (Figure 5.2). The exchange reaction can be written:

$$2\text{Na-Clay} + Ca^{++} = \text{Ca-Clay} + 2Na^+ \qquad \text{Equation 5-12}$$

The equilibrium reaction constant can be written as:

$$K=(Na^+)^2(\text{Ca-Clay})/(Ca^{++})(\text{Na-Clay})^2 \qquad \text{Equation 5-13}$$

where ( ) represents the activity of the reactants. Hence, given the importance of the $(Na^+)^2/(Ca^{++})$ ratio, it is called the mass action ratio (MAR).

In general, high salinity, high charge density, low pH (specific case of high charge density) favor clay flocculation, while low salinity, low charge density, including high pH, favors deflocculation. Because divalent cations are much more effective at keeping clays flocculated, increasing $Ca^{++}$ sharply reduces flocculation salinity (also called the critical salt concentration), that is, the salinity at which a given type of clay stays flocculated. Figure 5.3 displays a simplified diagram from Scheuerman and Bergersen (1990) capturing the preceding discussion. Flocculation salinity lines are displayed for four clay types: smectites, mixed-layer smectite-illite, illite, and kaolinite. The slopes of the curves show that increasing $Ca^{++}$ concentration can sharply reduce the flocculation salinity. A solution with a fraction of calcium ions higher than 20 percent of the divalent cations will not generate any common clay dispersion at equilibrium. Because a formation water is in equilibrium with the solid phases present in the formation, all formation water chemical analyses should fall either in the vicinity of the salinity line or clearly outside of it. The location of these analysis points is a useful indication of the nature of the clays in equilibrium with the formation water. If, for example, a lot of the data points fell inside the smectite salinity line, it suggests that the formation water is not in contact with the smectite clays, if present in the formation.

The following discussion relies heavily on the 1990 SPE paper by Scheuerman and Bergersen. When injecting fresher water, two things need to be appraised: position of the injected water relative to the flocculation salinity line (Figure 5.3) and availability of

Ca cations. Fresh water is typically Ca-rich and clays at equilibrium with dilute water tend to incorporate a higher proportion of divalent cations into their exchange sites. Thus, in the initial stages of the injection, when the system is still not at equilibrium, clay will tend to strip Ca from the water to incorporate it into its mineral structure. However, by doing this, the Ca concentration in the water is reduced and the injected water position on the salinity plot may be considerably shifted to the left in the deflocculation and permeability impairment zone (Scheuerman and Bergersen, 1990) and cause damage farther downstream. How much Ca will be stripped from the solution before clay and solution are at equilibrium depends on the cation exchange capacity of the formation. Scheuerman and Bergersen (1990) mentioned a study of a Maverick Basin core where 400 pore volumes of Carrizo-Wilcox water were needed before reaching equilibrium. During that transient phase, clays were deflocculated and mobilized. However, a simple $CaCl_2$ pretreatment before injection of the Carrizo-Wilcox water prevented any detrimental effect by saturating the clay exchange sites and by avoiding cation stripping.

The impact of cation stripping can be estimated by computing the ratio of the MAR of the formation water to that of the injection water. Table 5.4 highlights one of the paper conclusions. If the MAR of the injection water is higher than that of the formation water, no clay mobilization is likely. Otherwise, pretreatment is suggested or recommended. It can be easily determined that the MAR of a concentrate is 4 times (as 4 is the RO concentration factor retained in this study) that of the initial feed water:

$$\left(MAR_{i/f}\right)_{fresh} = \frac{\left(Na_{fresh}\right)_i^2 / \left(Ca_{fresh}\right)_i}{\left(Na\right)_i^2 / \left(Ca\right)_i} \qquad \text{Equation 5-14}$$

$$\left(MAR_{i/f}\right)_{conc} = \frac{\left(Na_{conc}\right)_i^2 / \left(Ca_{conc}\right)_i}{\left(Na\right)_i^2 / \left(Ca\right)_i} = \frac{\left(4Na_{fresh}\right)_i^2 / \left(4Ca_{fresh}\right)_i}{\left(Na\right)_i^2 / \left(Ca\right)_i} = 4\left(MAR_{i/f}\right)_{fresh} \qquad \text{Equation 5-15}$$

This suggests that, relative to clay sensitivity, if no problem was encountered during historical injection of fresh water, none will be during concentrate inkection. This may not be true relative to the scaling problem.

### 5.5.4 Organic Material

Organic deposition leading to formation damage can be generated by mechanical accumulation and filtering if the injectate is mixed with produced waters with remaining hydrocarbons (e.g., paraffins and asphaltenes), but it can also occur by microorganism growth. Microorganisms act by two mechanisms: accumulation of live or dead cell and help in precipitating bacterial byproducts. To survive and multiply, microorganisms need a source of food (to build more of themselves), a source of energy (to fuel the redox chemical reactions needed to move and grow), an electron acceptor (to perform the chemical reactions), and some nutrients and trace elements. Usually the food source will include local hydrocarbons, lignin and other decayed vegetal material, and possibly migrating methane. The energy source is also typically the same as that of the food source. The electron acceptor, typically $O_2$ for aerobic bacteria at the surface, is sulfate, ferric iron, or $CO_2$ (bicarbonate) in the subsurface. A common group of deep-formation dwelling anaerobic bacteria are sulfate-reducing bacteria. The waste product from sulfate reduction is $H_2S$ or one of its ionic forms, $S^{2-}$ or $HS^-$. Sulfide can then react with iron to precipitate poorly soluble iron sulfides. Even if a biocide is added to the concentrate waste stream, killing microorganisms injected along with the water, resident bacteria can still be active in the formation. Some sulfate-reducing bacteria are salt-tolerant. They can be active at salinities as high as 100,000 mg/L and temperatures above the maximum considered in this study (60°C).

### 5.5.5 Formation Damage Control and Solutions

In the past century or so of oil and gas production, the oil and gas industry has come up with solutions for most of the operational problems they encountered. The following subsections describe a few approaches taken by the industry to deal with the problems described above. The solutions described below do not pretend to be exhaustive but a demonstration of the capacity of the industry to tackle formation damage. No attempt was made to look at the cost of the different treatments and how they would impact the price of treated drinking water.

#### 5.5.5.1 Chemical and Physical Solutions

Acidizing (by injection of hydrochloric acid or sulfuric acid) is used to stimulate production in carbonates and to treat formation damage (particularly carbonate scales) in all formations. Hydrochloric acid (HCl) has the drawback of adding corrosion-enhancing chloride ions, unless corrosion inhibitors are added, while sulfuric acid could increase scale-prone sulfate ion concentration, which might be a problem, especially if barium is present. As a general rule sulfuric acid is used for scale control, while scale removal is done with hydrochloric acid. Hydrofluoric acid (HF) will dissolve siliceous materials, especially clays and feldspar, but not quartz, whose dissolution kinetics is slower. HF is typically mixed with hydrochloric acid to keep the pH low when it spends, thereby preventing detrimental precipitates such as carbonates. The mixture is called “mud acid.” Strongly alkaline agents (NaOH or KOH) are widely used to remove calcium sulfate deposits.

$CaCl_2$ brine treatment reduces water sensitivity of the clay mineral. The Ca from the brine will saturate the sensitive clays, preventing cation stripping and deflocculation (Scheuerman and Bergersen, 1990). Farther away from the well bore, mixing with the resident formation water will limit cation stripping. A buffer of NaCl or KCl is also used to eliminate fine deflocculation and migration. Clay stabilizers (e.g., Zr salt, hydroxy aluminum, and dimethyldicocoammonium chloride) that irreversibly bind clay particles and other fines to the substrate or to each other are also used. Tang and Morrow (2002) state that the presence of crude oil reduces fine production and limits permeability loss.

Hydraulic fracturing is also used to treat damaged wells and improve performance of low-permeability wells (e.g., Reynolds and Kiker, 2003, p. 8).

#### 5.5.5.2 Operational Solutions

Surface treatment of injected fluids with filters, flocculating chemicals (cut-off size typically around 2-4 microns) to prevent plugging is currently done. Some operators find this of too high maintenance and do regular backflowing of injection wells to remove impurities (Reynolds and Kiker, 2003, p. 45). $O_2$ scavengers are also used at the surface to avoid oxidation of reduced material downhole (if the system is open). A typical scavenger used in water treatment is sodium sulfite ($Na_2SO_3$). This must be seriously considered because it could create sulfate-related problems downhole. We have already discussed scale inhibitors. There are hundreds of them marketed by oil-field service companies. Biocides are also used to kill bacteria but may be effective only in killing bacteria injected from the surface with the water and not the indigenous bacteria within the formation farther away from the well.

If no clay stabilizers are used, as advised by some consultants and service companies, salinity shock and fine deflocculation can be reduced by a gradual change in the salinity and ionic makeup of the invading water. Injecting a buffer solution compatible with both formation water and injectate is also an approach that works. Kharaka et al. (1997, p. 1016) and Rosenbauer et al. (1992) described the case where injection of a brine with a high sulfate concentration and low calcium concentration into a formation water with the reverse characteristics could be avoided by injecting a buffer of surface water. Common practice in the field of deep well injection of hazardous wastes is also to inject a buffer waste between two chemically incompatible wastes.

Even if fine mobilization does occur, lowering fluid velocity could help keep particles from bridging pores. This can be accomplished by decreasing flow rates or increasing the number of perforations or shot density. Fines will squeeze one by one through the pore throats and not bridge pores.

Table 5.1. Locations of deep-well injection disposal of RO and EDR concentrates as of 1999

| Plant Name | State | Type | Design Capacity (MGD) |
|---|---|---|---|
| Burnt Store RO Plant | FL | Brackish Reverse Osmosis | 0.56 |
| Englewood Water District RO Plant | FL | Brackish Reverse Osmosis | 3.00 |
| Knight Island Utilities Inc. | FL | Brackish Reverse Osmosis | 0.90 |
| Marco Island RO Plant | FL | Brackish Reverse Osmosis | 6.00 |
| Miramar West Plant | FL | Nanofiltration | 4.50 |
| North Collier County, FL | FL | Brackish Reverse Osmosis | 20.00 |
| Plantation, FL WTP | FL | Nanofiltration | 12.00 |
| Plantation, FL, City of | FL | Brackish Reverse Osmosis | 6.00 |
| Sanibel Island WTP | FL | Brackish Reverse Osmosis | 4.70 |
| T. Mabry Carlton EDR Facility | FL | Electrodialysis Reversal | 12.00 |

From Mickley (2001)
MGD = millions gallons a day

Table 5.2. Impact of environmental parameters on solubility of scale-forming minerals

| | Increasing Temperature | Increasing Pressure | Increasing Salinity | Increasing pH | Increasing $P_{CO2}$ |
|---|---|---|---|---|---|
| Calcite ($CaCO_3$) | decrease | increase | increase | decrease | increase but less pronounced as temperature increases |
| Gypsum ($CaSO_4.2H_2O$) | increase up to 38°C then slight decrease | increase | increase up to 150 g/L | none | none |
| Barite ($BaSO_4$) | increase up to 100°C | increase | increase | none | none |
| Celestite ($SrSO_4$) | decrease | increase | increase up to 175 g/L | none | none |
| Silica ($SiO_2$) | increase | increase | decrease | increase | none |

Table 5.3. Physical characteristics of clay minerals

| Clay type | CEC[1] | Expansion[2] | Reactivity[3] | Causes for Formation Damage |
|---|---|---|---|---|
| Kaolinite | Very Low | None | Low | Fine migration |
| Illite | Low | None | Low | Fine migration |
| Chlorite | Low | None | Low | Fine migration |
| Vermiculite | Very High | High | High | Swelling, deflocculation |
| Smectites | High | High | High | Swelling, deflocculation |

1 – Cation Exchange Capacity
2 – Expansion of mixed layer clays
3 – Reaction with the clay minerals

Table 5.4. Criteria for requiring formation pretreatment (Scheuerman and Bergersen, 1990, Table 3)

| Clay type | Treatment recommended if $MAR_{i/j}$ | Treatment suggested if $MAR_{i/j}$ |
|---|---|---|
| Kaolinite | <0.15 | <0.3 |
| Illite | <0.3 | <0.5 |
| Chlorite | N/A | N/A |
| Smectites | <0.5 | <1.0 |

$MAR_{i/j}$=Mass Action Ratio of injection water / Mass Action Ratio of formation water

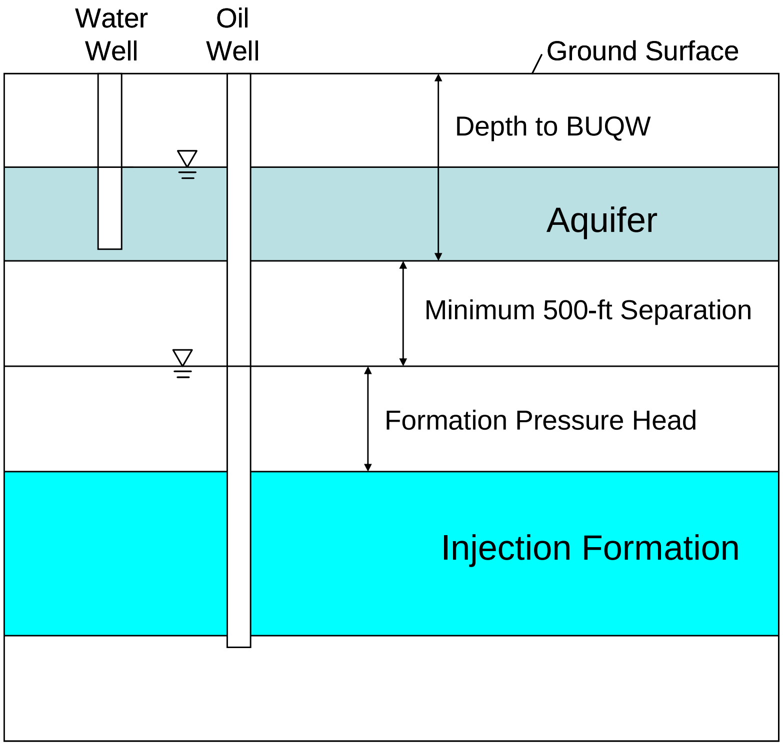

Figure 5.1. Cartoon showing AOR principles

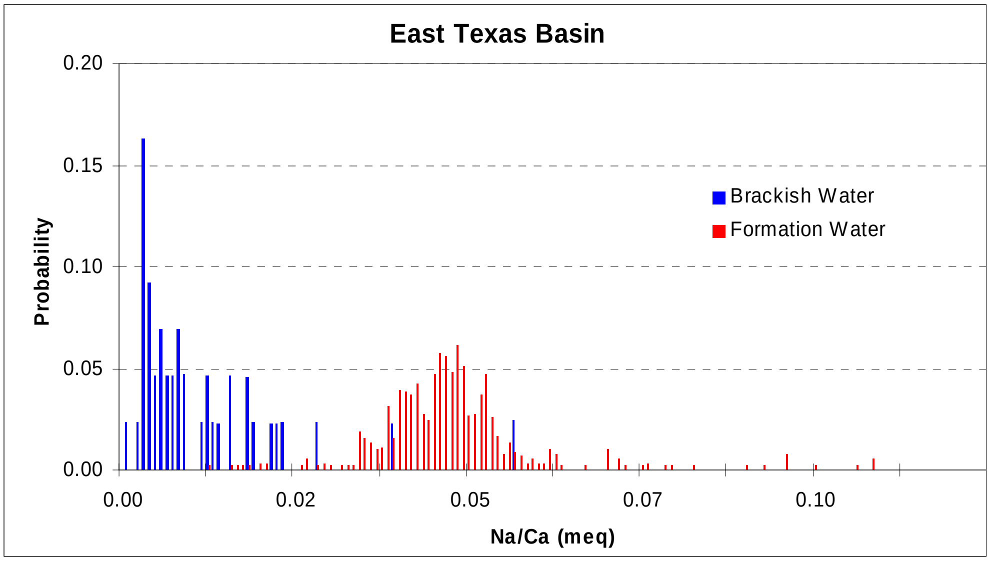

NOTE: Dark bars=brackish water; light bars=formation water

Figure 5.2. Distribution of Na/Ca ratio in the East Texas Basin

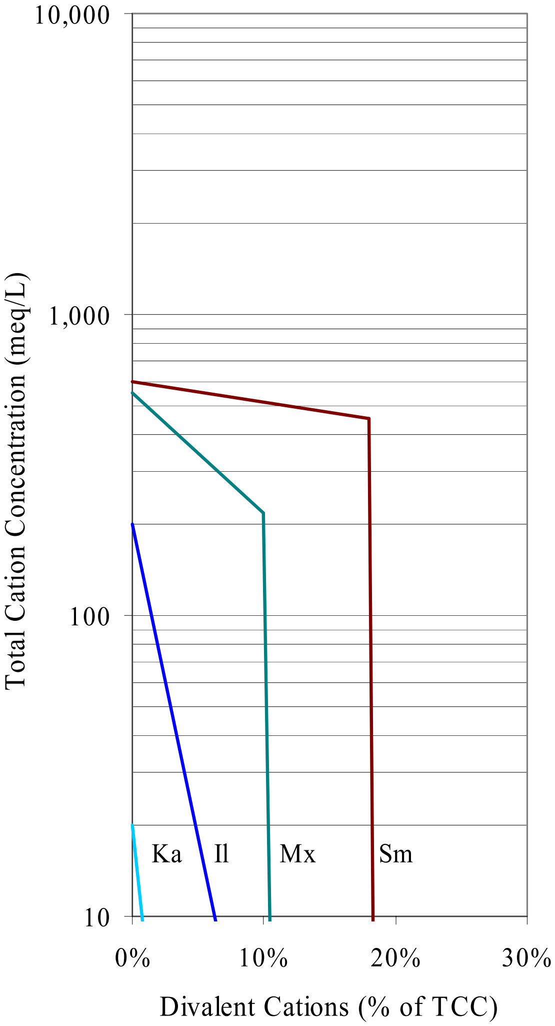

Ka=kaolinite; Il=illite; Mx=mixed layers; Sm=smectite
TCC=Total Cation Concentration

Note: any water inside the delineated domain will deflocculate the corresponding clay.

Figure 5.3. Template for water sensitivity analysis

# 6 Presentation of the Analysis areas

After a concise presentation underlining the position of the analysis areas in Texas geology, we detail for each of the six analysis areas (1) mineralogy, petrography, and reservoir description; (2) porosity and permeability; (3) nature of the formation waters; and (4) nature of the overlying brackish water aquifers. The last subsection describes additional parameters. The rationale for choosing the six analysis areas is presented in Sections 3.2 and 3.3. This section 1 will detail the relevant specifics of each area. They encompass an array of conditions large enough to cover most basins and formations not specifically investigated in this study. In all following sections, the different areas will be presented from north to south and west to east starting with the Anadarko Basin, moving to the Permian and East Texas Basins, then to the Fort Worth Basin, and finally to the Maverick and southern Gulf Coast Basins. The literature is extremely rich and abundant on all those basins because they have been producing oil and gas for decades and have been extensively studied from both geological and exploitation standpoints. It is out of the scope of this report to give a detailed summary of the geology and history of each basin. Some of the relevant literature will be referenced.

## *6.1 General Geology*

The following section gives an overview of Texas geology summarized from Ewing (1991). Most of West and Central Texas is underlain by Precambrian rocks that crop out mostly in the Llano Uplift in Central Texas and locally in the Trans-Pecos area. Starting in the Cambrian period, about 550 million years ago, failed continental rifting resulted in widespread deposition of shelf sediments on a stable craton (e.g., Ellenburger Group). Carbonate and clastic deposition continued until late Devonian, 350 million years ago. Thickness of the deposits varies, with a maximum in the ancestral Anadarko Basin and total removal by erosion of some formations along a broad arch oriented NW-SE on the Amarillo-Llano Uplift axis. Beginning in the Mississippian period (starting 350 million years ago), the passive-margin history of rifting and subsidence was replaced by extensive deep marine sedimentation and tectonic convergence on the eastern flank of the continental margin. This convergence episode yielded the so-called Ouachita Mountains, now eroded and buried, whose trace approximately follows the current Balcones Fault

Zone that runs west from San Antonio and northeast through Austin to the east of Dallas. Behind the orogenic belt, during and after the compressive event, sedimentation continued in and around several inland marine basins, north and west of the current Balcones Fault Zone. Sedimentation was thicker in the basins and thinner or absent on platforms and arches. During these times (320 to 270 million years ago) major subsidence and sediment accumulation, partially fed by the erosion of the Ouachita Mountains, occurred in the Permian Basin, including the Delaware and Midland Basins separated by the Central Platform Uplift. Farther north, the Anadarko Basin is separated from the Midland Basin by another basin and two structural highs. The Anadarko Basin also underwent abundant sedimentation during the Pennsylvanian and Permian and included coarse granitic detritus ("granite wash") from the Amarillo Uplift. The Fort Worth Basin is also filled with Pennsylvanian and Permian sediments.

Beginning in Triassic time (250 million years ago), Texas was again subject to extension and volcanism, leading to Jurassic rifting of the continental margin and creation of the Gulf of Mexico and Atlantic Ocean. The focus of major geologic events shifted to the eastern part of the state. The small rift basins that initially formed were buried under abundant salt accumulation (Louann Salt). As the weight of sediments increased, the salt became unstable and started locally to move upward in diapirs, a phenomenon still active today. During the Cretaceous, sediments deposited from shallow inland seas formed broad continental shelves that covered most of Texas. Abundant sedimentation in the East Texas and Maverick Basins occurred during the Cretaceous. In the Tertiary (starting 65 million years ago), as the Rocky Mountains to the west started rising, large river systems flowed toward the Gulf of Mexico, carrying an abundant sediment load, in the fashion of today's Mississippi River. All the area west of the old Ouachita Mountain range was also lifted, generating a local sediment source, including erosional detritus from the multiple Tertiary volcanic centers in West Texas and Mexico. Six major progradation events, where the sedimentation built out into the Gulf Coast Basin, include the Frio deltaic and strandplain sedimentation.

From a more hydrogeologic perspective, Kreitler (1989) presented an overview of Texas sedimentary basins, as well as a summary of basin-scale hydrological processes. A study with some overlap with this document was performed by Hovorka et al. (2000) on one or two formations in several sedimentary basins across the U.S., including the Frio Formation in the Gulf Coast Basin, the Woodbine Formation in the East Texas Basin, and the Granite Wash Formation in the Anadarko/Palo Duro Basins. The study was geared toward $CO_2$ injection for geological sequestration.

## 6.2 Petrography and Mineralogy

The mineralogy and petrography of each analysis area are described next. The discussion is summarized in Table 6.1. The formations can be divided into two groups according to their petrography: carbonate or silico-clastic. The San Andres Formation in the Permian Basin is mainly composed of carbonate deposited as such, while the five other formations consist of more or less “clean” sand. The range goes from nearly pure sand with little nonsilica grains to terrigenous sands mainly made of feldspars and rock fragments and their alteration products, such as clay and carbonates. According to Folk’s classification (Folk, 1980), sand has fewer than 25 percent foreign particles. More than 25 percent rock fragments and most the remainding comprised of quartz grains make the sample a litharenite, while more than 25 percent feldspar crystals in association with quartz grains make an arkose. All gradations exist between sand, arkose, and litharenite (lithic arkose = arkose with a nonnegligible fraction of rock fragments, feldspathic litharenite = litharenite with nonnegligible fraction of feldspars, subarkose = sand with some feldspar, and sublitharenite = sand with some rock fragments). The petrography and mineralogy of the formations are important considerations because they impact directly the potential chemical reactions during the injection process. Feldspars are much more reactive than quartz. The focus of the following description is on the cement and authigenic material in potential physical contact with the formation and injected water. This study does not model long-term subsurface reactions but investigates those able to impede the injection process, in particular the reaction with clay (see Section 5.5.3 for a list of clay types). The greatest risk of formation damage may be changing the ionic ratio of the formation water or the selectivity of ion exchange between water and clay minerals.

### 6.2.1 Anadarko Basin

***Introduction:***

The Anadarko Basin is the deepest Phanerozoic sedimentary basin within the North American craton (Ham and Wilson, 1967). During the Pennsylvanian orogenic period, the Wichita and Amarillo Uplifts (Figure 6.1) were separated from the Anadarko Basin by a series of faults that resulted in subsidence along the southern margin of the Anadarko Basin and accumulation of coarse arkosic granite wash materials from the uplifts (Dutton et al., 1993). The fluvial-deltaic Cleveland Formation was derived from the western margin of the basin that prograded eastward. Most tight gas occurs in the Granite Wash Formation. Outlines of the oil and gas fields present within the analysis areas are shown in Figure 3.8. A cross section of the analysis area is displayed in Figure 6.2a.

***Depositional Setting***

The Granite Wash is areally restricted close to the northern flank of the Amarillo Uplift (Dutton et al., 1993). These sediments were deposited in braided-stream, alluvial-fan, and fan-delta complexes (RRC, 1982). Local occurrences of interbedded marine shales and limestones indicate that marine transgression interrupted episodes of fan-delta deposition (Dutton, 1982, 1990). Tongues of tight gas of the Granite Wash in the north were probably part of the distal-fan deposition in near-shore marine bars (Dutton et al., 1993). The upward-coarsening log character of many tight-gas tongues indicate progradation; upward-fining trends and blocky intervals suggest aggradational processes; and thinner zones with spiky log expressions represent cyclically repeated deposits (Dutton et al., 1993).

The Cleveland Formation is a prolific natural gas producer, and stratigraphic boundaries of the formation are marked by regionally correlative high-gamma-ray correlative shales. The Cleveland Formation extends from the western terminus of the Anadarko Basin at least as far as the west-central Oklahoma. The Cleveland Formation mostly contains sandstone and shale, with carbonates restricted only in the upper part of the unit. Siliciclastics of the Cleveland Formation form mostly stacked, upward-coarsening deltaic facies.

### *Reservoir Description*

The tight Granite Wash section contains nine informal stratigraphic intervals, ranging in thickness from about 860 to 3,170 ft (RRC, 1982). Shale sections as much as 30 to 40 ft thick occur in the deep Anadarko Basin. Individual sections of the Granite Wash occur in intervals of 10 to greater than 120 ft. The log expressions in the nine stratigraphic units are variably upward coarsening, upward fining, blocky, and spiky. The trapping mechanism is stratigraphic, locally modified by anticlines. Reservoir pressures range from 1,800 to 2,000 psi. Formation temperature ranges from 160 to 210$^{o}$F.

Cleveland gas reservoirs are about 25,700 acres in areal extent (Kosters et al., 1989). Reservoir sandstones are as much as 65 ft thick but are locally 90 to 100 ft thick. Reservoir sandstones are generally continuous with sheetlike geometries. Reservoir thickness increasingly varies northward and westward. Bounding facies of the reservoirs are well-indurated, calcite-cemented prodelta and distal-front shale and silty/sandy shale that are less than 25 ft (Dutton et al., 1993). Reservoir pressures in the Cleveland range from 2,200 to 2,700 psi, and reservoir temperatures range from 145 to 160$^{o}$F.

### *Mineralogy and Diagenesis*

Sandstone compositions of the Granite Wash range from 50 percent potassium feldspar, 24 percent quartz, 16 percent clay (mostly sericite), 7 percent dolomite (as a cement), and 3 percent other. Other cements include calcite and siderite. As much as 35 to 40 percent of the feldspar grains are highly altered to sericite. High clay content, dolomite cement, poor sorting, and grain angularity contribute to significant reduction in porosity and permeability (RRC, 1982). Reservoir sandstones in the Cleveland Formation are feldspathic litharenites and lithic arkoses. Porosities in the Cleveland range from 4 to 14 percent. Permeability values of the core samples range from 0.0033 to 4.55 md, with an average of 0.15 md or less. The permeability of the sandstones is affected by large amounts of clay. Diagenetic cements and replacement minerals constitute between 10 and 34 percent of the rock volume. Illite, kaolinite, and chlorite are the main detrital clay minerals. Quartz composes an average of 7.3 percent of the whole rock volume; calcite, ankerite, and siderite comprise an average of 6.2 percent of the whole-rock volume, and authigenic clay (chlorite, illite, and kaolinite) has an average of 3 percent of the rock volume (Dutton et al., 1993).

### 6.2.2 Permian Basin

***Introduction:***

The San Andres Formation of Guadalupian/Permian age was chosen because of its high cumulative production. The part of the San Andres Formation included in this study lies mainly along the eastern side of the Central Basin Platform and the western side of the Midland Basin (Figure 6.1). The Central Basin Platform is an elongate carbonate platform that covered structurally positive basement rocks during the Permian Period (Ruppel and Cander, 1988). To its east, predominantly deeper-water siliciclastics and carbonates were deposited in the Midland Basin (Ruppel and Cander, 1988). The San Andres Formation on the Central Basin Platform is the fourth-largest oil play in the Permian Basin and has produced more than 2,150 MMbbl ($3.42 \times 10^8$ $m^3$) of oil from 52 reservoirs (Dutton et al., 2004). Outlines of the oil and gas fields present within the analysis areas are shown in Figure 3.9. A cross section of the analysis area is displayed in Figure 6.3a.

***Depositional Setting***

Carbonates and evaporites of the San Andres of the Central Basin Platform were deposited on a shallow-water shelf. Depositional environments varied from bar and bank complexes along the shelf edge to restricted subtidal lagoons and arid tidal flats toward the interior of the platform. Overall, depositional facies are locally distributed, resulting in highly heterogeneous reservoirs.

***Reservoir Description***

The San Andres-Grayburg Formation of the central platform of Texas and New Mexico has produced approximately 10 billion bbl of oil accounting for approximately 40 percent of the Permian Basin production. The McElroy field has produced about 0.7 billion bbl of oil. Solution gas is the primary drive mechanism, and most reservoirs underwent waterflood. Carbon dioxide is also commonly injected in the Permian Basin for tertiary recovery.

***Mineralogy and Diagenesis***

The dominant minerals of this carbonate-rich formation in the Central Basin Platform area are calcite, dolomite, and anhydrite. The main detrital rock types include fusulinid packstone and wackestone, skeletal grainstone, burrowed mudstone and skeletal wackestone, pisolite grainstone, cryptalgal mudstone, and fine-grained (siltstone and mudstone) silicilastics (Ruppel and Cander, 1988). Episodes of pervasive dolomitization affected the texture and fabric of the rock. Anhydrite was emplaced after dolomitization. Chalcedony and kaolinite form rare cements (Ruppel and Cander, 1988). To the north where more highly evaporatively concentrated brines formed, diagenesis formed a range of clay mineral compositions (Palmer, 1987).

### 6.2.3 East Texas Basin

#### *Introduction*

The oil reservoirs in the Woodbine Formation of Cretaceous age included in this study lie in the salt-structure province of the East Texas Basin on the northern flank of the Sabine uplift. The Woodbine Formation was deposited in a complex of fluvial, deltaic, and strandplain depositional systems (Galloway et al., 1982). Of the many reservoirs in the Woodbine play, five have each produced more than 1.6 $10^6$ $m^3$ of crude oil (Galloway et al. 1983). Outlines of the oil and gas fields present within the analysis areas are shown in Figure 3.10. The East Texas Basin was extensively studied in the 1980’s, when it was considered for deep geological disposal of high-level nuclear waste. A cross section of the analysis area is displayed in Figure 6.4a.

#### *Depositional Setting*

The East Texas Basin is located between the Muenster Arch / Ouachita Fold Belt to the west and the Sabine Uplift to the east. It is comprised of Cretaceous platform deposits transitioning to alternating delta/fluvio-deltaic deposits of Paleocene/Eocene and deep-sea deposits. The Woodbine Formation consists of sediments deposited in many varied environments: fluvial, deltaic, shelf, and deep marine.

#### *Reservoir Description*

The East Texas Basin Woodbine Formation contains one of the world’s most prolific plays (Galloway et al., 1983). The super-giant East Texas field in Upshur, Gregg, Smith, and Rusk Counties has produced about 5 billion bbl of oil with its excellent recovery due to a strong water drive, early pressure maintenance by injecting water below the oil-water contact, gravity-stable displacement, low residual oil saturation, and good management practices enforced early on by the RRC. The giant Hawkins field in Wood

County and the Van field in Van Zandt County produced 0.8 and 0.5 billion bbl, respectively.

### *Mineralogy and Diagenesis*

The Woodbine Formation includes volcaniclastic sandstones with interbedded shale and conglomerate with igneous and volcanic rock fragments (Belk et al., 1986). Sands may have been derived from the Paleozoic sediments of the Ozark Uplift in Oklahoma and Arkansas, with a secondary source of volcanic material in southwestern Arkansas (Beall, 1964). Igneous material is much more common in the upper Woodbine but is found throughout the Woodbine section in Texas (Belk et al., 1986).

The following mineralogy summary is mostly from Belk et al. (1986) which describes well the formation close to the source of sediments. Most sandstones have less than 10 percent quartz but abundant oligoclase feldspar, Ti-rich pyroxene, and magnetite. Volcanic rock fragments (VRFs) compose 49 percent of sand grains. Volcanic arenites and feldspathic volcanic arenites are interbedded with siltstones and conglomerates. The sand fraction consists of volcanic rock fragments, feldspar, quartz, chert, clay clasts, and heavy minerals such as hematite, magnetite, zircon, leucoxene tourmaline, apatite, and amphiboles. The most common detrital VRF is trachytic-textured igneous rock. VRFs feldspars are probably oligoclase and some sanidine. Common authigenic cements include calcite, dolomite, ankerite, and quartz (Uziemblo and Petersen, 1983). The gravel fraction includes novaculite (variety of chert), clay clasts, and volcanic cobbles totally altered to smectite. The volcanic components include pheno-nepheline tephrites, pheno-nepheline basanites, and pheno-andesites (Belk et al., 1986).

The silt- and clay-sized fraction consists of feldspar, quartz, VRFs, clay clasts, smectite from diagenetic alteration of VRFs, and detrital calcite and biotite (Belk et al., 1986). Uziemblo and Petersen (1983) identified clay minerals including kaolinite, chlorite, illite, and smectite. Beall (1964) described varying sodium and calcium ratios in smectite across the western flank of the East Texas Basin. The higher Na-smectite composition toward the center of the basin probably reflects the distribution of formation water composition (Kreitler et al., 1987). Beall (1964) also found illite clay in the Woodbine Formation.

Wagner (1987) described the mineralogy of the Woodbine Formation in the giant Hawkins oil field (Figure 3.10) as fine- to coarse-grained moderately sorted sandstones with abundant quartz grains, secondary overgrowths, varying amounts of clay, including authigenic chlorite and kaolinite, and minor amounts of feldspar.

### 6.2.4 Fort Worth Basin

#### *Introduction*

The Fort Worth Basin is an asymmetric foreland basin located in North Texas, formed during the Early to Middle Pennsylvanian Period in response to tectonic stresses that also produced the Ouachita Thrust Belt (Thompson, 1982). The basin has an axis about 200 miles long and is no more than 100-mile wide. It is bounded by the Red River and Muenster Arches to the north, by the Broad Bend Arch to the west, and by the Llano Uplift to the south. The basin covers about 20,300 square miles, with the deepest sections in the east-northeast and shallowest in the west. Paleozoic rocks in the Fort Worth Basin have a maximum thickness of 12,000 ft. Outlines of the oil and gas fields present within the analysis areas are shown in Figure 3.11. A cross section of the analysis area is displayed in Figure 6.5a.

#### *Depositional Setting*

The Atoka Group was deposited in three distinct packages of terrigenous deposits: (1) the lower Atoka formed from a fluvially dominated fan delta system, (2) the upper Atoka "Davis" formed from a coalesced wave-dominated delta, and (3) the upper Atoka "post-Davis", which is a thin, poorly integrated, fluvially dominated fan-delta system. The Atoka Group does not outcrop in the Fort Worth Basin. Subsurface Atokan strata have been known as "Bend Conglomerate", "Big Saline", "Caddo Conglomerate", "Lampasas Series", "Marble Falls Conglomerate", and "Atoka Group" (Thompson, 1982). The Atokan Group of sediments is as much as 5,900 ft thick near the leading edges of the Ouachita Thrust Belt (Johnson et al., 1988). The Lower Atoka is characterized by highly digitate and elongate net sandstone geometry, extensively interfingered terrigenous and carbonate units, and progradation facies sequences in which contemporaneous faulting influenced facies distribution. The upper Atoka "Davis" is characterized by a thick and strike-oriented sandstone geometry that suggests concurrent progradation and aggradation in a system of coalesced wave-dominated deltas. The upper

Atoka “post-Davis” is also characterized by a highly digitate sandstone geometry and a progradational facies sequence suggesting resumption of fluvially dominated fan-delta deposition (Thompson, 1982).

### *Reservoir Description*

The individual sandstone units in the Lower Atoka are thicker in the east and characterized by blocky electric log patterns (Thompson, 1982). To the west the sandstone units progressively break up into a series of thin, discontinuous beds averaging 10 ft in thickness. The primary source of the Lower Atoka was the Ouachita Thrust Belt. The upper Atoka “Davis” is characterized by a thick, strike-oriented sandstone geometry and maximum thickness trends concentrated along a narrow zone. Individual sandstone units average 30 ft in thickness and are separated by thick shale sequences (Figure 6.5b). The Davis sandstone thickens southeastward from less than 20 ft along the northern and western flanks of the Fort Worth basin to as much as 1,200 ft in Parker and Dallas Counties (Thompson, 1982). In Palo Pinto and Parker Counties, the unit is about 50 to greater than 100 ft thick. Sandstone packages in the upper Atoka “post Davis” are thicker in the east and break up westward into thin stringers. In the west (Archer, Young, and Stephens Counties), sandstone units average 5 ft in thickness. In the production zones, the reservoir pressures range from 200, to 2,000 psi, with considerable variation among zones, suggesting that the individual zones act as an individual reservoir with little intercommunication between zones (Thompson, 1982). Three styles of reservoir compartmentalization were identified in the Fort Worth Basin: structural, stratigraphic, and a combination of the two. Structural compartments are caused by low-displacement faulting, most commonly associated with karst collapse in deeper carbonate rocks, that produced structurally isolated fault blocks. The faulting is widespread, but subtle, and neither vertical displacements nor fault-block geometries can be mapped without 3-D seismic data. Stratigraphic compartments may be bounded laterally by facies transitions or complete porosity occlusion caused by diagenetic processes and vertically by the impermeable surface or sequence boundaries. Combination-style compartments have both structural and stratigraphic elements (Hamilton et al., 1997).

### *Mineralogy and Diagenesis*

Davis reservoir sandstones are quartz-rich feldspathic litharenite (Thompson, 1982). Typical sandstones contain abundant shale interbeds, plagioclase is the most abundant feldspar, and detrital organic matter is as much as 8 percent of the volume of mudstones and muddy sandstones. Detrital clay is composed of illite, chlorite, kaolinite, and clay-size quartz. Porosity development is primarily controlled by depositional environment. Highest porosity occurs in chert conglomerates deposited under high-energy conditions. Porosity includes original porosity remaining between quartz overgrowths and secondary porosity produced by dissolution of chert grains. Pore spaces are angular, moderately interconnected and 0.04 to 2 mm wide, with an average width of 0.8 mm. Secondary pore spaces are slightly interconnected and range from 0.6 to 3 mm, with an average width of 1 mm. Porosity in the medium- to fine-grained sandstones range between 8 and 12 percent. Chert conglomerates show permeability that averages between 2,000 and 3,000 md. The medium- to fine-grained sandstones have permeability of typically less than 1 md because of lack of interconnection between the dominantly secondary pore spaces.

Basic diagenetic sequence in the sandstones is (1) compaction resulting in stylolitization and development of pseudomatrix, (2) quartz overgrowth, and (3) dissolution of chert, feldspar, and metamorphic and volcanic rock fragments. Diagenetic minerals include replacement cements that may compose as much as 25 percent of the whole rock volume that include quartz, calcite, ankerite, siderite, chlorite, illite, kaolinite, and pyrite. Quartz cement consists of up to about 11 percent sandstone volume in clean sandstones. Chlorite cement volume averages 3 percent and carbonate cement 2 percent of rock volume (Thompson, 1982).

## 6.2.5 Maverick Basin

### *Introduction*

The Maverick Basin of southwest Texas forms the easternmost part of the Rio Grande Embayment of the Gulf Coast Basin. The Maverick Basin is separated from the East Texas Embayment by the San Marcos Arch that trends southeastward from the Llano Uplift (Figure 6.6). The Maverick Basin is bounded on the north by the Balcones Fault Zone and on the northwest by the Devils River Uplift. On the west, the basin is separated by the southeastward–trending Salado Arch. Smaller structural features include the Chittim Anticline and the Pearsall Ridge. No large growth faults occur in the basin. Numerous basaltic volcanic plugs occur in the northern part of the basin (Simmons, 1967). The Cretaceous San Miguel and Olmos Formations are the most prolific reservoirs in the Maverick Basin. Outlines of the oil and gas fields present within the analysis areas are shown in Figure 3.12. A cross section of the analysis area is displayed in Figure 6.6a.

The San Miguel Formation is predominantly an oil play (Galloway et al., 1983) with a cumulative production of 81.8 Bcf or 2.9 percent of the total production in Texas (Kosters et al., 1989). Catarina Southwest is a major gas play, with a total production of 51.4 Bcf in 1978. Big Wells oil reservoir is relatively tight, and wells require hydraulic fracturing to stimulate production. The reservoir shows minimal interwell variability, excellent internal continuity, and maximum recovery efficiency (Tyler et al., 1986).

The Olmos Formation overlies the lowermost clastic wedge, the San Miguel Formation, and is overlain by the uppermost clastic wedge, the Escondido Formation (Figure 6.6b). Tight gas sandstones occur within the Olmos Formation, with 973 tight completions having a cumulative production of 298.6 Bcf and an estimated ultimate recovery of 408 Bcf (Hugman et al., 1992).

### ***Depositional Setting***

The San Miguel Formation is predominantly an oil play (Galloway and others, 1983). It contains only three large gas reservoirs with a cumulative production of 81.8 billion cubic feet (Bcf) or 2.9 percent of the total production from Texas Gulf Coast Cretaceous gas plays (Kosters and others, 1989). Catarina southwest is a major gas play with a total production of 51.4 Bcf in 1978. Big Wells oil reservoir is relatively tight and wells require hydraulic fracturing to stimulate production. The reservoir shows minimal interwell variability, excellent internal continuity and maximum recovery efficiency (Tyler and others, 1986).

The Olmos Formation is exposed around the Chittim Anticline in Maverick County, and the formation extends in the subsurface to the southeast in Webb and La Salle Counties. Olmos deposition occurs in two main depocenters: (1) the western depocenter (Catarina Delta System), having a highly wave reworked, strike-elongated delta complex (Unit A), followed by more fluvially dominated delta systems (Units B and

C) and (2) the eastern depocenter (Rocky Creek Barrier/Strand Plain System), having again a wave-dominated delta complex (Unit F) followed by wave-modified deltaic sedimentation (Units G and H). (Tyler and Ambrose, 1986). Units D and E form thick retrogradational coastal interdeltaic complexes. (Figure 6.6b). Sand bodies are composed of sharply based, thin-bedded sandstones that are massive, horizontally laminated, or, more rarely, low-angle crossbedded. Sandstones grade upward into thoroughly bioturbated silty sandstones and sandy mudstones. These beds are interpreted to be storm deposits derived from the nearby deltaic headland.

### ***Reservoir Description***

The sandstones of the San Miguel Formation, dominated by upward coarsening cycles, are very fine-grained and range from coarse siltstone to fine sandstone. Sandstone A is up to 43 miles long and 8 to 14 miles wide, centering at the corner of Zavala, Frio, Dimmit and La Salle Counties. Sandstone A is concentrated in three main “pods” or depocenters with a thickness of 130 ft. Sandstone B is strike aligned, similar to A, and is up to 54 miles long. Sandstone C, better known as Atlas or Elaine Sandstone, is 45 miles long and 30 miles wide with net sandstone 130 ft thick (Weise, 1980). Sandstone D better known as the “basal San Miguel” sandstone forms an arcuate trend with the net sandstone section reaching a maximum of up to 95 ft. Sandstone E, known as the “Big Wells” Sandstone, is 35 miles long and 18 miles wide with a net sandstone thickness of 90 ft. Sandstone F is at least 60 miles long and lies updip of Sandstone E with a net sandstone thickness of 90 ft. Sandstone G known as the “torch” or the “King” or the “Second Sand Miguel” is up to 60 miles long with a net sandstone thickness of 140 ft. The youngest of the units Sandstone I is 60 miles long and 22 miles wide with a maximum net sandstone thickness of 80 ft. Two types of hydrocarbon traps are common in the San Miguel sandstones: (1) structural traps over volcanic plugs and (2) stratigraphic traps formed by updip pinch-out of porous sandstones.

Downdip from the Lower Cretaceous shelf edge, the Olmos sandstones are informally designated as Olmos “A” and underlying Olmos “B”. Barrow and Asquith (1992) showed the Olmos to contain at least nine individual sandstone bodies (Figure 6.6b). Unit A sandstones are as much as 60 ft thick, display upward–coarsening SP log patterns, and are arranged in a 75-mile long, strike-elongate, sandstone-rich trend. Unit B sandstones are lobate and digitate, and axes are as much as 120 ft thick. Potential reservoirs are dip-elongate upward-fining channel sandstones (70 to 100 ft thick); upward-coarsening, channel-mouth-bar sandstones (20 to 50 ft thick); and thin, muddy, delta-front sandstones. Unit C contains a maximum of 80 ft of sandstone in southern Dimmit County and a strike-oriented system with as much as 100 ft of sandstone in northwestern Webb County (Dutton et al., 1993). Unit D is centered in northwestern Webb County, consisting of a major strike-elongate belt with as much as 90 ft of sandstone. Unit E was deposited as a marine onlap with small-scale (10 ft thick) sandstones of reservoir potential. In the updip trend, the net pay thickness ranges from 50 to 250 ft with net pay thickness of 50 ft in the downdip trend. Net pay thickness ranges from 12 to 82 ft for the Olmos overall (Finley, 1984). Strike-oriented belts of high production parallel sand thickness trends. However, highest production occurs in the longshore-distal part of the trend, where sand thicknesses are generally lower than in the area proximal to the delta. This may be due to increased concentrations of calcite in proximal areas. Hydrocarbon pore volume corrected for volume of clay has been calculated from available log suites and compared with cumulative gas production. Gas recovery efficiency varies across the trend; significant reserves remain in areas where average drainage radius is much less than regulated well spacing.

### *Mineralogy and Diagenesis*

Thin section examinations indicate that the sandstones of the San Miguel Formation are dominantly arkosic in composition. Calcic plagioclases are most abundant compared with potassium feldspars and albite. A higher percentage of quartz is found in the coarsest parts of the sandstone. Sandstones of the Olmos Formation are subarkose to sublitharenite in composition and are composed of quartz, clay, feldspar, and rock fragments. The clay minerals are mainly detrital that include subequal amounts of mixed layer illite-smectite, and Fe–rich chlorite composes up to 30 percent of some sandstones (Snedden and Jumper, 1990). Porosity determined from thin sections of the San Miguel Formation shows an upward increase due to a decrease in the clay content, ranging from 10 to 30 percent. Highest porosity occurs in areas where feldspar and shell fragments have been leached. Original porosity is destroyed in some zones due to calcite cementation. The cemented zones exhibit low spontaneous potential (SP) and high resistivity values on the electric log. Thin limestone beds that are silty to sandy micrites are nonporous. Permeability ranges from 0.1 to 65 md with an average of 6 md. Core, SEM, and petrographic analyses of the Olmos Formation indicate that porosity, which ranges from 6 to 16 percent and averages slightly under 10 percent, is 80 percent primary macroporosity, 10 percent secondary macroporosity, and 10 percent primary microporosity. The most common cements in the San Miguel Formation are calcite and quartz overgrowths. Other diagenetic minerals are kaolinite, feldspar, illite (clay rims), pyrite, and hematite (Loucks et al., 1979). Diagenetic kaolinite occupies some primary intergranular pore spaces, as well as central parts of larger cavities (Weise, 1980). The very fine grain size and high clay content result in low permeability, which ranges from 0.01 to 8 md (Snedden and Jumper, 1990). Finley (1984) documented median permeabilities ranging from 0.034 to 0.072 md from 149 wells with permeabilities lower in the downdip than in updip sandstones. Olmos reservoirs are overpressured, and fractures and faults may define pressure compartments in this unit. Dissolution of feldspar, calcite cement, and shale clasts in the Olmos Formation contributes to secondary porosity. Secondary calcite further reduces porosity and forms the updip trapping mechanism.

### 6.2.6 Southern Gulf Coast Basin

#### *Introduction*

The southern Gulf Coast Basin includes six major progradational sedimentary packages of Tertiary and Quaternary age, underlain by older Mesozoic formations that record the early evolution of the basin (Galloway et al., 2000). Zones of growth faulting mark the basinward movement of the shelf edge. Fault-bounded reservoir compartments create many structural traps in the Cenozoic stratigraphic section of the southern Gulf Coast Basin. Outlines of the oil and gas fields present within the analysis areas are shown in Figure 3.13. A cross section of the analysis area is displayed in Figure 6.7a.

#### *Depositional Setting*

The Frio Formation composes one of the major progradations into the Gulf of Mexico (Figure 6.7b). In the Frio Formation, hydrocarbons are trapped in the downthrown side of down-to-the-basin faults along the Vicksburg-Frio fault zone (Galloway et al., 1983). The Frio Formation of South Texas was deposited in a complex of fluvial, deltaic, strandplain, and barrier depositional systems (Galloway et al., 1982). Vertically stacked reservoirs in multiple horizons of permeable deposits are typical of the Frio Formation.

### *Reservoir Description*

The sheer number of attractive targets makes a high-level study such as this incomplete. The Frio Formation in Texas has produced 6 billion bbl of oil and 60 trillion cubic ft of gas. Shallow saline sections of the Gulf Coast basin are hydrostatic. Beyond depths of 8,000 to 10,000 ft, the formations become overpressured in the so-called geopressured zone.

### *Mineralogy and Diagenesis*

Capuano et al. (1989, p. 53), citing different sources, summarized the petrography of Frio and other Gulf Coast sandstones. Quartz is a major component, followed by feldspar and rock fragments, which generally make up 5 to 50 percent of the total rock. Clay content increases with depth and also undergoes a mineralogical change as smectite gives way to illite at a depth of ~9,000 ft (Loucks et al., 1979). Carbonate cementation is also common and occurs predominantly as calcite. Calcite cement averages 5 percent in volume (Land, 1984). The lower Gulf Coast sandstones, i.e. in the analysis area, have a higher proportion (~60 to 80 percent) of volcanic rock and carbonate rock fragments and plagioclase and orthoclase feldspars than their northern counterparts (Loucks et al., 1977, their Figure 5) because of their proximity to the then-active volcanic areas in Mexico and West Texas. Rock fragments compose half to more than 75 percent of the nonquartz grains. Consolidation history includes a reduction in porosity (that can rebound with a leached secondary porosity but only beyond depths considered in this study), feldspar leaching, creation of some quartz and feldspar overgrowth, formation of clay coats and rims, and production of a calcite cement.

In a more detailed analysis, Lindquist (1977) completed a classic study of the mineralogy and diagenesis of reservoir sandstones in the Frio Formation, focusing on a analysis area in Nueces, Willacy, and Hidalgo Counties that probably is representative of the Frio in the southern Gulf Coast Basin. Texture and mineralogy varies with depositional system. In the depocenters of deltaic and nearshore coastal complex environments, one finds mineralogically immature, fine-grained, moderately well sorted sandstones. Feldspathic litharenites to lithic arkoses near the depocenters are low in quartz (20-30 percent), and rich in feldspar and VRF (up to 50 percent VRF) (Lindquist, 1977; Loucks et al., 1986). VRFs are predominantly rhyolites and trachytes and normally silicified or altered to chlorite (Lindquist, 1977; Loucks et al., 1986; Grigsby and Kerr, 1991). Carbonate rock fragments, mainly from caliche deposits, are also frequent (Loucks et al., 1986). The diagenetic sequence is well established (Lindquist, 1977; Loucks et al., 1986):

1- At shallow to moderate depth of burial in normal pressure regime: cementation by micrite replacing feldspar, feldspar overgrowths on feldspar, quartz overgrowths, sparry calcite replacing feldspar, and some pyrite; primary porosity is reduced to several percent and permeability reduced to less than several tens of millidarcys.

2- At greater depth in the transition zone at the top of geopressure (~10,000 ft): dissolution of calcite increases porosity to more than 30 percent and increases permeability to several hundred millidarcys.

3- At greater depth in the geopressure zone: postdissolution recementation by kaolinite, ferroan calcite and dolomite cements, ankerite, analcime, zeolite (laumontite?), and more pyrite, which causes reduction in secondary porosity and permeability.

Lindquist (1977) also found that porosity and permeability in the depocenter areas depends on the extensiveness of early cementation. Grigsby and Kerr (1991) found that the middle Frio is composed mainly of lithic arkoses to feldspathic litharenites with abundant glass shards and volcanic-ash-rich matrix. Devitrification yielded analcime and mixed-layer illite-smectite minerals (Kerr and Grigsby, 1991). Galloway (1977) also suggested that alteration of volcanic clasts yielded montmorillonite. In the middle Frio much of the higher porosities are ineffective owing to authigenic cementation. Morton and Land (1987) pointed out that the formation waters in the Frio Formation are mainly Na-Cl along the San Marcos Arch but Ca-Cl to the south in the Gulf Basin.

## *6.3 Porosity and Permeability*

Permeability and porosity data that we examined from the analysis areas are extremely variable within the same formation, as a function of the depositional setting. Sources for porosity and permeability include a Core Laboratories report (1972b), digital compilation of the oil and gas atlases published by BEG in Holtz et al. (1991) and Garrett et al. (1991), data from H1 forms downloaded from the RRC website or gathered from older paper copies. Only minimal effort was made to ensure no data doubling by merging the different data sets. Permeability distribution is very dependant upon the depositional pattern, and a map of the permeability values may look random until depositional system contours are superimposed onto the map. Porosity and permeability are generally lower in the Paleozoic basins than in the Cretaceous and Tertiary basins. The porosity-permeability cross plots show that these two parameters are linearly correlated in the analysis areas with a linear correlation coefficient of 0.5 or higher. These correlation coefficients will be used when a distribution of the flow rates will be computed (Section 1). It is beyond the scope of this study to do a thorough analysis of the spatial distribution of the permeability; rather, we hypothesize as a first approximation that the data points gathered from various sources represent the permeability variability of a standard field. We also merged porosity or permeability data from oil and gas fields. Holtz and McRae (1995) showed that, in the southern Gulf Coast, there is no difference in permeability and porosity statistical attributes between oil and gas fields. The concept of relative permeability is also very important in multiphase flow systems such as injection of water into oil/gas reservoirs. It is again beyond the scope of the study to do a thorough analysis of relative permeability.

### 6.3.1 Anadarko Basin

Porosity in the Granite Wash ranges from 4 to 20 percent with an average of 8.5 percent. Permeabilities are moderate varying from about 9 to 100 mD with a mean of 23 mD. Porosity and permeability show poor correlation (Figure 5.22). At high porosity some of the sandstones have very low permeability, presumably due to an absence of interconnection between the pore spaces due to alteration of framework detrital minerals and formation of cements bridging the pore spaces.

### 6.3.2 Permian Basin

Sampling locations for the porosity in the San Andres–Grayburg Formation are displayed in Figure 6.9a. Porosity ranges from 2 to more than 20 percent with most of the values between 5 and 10 percent. Permeability sampling locations are shown on Figure 6.9c. Permeability ranges from 1 md to more than 100 md (Figure 6.9d) and seem not to be a function of depth within the data set (Figure 6.9b).

### 6.3.3 East Texas Basin

Porosity and permeability sampling locations are shown on Figure 6.10a and c, respectively. Porosity varies from less then 20 percent to more than 35 percent with most of the values between 25 and 30 percent (Figure 6.10d). Permeability covers a large range from approximately 10 md to more than 5,000 md (Figure 6.10d). The parameters are connected through a strong positive linear correlation. At the sampling scale, there is no evidence of a variation with depth (Figure 6.10b).

### 6.3.4 Fort Worth Basin

Porosity, permeability, and their relationship to well depth are shown in Figure 6.11. Porosity remains uniform at about 10 to 12 percent throughout the plotted depth intervals. Permeability varies in orders of magnitude. The more permeable units occur at depths between 3000 and 4000 ft. Porosity and permeability cross plots suggest a slight increase in permeability with increase in porosity.

### 6.3.5 Maverick Basin

Porosity, permeability, and their relationship to well depth for samples from the San Miguel and the Olmos Formations are shown in Figure 6.12. Porosity shows no trend with depth. High porosity is equally observed both at shallow and deeper intervals, indicating their development due to secondary porosity along discrete reservoir intervals. Porosity and permeability plots suggest a poor correlation between them. At high porosity some of the sandstones have low permeability. This is presumably caused by an absence of interconnection between the pore spaces and formation of cements that bridged the pore spaces.

### 6.3.6 Southern Gulf Coast Basin

Controls on the distribution of permeability and porosity in the Frio Formation have been extensively studied. Porosity is primarily related to depositional facies, with very high permeability in clean sandstones. No true depth trend is noticeable in the data set (Figure 6.13b), although Loucks et al. (1986) discerned one, but for a larger depth range. Holtz and McRae (1995) studied the porosity, permeability, and other parameters of the Frio Formation in the southern Gulf Coast Basin analysis area. They used a data set largely overlapping that used in this study. They concluded that permeability and porosity are strongly correlated with the depositional facies. They also developed statistical distribution functions for permeability and porosity. However, although we did make use of the porosity and permeability distributions in this document, we directly sampled the data set randomly rather than fitting it to a functional statistical distribution. Porosity and permeability sampling locations for the study and neighboring areas are presented in Figure 6.13a and c. A strong positive linear correlation exists between porosity and permeability in the analysis area (Figure 6.13d).

## *6.4 Formation Waters*

Collins (1987) presented a condensed summary of produced waters in the U.S. and of their properties. A more detailed analysis is available in Collins (1975). The major anion in most oil fields is chloride. Other anions include bicarbonate, sulfate, carbonate, fluoride, and organic acid salts. The major cations are sodium, calcium, and magnesium. Other cations are potassium, strontium, and barium. The pH of produced waters is typically controlled by the carbonate system. The redox potential Eh of produced waters is often reducing/negative. If the produced waters are exposed to the atmosphere, the Eh becomes positive. Eh status is important for understanding solubility of sulfur and metals such as iron. In addition, pH and Eh are the two most difficult parameters to measure accurately in situ. There are many potential sources of error in the collection and analysis of formation water samples (Appendix 3). Dissolved gases are frequent in formation waters and can easily volatilize if no precautions are taken. They are $CH_4$, $CO_2$, $N_2$, and $H_2S$, in addition to hydrocarbons. Measured temperature may be inaccurate. Outgassing, particularly of carbon dioxide, is another concern. The presence of dissolved hydrocarbons in the water also contributes to sampling difficulties because organic acids play a role in alkalinity determination. Barite is used in drilling mud and can lead to sample contamination. Ba concentrations examined and used in this study are reasonable, and no contamination is assumed. It is, however, safe to assume that formation waters are close to thermodynamic equilibrium, with some of the minerals composing the rock framework or undergoing slow-kinetics reactions. Ca concentrations are most likely determined by equilibrium with calcite, ubiquitous in the formations. Dissolved silica is controlled by amorphous silica solubility.

We used three types of sources to access information about formation waters: the USGS-produced waters database (USGS, 2002), data ordered from a vendor (IHS Energy Group, formerly Petroleum Information/Dwights), and data gathered from publications, particularly BEG publications. The total number of samples is presented in Table 6.2. A major issue was to locate the chemical analysis actual field locations. Additional work was done to obtain locational coordinates for as many of these data as possible. Locational data came from both a cross-listing of API well numbers and from field, lease, and well data obtained from a commercial license of data at drillinginfo.com.

The USGS database contains a total of 14,059 records for the state of Texas (Figure 6.14). It provides major ion concentration (Ca, Mg, Na, sometimes K, Cl, $SO_4^{2-}$, $HCO_3^-/CO_3^{2-}$), TDS, and pH in addition to location and reservoir information. The USGS database also provides a flag about the quality of the analysis. Because the information is used for geochemical modeling, the highest possible quality is needed. Details about the procedure are given in Appendix 4. However, no information is provided about important minor elements such as Si, Ba, or Sr. Chemical analyses of Fe and $H_2S$, which could figure significantly in the success of an injection well are also lacking. TDS of produced waters (Table 6.3 and Figure 6.15) varies on average from less than that of seawater (35,000 mg/L) in the San Miguel-Olmos Formation in the Maverick Basin to more than 130,000 mg/L in the Fort Worth Atoka Group. Average TDS values were used in the computation of density which was used in the AOR calculations. For each analysis area, we present a location map of the samples with size-coded symbols, as well as a Durov displaying the variability of the sample chemical composition in a given field.

### 6.4.1 Anadarko Basin

Formation water compositions from the analysis areas of the Anadarko Basin are included in Figure 6.16. Most of the data included in the figure were purchased from IHS Energy. Formation waters from the analysis area show considerable variability in chemical composition. Chemical compositions of the water are represented by Durov diagram (Figure 6.16b). TDS ranges from less than 50,000 mg/L to as high as 450,000 mg/L. Most of the formation waters are primarily Na-Cl type with minor concentrations of Ca. High variability in the ionic compositions between samples probably indicate influences of different source water, variability in formation lithology, and varying rates of chemical reactions between the matrix and the formation water.

### 6.4.2 Permian Basin

For the San Andres Formation in the Permian Basin, data were taken from Dutton and Orr (1986) and Bein and Dutton (1993). These data include chemical analyses of more than 160 formation-water samples from San Andres oil fields, including data from the northern shelf of the Midland Basin. To extend these data farther south along the Central Basin Platform, a data-purchase query was submitted to IHS Energy Group. The data set was complemented by relevant samples of the USGS database. Figure 6.17 suggests that the IHS and USGS data sets belong to the same population. TDS varies from 10,000 mg/L (sample likely contaminated and diluted by condensed water) to almost 400,000 mg/L. The average TDS is 82,000 mg/L. Recorded values for pH vary between 6 and 9. The formation water is dominated by sodium chloride with some sulfate and calcium and magnesium cations. In addition, it is well known that the San Andres Formation is $H_2S$-rich. However, none of the analyses used in this study report $H_2S$ concentrations, casting doubt on the accuracy of the analyses for pH and other volatiles.

### 6.4.3 East Texas Basin

Data on chemical composition of saline formation waters in the Woodbine Formation in East Texas were digitized from tables reported in Kreitler et al. (1987). This source lists data by well in various oil fields but lacks locational information on the wells. Locations for 47 fields were obtained using commercial data from www.drillinginfo.com available under license to the Bureau of Economic Geology. These 47 fields correspond to chemical-composition data for 131 samples. The data set was complemented by the USGS database. Figure 6.18 suggests that both data sets come from the same population, although data from Kreitler et al. (1987) look consistently higher despite a commingled spatial origin. TDS varies from less than 10,000 mg/L to almost 120,000 mg/L with an average of 57,000 mg/L. The water is dominated by sodium chloride with some amount of calcium. Values for pH vary from 6 to 8.

### 6.4.4 Fort Worth Basin

Locations of formation water samples from the analysis areas of the Fort Worth Basin are shown in Figure 6.19a. Most of the formation water composition data were purchased from IHS Energy. Most of the formation waters from the analysis area are brine in composition. Chemical compositions of the formation waters are represented by Durov diagram (Figure 6.19b). Most of the waters are Na-Cl type with minor concentrations of Ca and $SO_4$. TDS composition of the formation water varies considerably, from about 50,000 to 3000,000 mg/L.

### 6.4.5 Maverick Basin

Produced water compositions from the analysis areas of the Maverick Basin are shown in Figure 6.20. Most of the formation water composition data were purchased from IHS Energy. The formations waters in the Maverick Basin are mostly very saline to brine in composition. Chemical composition of the waters is represented by Durov diagram (Figure 6.20b). Most of the formation waters are primarily Na-Cl type with minor concentrations of Ca. TDS of the formation waters ranges from less than 1,000 to about 120,000 mg/L.

### 6.4.6 Southern Gulf Coast Basin

Data on chemical composition of saline formation waters in the Frio Formation in South Texas were digitized from tables reported in Kreitler et al. (1988) and Kreitler and Richter (1986). These data include 186 samples from Jim Wells, Nueces, Kleberg, and San Patricio Counties and additional data for the Frio in other surrounding counties for statistical comparison. The data set was complemented by the USGS database. Morton and Land (1987) did an extensive study on the chemical variations of Frio brines along the Texas Gulf Coast. Variability in the chemical composition of the brines is also evidenced in Figure 6.21, although the formation water is dominantly sodium chloride with a strong calcium and bicarbonate component. TDS varies from approximately 10,000 mg/L to almost 250,000 mg/L. Average TDS is 51,000 mg/L. Values of pH cover a large range varying from 5 to more than 9.

## *6.5 Aquifers and Brackish Water Sources*

Relevant brackish water composition data files were all downloaded from the TWDB online Groundwater Database with the guidance of the brackish water report by LBG-Guyton Associates (2003). Internal consistency of the water analyses were checked according to the guidelines outlined in Appendix 3. As a general rule, groundwater TDS increases with depth and distance from the recharge areas, as observed on the maps of major and minor aquifers in Texas (Ashworth and Hopkins, 1995). Residence time increases along flowpaths and allows for the initially fresh recharging water to dissolve more solutes. However, the picture can be and generally is considerably more complex, with mixing of water of different sources, including deep brines. Brackish waters are also typically found in the confined section of the aquifer. Man-made or natural (e.g., halite outcrops or subcrops) surface contamination could also occur, as observed along the Canadian and Red Rivers. Typical ion compositions reported in chemical analyses are for Ca, Mg, Na, Cl, $HCO_3$, and $SO_4$. K is sometimes also reported either as Na+K or independently. $SiO_2$, Fe, Ba, and Sr are also sometimes reported, especially when they might cause water quality problems. Table 6.4 shows the saturation indices for scale-forming calcite, gypsum, barite, and silica. For the most part, the feed waters are undersaturated relative to these minerals.

### 6.5.1 Anadarko Basin

The main aquifer in the analysis area of the Anadarko Basin is the Ogallala aquifer, the major water-bearing unit in the High Plains of Texas. The Ogallala aquifer is composed of sand, gravel, clay, and silt deposits (Ashworth and Hopkins, 1995). Groundwater moves slowly southeastward to the caprock edge or eastern escarpment of the High Plains. Coarse-grained sediments in the channels have the greatest permeability and supply water to wells of up to 2,000 gpm (Ashworth and Hopkins, 1995). Average yield of the Ogallala aquifer is 500 gpm. Chemical quality of the water in the aquifer is generally fresh; however, both chloride and total dissolved solids increase from north to south.

The Dockum aquifer also occupies the western portion of the analysis area. The aquifer underlies much of the Ogallala Formation. The primary water-bearing zone in the formation, the Santa Rosa, consists of up to 700 ft of sand and conglomerate, interbedded with layers of silt and shale. Concentrations of dissolved solids in the groundwater range from less than 1,000 mg/L near the eastern outcrop to more than 20,000 mg/L in the deeper parts of the aquifer to the west (Ashworth and Hopkins, 1995).

Brackish groundwater occurs in the analysis areas of the Anadarko Basin (Figure 6.22a). The Alluvium and the Dockum aquifers are more saline than the Ogallala aquifer. Average compositions of the major and trace elements in the Ogallala, Dockum and Alluvium aquifers have been included in Table 6.5. Higher chloride concentrations occur in these groundwaters than that of sodium and sulfate. Representation of the brackish groundwater in Piper and Durov diagrams suggests that most of the brackish groundwater in the analysis area falls from Ca-$HCO_3$ to Na-Cl chemical facies (Figure 6.22c). TDS of the brackish waters range from 1,000 to about 7,000 mg/L. pH of the waters ranges from 7 to 9. TDS composition versus depth plot indicates that the brackish groundwater is readily available at shallow to moderate depths in this area, suggesting no additional cost of pumping (Figure 6.22b). Trace concentrations of Ba, F, Fe, and $SiO_2$ occur in this groundwater, with potential for scale formation during desalination unless appropriately treated.

### 6.5.2 Permian Basin

Aquifers covering all or part of the Permian Basin analysis area are the Ogallala aquifer, the Santa Rosa Formation, base of the Dockum Formation, and, to a lesser extent, the Rustler aquifer. A description of the Ogallala and Dockum aquifers has been made in Section 6.5.1. The Rustler aquifer underlies the Dockum Formation. It consists mainly of limestone, dolomite, and gypsum beds. Salinity information on the aquifer is scarce but is likely the same as or higher than that of the Dockum. Only one sample of the Rustler aquifer is included in the analysis. A sample location map is provided in Figure 6.23a. The low sample density in the analysis area was offset by adding samples from neighboring counties. TDS values vary from 1,000 to 10,000 mg/L but cluster between 1,000 and 4,000 mg/L (Figure 6.23b). A large variability in chemical composition characterizes the samples.

### 6.5.3 East Texas Basin

Several East Texas Basin aquifers from the Claiborne Group (Sparta, Queen City, Carrizo) and from the Wilcox Group in the Eocene/Paleocene are considered fresh. The main underlying Cretaceous water-bearing formations are, starting with the youngest: the Nacatoch Formation, the Sub-Clarksville Formation corresponding to the Eagle Ford Formation, the Woodbine Formation, and then the Paluxy Formation laterally transitioning to the Edwards Formation. LBG-Guyton qualifies the brackish water availability of the regional water planning group D (North East Texas) as high. There are three possible sources of brackish waters: (1) confined sections of regional aquifers such as the Carrizo-Wilcox aquifer and maybe the Nacatoch aquifer; (2) shallow surficial aquifers such as the Queen City aquifer of water quality degraded by previous oil exploitation practices (pits for saltwater disposal discontinued in 1968 following a ruling by the RRC); (3) surface waters of poor quality because of upstream Permian outcrops or subcrops rich in evaporites. The Queen City does not seem to have a saltwater disposal problem, maybe because recharge fluxes are high. The Nacatoch aquifer is characterized as a minor aquifer in Texas. The Mexia-Talco Fault Zone interrupts the normal downdip flow of groundwater from the outcrop area. The segment underlying the East Texas Basin is beyond the fault zone and is likely saline (>10,000 mg/L), although few data have been reported (LBG Guyton Associates, 2003). The main source of brackish water is then the Carrizo-Wilcox aquifer.

The Carrizo-Wilcox is a major aquifer in Texas whose water availability has been recently described in a GAM ( groundwater Availability Model) model (Fryar et al., 2003). The Carrizo-Wilcox aquifer provides large volumes of fresh water but also contains abundant volumes of brackish water in deeper sections (Table 3.1) within the TWDB-defined limits of usable water (<3,000 mg/L) (Figure 6.24b).

### 6.5.4 Fort Worth Basin

The main aquifer in the analysis area of the Fort-Worth Basin is the Cretaceous-aged sediments of the Trinity Group that occur in a band from the Red River in North Texas to the Hill Country of South-Central Texas. Formations in the Trinity Group (from youngest to oldest) are the Paluxy, Glen Rose, and Twin Mountains-Travis Peak (Ashworth and Hopkins, 1995). Where the Glen Rose is thin or missing, the Paluxy and the Twin Mountains coalesce to form the Antlers Formation. The Antlers consists of up to 900 ft of sand and gravel and is used for irrigation. The Twin Mountains is the most prolific of the Trinity aquifers in North-Central Texas. Extensive development of the Trinity aquifer has occurred in the Fort Worth-Dallas region, where water levels have dropped as much as 550 ft (Ashworth and Hopkins, 1995).

Brackish to slightly-saline groundwater widely occur in the analysis areas of the Fort Worth Basin (Figure 6.25a). Average compositions of the major and trace elements in the Trinity, Graham, and Alluvium aquifers are presented in Table 6.6. Considerably more chloride occurs in the groundwater than sodium or sulfate. Representation of the brackish groundwater in Piper and Durov diagrams indicates that the groundwater in the analysis area belongs to Ca-$HCO_3$ to Na-Cl chemical facies (Figure 6.25c). TDS of the waters ranges from about 1,000 to 8,000 mg/L. TDS composition versus depth plot indicates that the brackish groundwater is readily available at shallow to moderate depths in this area, suggesting no additional cost of pumping (Figure 6.25b). Trace concentrations of Ba, F, Fe, and $SiO_2$ occur in this groundwater with potential for scale formation during desalination unless appropriately treated.

### 6.5.5 Maverick Basin

The main aquifer in the Maverick Basin analysis area is the southern portion of the Carrizo-Wilcox aquifer. The aquifer consists of fluvial-deltaic sediments of the upper Paleocene and Lower Eocene Wilcox Group and Carrizo Sand. The aquifer is bounded below by the marine clay deposits of the Midway Group and above by the Reklaw and Bigford Formations that represent a semiconfining unit between the Carrizo Sand and the shallow Queen City aquifer. These depositional sequences in ascending order are the lower Wilcox, the upper Wilcox, the Carrizo, the Queen City, the Sparta, the Yegua-

Cockfield, the Jackson, and the Vicksburg-Frio. Each of these sequences is bounded by marine shales (Galloway et al., 1994).

Brackish groundwater in the Carrizo-Wilcox, Queen City-Sparta, and Alluvium aquifers in the analysis area is moderately saline in composition (Figure 6.26a). TDS concentrations range from 1,000 to about 7,000 mg/L, with nearly equal concentrations of sodium (182 to 294 mg/L) and chloride (180 to 354 mg/L). Sulfate concentrations range from 122 to 183 mg/L (Table 6.7). Representation of the brackish groundwater from the analysis area in Piper diagrams indicates that the groundwater in the analysis area falls into Ca-$HCO_3$ to Na-Cl chemical facies (Figure 6.26c). TDS composition versus depth plot indicates that the brackish groundwater is readily available at shallow to moderate depths in this area, suggesting no additional cost of pumping (Figure 6.26b).

Trace concentrations of Ba, F, Fe, Cu, and $SiO_2$ occur in the groundwater, with a potential for scale formation during desalination unless appropriately treated. Radium, a naturally occurring radionuclide, also occurs in the groundwater in the analysis area. Nearly 20 percent of the groundwater exceeds the primary MCL of 5 picoCuries per liter (pCi/L) for drinking water. Alpha particles exceed the MCL in 7 percent of the wells (Deeds et al., 2003). Thus, if these radionuclides are not removed by treatment prior to desalination, their concentration will most likely increase in the concentrate, posing additional disposal problems.

### 6.5.6 Southern Gulf Coast Basin

The Gulf coast aquifer system in the southern Gulf Coast Basin is composed of three main aquifers: Chicot, Evangeline, and Jasper aquifers from shallowest to deepest (Ashworth and Hopkins, 1995). The system is composed of interbedded silt, sand, and clay sediment of Cenozoic age. In the analysis area, the maximum sand thickness is approximately 700 ft. Brackish water is available at shallow depths (LBG-Guyton Associates, 2003) in significant volumes (Table 3.1) within the TWDB-defined limits of usable water (<3,000 mg/L) (Figure 6.27a) across much of the analysis area.

## 6.6 Additional Parameters

Next we describe miscellaneous parameters used in the course of the calculations: average variations of temperature and pressure with depth, determination of a median sample for the formation waters, and formation compressibility.

Temperature at depth can be measured or determined by the local geothermal gradient $g_T$ when no measurement is available or when the data are not reliable. The average geothermal gradient was computed by digitizing contour lines crossing relevant counties from the "geothermal map of Texas" (Woodruff et al., 1984). The contour lines were constructed mainly from the Woodbine and younger formations. Average gradient within a county was calculated by integrating the gradient over the county with the "Spatial Analyst" tool featured in Arc Info. The county-averaged temperature gradients were then averaged over the analysis area (Table 6.8). Surface temperatures at the analysis areas are approximated by average yearly temperature at selected cities located in the chosen basin or close to it. Temperature $T$ as a function of depth $D$ is then expressed by $T(^{o}\mathrm{C})=5/9(T_0+g_rD/100-32)$ ($D$ in ft, $g_r$ in $^{o}$F/100ft), where $T_0$ is the surface temperature in $^{o}$F. The depth is computed as the midpoint between the upper and lower perforation or, when no depth is available, as the average depth of the available data points.

Because most geochemical samples do not provide pressure data and pressure is important to estimate mineral solubility, it had to be estimated from depth. This was done by fitting a line through the form H15 data set. Pressure $P$ as a function of depth is then expressed by, where $\alpha_P$ is the pressure slope (results are presented in Table 6.8):

$$P(\mathrm{psi})=\alpha_P D \ (D \text{ in ft}) \qquad \text{Equation 6-1}$$

Compressibility $c$ is the specific change in volume $V$ in response to a change in overburden pressure $\overline{\sigma}$, while the pore pressure $p$ stays constant. Matrix and water compressibility are considered isotropic, while only the vertical component of bulk compressibility is of interest in this study. Compressibility of the San Andres Formation and the Woodbine Formation are given at $9.5\mathrm{x}10^{-6}$ psi$^{-1}$ and $3.3\mathrm{x}10^{-6}$ psi$^{-1}$, respectively, in Figure 26.8 of Bass (1987). The same figure also assumes a porosity of 24 percent for the Woodbine Fm. and ~2 percent for the San Andres Fm., which is on the low side of the porosity range we report.

Table 6.1. Petrography and mineralogy summary

| Basin | Main Composition of Matrix | Cement | Additional Authigenic Material in Minor Amounts |
|---|---|---|---|
| **Anadarko** | | | |
| Quartz, feldspar, and clay | | Dolomite, calcite, and siderite | Chlorite, illite, and kaolinite |
| **Permian** | | | |
| Calcite, dolomite, anhydrite | | Rare cement: chalcedony and kaolinite | |
| **East Texas** | | | |
| Quartz, feldspars, volcanic rock fragments. More quartz to the south | | Calcite, dolomite, ankerite, quartz | Smectite, chlorite |
| **Fort Worth** | | | |
| Plagioclase, organic matter, quartz and clay | | Quartz, calcite, ankerite, and siderite | Chlorite, illite, kaolinite, and pyrite |
| **Maverick** | | | |
| Quartz, clay, feldspar, and rock fragments | | Calcite and quartz overgrowths | Kaolinite, feldspar, illite, pyrite and hematite |
| **Southern Gulf Coast** | | | |
| Quartz, feldspars, volcanic rock fragments sometimes altered to chlorite, carbonate rock fragments | | Calcite, ankerite | Kaolinite, smectites |

Table 6.2. Number of formation and brackish water samples used in the analysis

| Basin | Formation Water | Concentrate | Number of Possible Combinations (Fm. x Conc.) |
|---|---|---|---|
| Anadarko | 113 | 59 | 6,667 |
| Permian | 260 | 297 | 77,220 |
| East Texas | 381 | 52 | 19,812 |
| Fort Worth | 20 | 462 | 9,240 |
| Maverick | 131 | 150 | 19,650 |
| Southern Gulf Coast | 654 | 525 | 343,350 |

Table 6.3. Average formation water TDS

| Basin | Average TDS (g/L) | Average Density* |
|---|---|---|
| Anadarko | 104 | 1.071 |
| Permian | 82 | 1.056 |
| East Texas | 57 | 1.039 |
| Fort Worth | 136 | 1.093 |
| Maverick | 33 | 1.023 |
| Southern Gulf Coast | 51 | 1.035 |

* From Kharaka et al. (1988) formula for density as a function of TDS

Table 6.4. Saturation index of scale-forming minerals in the feed water

| | | Calcite SI | Gypsum SI | Barite SI | Silica SI |
|---|---|---|---|---|---|
| **Anadarko Basin** | | | | | |
| Raw Feed Water | Nb | 57 | 57 | 9 | 55 |
| | 5th | -0.84 | -1.91 | 0.15 | -0.95 |
| | Med | -0.49 | -0.96 | 0.31 | -0.63 |
| | 95th | -0.05 | -0.01 | 0.86 | -0.36 |
| **Permian Basin** | | | | | |
| Raw Feed Water | Nb | 297 | 297 | 35 | 262 |
| | 5th | -1.02 | -1.81 | -0.23 | -1.13 |
| | Med | -0.28 | -0.98 | -0.03 | -0.71 |
| | 95th | 0.07 | -0.23 | 0.40 | -0.20 |
| **East Texas Basin** | | | | | |
| Raw Feed Water | Nb | 52 | 43 | N/A | 39 |
| | 5th | -1.57 | -4.49 | N/A | -1.04 |
| | Med | -1.18 | -3.32 | N/A | -0.94 |
| | 95th | 0.04 | -0.15 | N/A | -0.32 |
| **Fort Worth Basin** | | | | | |
| Raw Feed Water | Nb | 460 | 457 | 3 | 427 |
| | 5th | -1.34 | -3.21 | -3.21 | -0.31 |
| | Med | -0.06 | -1.52 | -1.52 | -0.11 |
| | 95th | 0.35 | -0.69 | -0.69 | -0.02 |
| **Maverick Basin** | | | | | |
| Raw Feed Water | Nb | 148 | 148 | N/A | 144 |
| | 5th | -1.45 | -3.31 | N/A | -1.07 |
| | Med | -0.23 | -1.32 | N/A | -0.83 |
| | 95th | 0.30 | -0.47 | N/A | -0.42 |
| **South Texas Fields** | | | | | |
| Raw Feed Water | Nb | 525 | 525 | 69 | 462 |
| | 5th | -1.31 | -3.06 | -0.21 | -1.00 |
| | Med | -0.69 | -1.87 | -0.05 | -0.79 |
| | 95th | 0.07 | -1.01 | 0.34 | -0.17 |

Nb=Number of data points; 5th=5th Percentile; Med=Median; 95th=95th Percentile

## Table 6.5. Major and trace element compositions of the groundwater, Anadarko Basin

| Analyses Areas | Parameters | Major Elements (mg/l) | | | | | | | | Trace Elements (ug/l) | | |
|---|---|---|---|---|---|---|---|---|---|---|---|---|
| | | TDS | Ca | Mg | Na | HCO3 | SO4 | Cl | SiO2 | Ba | Fe | Cu |
| Anadarko Basin | | | | | | | | | | | | |
| Alluvium Aquifer | Average | 1553 | 235 | 95 | 131 | 232 | 297 | 527 | 30 | NA | NA | NA |
| | Standard Deviation | 2563 | 394 | 188 | 235 | 29 | 622 | 1115 | 12 | NA | NA | NA |
| | Maximum | 6136 | 940 | 432 | 550 | 267 | 1410 | 2520 | 51 | NA | NA | NA |
| | Minimum | 305 | 52 | 5 | 12 | 192 | 12 | 2 | 22 | NA | NA | NA |
| Ogallala Aquifer | Average | 1492 | 142 | 45 | 271 | 225 | 295 | 403 | 25 | 110 | 33 | 110 |
| | Standard Deviation | 473 | 106 | 37 | 136 | 47 | 254 | 352 | 3 | 54 | 38 | 54 |
| | Maximum | 2816 | 360 | 188 | 600 | 301 | 1090 | 1540 | 35 | 352 | 430 | 352 |
| | Minimum | 1013 | 24 | 13 | 72 | 89 | 9 | 27 | 19 | 25 | 0 | 25 |
| Ogallala and Dockum Aquifer | Average | 464 | 28 | 46 | 25 | 1 | 42 | 24 | 28 | 69 | 146 | 69 |
| | Standard Deviation | 114 | 5 | 15 | 9 | 0 | 22 | 64 | 5 | 26 | 208 | 26 |
| | Maximum | 1304 | 43 | 140 | 83 | 2 | 180 | 580 | 43 | 137 | 673 | 137 |
| | Minimum | 329 | 17 | 23 | 7 | 1 | 6 | 5 | 17 | 37 | 0 | 37 |
| Dockum Aquifer | Average | 1912 | 142 | 75 | 355 | 285 | 637 | 357 | 35 | 59 | 196 | 101 |
| | Standard Deviation | 2246 | 176 | 105 | 517 | 106 | 1059 | 565 | 21 | 28 | 369 | 109 |
| | Maximum | 8224 | 566 | 525 | 1880 | 473 | 3840 | 1879 | 83 | 124 | 1363 | 352 |
| | Minimum | 442 | 8 | 5 | 17 | 55 | 24 | 16 | 8 | 15 | 4 | 25 |

## Table 6.6. Major and trace element compositions of the groundwater, Fort Worth Basin

| Analyses Areas | Parameters | Major Elements (mg/l) | | | | | | | | Trace Elements (ug/l) | | |
|---|---|---|---|---|---|---|---|---|---|---|---|---|
| Fort Worth Basin | | | | | | | | | | | | |
| | | TDS | Ca | Mg | Na | $HCO_3$ | $SO_4$ | Cl | $SiO_2$ | F | Ba | Cu |
| Alluvium Aquifer | Average | 1356 | 242 | 96 | 387 | 398 | 401 | 759 | 16 | 1 | 53 | NA |
| | Standard Deviation | 959 | 149 | 88 | 287 | 114 | 359 | 630 | 4 | 0 | 31 | NA |
| | Maximum | 5308 | 655 | 497 | 1480 | 615 | 1450 | 2700 | 27 | 2 | 97 | NA |
| | Minimum | 289 | 38 | 29 | 130 | 146 | 9 | 149 | 2 | 0 | 20 | NA |
| Trinity Aquifer | Average | 2469 | 102 | 27 | 724 | 506 | 219 | 872 | 13 | 1 | 87 | NA |
| | Standard Deviation | 6159 | 140 | 34 | 2519 | 173 | 235 | 3455 | 4 | 1 | 138 | NA |
| | Maximum | 58633 | 730 | 176 | 23754 | 1057 | 1504 | 32313 | 20 | 12 | 526 | NA |
| | Minimum | 1001 | 1 | 0 | 77 | 140 | 0 | 52 | 2 | 0 | 20 | NA |
| Graham Aquifer | Average | 2052 | 139 | 37 | 578 | 431 | 310 | 754 | 13 | NA | NA | NA |
| | Standard Deviation | 1165 | 143 | 37 | 473 | 104 | 343 | 744 | 4 | NA | NA | NA |
| | Maximum | 5851 | 800 | 248 | 2210 | 752 | 1870 | 3350 | 28 | NA | NA | NA |
| | Minimum | 1008 | 5 | 1 | 55 | 128 | 0 | 57 | 7 | NA | NA | NA |

## Table 6.7. Major and trace element compositions of the groundwater, Maverick Basin

| Analyses Areas | Parameters | Major Elements (mg/l) | | | | | | | | Trace Elements (ug/l) | | | |
|---|---|---|---|---|---|---|---|---|---|---|---|---|---|
| Maverick Basin | | **TDS** | **Ca** | **Mg** | **Na** | **$HCO_3$** | **$SO_4$** | **Cl** | **$SiO_2$** | **Ba** | **F (mg/l)** | **Fe** | **Cu** |
| Alluvium aquifer | Average | 1,233 | 153 | 28 | 178 | 289 | 264 | 528 | 42 | 68 | 1 | 21 | 15 |
| | Standard Deviation | 781 | 67 | 17 | 209 | 76 | 221 | 357 | 15 | 76 | 0 | 16 | 9 |
| | Maximum | 3,295 | 277 | 58 | 746 | 411 | 690 | 1,159 | 57 | 327 | 1 | 80 | 42 |
| | Minimum | 439 | 74 | 6 | 19 | 207 | 88 | 202 | 22 | 19 | 0 | 10 | 3 |
| Carrizo aquifer | Average | 2,027 | 86 | 21 | 538 | 543 | 250 | 557 | 20 | 92 | 0 | 374 | 9 |
| | Standard Deviation | 1,044 | 118 | 28 | 417 | 363 | 204 | 528 | 7 | 69 | 1 | 682 | 10 |
| | Maximum | 5,639 | 550 | 137 | 2,040 | 1,617 | 831 | 2,609 | 36 | 802 | 4 | 6,860 | 92 |
| | Minimum | 1,034 | 2 | 0 | 64 | 43 | 1 | 76 | 2 | 0 | 0 | 0 | 0 |
| Queen City aquifer | Average | 1,494 | 110 | 28 | 311 | 360 | 232 | 411 | 20 | 97 | 1 | 854 | 9 |
| | Standard Deviation | 900 | 170 | 23 | 145 | 98 | 193 | 449 | 13 | 160 | 1 | 1,269 | 10 |
| | Maximum | 4,285 | 713 | 81 | 565 | 505 | 872 | 1,910 | 68 | 500 | 2 | 5,330 | 35 |
| | Minimum | 437 | 4 | 3 | 29 | 189 | 34 | 12 | 10 | 15 | 0 | 15 | 1 |
| Carrizo-Wilcox aquifer | Average | 2,017 | 145 | 33 | 466 | 352 | 333 | 645 | 22 | 54 | 0 | 214 | 12 |
| | Standard Deviation | 1,322 | 152 | 29 | 453 | 151 | 315 | 598 | 13 | 32 | 1 | 298 | 20 |
| | Maximum | 6,663 | 762 | 137 | 1,933 | 976 | 1,779 | 2,609 | 68 | 105 | 1 | 920 | 57 |
| | Minimum | 1,003 | 2 | 1 | 19 | 43 | 39 | 79 | 2 | 16 | 0 | 10 | 1 |
| Wilcox aquifer | Average | 2,445 | 125 | 28 | 705 | 385 | 556 | 800 | 24 | 72 | 1 | 214 | 24 |
| | Standard Deviation | 2,234 | 131 | 39 | 762 | 188 | 687 | 977 | 11 | 48 | 1 | 298 | 65 |
| | Maximum | 6,663 | 353 | 121 | 1,840 | 744 | 1,779 | 2,435 | 51 | 147 | 2 | 920 | 229 |
| | Minimum | 437 | 2 | 1 | 87 | 99 | 53 | 70 | 15 | 8 | 0 | 10 | 2 |

Table 6.8. Data for temperature/depth and pressure/depth functions

| Basin | Surface Temperature ($^oF$) | Temperature Gradient ($^oF/100ft$) | Pressure Slope ($psi^{-1}$) |
|---|---|---|---|
| **Anadarko** | 63.5<br>(Wichita Fall) | 1.5 | 0.164 |
| **Permian** | 63<br>(Midland) | 1.180 | 0.312 |
| **East Texas** | 65<br>(Tyler) | 1.724 | 0.290 |
| **Fort Worth** | 67<br>(Waco) | 1.75 | 0.303 |
| **Maverick** | 72<br>(Brownsville) | 1.5 | 0.318 |
| **Sth. Gulf Coast** | 72<br>(Brownsville – Corpus Christi) | 1.667 | 0.327 |

Note: hydrostatic pressure slope is 0.433 $psi^{-1}$.

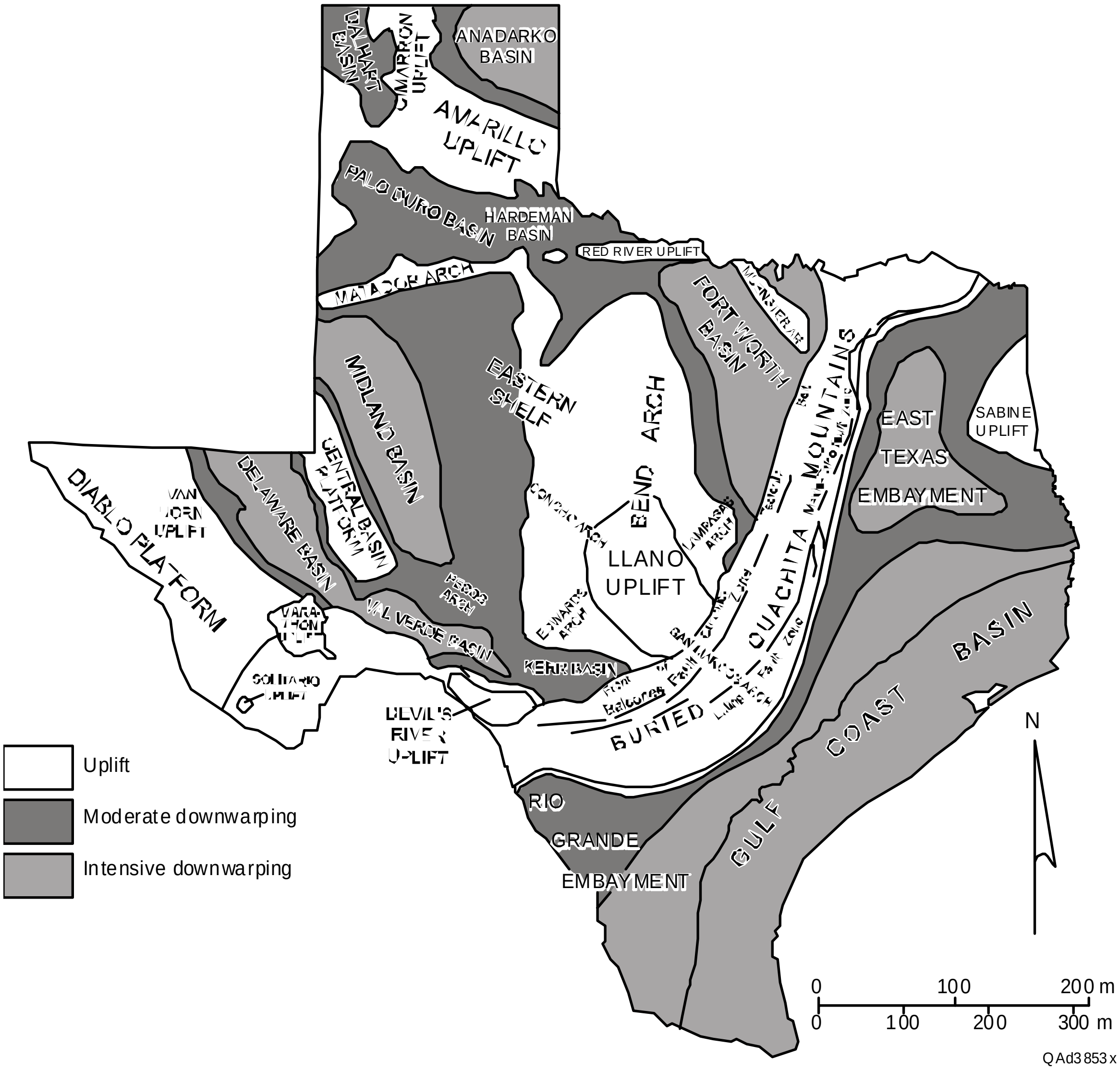

Figure 6.1. Generalized tectonic map of Texas showing location of sedimentary basins (modified from Kreitler, 1989)

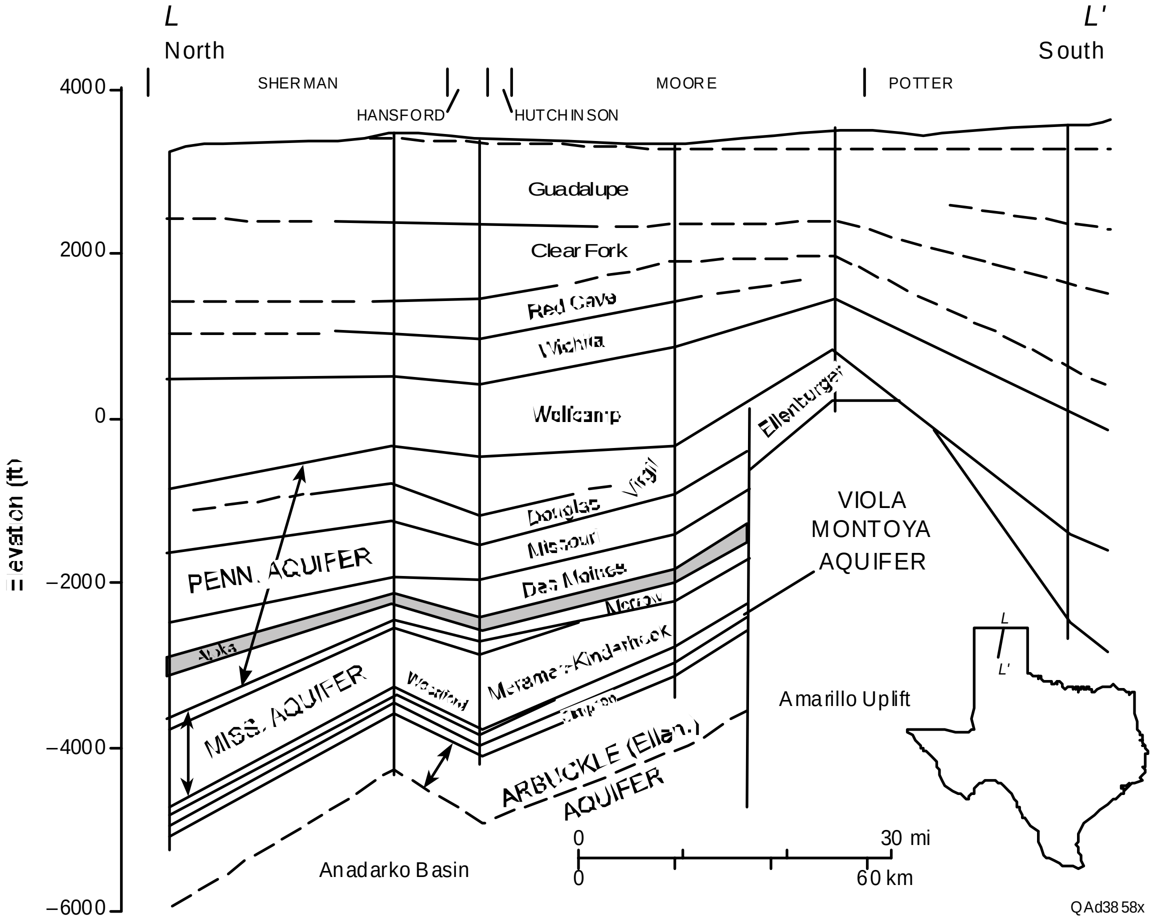

Figure 6.2. Anadarko Basin: simplified cross section across the analysis area (modified from Core Laboratories Inc., 1972a)

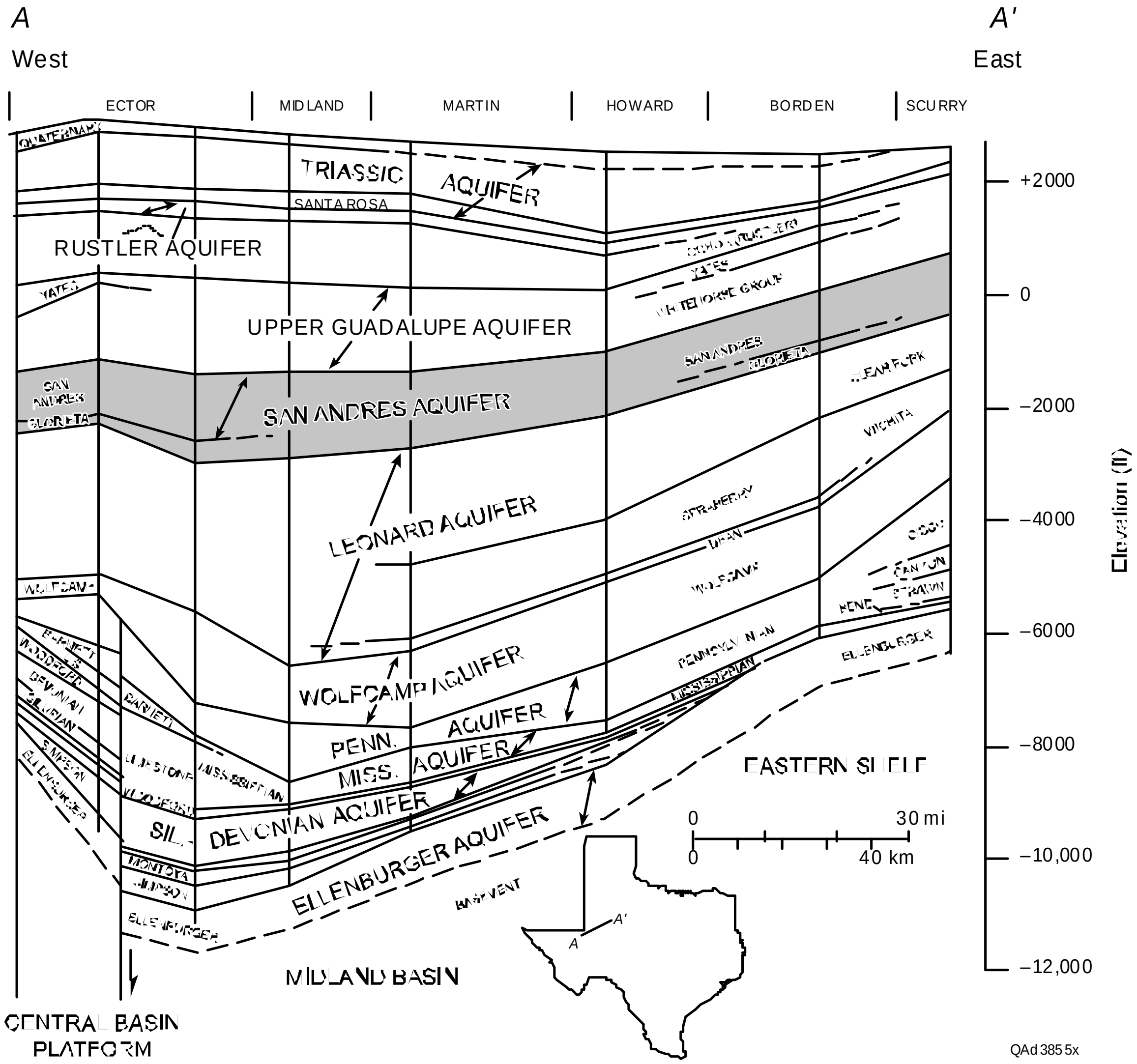

Figure 6.3. Permian Basin: simplified cross section across the analysis area (modified from Core Laboratories Inc., 1972a)

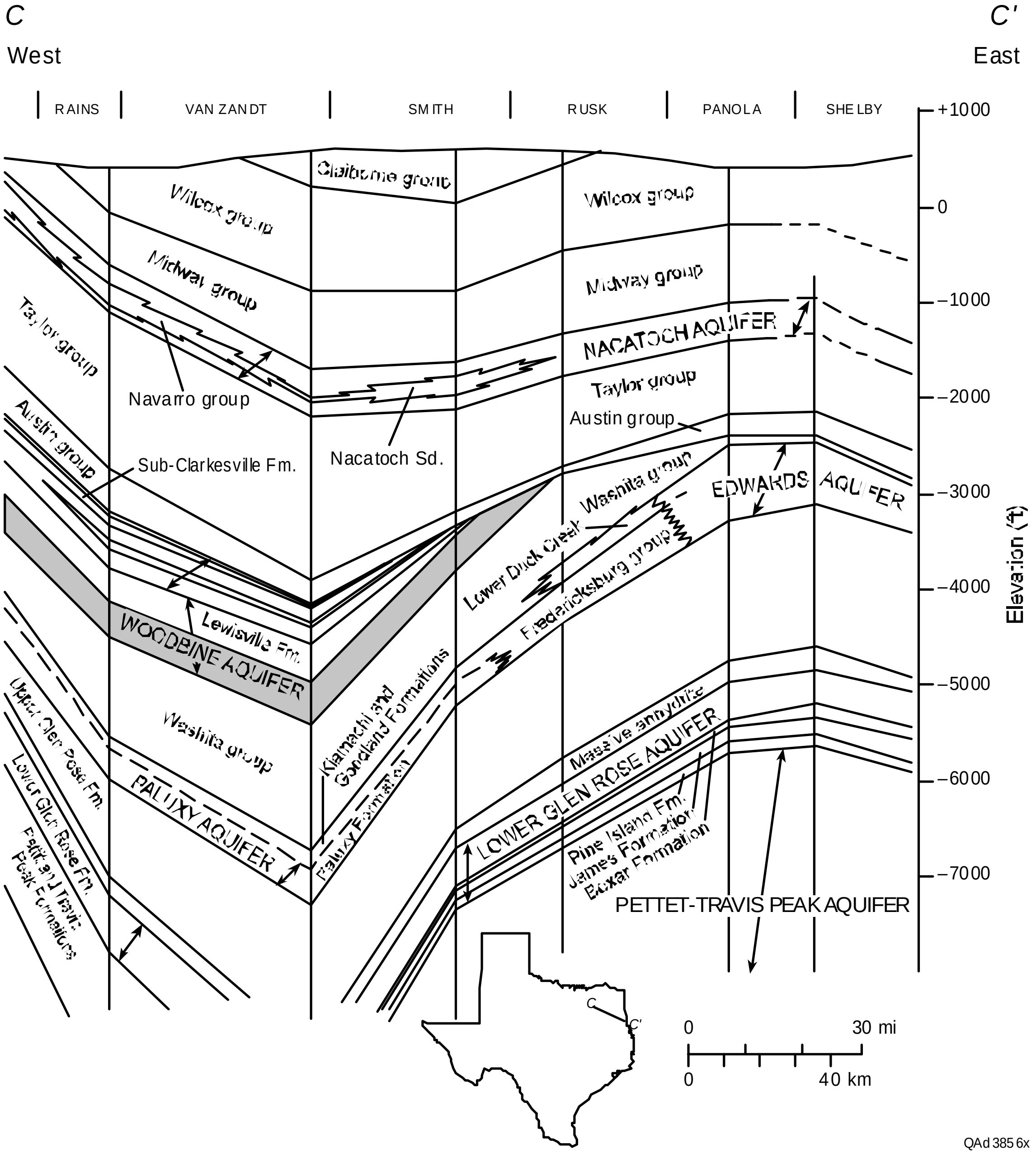

Figure 6.4. East Texas Basin: simplified cross section across the analysis area (modified from Core Laboratories Inc., 1972a)

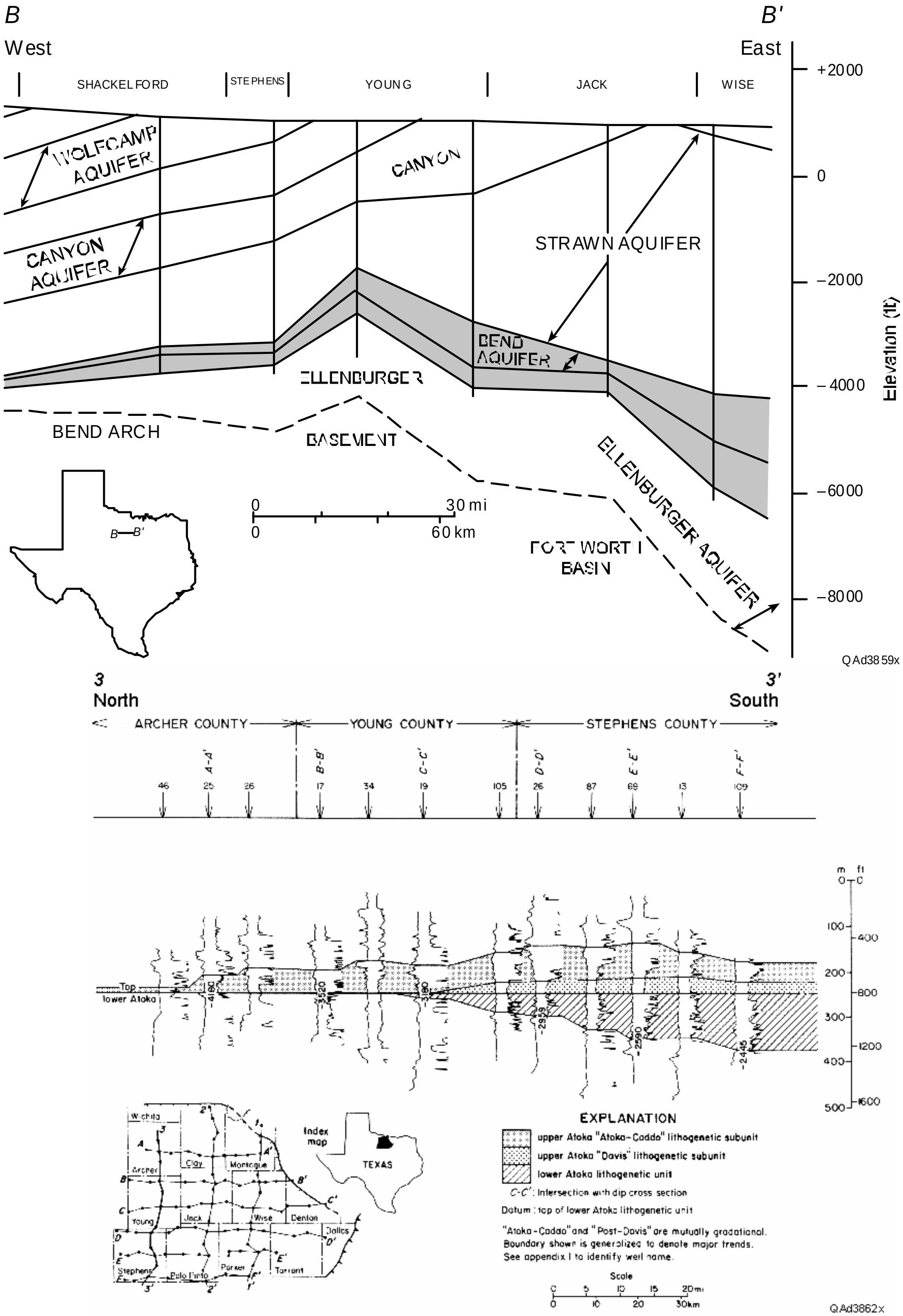

Figure 6.5. Fort Worth Basin: (a) simplified cross section across the analysis area (modified from Core Laboratories Inc., 1972a); (b) cross section through Young and Stephens Counties showing distribution and geometry of the Atoka reservoir units (adapted from Thompson, 1982)

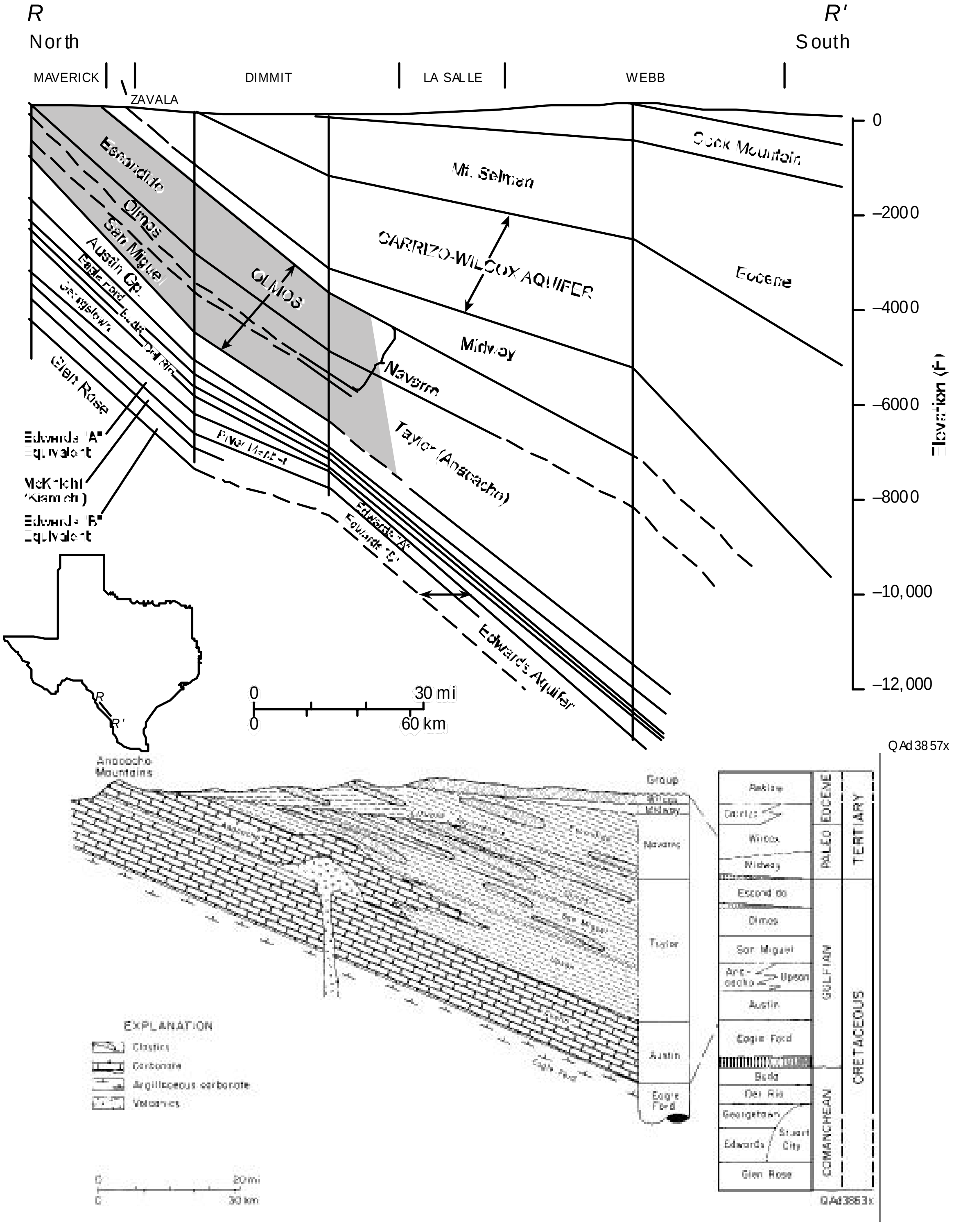

Figure 6.6. Maverick Basin: (a) simplified cross section across the analysis area (modified from Core Laboratories Inc., 1972a); (b) stratigraphic-cross section showing in detail distribution and geometry of the Olmos and the San Miguel reservoir sandstones. Distribution of the volcanic plug is also shown (adapted from Weise, 1980)

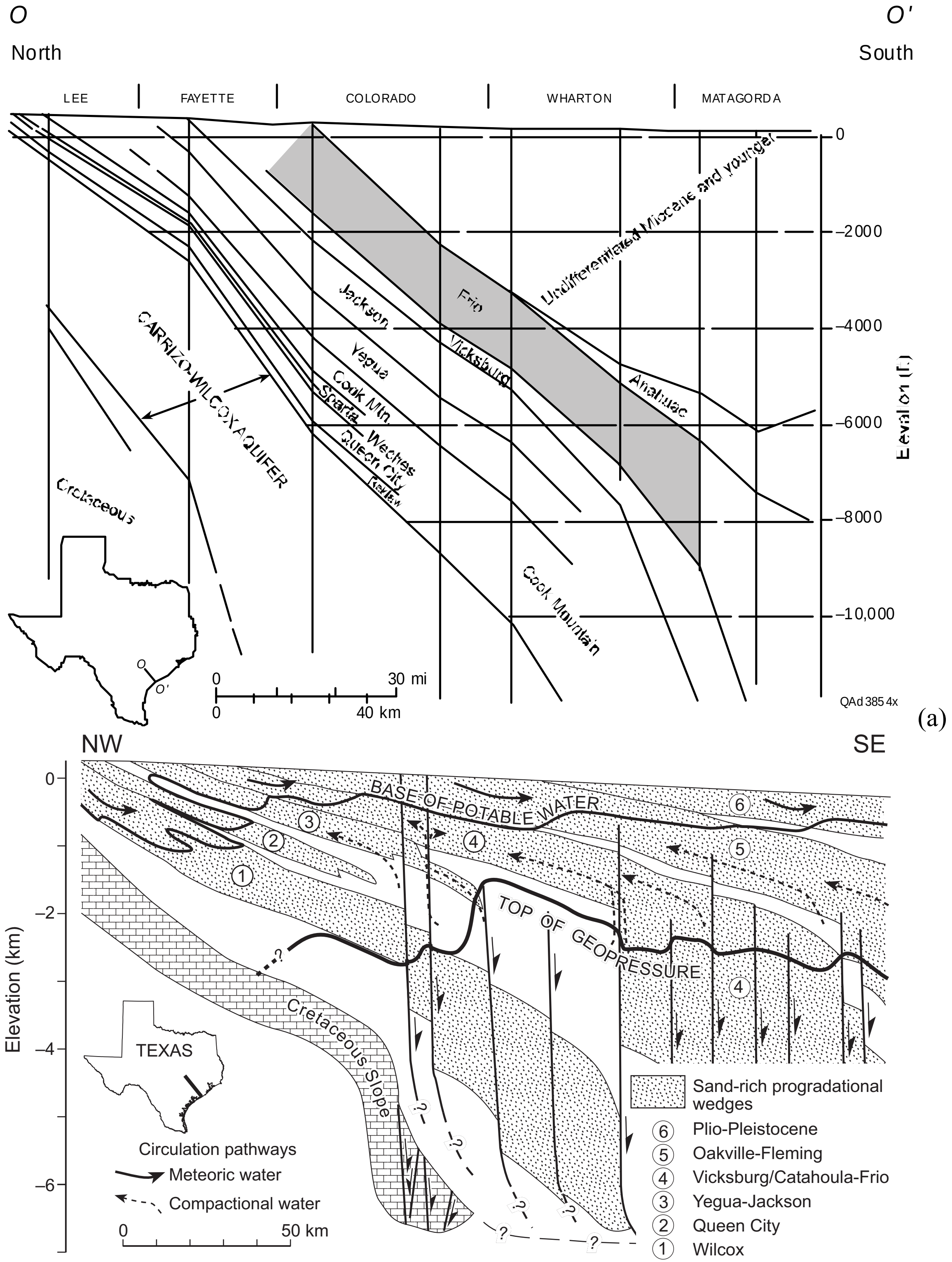

Figure 6.7. Southern Gulf Coast: (a) simplified cross section (modified from Core Laboratories Inc., 1972a); (b) major sand-rich progradational packages and growth fault zones beneath the Texas coastal plain (adapted from Galloway, 1982, and Galloway et al., 1982)

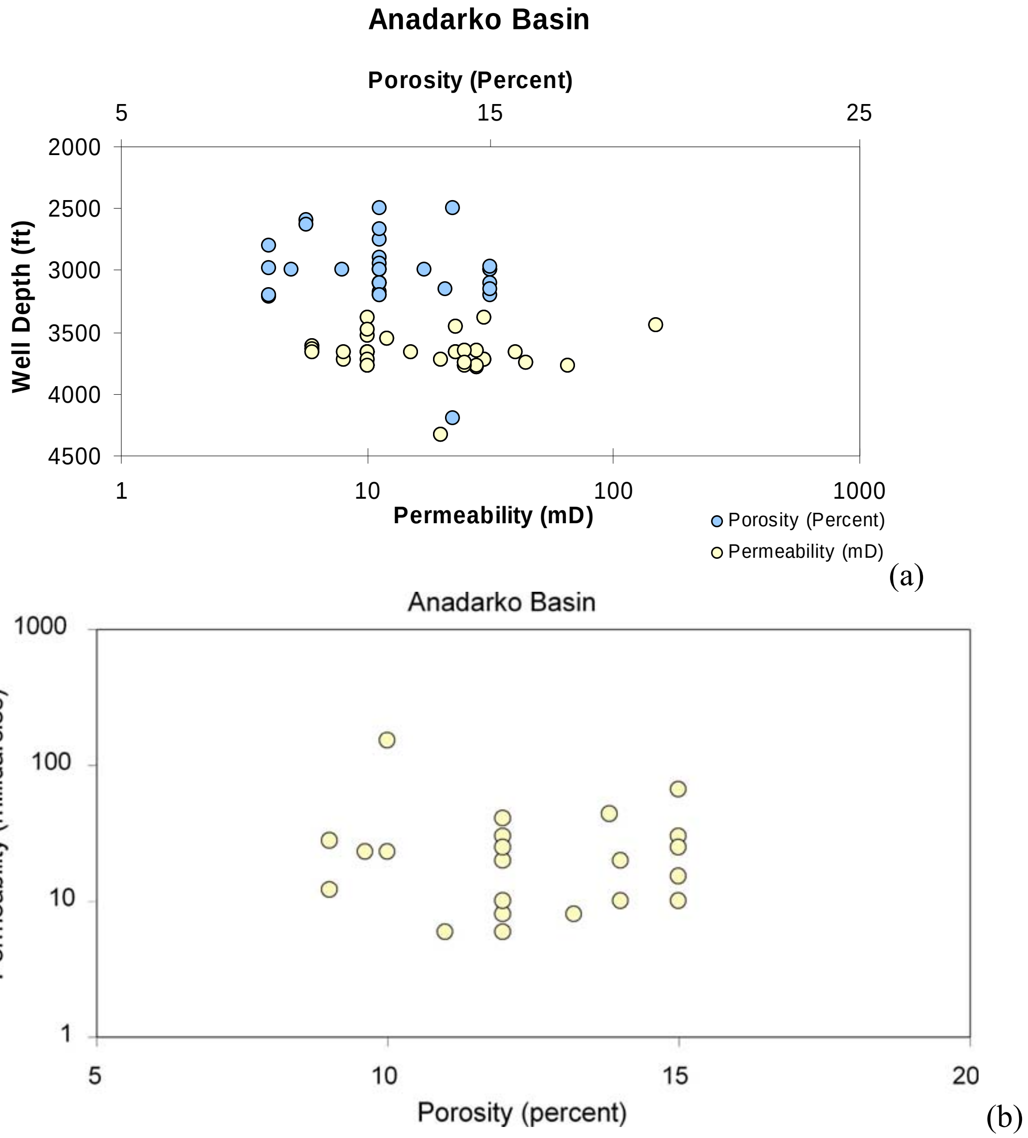

Figure 6.8. (a) Porosity, permeability trend with increasing well depth, and (b) porosity-permeability relationship in the producing reservoirs of the Anadarko Basin

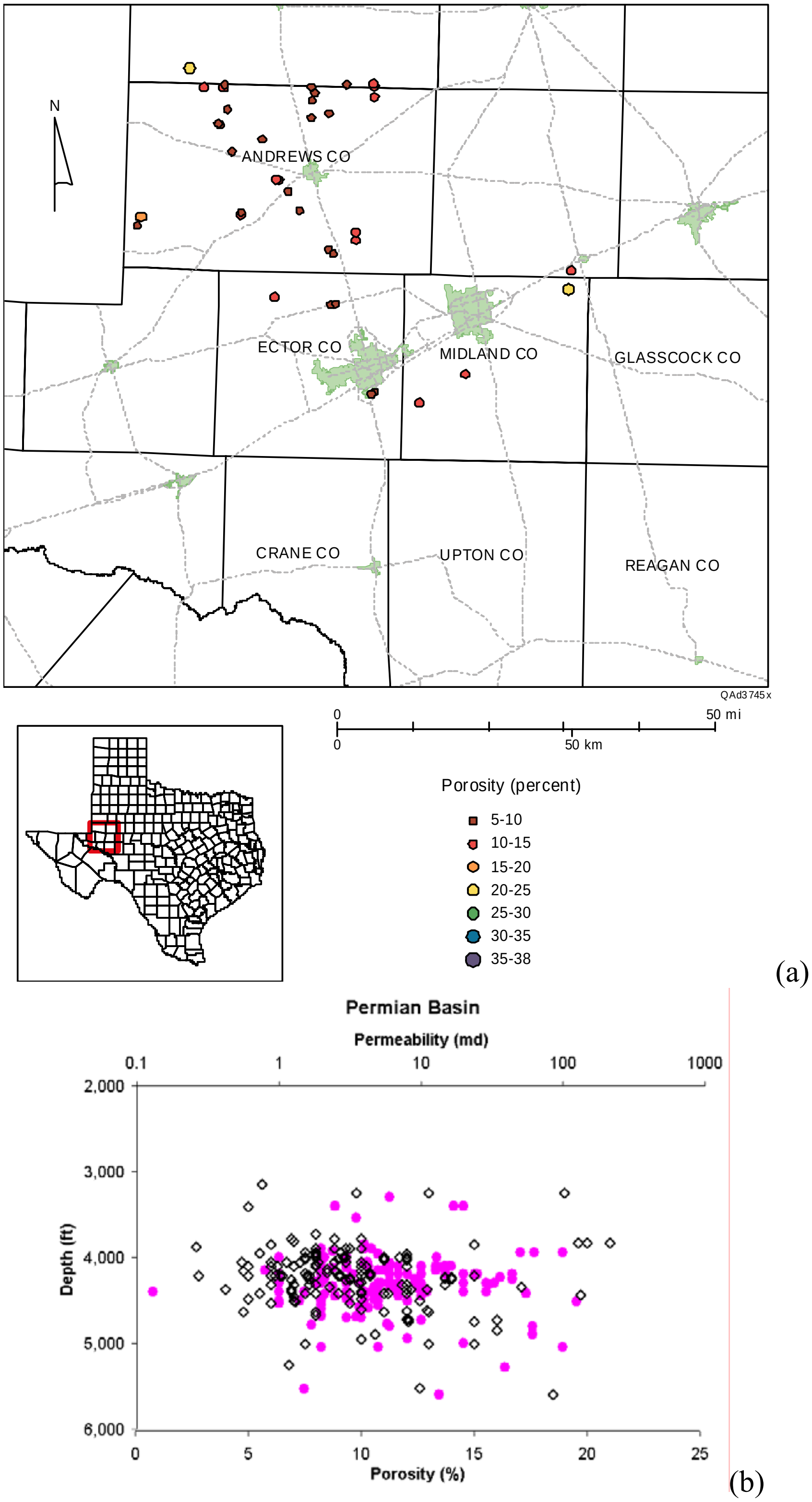

open diamonds = porosity; circles = permeability

Figure 6.9. (a) Spatial distribution of porosity; (b) permeability and porosity variations with depth; (c) spatial distribution of permeability; (d) permeability-porosity cross plot (San Andres Formation)

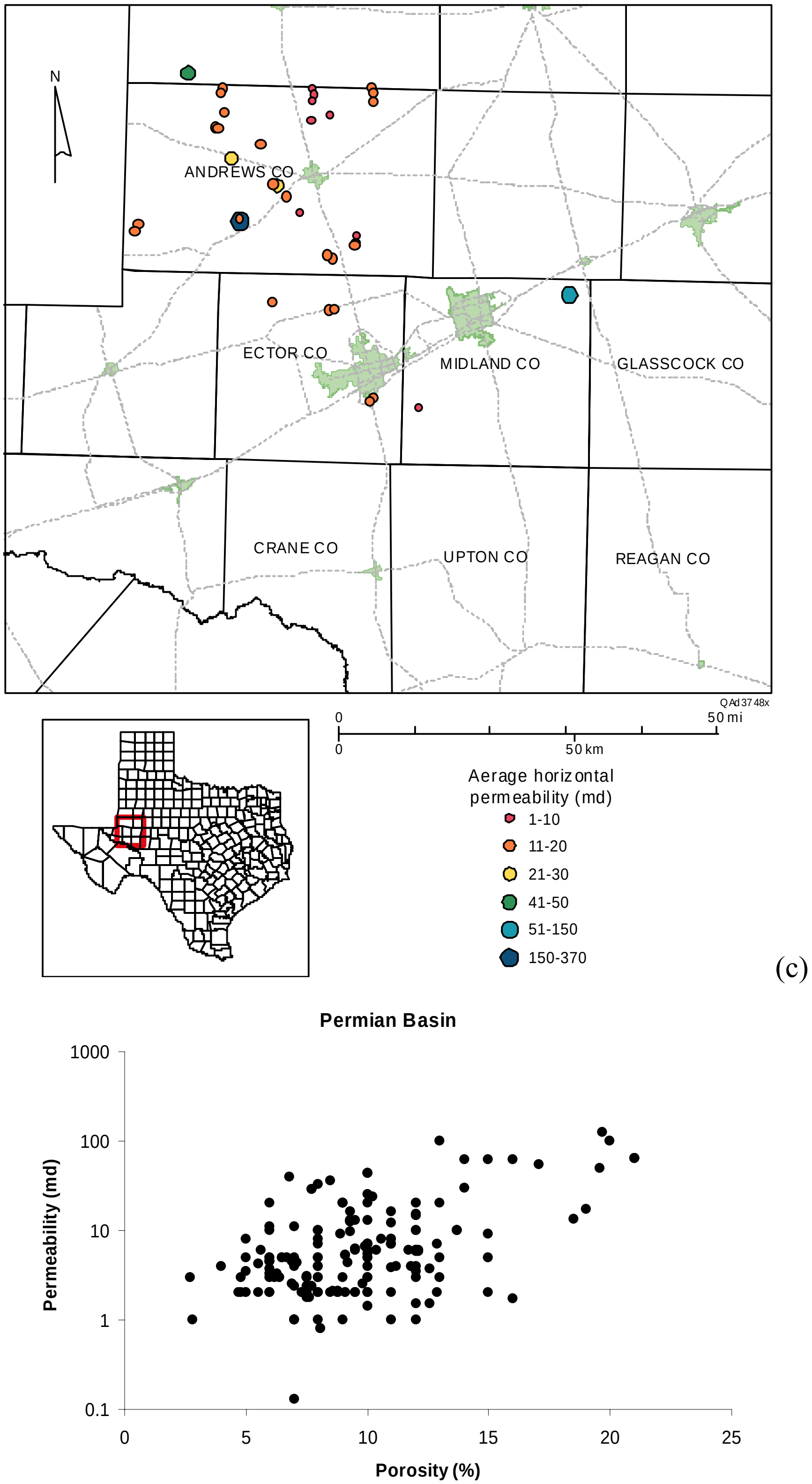

Figure 6.9 (continued). (a) Spatial distribution of porosity; (b) permeability and porosity variations with depth; (c) spatial distribution of permeability; (d) permeability-porosity cross plot (San Andres Formation)

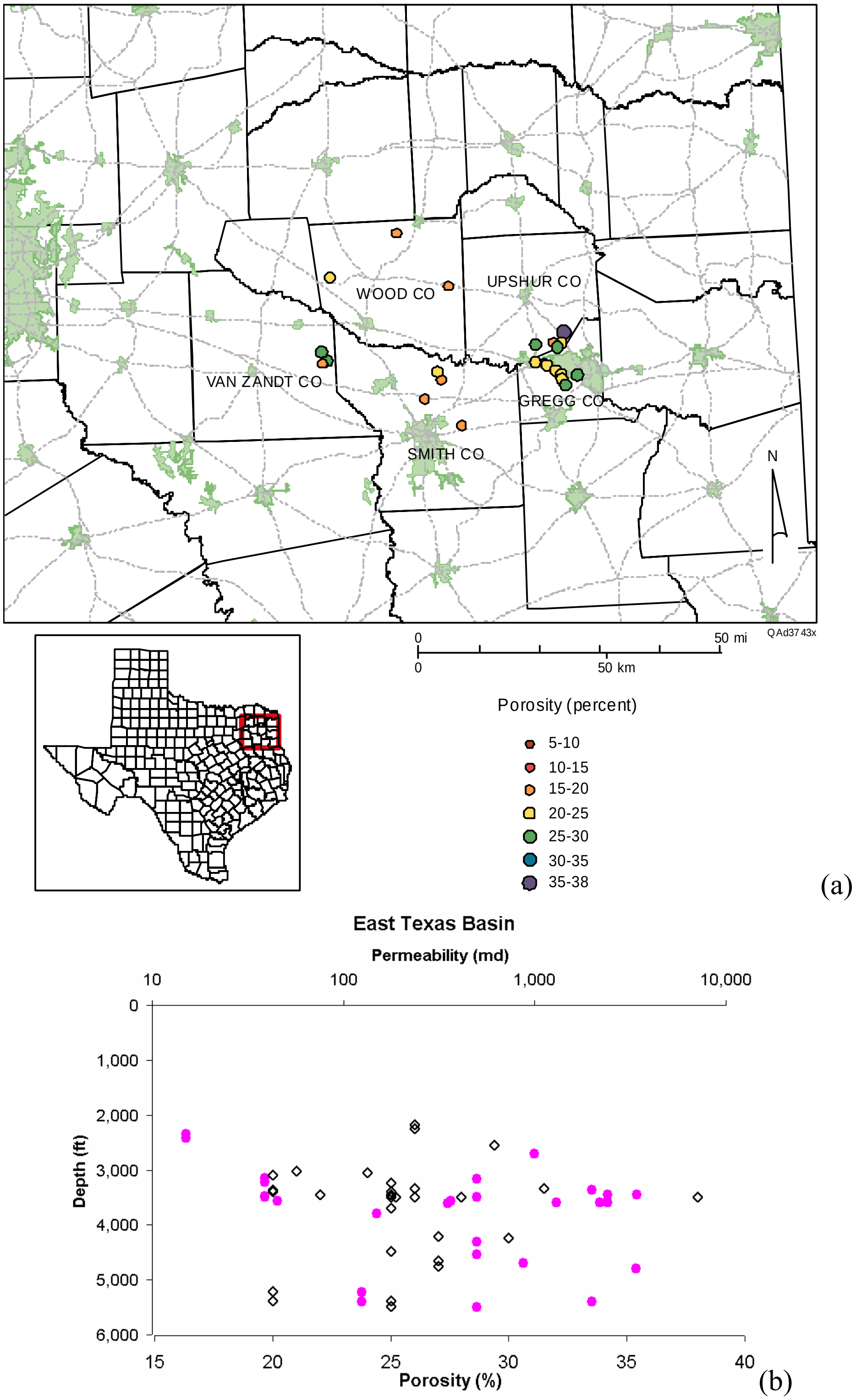

open diamonds = porosity; circles = permeability

Figure 6.10. (a) Spatial distribution of porosity; (b) permeability and porosity variations with depth; (c) spatial distribution of permeability; (d) permeability-porosity cross plot (Woodbine Formation)

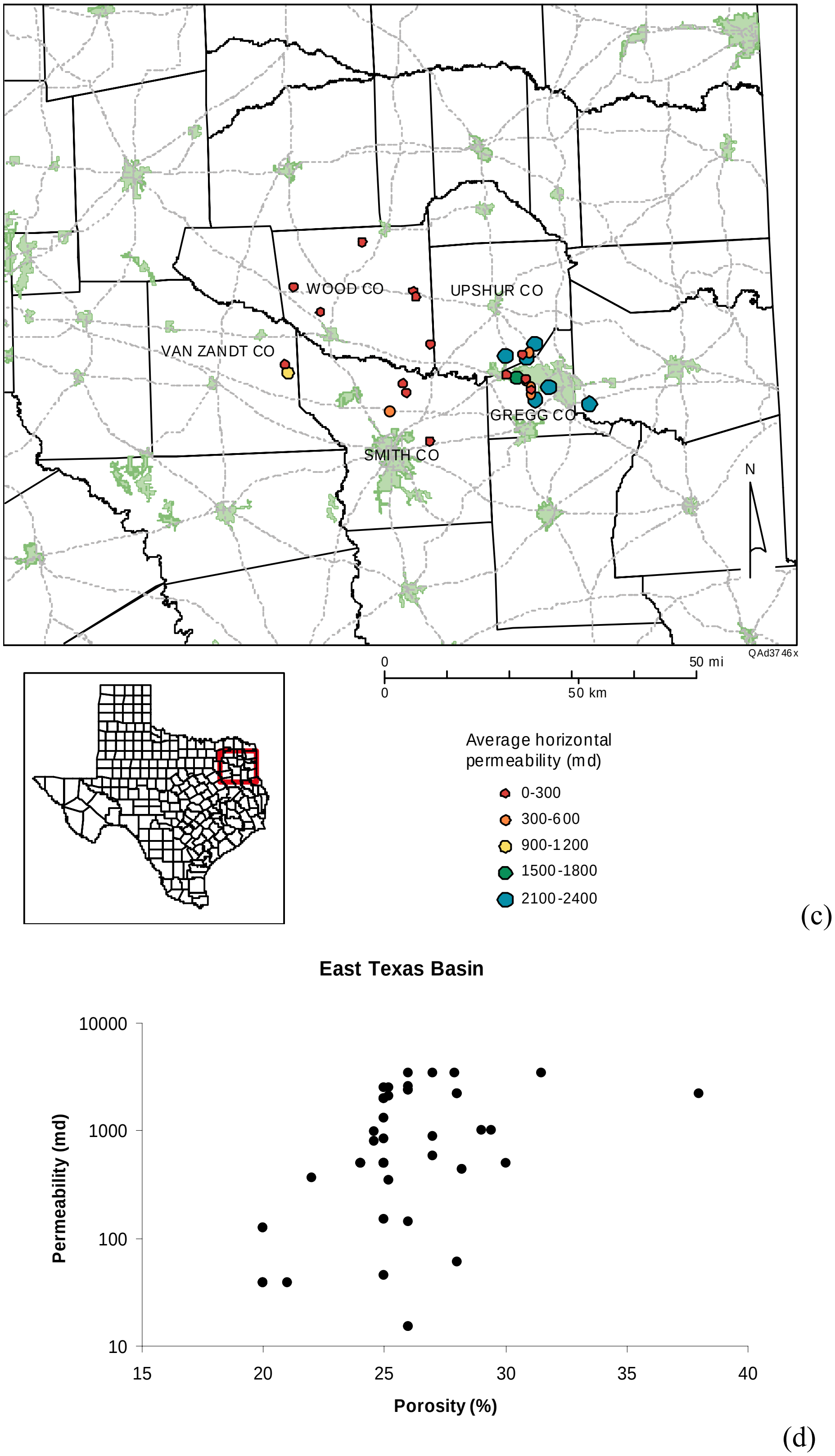

Figure 6.10 (continued). (a) Spatial distribution of porosity; (b) permeability and porosity variations with depth; (c) spatial distribution of permeability; (d) permeability-porosity cross plot (Woodbine Formation)

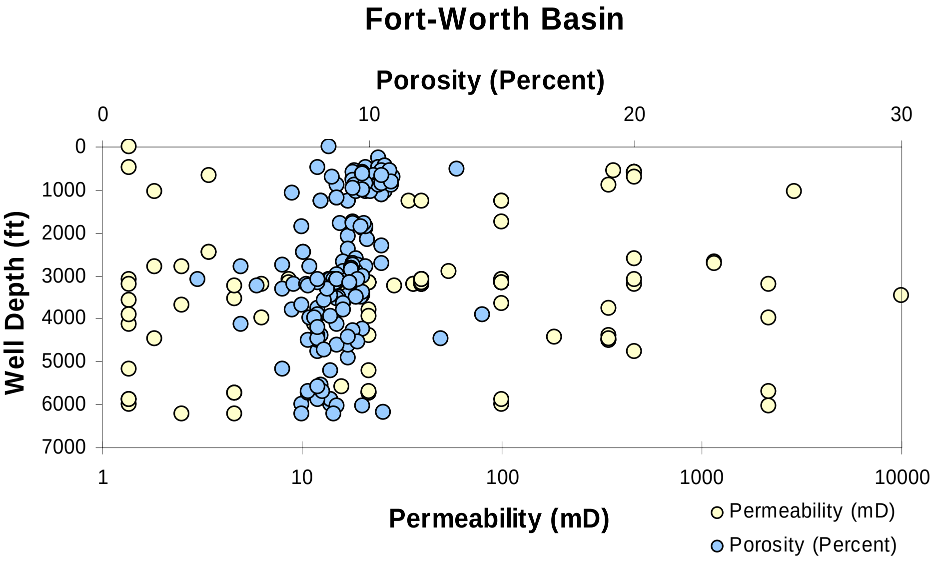

(a)

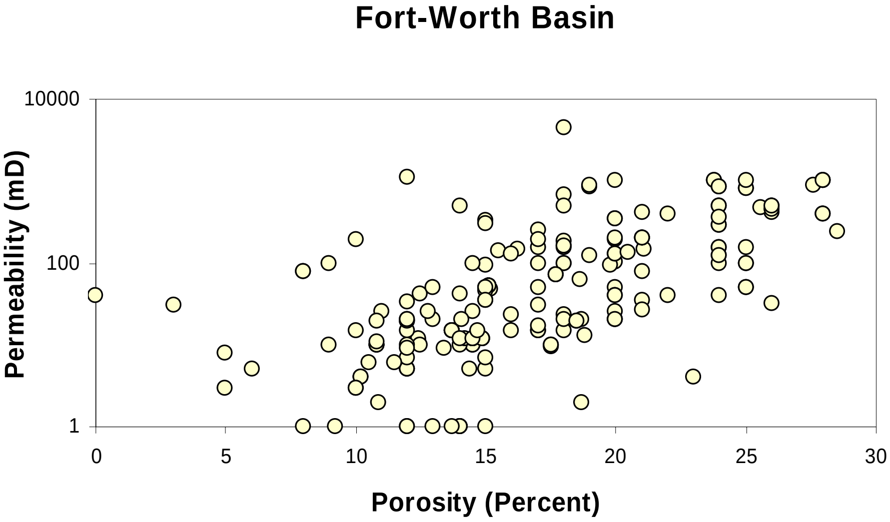

(b)

Figure 6.11. (a) Porosity, permeability trend with increasing well depth, and (b) porosity-permeability relationship in the producing reservoirs of the Fort Worth Basin

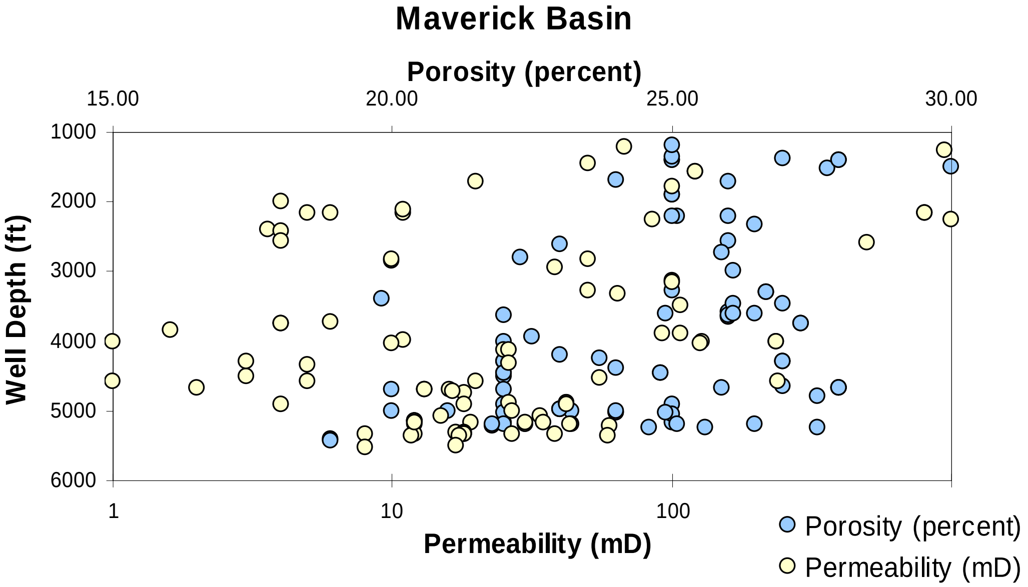

(a)

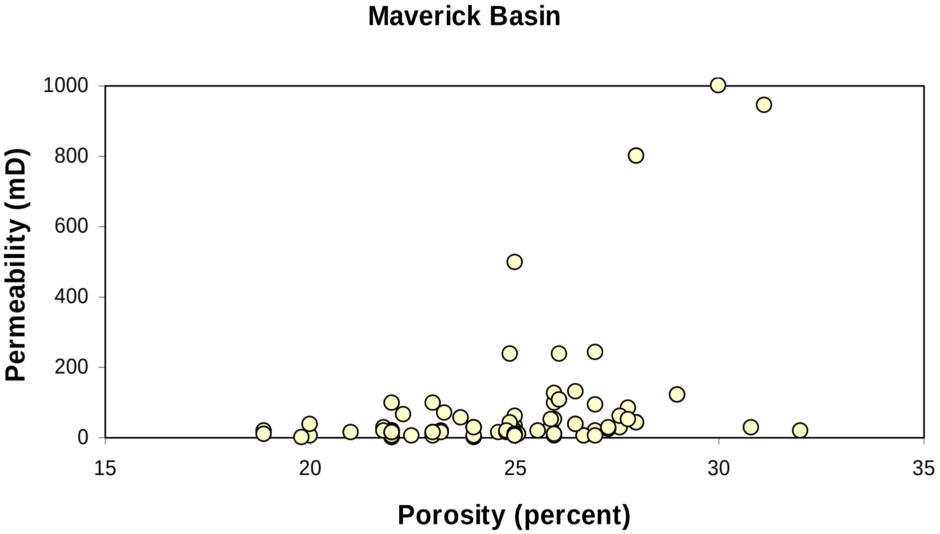

(b)

Figure 6.12. (a) Porosity, permeability trend with increasing well depth, and (b) porosity-permeability relationship in the producing reservoirs of the Maverick Basin

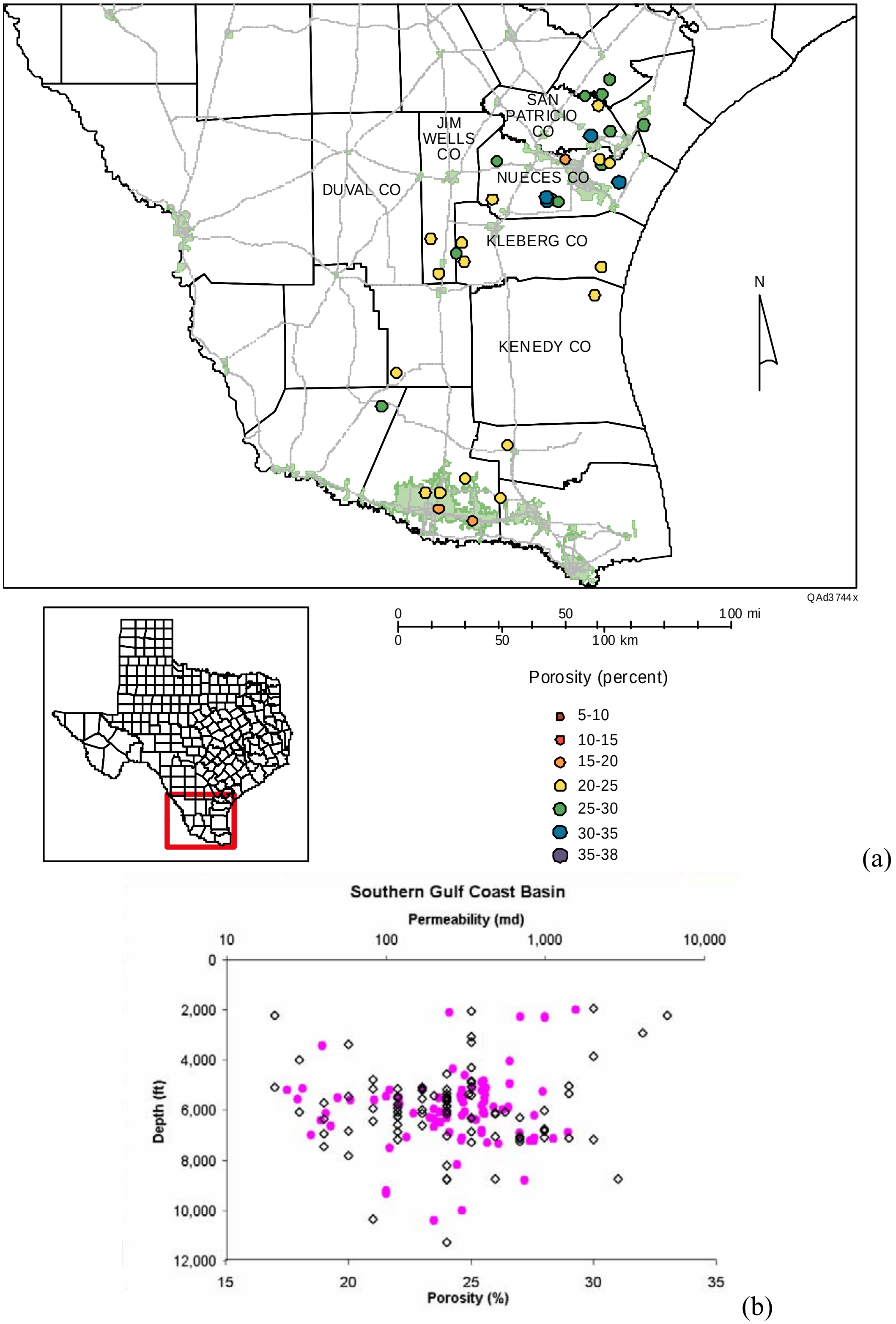

open diamonds = porosity; circles = permeability

Figure 6.13. (a) Spatial distribution of porosity; (b) permeability and porosity variations with depth; (c) spatial distribution of permeability; (d) permeability-porosity cross plot (Frio Formation)

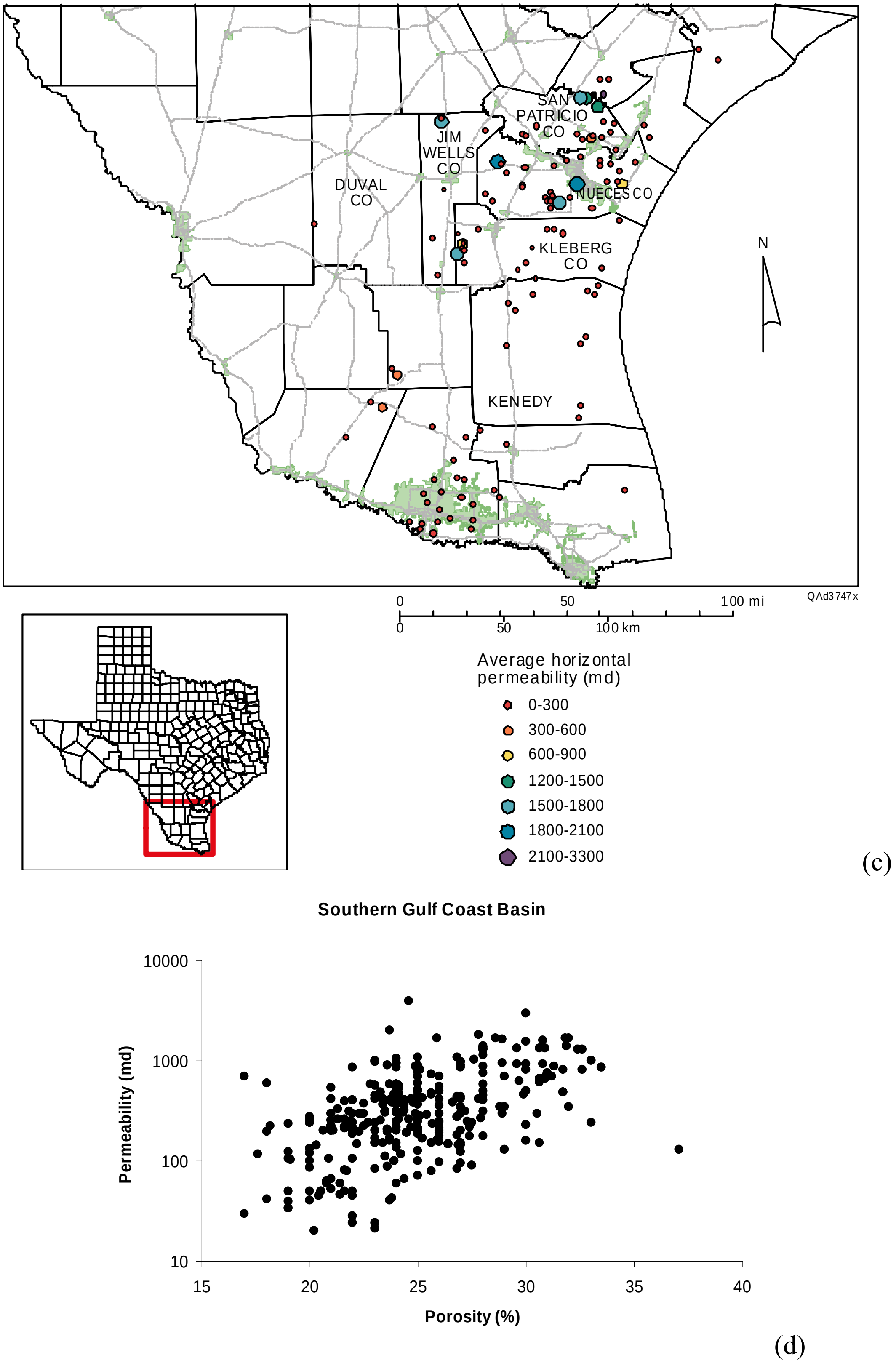

Figure 6.13 (continued). (a) Spatial distribution of porosity; (b) permeability and porosity variations with depth; (c) spatial distribution of permeability; (d) permeability-porosity cross plot (Frio Formation)

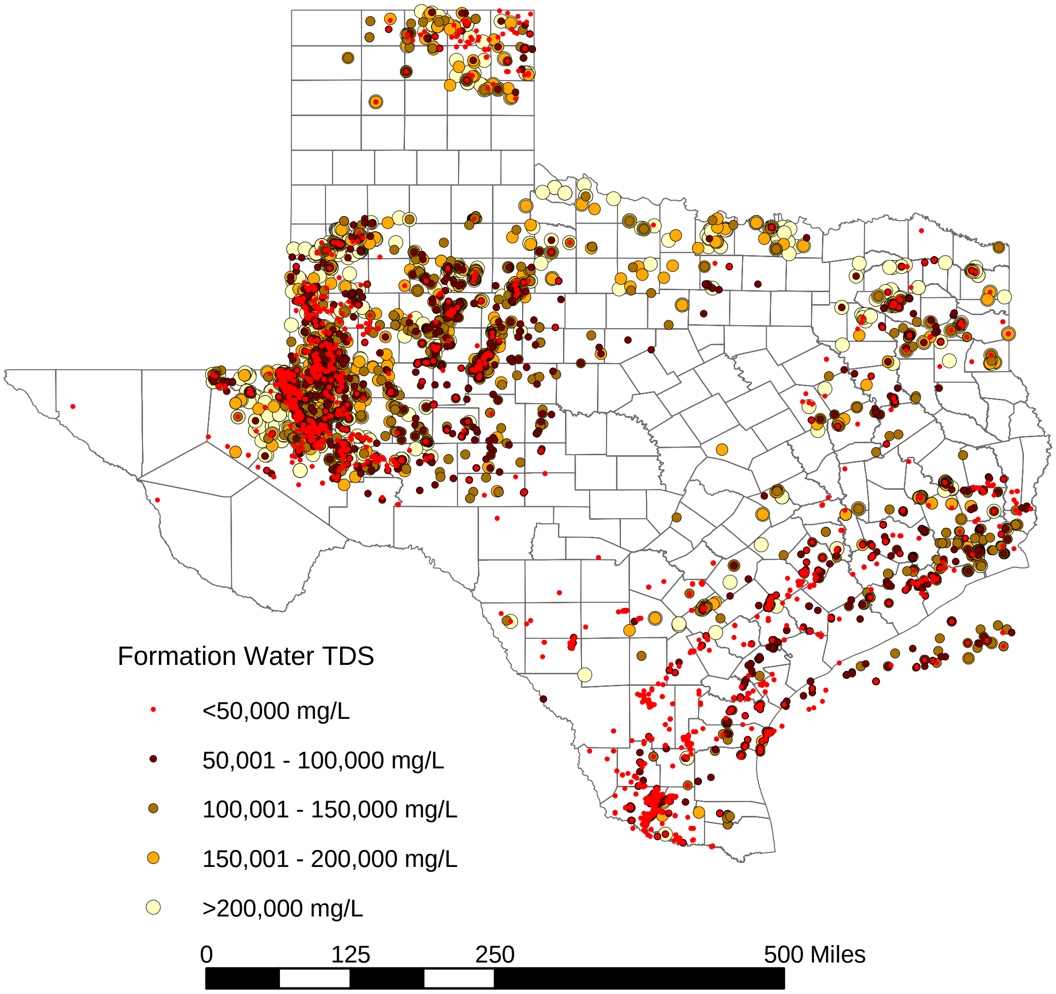

Figure 6.14. Map of formation water TDS in Texas (USGS database, 2002)

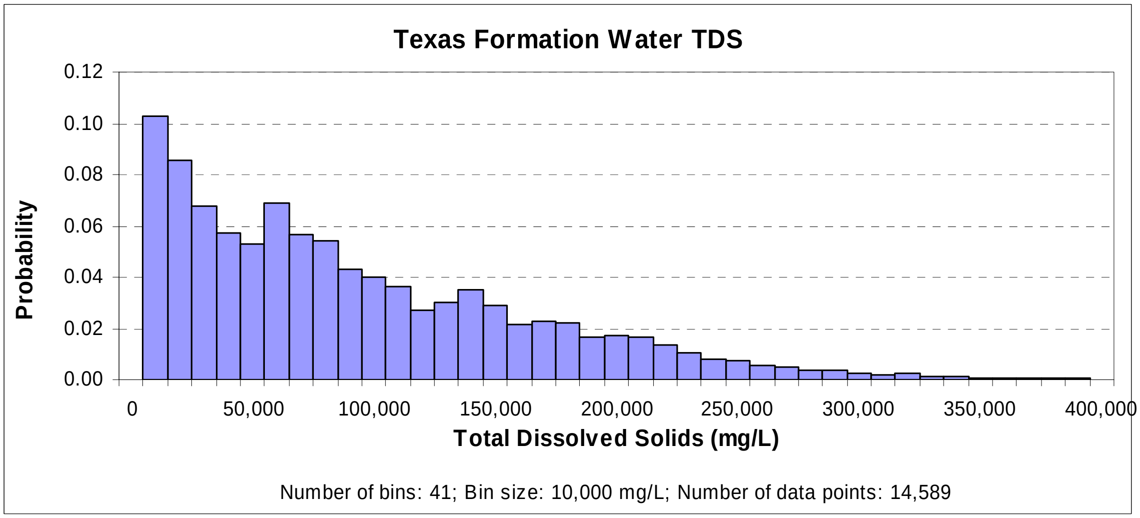

Figure 6.15. Histogram of formation water TDS in Texas (USGS database, 2002)

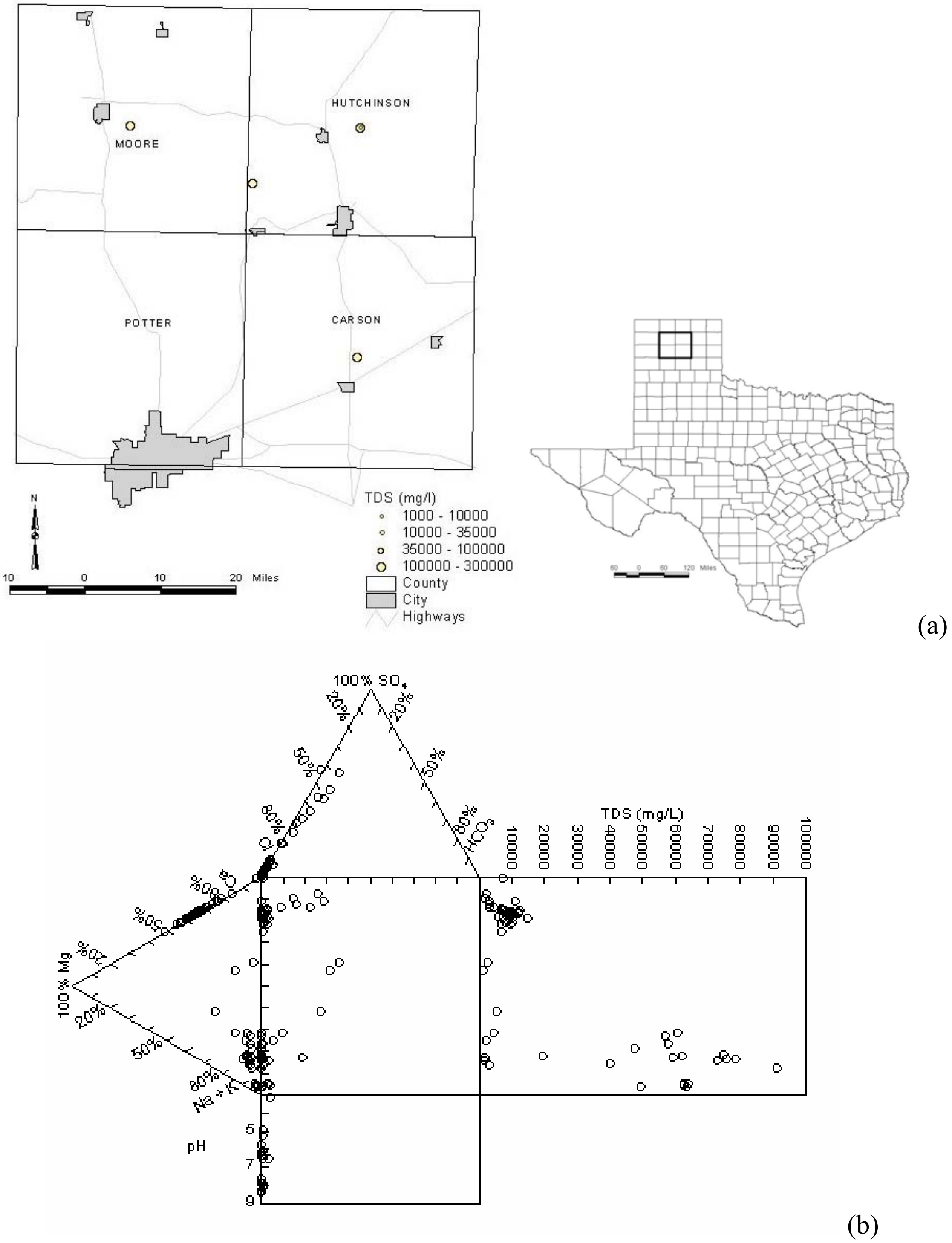

Figure 6.16. (a) Spatial distribution of TDS compositions; (b) Durov plots of formation samples (Anadarko Basin)

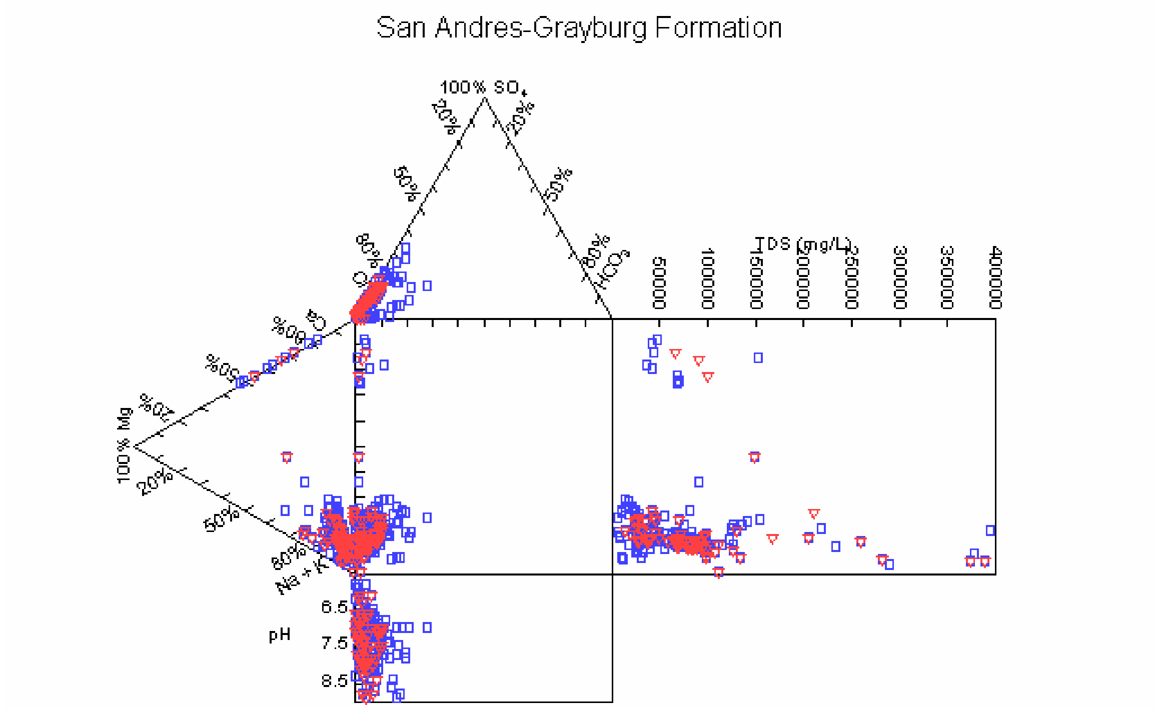

(blue squares = USGS data; red triangles = IHS data)

Figure 6.17. Durov plots of the San Andres-Grayburg Formation samples (Permian Basin)

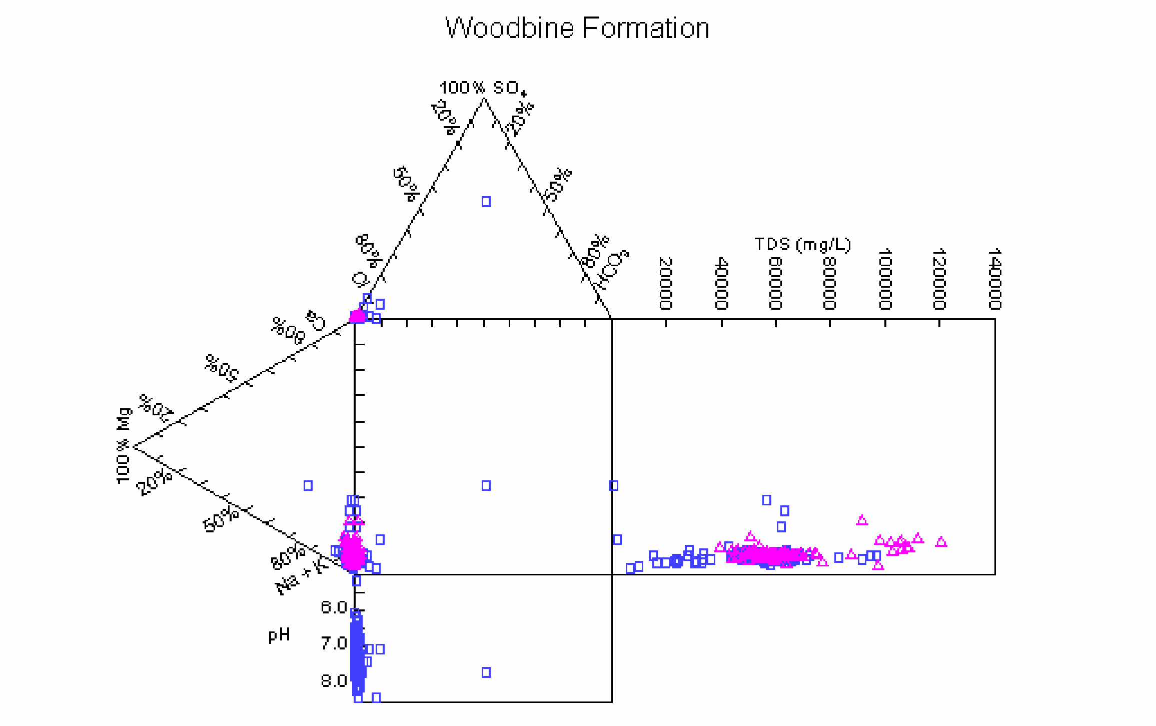

(blue squares = USGS data; pink triangles = Kreitler, 1987 data)

Figure 6.18. Durov plots of the Woodbine Formation samples (East Texas Basin)

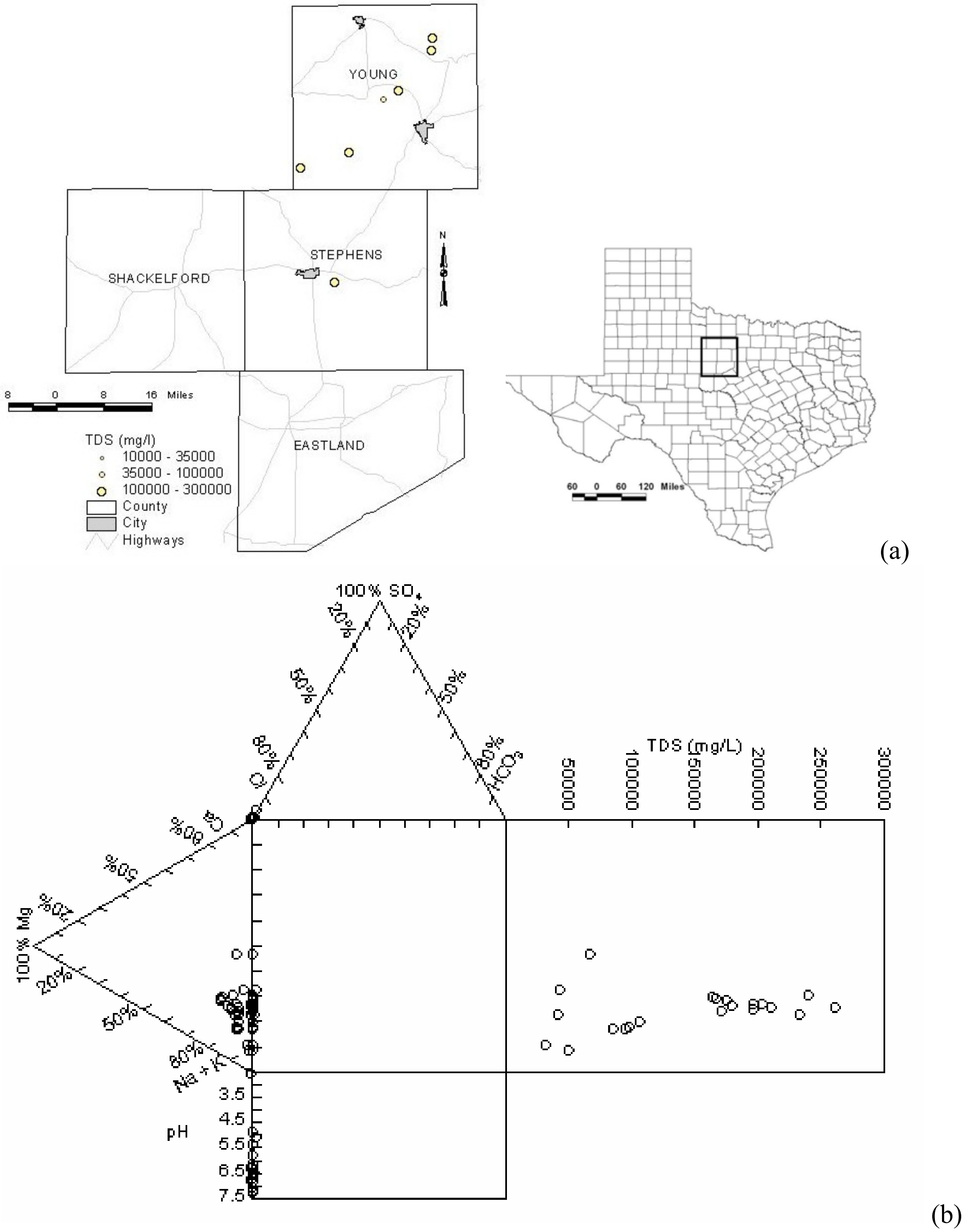

Figure 6.19. (a) Spatial distribution of TDS compositions; (b) Durov plots of formation samples (Fort Worth Basin)

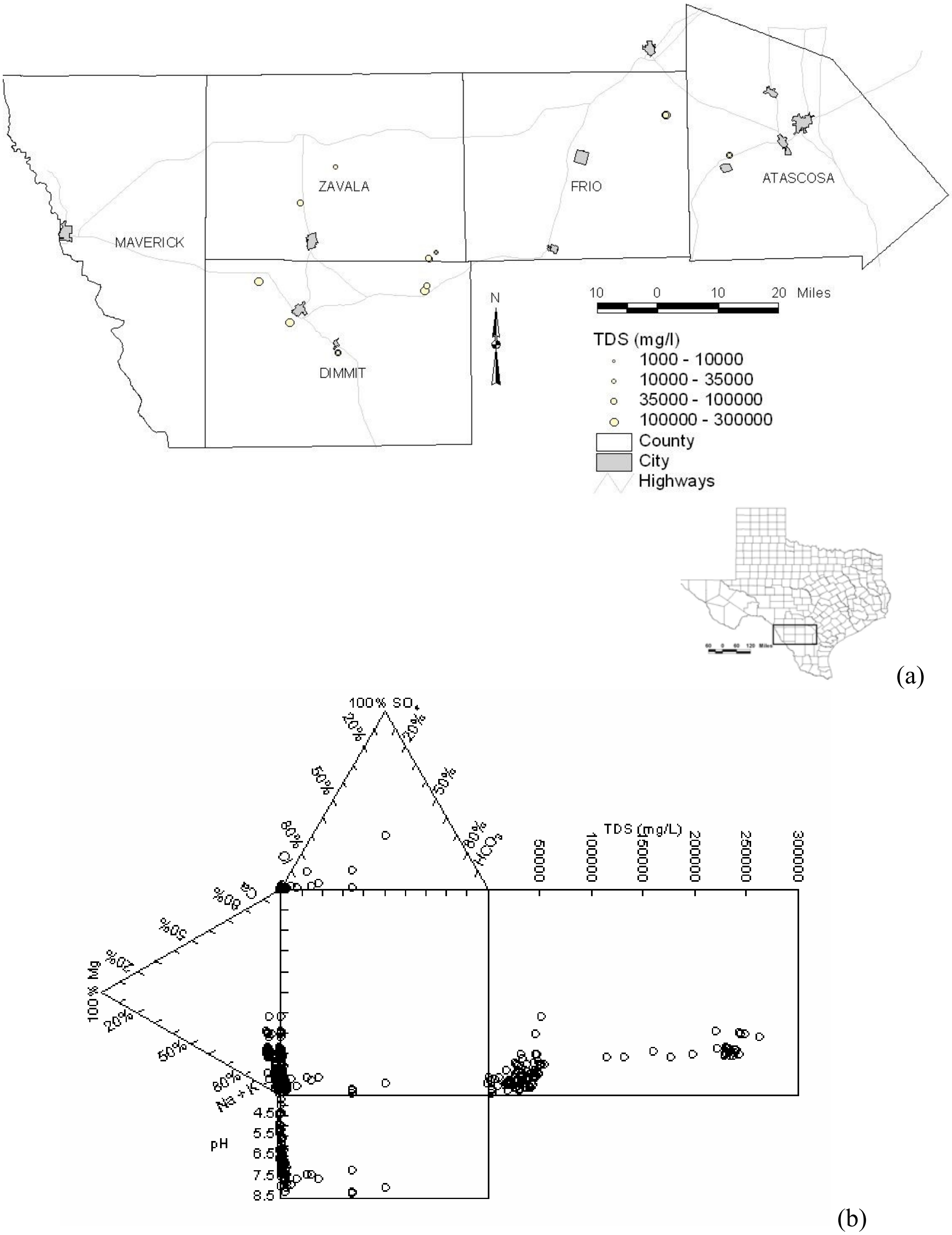

Figure 6.20. (a) Spatial distribution of TDS compositions; (b) Durov plots of the San Miguel–Olmos Formation samples (Maverick Basin)

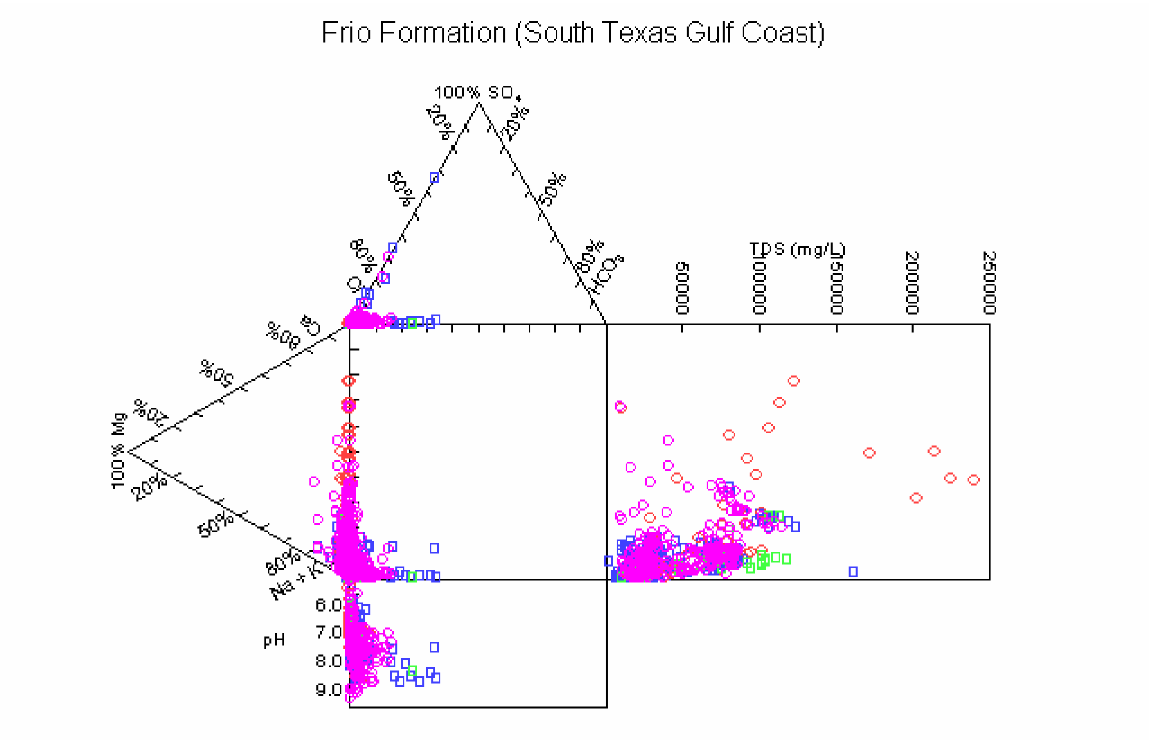

(blue squares = USGS data; orange diamonds = Kreitler et al., 1988; green squares =; Kreitler et al., 1988; pink circles = Kreitler and Richter, 1986)

Figure 6.21. Durov plots of the Frio Formation samples (Southern Gulf Coast Basin)

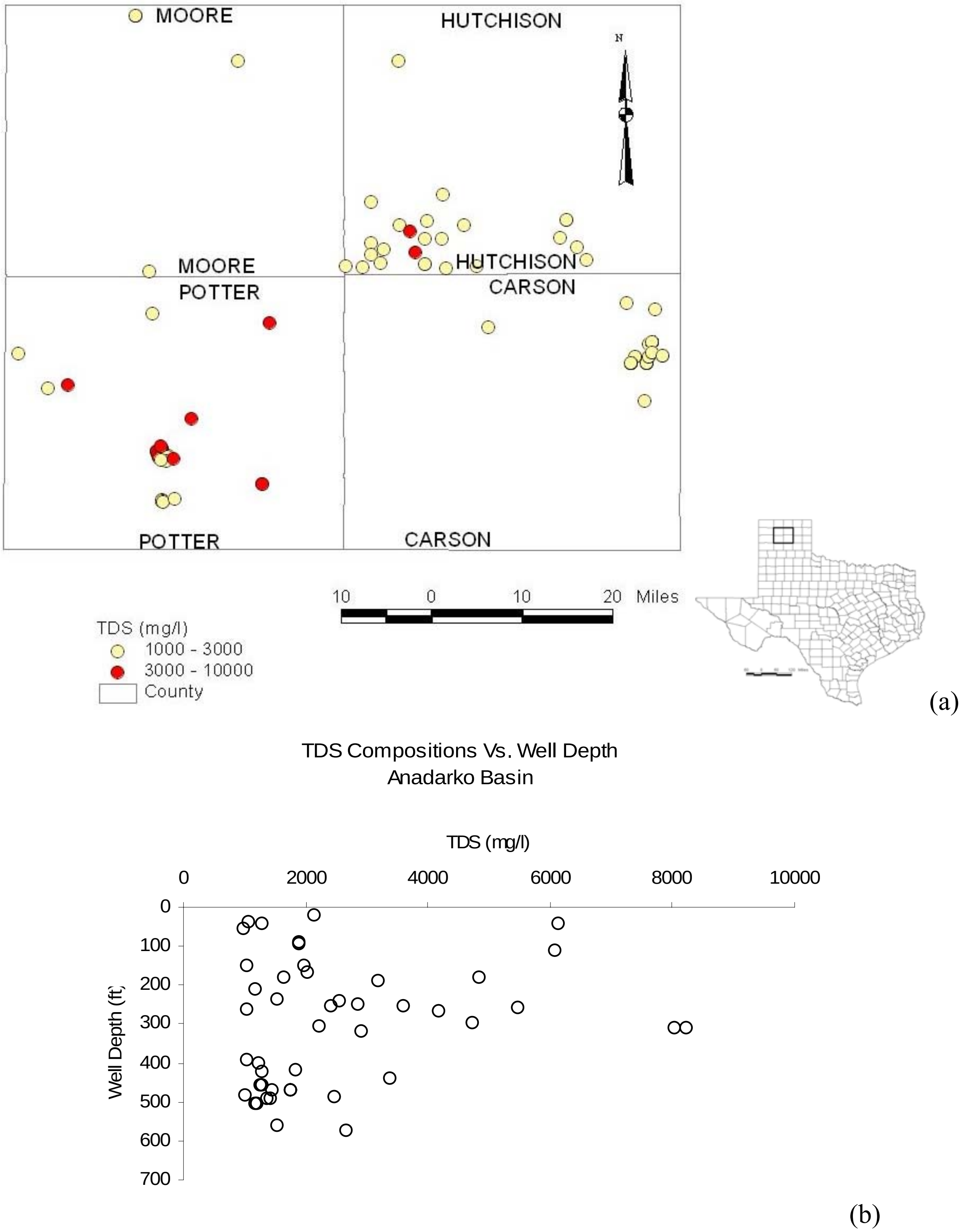

Figure 6.22. (a) Sample location map with TDS; (b) TDS versus depth plot; and (c) Piper and Durov plots of feed water (Anadarko Basin)

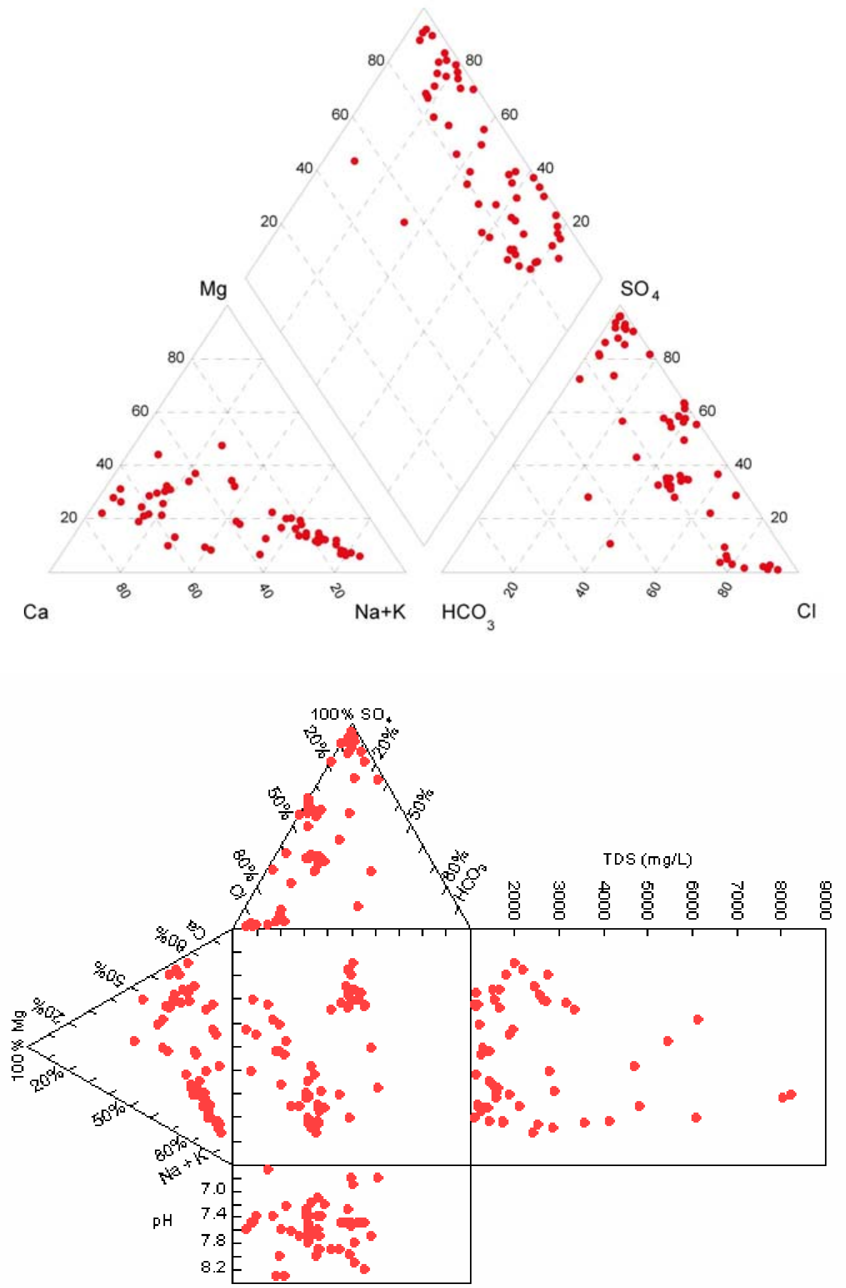

(c)

Figure 6.22 (continued): (a) Sample location map with TDS; (b) TDS versus depth plot; and (c) Piper and Durov plots of feed water (Anadarko Basin)

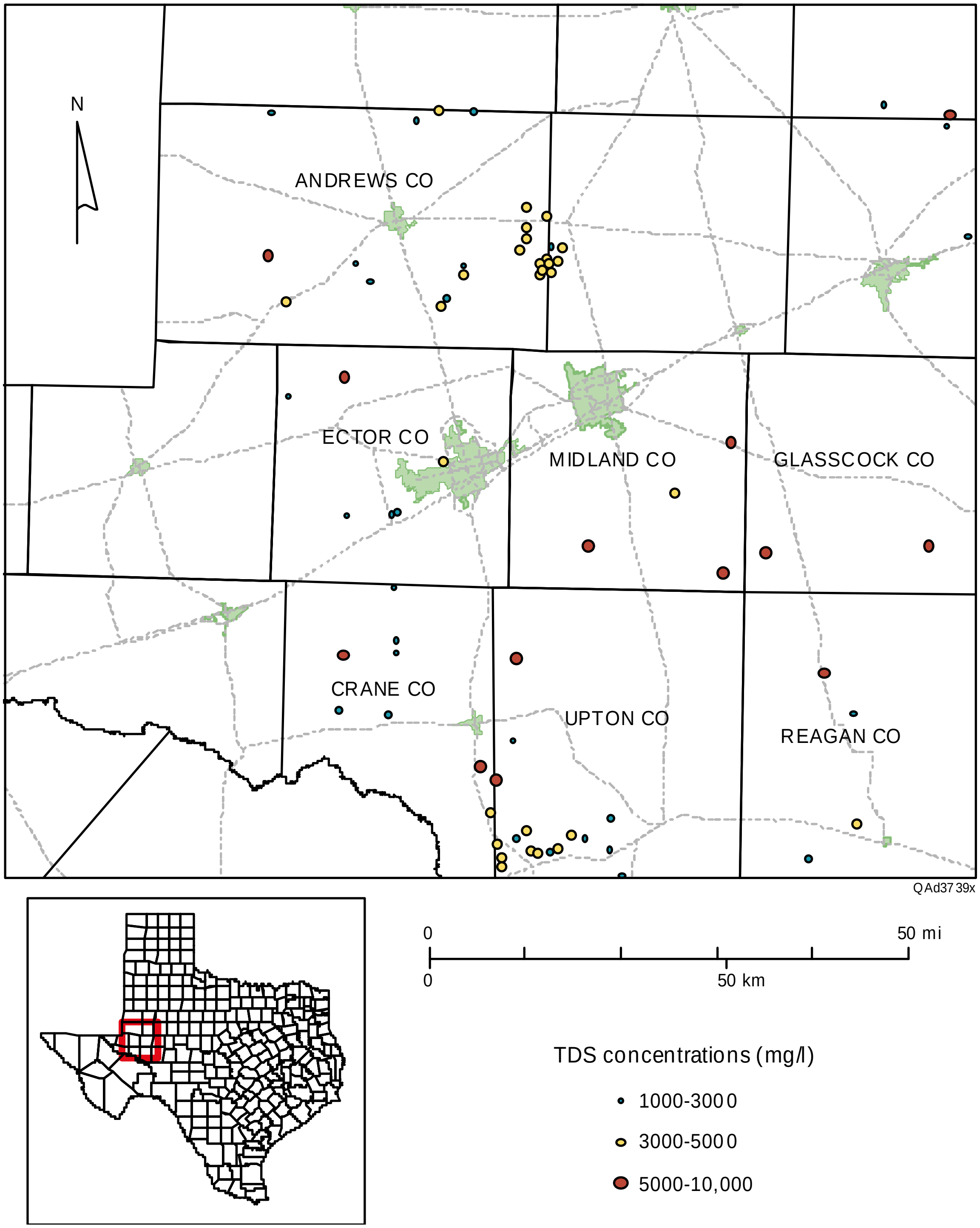

(a)

Figure 6.23. (a) Sample location map with TDS; and (b) Piper and Durov plots of feed water, Permian Basin (Ogallala and Dockum aquifers)

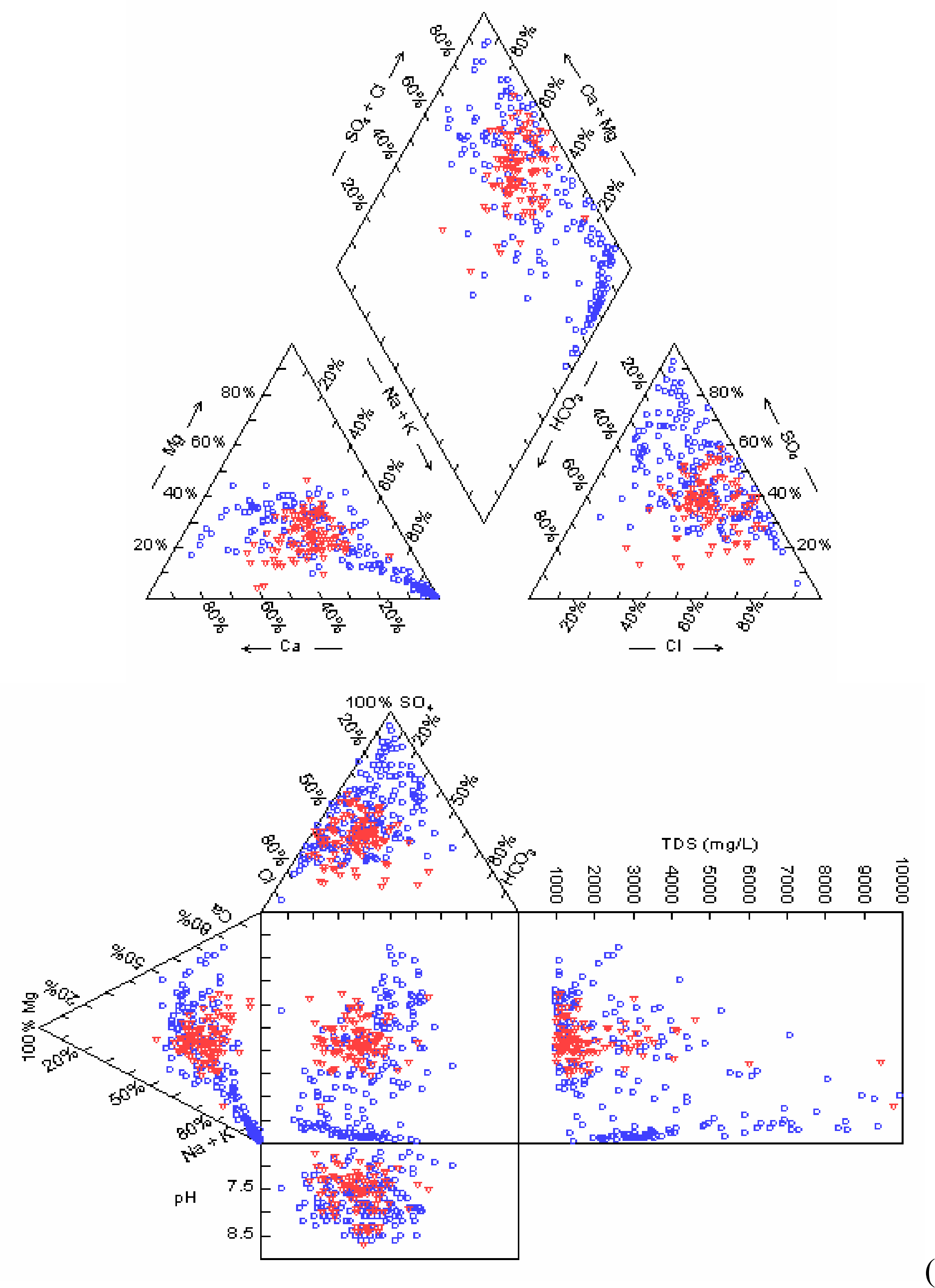

(b)

blue circles = Dockum aquifer; red triangles = Ogallala aquifer

Figure 6.23 (continued). (a) Sample location map with TDS; and (b) Piper and Durov plots of feed water, Permian Basin (Ogallala and Dockum aquifers)

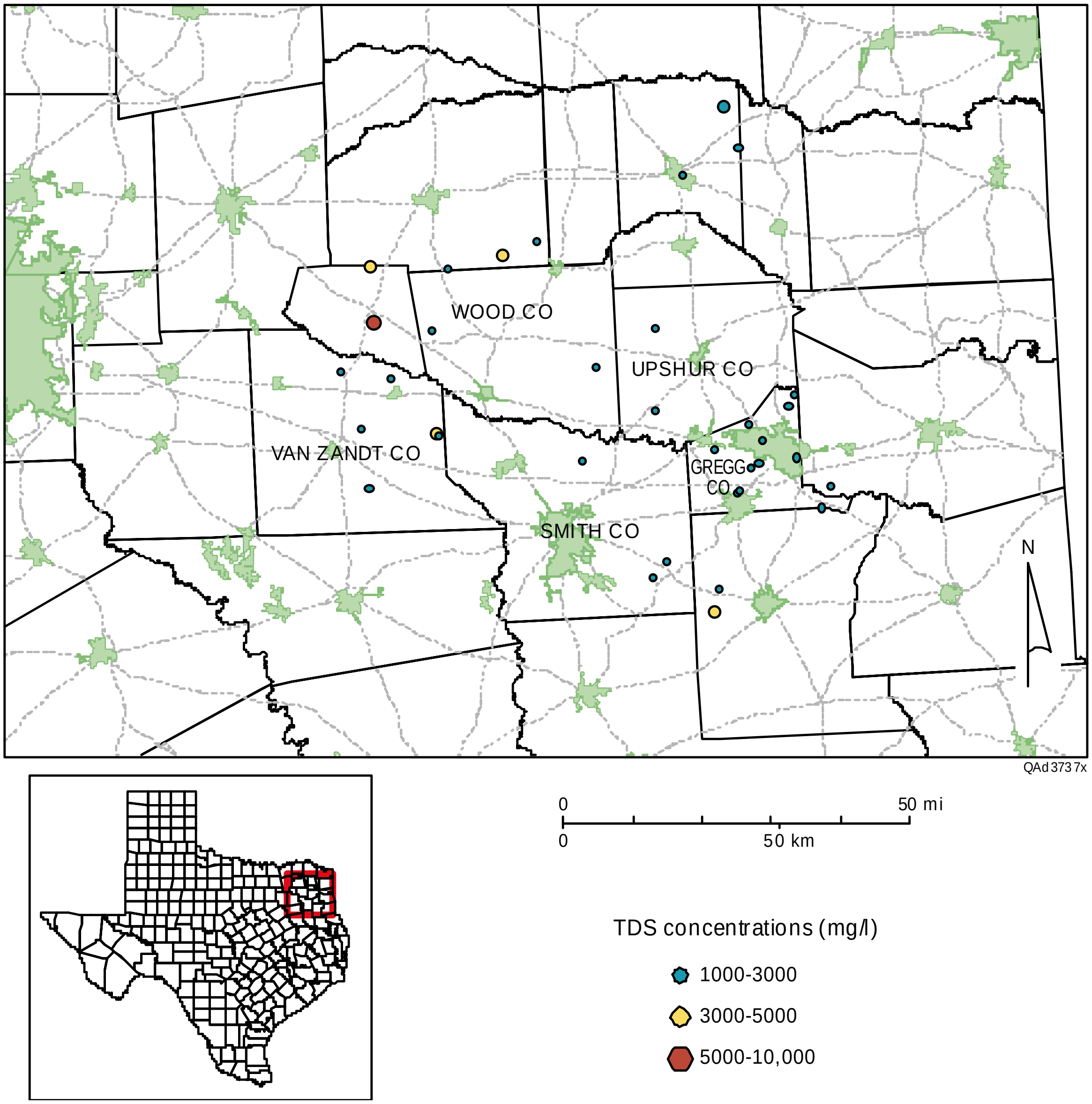

(a)

Figure 6.24. (a) Sample location map with TDS and (b) Piper and Durov plots of feed water, East Texas Basin (Carrizo aquifer)

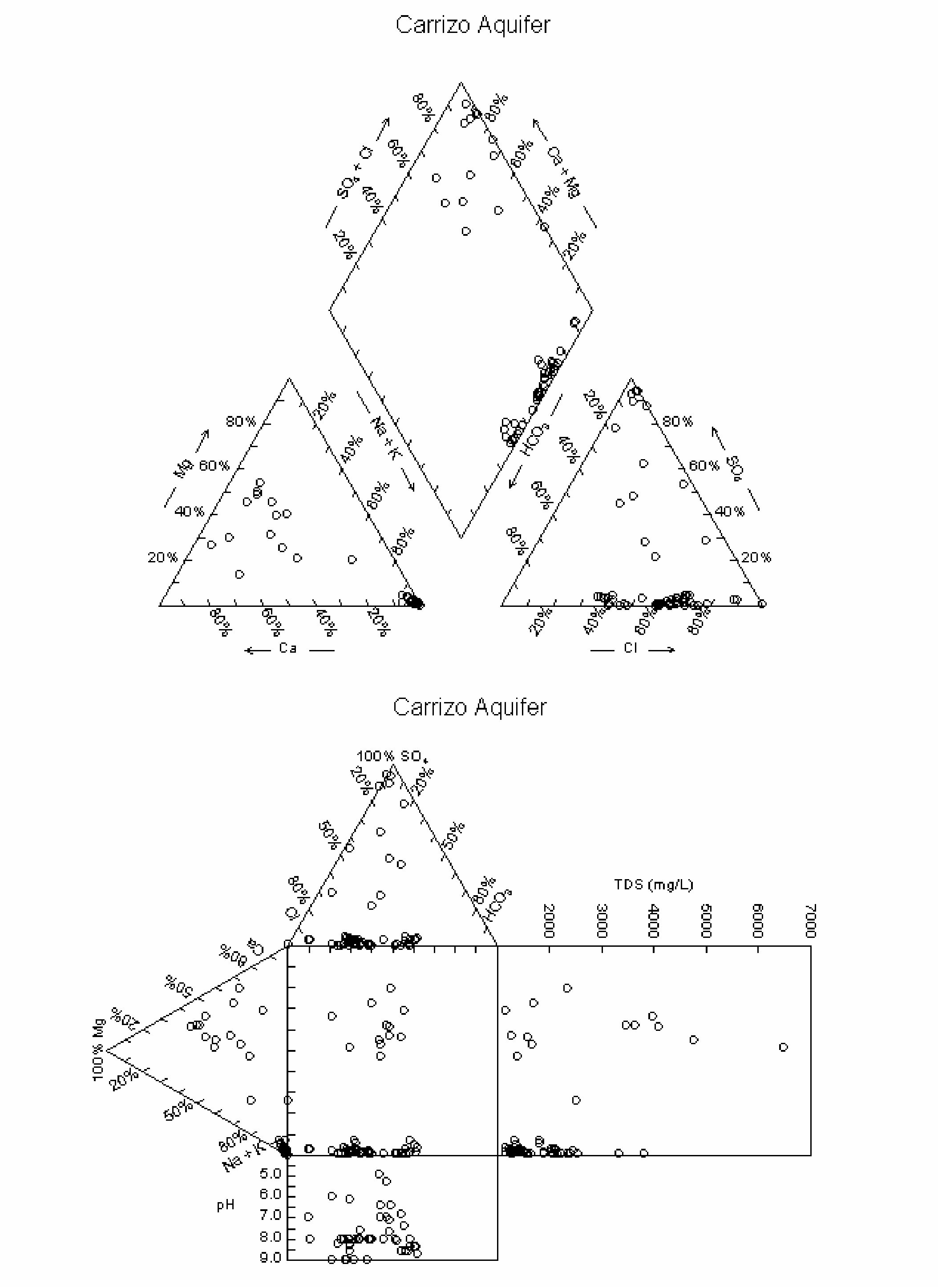

(b)

Figure 6.24 (continued). (a) Sample location map with TDS and (b) Piper and Durov plots of feed water, East Texas Basin (Carrizo aquifer)

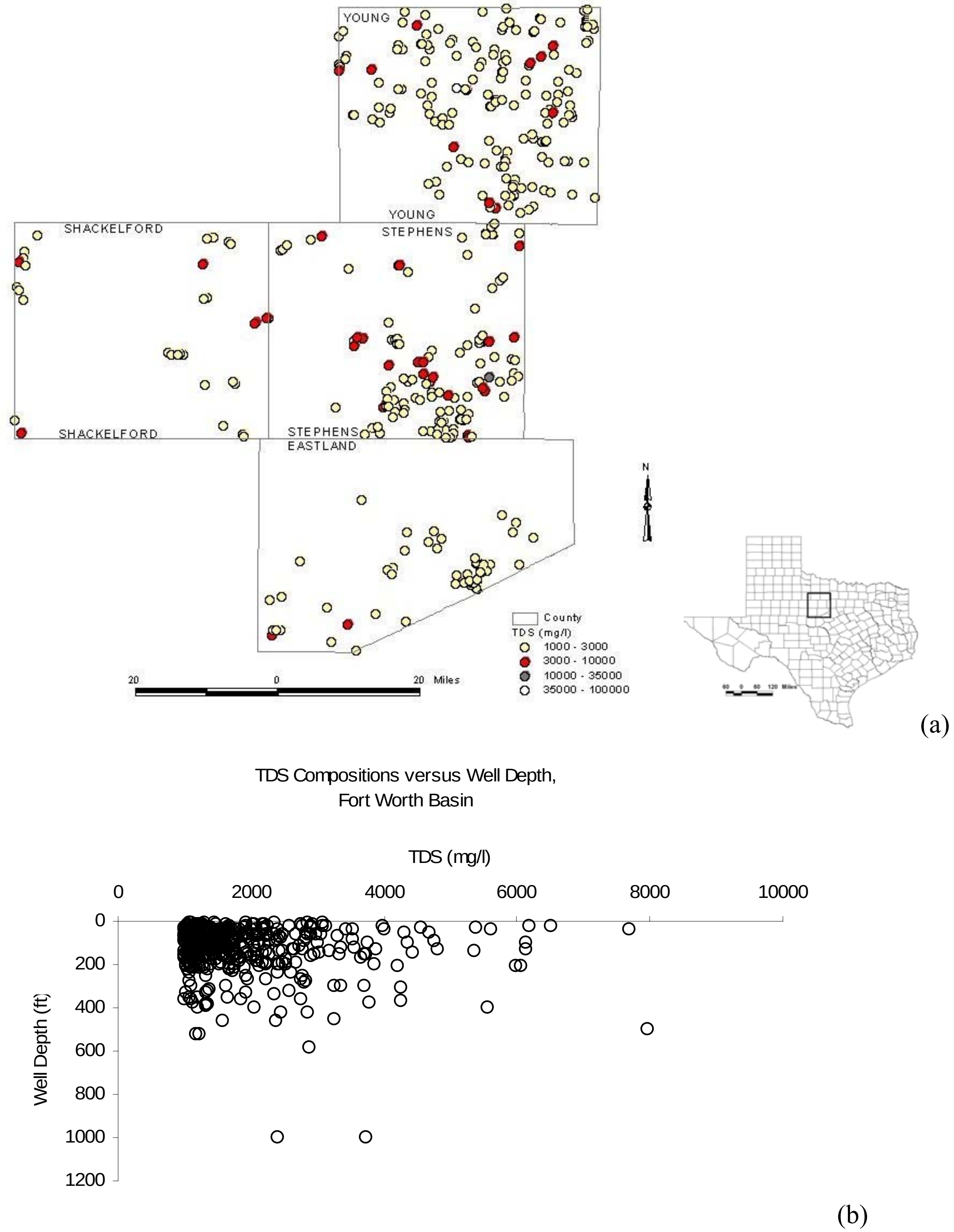

Figure 6.25. (a) Sample location map with TDS; (b) TDS versus depth plot; and (c) Piper and Durov plots of feed water, Fort Worth Basin

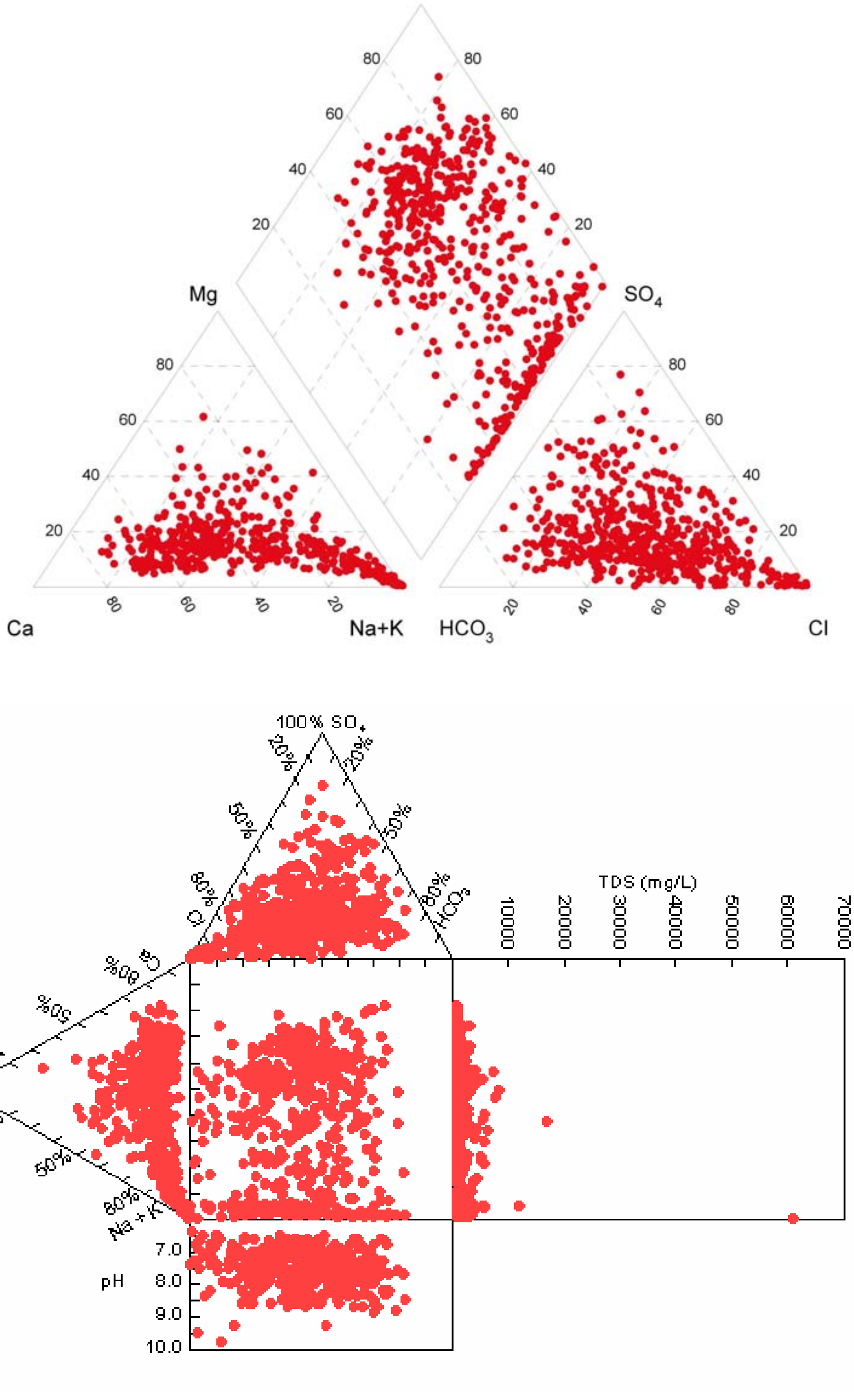

(c)

Figure 6.25 (continued). (a) Sample location map with TDS; (b) TDS versus depth plot; and (c) Piper and Durov plots of feed water, Fort Worth Basin

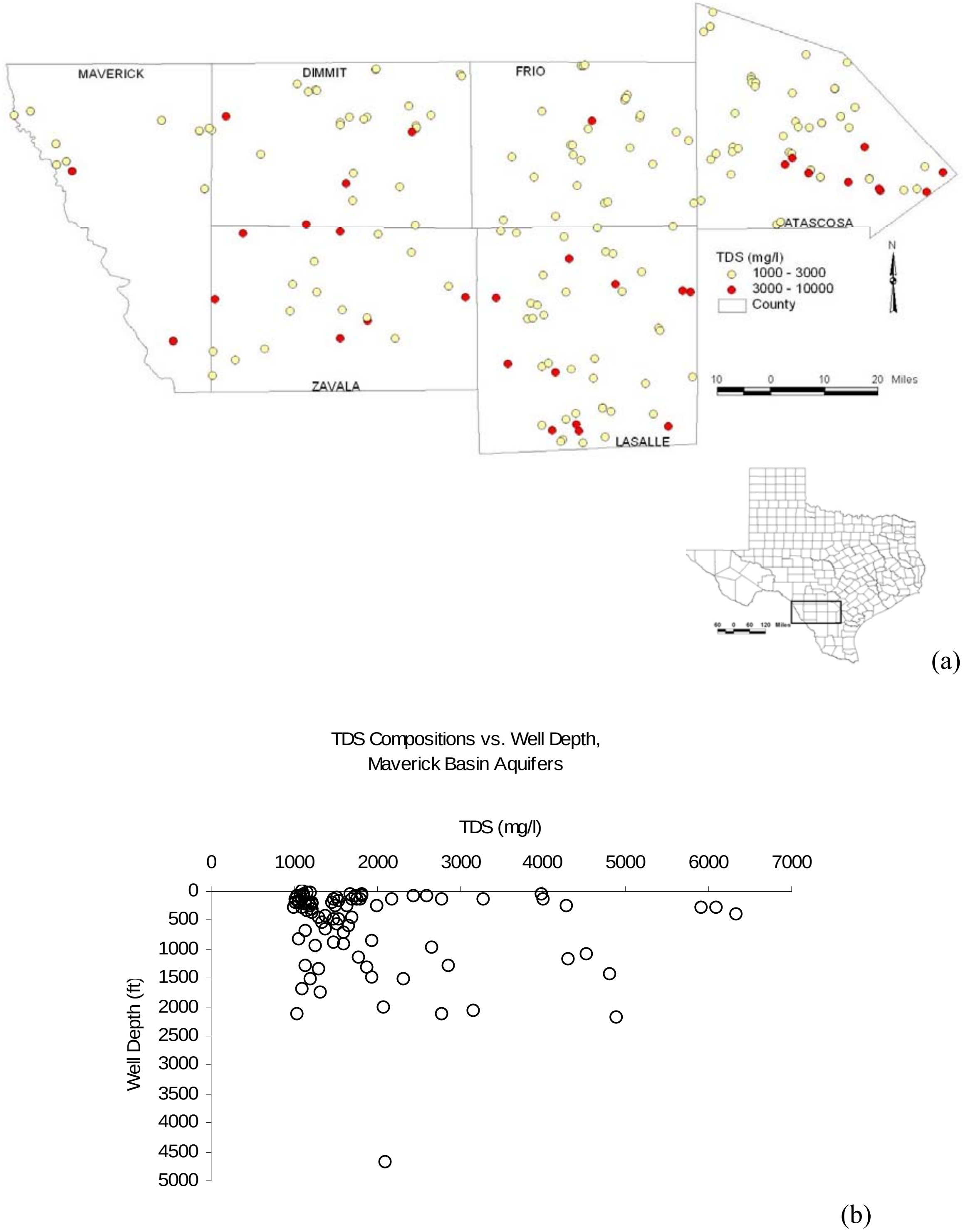

Figure 6.26. (a) Sample location map with TDS; (b) TDS versus depth plot; and (c) Piper and Durov plots of feed water, Maverick Basin (Carrizo-Wilcox aquifer)

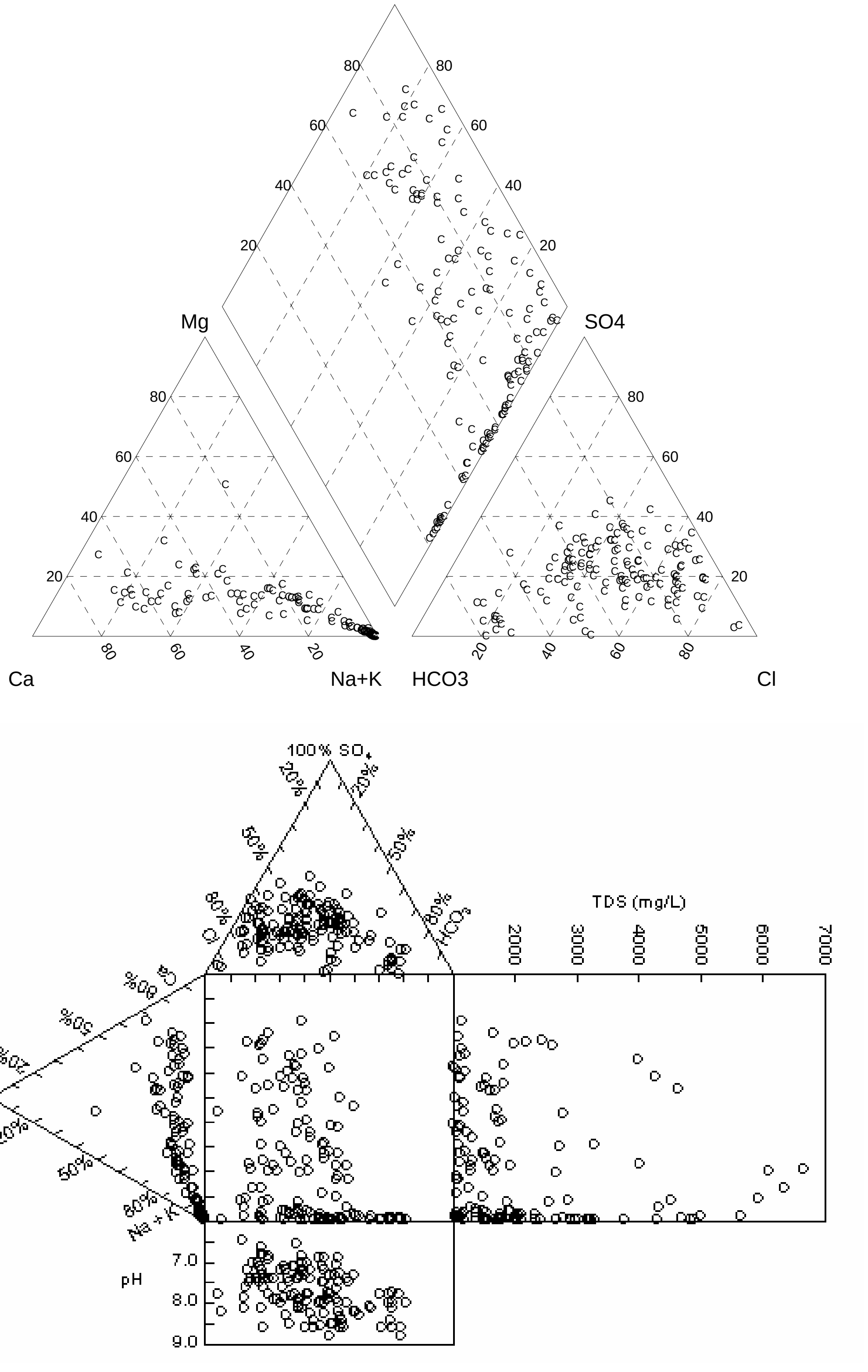

Figure 6.26 (continued). (a) Sample location map with TDS; (b) TDS versus depth plot; and (c) Piper and Durov plots of feed water, Maverick Basin (Carrizo-Wilcox aquifer)

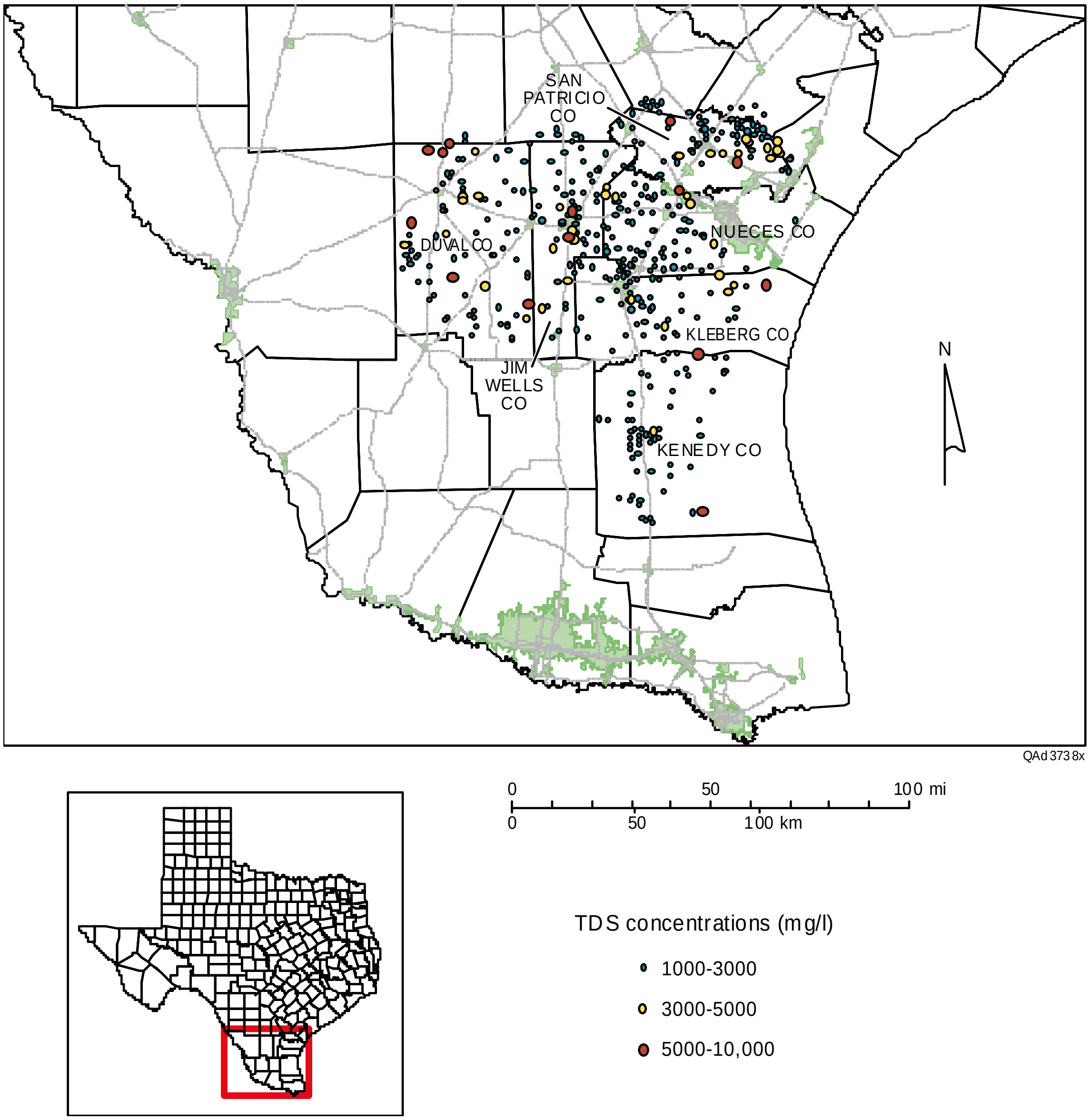

(a)

Figure 6.27. (a) Sample location map with TDS and (b) Piper and Durov plots of feed water, South Texas Fields (Gulf Coast aquifers)

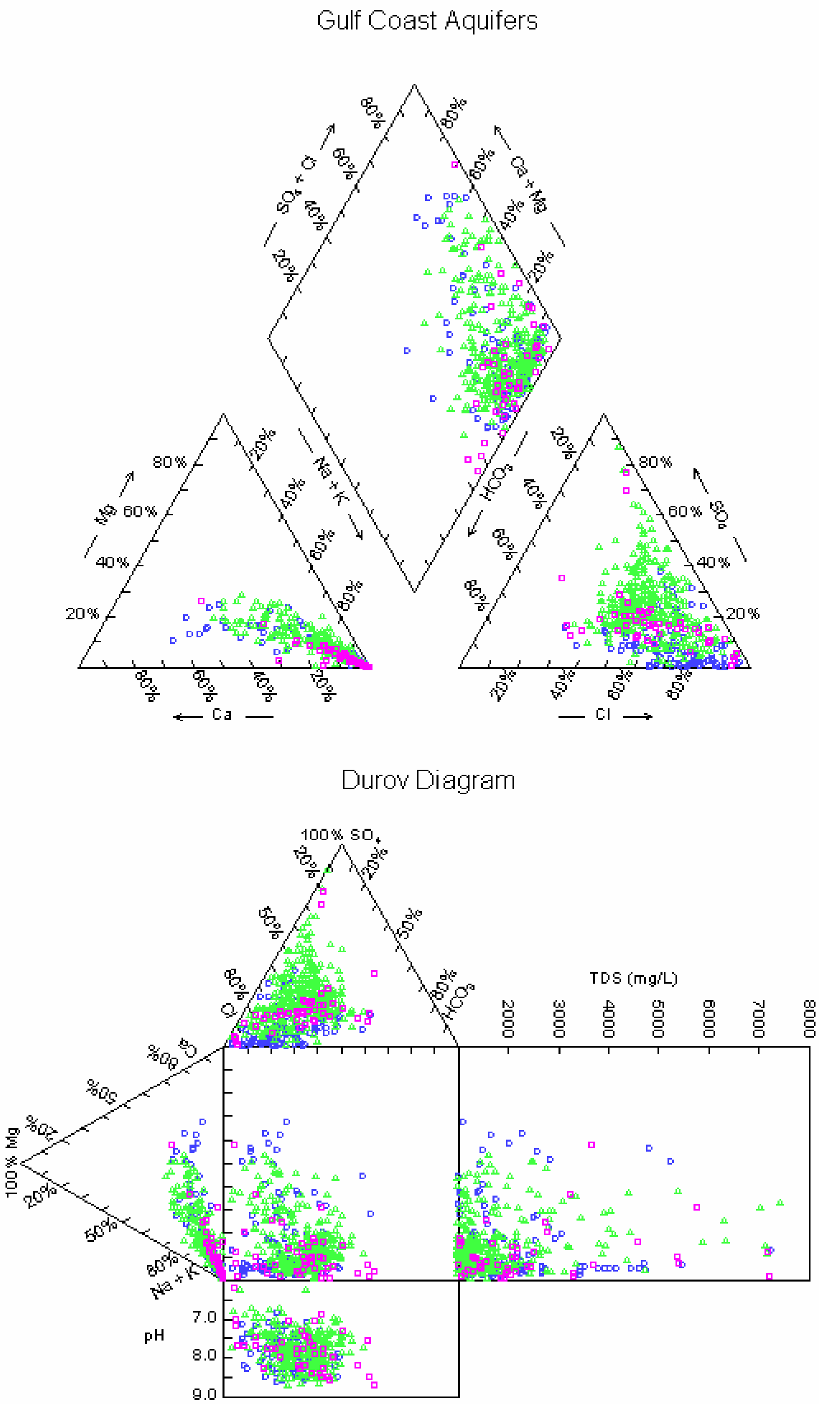

Gulf Coast Aquifers

Durov Diagram

(b)

(blue circles = Chicot aquifer; green triangles = Evangeline Aquifer ; purple squares = Catahoula Aquifer)

Figure 6.27 (continued). (a) Sample location map with TDS and (b) Piper and Durov plots of feed water, South Texas Fields (Gulf Coast aquifers)

# 7 Results of the Area-Specific Studies

In this section, we present the general results of the study. In Section 7.1, we discuss the results on the formation pressure assessment and its implication for the variance of Area of Review studies. In the following sections, we introduce the details of the methodology and results of the batch geochemical modeling (Section 7.2) and of the water sensitivity analyses (Section 7.3). In Sections 7.4 and 7.5, we present a succinct history of water injection in Texas oil-fields and address injection rate issues.

## *7.1 Results of AOR Studies*

The AOR studies show that a significant portion of wells would qualify for a variance of AOR (Table 7.1), although reported fluid levels in shut-in wells and BUQWs are highly variable within the fields. This large percentage is due in part to the fact that the fields have been pressure depleted (Figure 7.1 and Table 6.8). For each analysis area (Figure 7.2 to Figure 7.7), three plots are presented. The first plot shows the distribution of the depth to top of fluids (TOF) and the depth to the base of the usable quality water (BUQW). The second plot ("H15TOP-BUQW") is built by taking the separation between the top of fluid and the base of the usable quality water on a well-by-well basis. The separation between the top of fluid and the base of the usable quality water for each well is then averaged across a given field. Those averaged field separations are used to build the histograms. The third plot ("MinTOF-MaxBUQW") shows a similar distribution, but, except for being done on a well-by-well basis, the separation is computed on a field by field basis by taking the difference between the lowest BUQW of the field and the highest TOF, even if not from the same well.

The very large pressure depletion in the Anadarko Basin (Figure 7.1a) indicates that a large fraction of the fields may qualify for an AOR (~67 percent - Table 7.1). Between 50 and 60 percent of the fields from the Permian Basin (Figure 7.3), East Texas Basin (Figure 7.4), and Fort Worth Basin (Figure 7.5) may qualify for a variance of the Area of Review. The Maverick Basin (Figure 7.6) is an anomaly among the six analysis areas because only 35.5 percent of its fields look favorable for a variance of the Area of Review. The percentage of fields with a separation >500 ft fall into the main group at ~56 percent in the southern Gulf Coast Basin (Figure 7.7).

## *7.2 Batch Geochemical Modeling*

### 7.2.1 Template for Studies

It was beyond the scope of this study to do a detailed geochemical analysis that would include reaction with various solid phases. Batch modeling assumes total and thorough mixing, which is not likely to occur in the subsurface unless the formation is extensively fractured and contains large openings or other dissolution voids. Batch modeling is essentially an end member of all the possible outcomes at the injection zone. Considering the extent of mixing is important because it will occur only at the interface of the moving water. The batch modeling was done in two steps with two sets of data:

- Step 1: the purpose of this step is to compute the concentrate composition using PHREEQC (Parkhurst and Appelo, 2002). PHREEQC is a conventional batch geochemical code developed by the USGS. Its use is legitimate because the ionic strength of the concentrate is typically below that of seawater, which is often cited as the upper limit for use of those conventional models. The Debye-Huckel formulation, used in most geochemical codes, is valid up to the ionic strength of seawater (~0.3) and to 0.8-1 in a semiquantitative fashion.
- Step 2: the purpose of Step 2 is to compute the *SI* of a batch mixture of formation water and concentrate in four proportions (0.2/0.8 – 0.4/0.6 – 0.6/0.4 – 0.8/0.2). The calculation was done with SOLMINEQ (Kharaka et al., 1988), another USGS code able to handle aqueous reactions in high ionic-strength brines by using Pitzer formalism for activity coefficients. Results were spot-checked using PHRQPITZ (Plummer et al., 1988), another USGS code also able to handle high salinity solutions.

A script, written in visual basic and launched from an Excel© spreadsheet, allows for multiple runs without user intervention. The results are then tabulated. Two sets of concentrates were used: one with no treatment and another one with acid added so that the concentrate pH is 6. The value of 6 was retained as reasonable after reviewing the technical literature (see Section 4.4).

As described in Section 4.3, the concentrate is obtained by simply multiplying all concentration values by a factor of 4. This is done by using the "REACTION" keyword in PHREEQC, which in this study removes 75 percent of the water initially present. This is equivalent to enrichment by a factor of 4 of all species. The system is assumed closed, that is, it is not reequilibrated with atmospheric $CO_2$. Atmospheric $O_2$ has no impact on the results because redox reactions are not modeled. In the geochemical runs where we acidified the waters, the pH was forced to a value of 6 by using a fictitious species (Fix_pH). We assumed that the acid added was sulfuric acid. It introduces sulfate into the concentrate, but this is conservative relative to sulfate scaling because chloride ions introduced by hydrochloric acid have no impact on scaling.

SOLMINEQ requires several input data sets. Concentrate composition was internally recomputed at a temperature of $25^{o}C$ before being mixed with the formation water. The final temperature of the mixture is a direct function of the proportion of each water in the mixture. Temperature of the formation water was determined according to the thermal gradient and not from the so-called sampling temperature which may not be representative of the downhole conditions. When average screen depth was not available, the average of the available samples was used instead. Because pressure has an impact on mineral solubility, SOLMINEQ also requires pressure data. Because pressure data is typically not available at the same location where sampling was done, pressure was inferred using a linear relationship between depth and pressure (Section 6.6 and Table 6.8). The relationship was derived from the Form H15 database that was assumed representative of the downhole conditions. It is understood that there is a lot of variability in pressure as seen on Figure 7.1, but it was felt that this was better and more conservative than the alternative of using a hydrostatic pressure assumption because scaling tendency typically decreases with increasing pressure.

As in all geochemical modeling, the choice and accuracy of the thermodynamic database is important. This is especially true for modeling of brines. The database provided with the PHREEQC software, used to model solutions with ionic strength less than that of seawater, has been tested across the country in countless projects, and we have high confidence on the accuracy of the program output. On the other hand, there is limited information on the interaction coefficients used in the Pitzer formulation, especially at pressure and temperature higher than standard conditions. In that sense, the results are only qualitative because of high uncertainties of the values of these coefficients in the environmental conditions prevalent in this study. In addition, multiple chemical interactions can occur in the subsurface: precipitation, co-precipitation, redox reactions, and ion exchange. However, if they can all be handled by a code such as PHREEQC for low ionic-strength solutions, theoretical developments of the Pitzer formulation, needed in this study, have not yet produced a satisfying approach to modeling ion exchange. SOLMINEQ is also limited to equilibration with one mineral. For these reasons, no attempt was made to quantify the amount of material that could precipitate but, rather, whether it could precipitate.

We used a statistical approach combined with Monte Carlo trials to analyze the results of mixing formation water and concentrate partly on the basis of the assumption that spatial variability in the composition of the feed water translates into temporal variability. Water-quality variations are generally related to permeability variations. As time goes on, brackish water pumping draws additional water from low-permeability pockets and from the surrounding layers confining the aquifer. These waters are typically more saline and possibly of a different ionic makeup. There are multiple instances across the state and the country of more saline water being drained progressively into the well field cone of depression and degrading the water quality. The second reason is that the relative location of the brackish water well field and of the concentrate disposal well is obviously not known, justifying random pairing of concentrate and formation samples. The total number of combinations varies from less than 10,000 in the Forth Worth Basin to almost 350,000 in the southern Gulf Coast Basin (Table 6.2). It should be noted that the number of potential combinations is not connected to the actual variability in the field. We used a subset of 5,000 combinations, selected at random, after having checked that the salient features of the results were reproduced for the Permian Basin data sets.

### 7.2.2 Results

Results of the geochemical model runs are reported in the form of histograms. The important observation is that some of the concentrate/formation water combinations produced above the threshold saturation index. The theoretical threshold for precipitation is a saturation index of $SI=0$, although kinetics may render the reaction so slow that it has no real impact. As described in Section 4.4, addition of antiscalant products will increase the threshold to approximately a value of 2. This value of 2 is retained as the saturation index beyond which recurrent scaling problems could occur during the injection. It is, however, important to remember that the SI values result from the assumption of total mixing. In the subsurface, formation water and injected concentrate will not mixed as much as assumed in this section. The concentrate will displace the resident formation water. The injection front will also be somewhat blurred by diffusive forces.

The feed water saturation indices were already presented in Table 6.4. The potential feed waters are mainly undersaturated relative to calcite, gypsum, and silica. Barite saturation index from some basins, particularly the Anadarko Basin, suggests that the water is supersaturated with respect to this mineral. However, given the low solubility of barite, the higher saturation indices may also be due to erroneous temperature field measurements. Table 7.2 presents the six analysis-area saturation indices for the concentrate, both acidified and with no treatment, the formation water and the mixed solutions of formation water and concentrate in different proportions. The median, 5th, and 95th percentiles are given, as well as the number of data points or number of statistical trials. The full distributions whose statistics are displayed in Table 7.2 are in the histograms of Figure 7.8 to Figure 7.20. Number of bins, bin size (generally 0.1 saturation index unit), and number of data points or trials are shown at the bottom of the histogram. Title of the histogram reflects the nature of the basin, the water type(s) analyzed, the mineral considered, and additional information such as addition of acid or no pretreatment.

Acidification of the concentrate drops the saturation index of calcite by one order of magnitude, bringing it to below a value of 0 in the large majority of cases. The other minerals analyzed (gypsum, barite, and silica) show small variations in *SI* owing to the change in ionic strength by the addition of acid and of sulfate ions (more evident for gypsum and barite). The amount of acid added is recorded in Figure 7.14, which shows a range (<300 ppm of sulfuric acid) consistent with desalination industry usage. If the increase in sulfate concentration leads to a barite scaling problem, hydrochloric acid can be used instead. Formation water from all analysis areas shows a supersaturated calcite, sometimes by one order of magnitude (for the median). It is common for calcium carbonate to be supersaturated in solution, but it could also correspond for some samples to sampling problems, such erroneous temperature or pH measurements. SOLMINEQ has the ability to equilibrate a solution with respect to a given mineral. Because calcite is widespread in the subsurface, this option could have been used. However, it would not have allowed comparison between analysis areas. Saturation indices for the mixing solutions are intermediate between those of formation water and acidified concentrate. All indices, except barite for one analysis area, are below the threshold of $SI$=2, beyond which it is assumed that scaling could happen even in the presence of commercially available antiscalant. Results are summarized in Figure 7.21. Figure 7.21 displays saturation indices in a concise way, suggesting that there is no superior site relative to scaling tendency. According to the modeling results of this study, calcite impacts equally all analysis areas; gypsum may not cause problems on average, but the Anadarko and Permian Basins are more prone than other analysis areas; silica does not seem to be able to produce significant scaling on average. Barite may be more of an issue, but data are insufficient to conclude with certainty.

## 7.3 Water Sensitivity Analyses

As described in Section 5.5.3 and emphasized by Warner and Lehr (1977, p. 174), water sensitivity of clay-bearing sandstones increases with decreasing water salinity, decreasing valence of the cations in solution, and increasing pH in the water. Two factors control whether injected waters/brine will cause formation clay-related impairment: (1) the water must have an adequate total cation and/or divalent cation concentration for prevention of clay deflocculation and (2) cation exchange during mixing must not reduce the divalent cation concentration (Schuerman and Bergersen, 1990). On the basis of clay types commonly encountered in the reservoirs, Schuerman and Bergersen (1990) developed compatibility guidelines for injection water. In the following figures, total cations are plotted against divalent cations. The most sensitive clay is montmorillonite, followed by mixed-layer clays and illite. Kaolinite is barely water sensitive and chlorite is not. The injection water and formation clay compatibility is then determined based on the positions of the water composition on the diagram.

Figure 7.22 to Figure 7.30 show the position on the diagram of the formation water and brackish water for the analysis areas. The information is sometimes presented by county. In the Anadarko (Figure 7.22a and b), Permian (Figure 7.23a), East Texas (Figure 7.25a), Fort Worth (Figure 7.27a and b), Maverick Basins (Figure 7.28a, b, and c), most of the data points fall outside the smectite salinity line, suggesting that the formation contains smectite in contact with the flowing water and that they are at equilibrium. In the southern Gulf Coast (Figure 7.29a), data points reach the illite salinity line. Because smectite clay is progressively transformed into illite with depth, some the previous figures were replotted by county with depth as an additional color-coded parameter. The best example of the transformation occurs just outside the southern Gulf Coast Basin analysis area in San Patricio County (Figure 7.29g), where there is a large depth range in the Frio Formation. It is clear that as the burial depth increases so does the proportion of illite (through mixed-layer illite-smectite stages). These mineralogical changes are highlighted by the composition changes of the formation water. It was out of the scope of this work to analyze the reactive transport phenomena leading to such changes. However, from a practical standpoint, it confirms that this type of plot can help in determining the clay type controlling the water sensitivity of the formation. The depth range in the San Andres Formation in the Permian Basin is too narrow for this process to be visible in the color-coded depth plots (Figure 7.23b, c, and d), although its initialization might be recognized on Figure 7.23d. The same holds true for the Woodbine Formation in the East Texas Basin (Figure 7.25b, c, and d). Our Woodbine data set contains a significant fraction of data points with no depth information. A trail toward the illite salinity line in Rusk County (Figure 7.25c) suggests that illite may be dominant in the southern part of the analysis area. Other counties in the southern Gulf Coast analysis area show a picture similar to that of San Patricio County (e.g., Figure 7.29f for Nueces County). Other plots (e.g., Figure 7.29c for Jim Wells County and Figure 7.29e for Kleberg County) suggest that formation waters are at equilibrium with mixed-layer clays rather than smectite even at shallow depths (<4,000ft). The overall picture tells that all formation water sensitivity is likely controlled by smectite except perhaps in the southern Gulf Coast Basin, where it may be controlled by mixed-layer clays and even possibly illite for the deeper sections of the Frio Formation.

The injected concentrate is likely not at equilibrium with the formation clays. However, all brackish water samples fall outside the smectite salinity line in the Anardarko Basin (Figure 7.22a and b). Approximately 75 percent of the concentrate data points (measured as points with a divalent cation fraction of TTC of at least 20 percent) falls outside the smectite salinity line in the Permian Basin (Figure 7.24). Table 7.3 shows a summary for all analysis areas of brackish water sample distribution relative to the illite and smectite salinity lines. Most of the Carrizo-Wilcox data points fall within the smectite salinity line, and only 65 percent outside the illite salinity line. Similarly the Fort Worth Basin analysis area contains more than half of the brackish water samples that fall inside the smectite salinity line (Figure 7.27a and b). Most of the brackish water samples in the Maverick Basin analysis area fall outside the smectite salinity line (Figure 7.28a, b, and c). The southern Gulf Coast analysis area has 29 and 58 percent of the data points outside the illite and smectite salinity line, respectively (Figure 7.30). As a partial conclusion, some basins, particularly the East Texas and Fort Worth Basins, could present a challenge for concentrate injection. The Anadarko and Permian Basin analysis areas should be easily amenable to concentrate injection. An intermediate statement can be made for the Maverick and southern Gulf Coast Basin analysis areas.

This first step of the water sensitivity approach eliminates those waters likely to generate formation damage unless operational precautions are taken. However, even seemingly compatible water can generate problems owing to cation stripping. The propensity of an injection water to undergo cation stripping is measured by the mass action ratio (MAR) ratio ($MAR_{i/f}$ = MAR of injected water / MAR of formation water). For the same reasons stated in Section 7.2, we used a statistical approach to analyze the issue. MAR of injection water and formation water and their distribution can easily be determined on a spreadsheet. However, the distribution of ratios is needed. The approach is then to sample each MAR data set at random, compute the ratio, and progressively build the statistical distribution. The statistical analyses were performed using the risk-analysis package Crystal Ball® running under Excel (Crystal Ball, 2001). Results are presented in the form of histograms (Figure 7.31) to be compared with guidelines displayed in Table 5.4. It follows that a water sensitivity pretreatment is needed in most combinations of concentrate / formation water.

## *7.4 Historical Account of Water Injection*

Economic factors often dictate the nature of the water selected for waterflood and pressure maintenance. Pumping and injecting fresh water may be cheaper than reinjecting produced waters or pumping water from saline aquifers, especially if they need treatment. In addition fresh water does not generate as much corrosion or clogging of pipes or pumping equipment or as fast. It is also generally accepted that a diluted brine leads to a higher oil recovery (e.g., Tang and Morrow, 1997). The last exhaustive compilation by the RRC of injection operations in Texas was done in 1982 (RRC, 1982). The document displays numerous tables with administrative, as well as technical, information on both active and abandoned projects. Figure 7.32, Table 7.4, and Table 7.5 show an historical perspective to water injection. Although there is no breakdown by producing formation, it is legitimate to draw conclusions from these histograms and tabulated data because most of the depleted fields of the analysis area were already producing in the first half of the 20th century and they often account for a significant percentage of basin cumulative production (see Figure 3.4 to Figure 3.7). In addition, early on, fresh water aquifers were not as stressed by human consumption demand as they are today, and fresh water was more readily used for the reasons outlined above.

It can be clearly seen that fresh water injection, mainly from the Ogallala aquifer, used to be very common in the Permian Basin. In the 1960's, almost 1 percent of the fresh water produced from the Ogallala aquifer in Texas was used in waterflood and pressure maintenance operations. Anadarko Basin reservoirs were also heavily waterflooded with Ogallala Formation water. A significant amount of fresh and brackish water was used in the Fort Worth Basin as well. The East Texas Basin also received fresh water in addition to produced water injection. The massive reinjection of produced waters from the East Texas field generated calcium sulfate, calcium carbonate, and silica scales in the treatment steps before water entered the injection wells (East Texas Saltwater Disposal Company, 1958, p.76). Aluminum and iron oxides were also precipitated, the former from alum being added for coagulation of particulates, the latter two from iron-based tubing. Average produced-water injection rate among the ~75 wells active in the 1940's and 1950's varied between 150 and 200 gpm. At the other end of the spectrum, in the southern Gulf Coast, very little water injection was done. This is actually true for the whole Texas Gulf Coast encompassing RRC districts 2, 3, and 4, including the Maverick Basin.

Inspection of a much smaller subset of data, a limited sampling of the H1 forms, revealed that most of the injection water is produced water. Table 7.6 shows results from a nonexhaustive examination of water sources for injection. Data are a mix of mainly recent activity (from 2000 onward) documented from the Worldwide Web and of older activity from the 1980's compiled from paper copies. The same pattern as in districtwide numbers is visible: there is major water injection in the Permian Basin, which was not under primary natural drive, and none in the southern Gulf Coast. An observation of significance is that, often times (26 out of 32), fresh water is mixed with produced waters, presumably to limit formation damage. There is a need to balance the reduction or lack of scaling in the pipe network with the potential of formation damage when using fresh/brackish water. That same usage of blending water of different origins could also apply to desalination wastes. This historical perspective proves that at least some reservoirs in all analysis area formations can accept fresh and brackish water in large amounts.

## 7.5 Injectivity Modeling

Existing formation pressures in the analysis area are considerably lower than the hydrostatic pressure (Figure 3.3). Figure 7.33 shows an aggregated distribution across the analysis areas of the reported average and maximum injection rate, whose median is 30 gpm and 60 gpm, respectively, while the 95th percentiles are ~150 gpm and ~230 gpm, respectively. A rate of 60 gpm translates into a rate slightly smaller than 0.1 MGD. On the other end, Class I injection wells along the Texas Gulf Coast inject at an average rate of 100 gpm (Section 5.1), but it could be much higher. Depending on the facility size, a cluster or multiple clusters of wells may be needed. A facility generating 1 MGD of concentrate would need a least 10 injection wells as currently operated.

The number of wells needed to meet the requirements of a typical desalination facility depends not only on the facility size but also on the average injection rate that can be sustained by the formation, itself a function of the permeability (see Section 5.4.3). The statistical analyses were performed using the risk-analysis package Crystal Ball® running under Excel (Crystal Ball, 2001) to generate the possible range of injection rates. Parameters were varied randomly (except porosity and permeability, which were varied according to their linear correlation coefficient) and injection rate results plotted on histograms (Figure 7.34 and Table 7.7). The described distributions include all collected porosity and permeability data and therefore are biased toward low injection rates. They may not be representative of the set of higher performing wells that will most likely be used to inject fluids. The median injection rate is about 10 gpm in the Paleozoic basins, while it reaches 278 and 466 gpm in the southern Gulf Coast and East Texas Basins, respectively. The rate could also be increased by screening more intervals and performing well stimulation.

Table 7.1. Percentage and number of fields with separation greater than 500 ft

| Basin | Percentage of Fields with Separation > 500ft | Number of Fields |
|---|---|---|
| Anadarko | 66.7% | 18 |
| Permian | 50.5% | 436 |
| East Texas | 56.8% | 139 |
| Fort Worth | 62.8% | 285 |
| Maverick | 35.5% | 121 |
| Southern Gulf Coast | 56.2% | 356 |

Table 7.2. Result summary of batch geochemical runs

| | | **Calcite SI** | **Gypsum SI** | **Barite SI** | **Silica SI** |
|---|---|---|---|---|---|
| **Anadarko Basin** | | | | | |
| Concentrate (acidified) | Nb | 57 | 57 | 9 | 55 |
| | 5th | -1.28 | -0.67 | 0.90 | -0.32 |
| | Med | -0.92 | -0.13 | 1.15 | -0.02 |
| | 95th | -0.44 | 0.72 | 1.68 | 0.25 |
| Concentrate (no treatment) | Nb | 57 | 57 | 9 | 55 |
| | 5th | 0.02 | -1.16 | 0.15 | -0.32 |
| | Med | 0.36 | -0.18 | 0.31 | -0.02 |
| | 95th | 0.79 | 0.72 | 0.86 | 0.25 |
| Downhole Batch Mixture (with acidified concentrate) | Nb | 19999 | 19990 | N/A | 24107 |
| | 5th | -0.72 | -0.68 | N/A | -1.03 |
| | Med | -0.11 | 0.14 | N/A | -0.45 |
| | 95th | 0.37 | 0.58 | N/A | 0.01 |
| Formation Water | Nb | (1,572) | (1,659) | N/A | N/A |
| | 5th | -1.40 | -1.78 | N/A | N/A |
| | Med | 0.77 | 0.24 | N/A | N/A |
| | 95th | 1.84 | 0.78 | N/A | N/A |
| **Permian Basin** | | | | | |
| Concentrate (acidified) | Nb | 297 | 297 | 35 | 262 |
| | 5th | -1.45 | -1.02 | 0.49 | -0.52 |
| | Med | -0.69 | -0.13 | 0.70 | -0.10 |
| | 95th | -0.35 | 0.51 | 1.16 | 0.42 |
| Concentrate (no treatment) | Nb | 297 | 297 | 35 | 262 |
| | 5th | -0.18 | -1.09 | 0.45 | -0.52 |
| | Med | 0.59 | -0.23 | 0.67 | -0.10 |
| | 95th | 0.89 | 0.50 | 1.10 | 0.41 |
| Downhole Batch Mixture (with acidified concentrate) | Nb | 20,000 | 19,990 | 2,300 | 17,692 |
| | 5th | -0.50 | -0.48 | -1.01 | -1.22 |
| | Med | 0.05 | -0.03 | -0.26 | -0.57 |
| | 95th | 0.73 | 0.25 | 0.34 | 0.08 |
| Formation Water | Nb | (4,878) | (5,000) | N/A | N/A |
| | 5th | 0.31 | -1.21 | N/A | N/A |
| | Med | 1.25 | 0.05 | N/A | N/A |
| | 95th | 1.91 | 0.20 | N/A | N/A |

Nb=Number of data points; 5th=5th Percentile; Med=Median; 95th=95th Percentile

Table 7.2 (continued). Result summary of batch geochemical runs

| | | Calcite SI | Gypsum SI | Barite SI | Silica SI |
|---|---|---|---|---|---|
| **East Texas Basin** | | | | | |
| Concentrate (acidified) | Nb | 52 | 52 | N/A | 39 |
| | 5th | -2.01 | -2.10 | N/A | -0.43 |
| | Med | -1.59 | -1.74 | N/A | -0.33 |
| | 95th | -0.35 | 0.48 | N/A | 0.32 |
| Concentrate (no treatment) | Nb | 52 | 43 | N/A | 39 |
| | 5th | -0.65 | -3.73 | N/A | -0.43 |
| | Med | -0.29 | -2.52 | N/A | -0.33 |
| | 95th | 0.84 | 0.58 | N/A | 0.32 |
| Downhole Batch Mixture (with acidified concentrate) | Nb | 19,581 | 19,350 | 320 | 14,233 |
| | 5th | -0.44 | -1.39 | 0.07 | -1.28 |
| | Med | -0.03 | -0.94 | 0.96 | -0.79 |
| | 95th | 0.36 | -0.01 | 2.72 | -0.18 |
| Formation Water | Nb | (4,980) | (5,000) | (84) | (11) |
| | 5th | 0.15 | -2.74 | -1.64 | -0.39 |
| | Med | 0.98 | -1.27 | 0.85 | -0.25 |
| | 95th | 1.33 | -0.89 | 2.22 | 0.16 |
| **Fort Worth Basin** | | | | | |
| Concentrate (acidified) | Nb | 427 | 460 | 3 | 427 |
| | 5th | -0.52 | -1.73 | 0.77 | -0.52 |
| | Med | -0.26 | -0.37 | 0.82 | -0.26 |
| | 95th | 0.00 | 0.15 | 0.84 | 0.00 |
| Concentrate (no treatment) | Nb | 460 | 460 | N/A | 427 |
| | 5th | -0.44 | -2.46 | N/A | -0.52 |
| | Med | 0.81 | -0.75 | N/A | -0.26 |
| | 95th | 1.19 | 0.06 | N/A | 0.00 |
| Downhole Batch Mixture (with acidified concentrate) | Nb | 26,875 | 26,876 | N/A | N/A |
| | 5th | N/A | N/A | N/A | N/A |
| | Med | -0.27 | -1.71 | N/A | N/A |
| | 95th | 0.89 | -0.66 | N/A | N/A |
| Formation Water | Nb | (4,496 | (4,511) | N/A | N/A |
| | 5th | N/A | N/A | N/A | N/A |
| | Med | 0.02 | -1.38 | N/A | N/A |
| | 95th | 1.08 | 0.74 | N/A | N/A |

Nb=Number of data points; 5th=5th Percentile; Med=Median; 95th=95th Percentile

Table 7.2 (continued). Result summary of batch geochemical runs

| | | Calcite SI | Gypsum SI | Barite SI | Silica SI |
|---|---|---|---|---|---|
| **Maverick Basin** | | | | | |
| Concentrate (acidified) | Nb | 148 | 148 | N/A | 148 |
| | 5th | -1.92 | -1.97 | N/A | -0.56 |
| | Med | -0.64 | -0.39 | N/A | -0.23 |
| | 95th | -0.07 | 0.30 | N/A | 0.20 |
| Concentrate (no treatment) | Nb | 144 | 148 | N/A | 144 |
| | 5th | -0.46 | -0.55 | N/A | -0.46 |
| | Med | -0.22 | 0.60 | N/A | -0.22 |
| | 95th | 0.20 | 1.13 | N/A | 0.20 |
| Downhole Batch Mixture (with acidified concentrate) | Nb | 28738 | 28178 | N/A | N/A |
| | 5th | -0.40 | -1.11 | N/A | N/A |
| | Med | 0.08 | -0.30 | N/A | N/A |
| | 95th | 0.35 | 0.27 | N/A | N/A |
| Formation Water | Nb | (3,668) | (4,381) | N/A | N/A |
| | 5th | -1.50 | -3.29 | N/A | N/A |
| | Med | 0.37 | -1.61 | N/A | N/A |
| | 95th | 0.95 | -0.19 | N/A | N/A |
| **South Texas Fields** | | | | | |
| Concentrate (acidified) | Nb | 525 | 525 | 69 | 462 |
| | 5th | -1.73 | -1.52 | 0.67 | -0.39 |
| | Med | -1.11 | -0.87 | 0.83 | -0.18 |
| | 95th | -0.30 | -0.22 | 1.49 | 0.45 |
| Concentrate (no treatment) | Nb | 525 | 525 | 69 | 462 |
| | 5th | -0.43 | -2.30 | 0.52 | -0.39 |
| | Med | 0.19 | -1.08 | 0.70 | -0.18 |
| | 95th | 0.89 | -0.29 | 1.07 | 0.45 |
| Downhole Batch Mixture (with acidified concentrate) | Nb | 19,999 | 19,999 | 4,128 | 18,043 |
| | 5th | -0.77 | -1.55 | -1.70 | -1.38 |
| | Med | -0.07 | -0.81 | -0.20 | -0.79 |
| | 95th | 0.58 | -0.20 | 2.03 | -0.22 |
| Formation Water | Nb | (2,656) | (5,000) | (400) | (779) |
| | 5th | -0.28 | -3.51 | -1.27 | -1.25 |
| | Med | 0.53 | -2.31 | 0.20 | -0.78 |
| | 95th | 1.06 | -0.97 | 1.38 | -0.39 |

Nb=Number of data points; 5th=5th Percentile; Med=Median; 95th=95th Percentile

Table 7.3. Fraction of concentrate data points outside the smectite and illite salinity line

| Basin | Fraction of Concentrate Data Points outside the Smectite Salinity Line | Fraction of Concentrate Data Points outside the Illite Salinity Line |
|---|---|---|
| Anadarko | 100% | 100% |
| Permian | 76% | 81% |
| East Texas | 9% | 65% |
| Fort Worth | 50% | 61% |
| Maverick | 50% | 58% |
| Southern Gulf Coast | 29% | 58% |

Table 7.4. Volume (thousand bbl) of injected water in 1981 and cumulative up to 1981

| RRC District (# of active wells) | Saltwater >3,500 ppm* | Brackish Water 1,000< - <3,500 ppm* | Fresh Water <1,000 ppm |
|---|---:|---:|---:|
| **District 10 including Anadarko Basin** | | | |
| 1981 (758) | 20,492 | 0 | 14,480 |
| Cumulative | 403,859 | 0 | 835,682 |
| **District 8 including Permian Basin** | | | |
| 1981 (9,899) | 617,235 | 440,352 | 81,245 |
| Cumulative | 9,204,619 | 8,345,495 | 2,032,220 |
| **Districts 5 then 6 including East Texas Basin** | | | |
| 1981 (169) | 9,344 | 37 | 1,028 |
| Cumulative | 184,401 | 162 | 15,605 |
| 1981 (502) | 57,498 | 2,425 | 24,611 |
| Cumulative | 645,0997 | 70,512 | 663,108 |
| **Districts 7B then 9 including Fort Worth Basin** | | | |
| 1981 (1,654) | 133,453 | 1,423 | 41,533 |
| Cumulative | 2,826,445 | 74,583 | 788,338 |
| 1981 (4,683) | 292,279 | 3,264 | 12,117 |
| Cumulative | 6,605,868 | 152,478 | 1,369,369 |
| **District 1 including Maverick Basin** | | | |
| 1981 (1,162) | 12,409 | 17,264 | 3,367 |
| Cumulative | 1,297,012 | 78,666 | 56,453 |
| **District 4 including Southern Gulf Coast Basin** | | | |
| 1981 (424) | 79,645 | 0 | 0 |
| Cumulative | 2,440,605 | 11,211 | 1,910 |
| **All Texas Districts** | | | |
| 1981 (27,160) | 2,211,593 | 518,745 | 597,325 |
| Cumulative | 32,672,449 | 9,689,473 | 14,655,851 |

Source: Table 4, RRC (1982)

* Cut-off values for brackish and saline water from RRC (1982)

Table 7.5. Districtwide average injection rate in wells active in 1981

| RRC District (# of active wells) | Injected Volume in 1981 (1,000 bbl) | Rate/Well (bbl/day)* | Rate/Well (gpm) |
|---|---|---|---|
| **District 10 including Anadarko Basin** | | | |
| 758 | 34,972 | 126.3 | 3.7 |
| **District 8 including Permian Basin** | | | |
| 9,899 | 1,138,832 | 315.0 | 9.2 |
| **Districts 5 then 6 including East Texas Basin** | | | |
| 671 | 94,943 | 387.4 | 11.3 |
| **Districts 7B then 9 including Fort Worth Basin** | | | |
| 6337 | 484,069 | 209.1 | 6.1 |
| **District 1 including Maverick Basin** | | | |
| 1,162 | 33,040 | 77.8 | 2.3 |
| **District 4 including Southern Gulf Coast Basin** | | | |
| 424 | 79,645 | 514.3 | 15.0 |
| **All Texas Districts** | | | |
| 27,160 | 3,327,663 | 335.4 | 9.8 |

Table 7.6. Selected injection information from form H1

| Number of Forms Examined | Number of Forms with Relevant Data | Number of Forms with Nonproduced Water Sources | Source | # |
|---|---|---|---|---|
| **Anadarko Basin** | | | | |
| 34 | 34 | 0 | | |
| **Permian Basin (injection into the San Andres – Grayburg Formations)** | | | | |
| 370 | 48 | 23 | Prod. water and Santa Rosa Fm. | 9 |
| | | | Prod. Water, Santa Rosa and Ogal. Fm. | 1 |
| | | | Prod. Water and Ogal. Fm. | 9 |
| | | | Ogallala Fm. | 1 |
| | | | Surface water and unidentified source | 3 |
| **East Texas Basin (injection into the Woodbine Formation)** | | | | |
| 47 | 47 | 2 | Lower Wilcox Fm. for polymer floods | 2 |
| **Fort Worth Basin** | | | | |
| 43 | 43 | 4 | Formation water from Caddo Lime/Conglomerate, and brackish/fresh water | 4 |
| **Maverick Basin** | | | | |
| 38 | 38 | 3 | Formation water, Olmos/ San Miguel Formation and commercially available fresh water | 3 |
| **Southern Gulf Coast Basin (injection into the Frio Formation)** | | | | |
| 41 | 41 | 0 | | |

Table 7.7. Computed injection rate statistics

| Basin | 5th Percentile Injection Rate (gpm) | Median Computed Injection Rate (gpm) | 95th Percentile Injection Rate (gpm) |
|---|---|---|---|
| **Anadarko** | | | |
| | 2.3 | 7.3 | 22.8 |
| **Permian** | | | |
| | 1.5 | 13.2 | 152.7 |
| **East Texas** | | | |
| | 16.1 | 466 | 3,347 |
| **Fort Worth** | | | |
| | 0.3 | 9.8 | 376.4 |
| **Maverick** | | | |
| | 0.3 | 6.3 | 269.9 |
| **Southern Gulf Coast** | | | |
| | 29.8 | 278 | 9,038 |

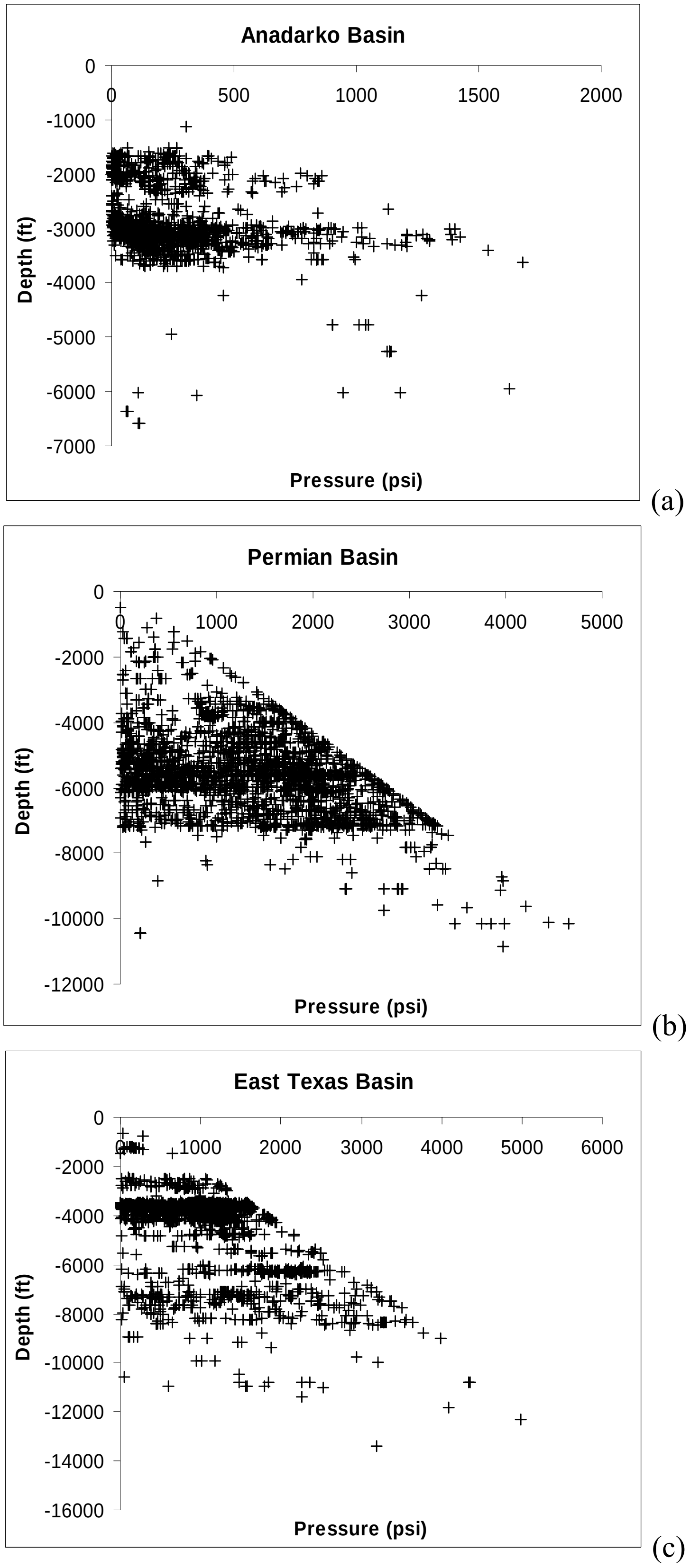

Figure 7.1. Pressure distribution from Form H15

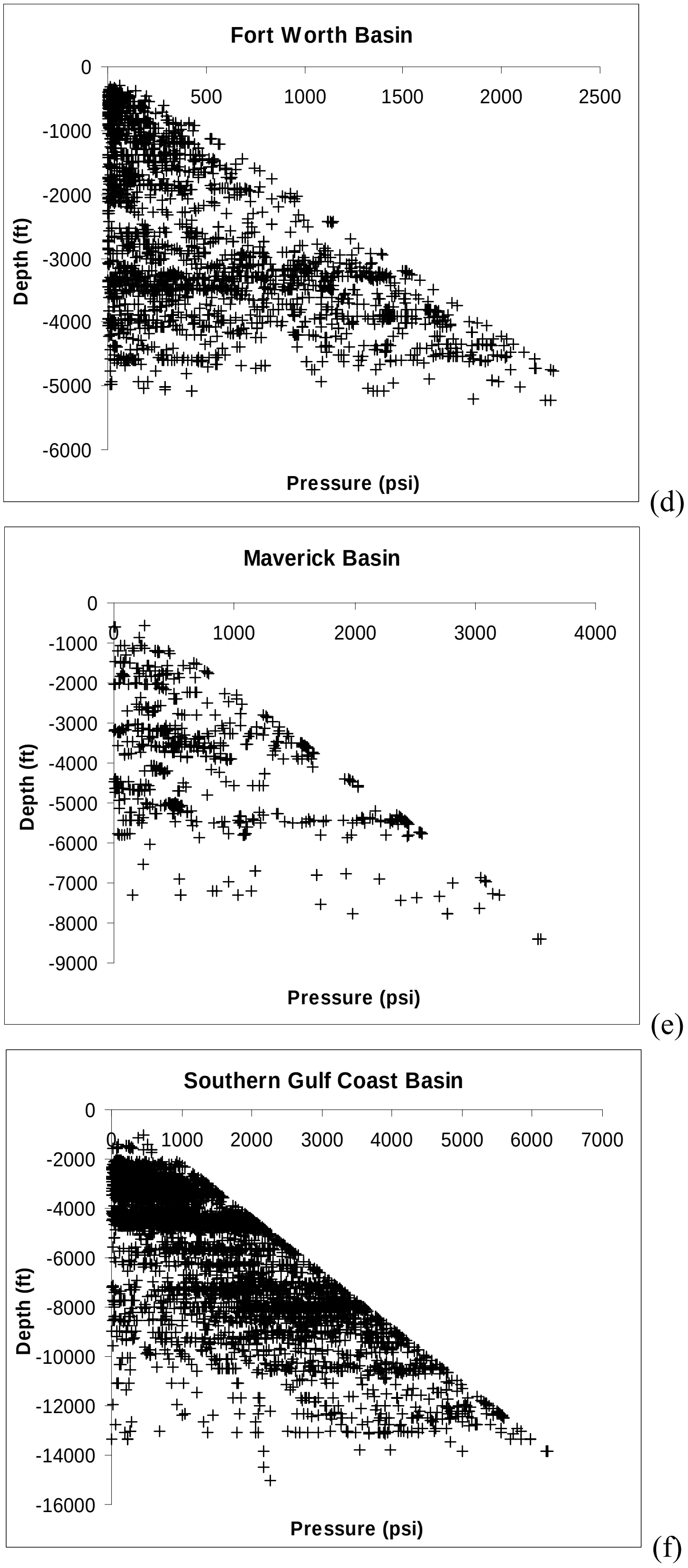

Figure 7.1 (continued). Pressure distribution from Form H15

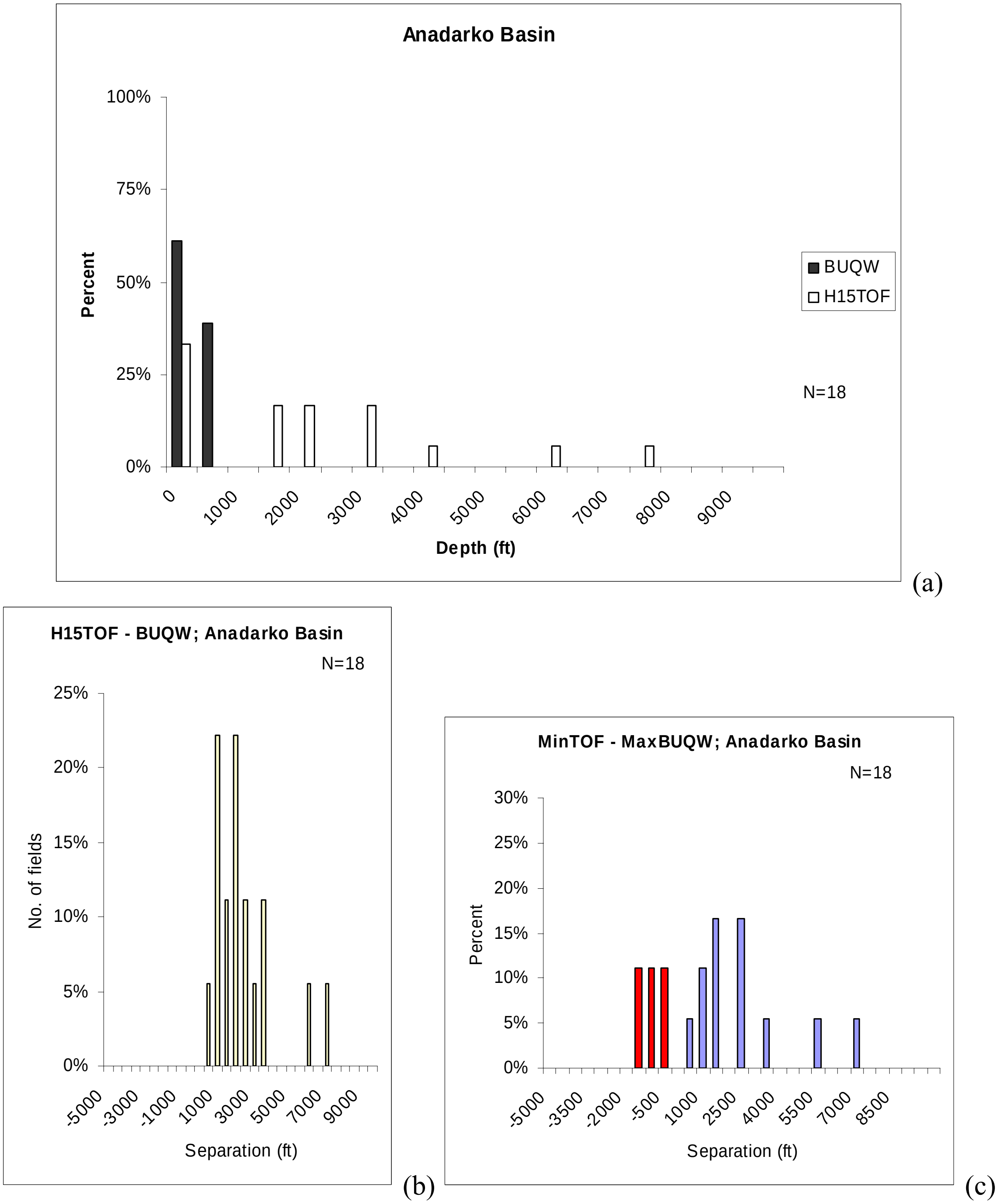

Figure 7.2. Variance of AOR study results (Anadarko Basin): (a) distribution of the depth to top of fluids (TOF) and the depth to the base of the usable quality water (BUQW); (b) distribution of field average of individual well separation between TOF and BUQW; (c) distribution of difference between maximum TOF and maximum BUQW across a given field. N=number of fields

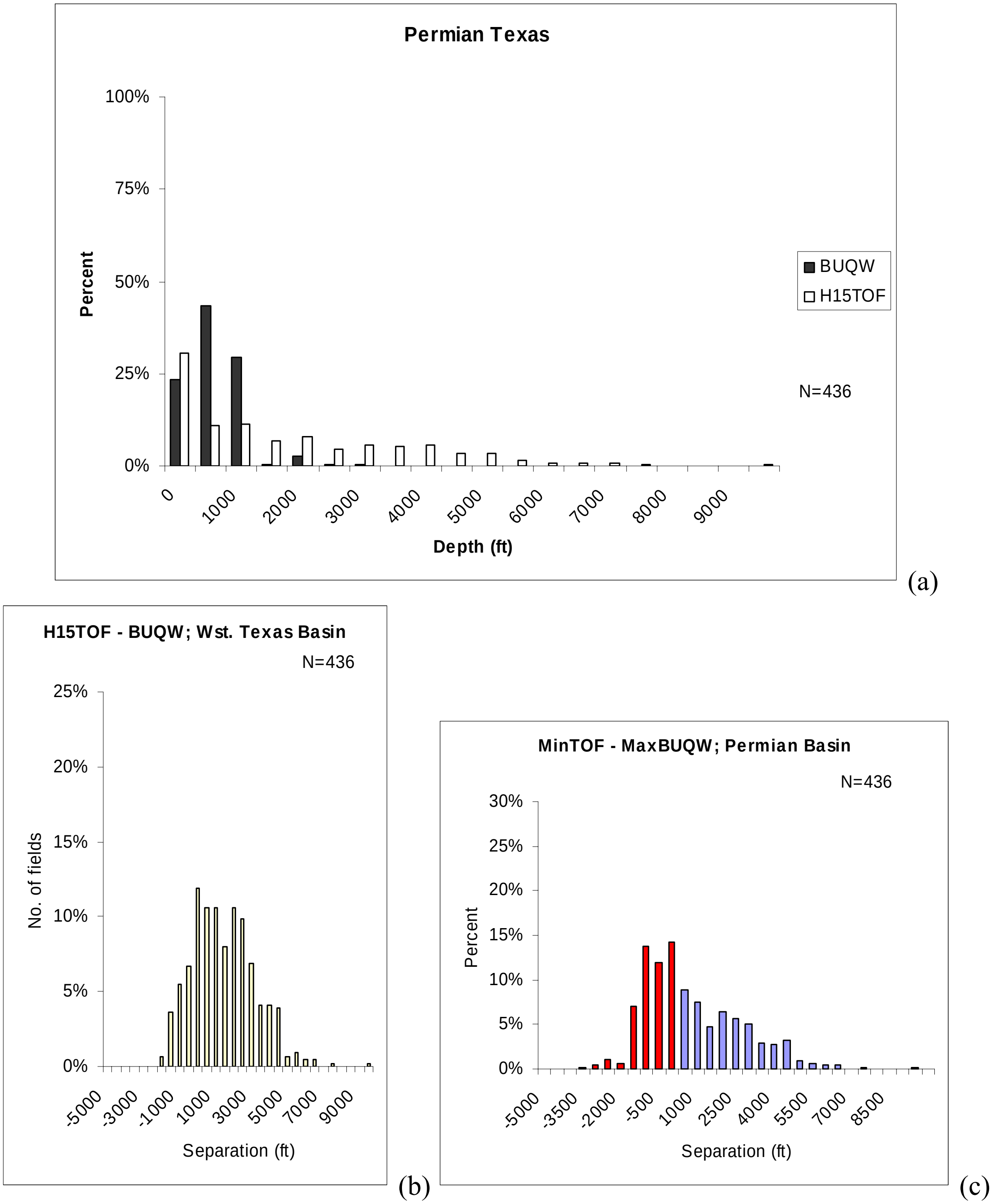

Figure 7.3. Variance of AOR study results (Permian Basin): (a) distribution of the depth to top of fluids (TOF) and the depth to the base of the usable quality water (BUQW); (b) distribution of field average of individual well separation between TOF and BUQW; (c) distribution of difference between maximum TOF and maximum BUQW across a given field. N=number of fields

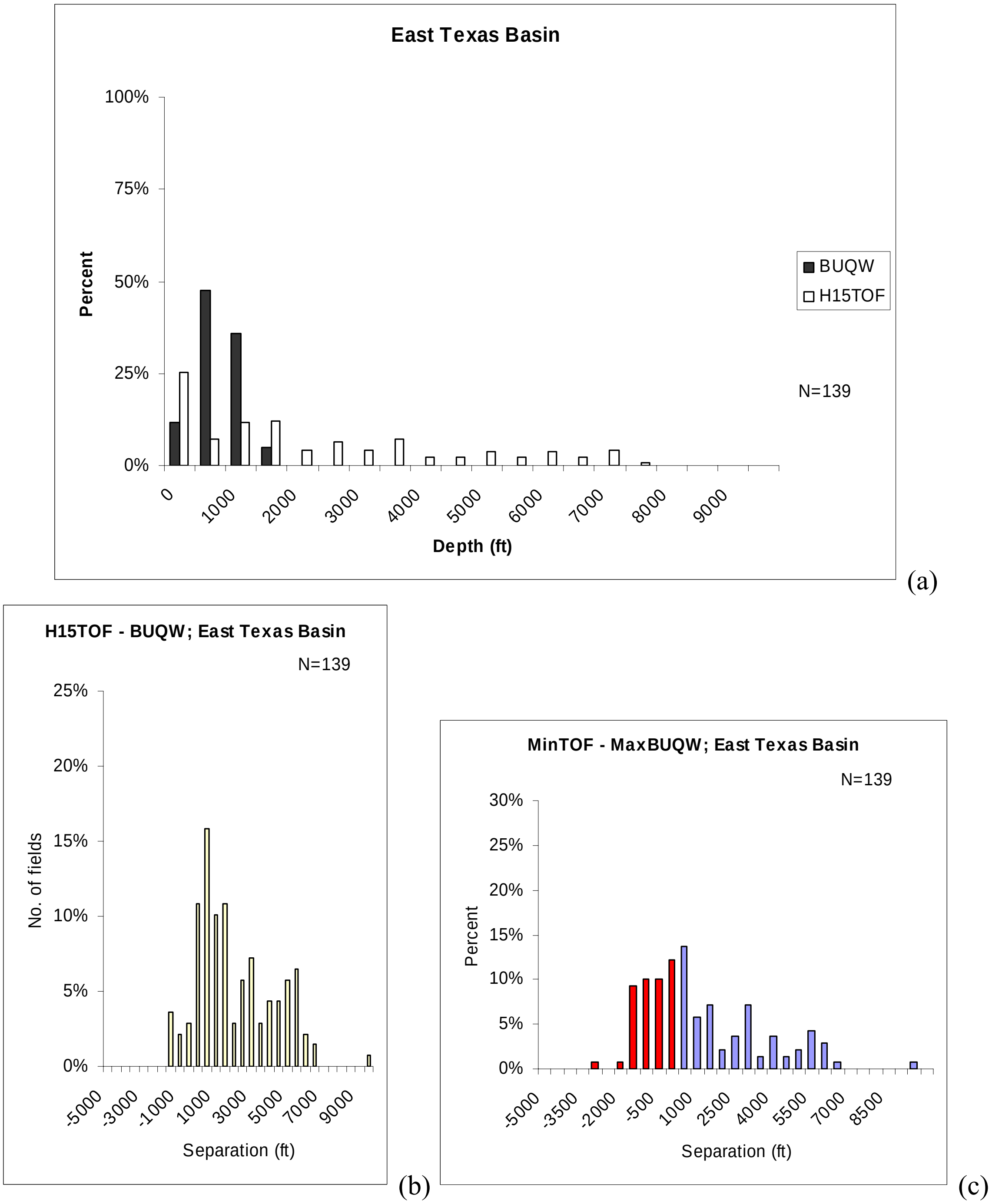

Figure 7.4. Variance of AOR study results (East Texas Basin): (a) distribution of the depth to top of fluids (TOF) and the depth to the base of the usable quality water (BUQW); (b) distribution of field average of individual well separation between TOF and BUQW; (c) distribution of difference between maximum TOF and maximum BUQW across a given field. N=number of fields

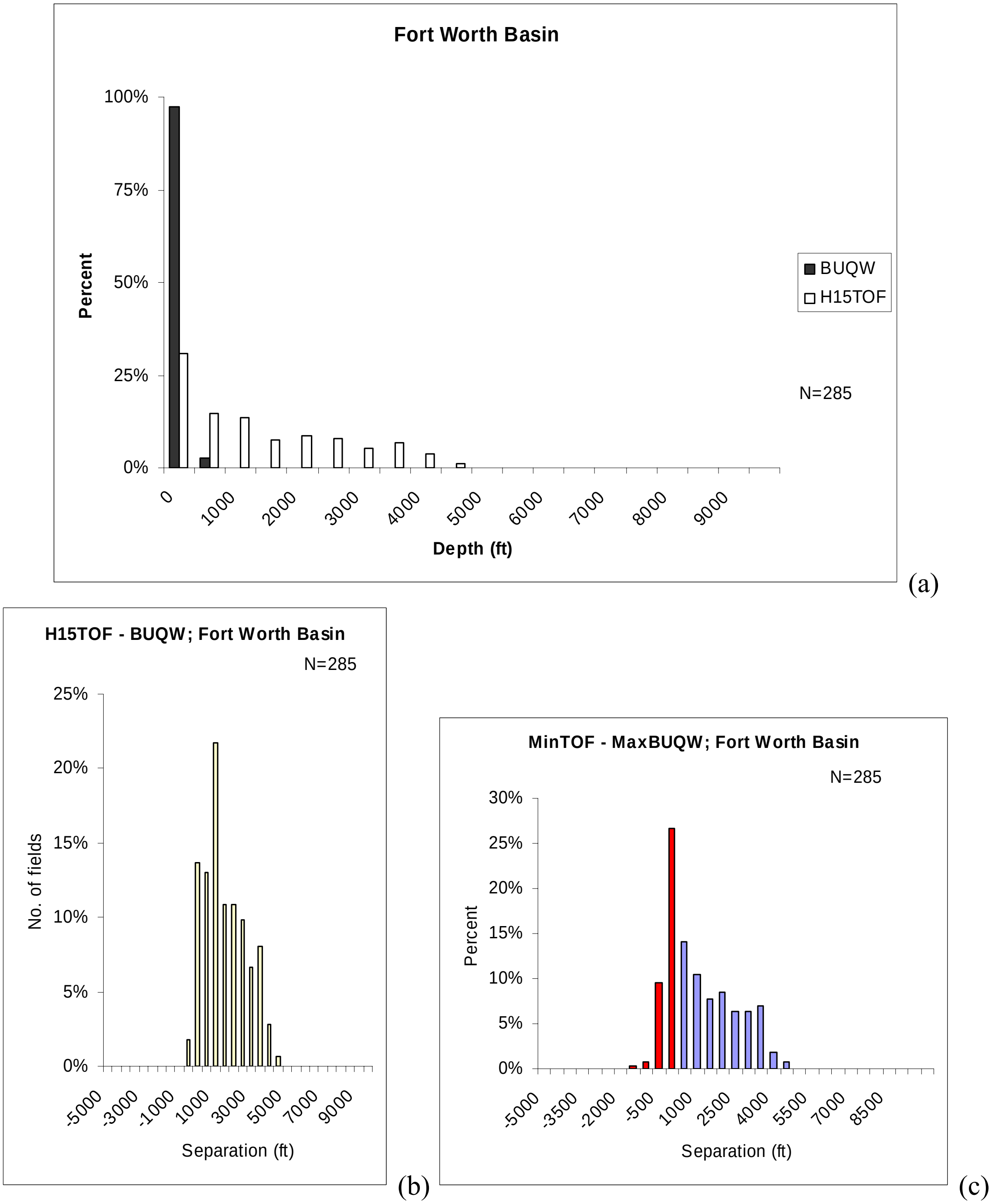

Figure 7.5. Variance of AOR study results (Fort Worth Basin): (a) distribution of the depth to top of fluids (TOF) and the depth to the base of the usable quality water (BUQW); (b) distribution of field average of individual well separation between TOF and BUQW; (c) distribution of difference between maximum TOF and maximum BUQW across a given field. N=number of fields

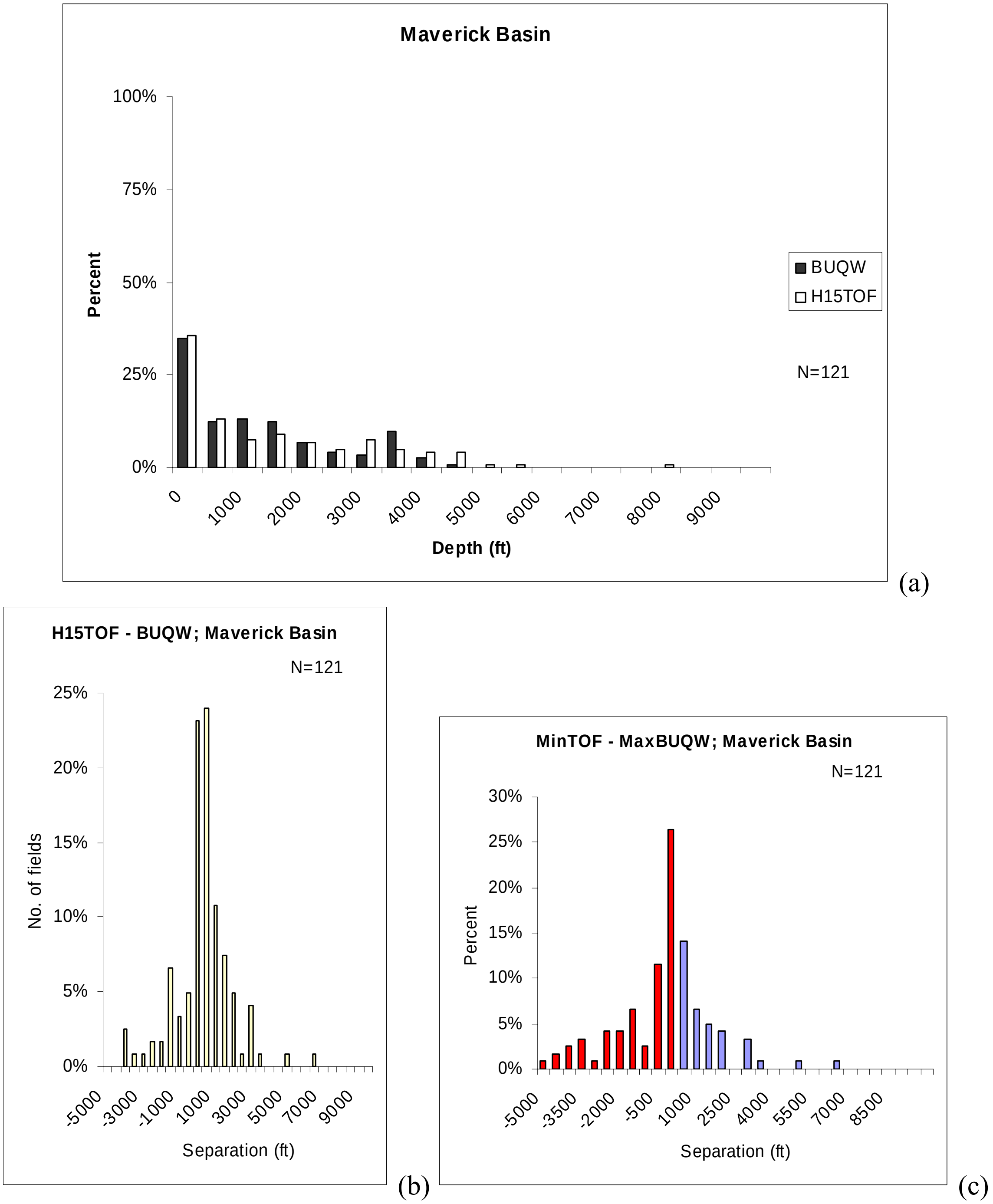

(a)

(b)

(c)

Figure 7.6. Variance of AOR study results (Maverick Basin): (a) distribution of the depth to top of fluids (TOF) and the depth to the base of the usable quality water (BUQW); (b) distribution of field average of individual well separation between TOF and BUQW; (c) distribution of difference between maximum TOF and maximum BUQW across a given field. N=number of fields

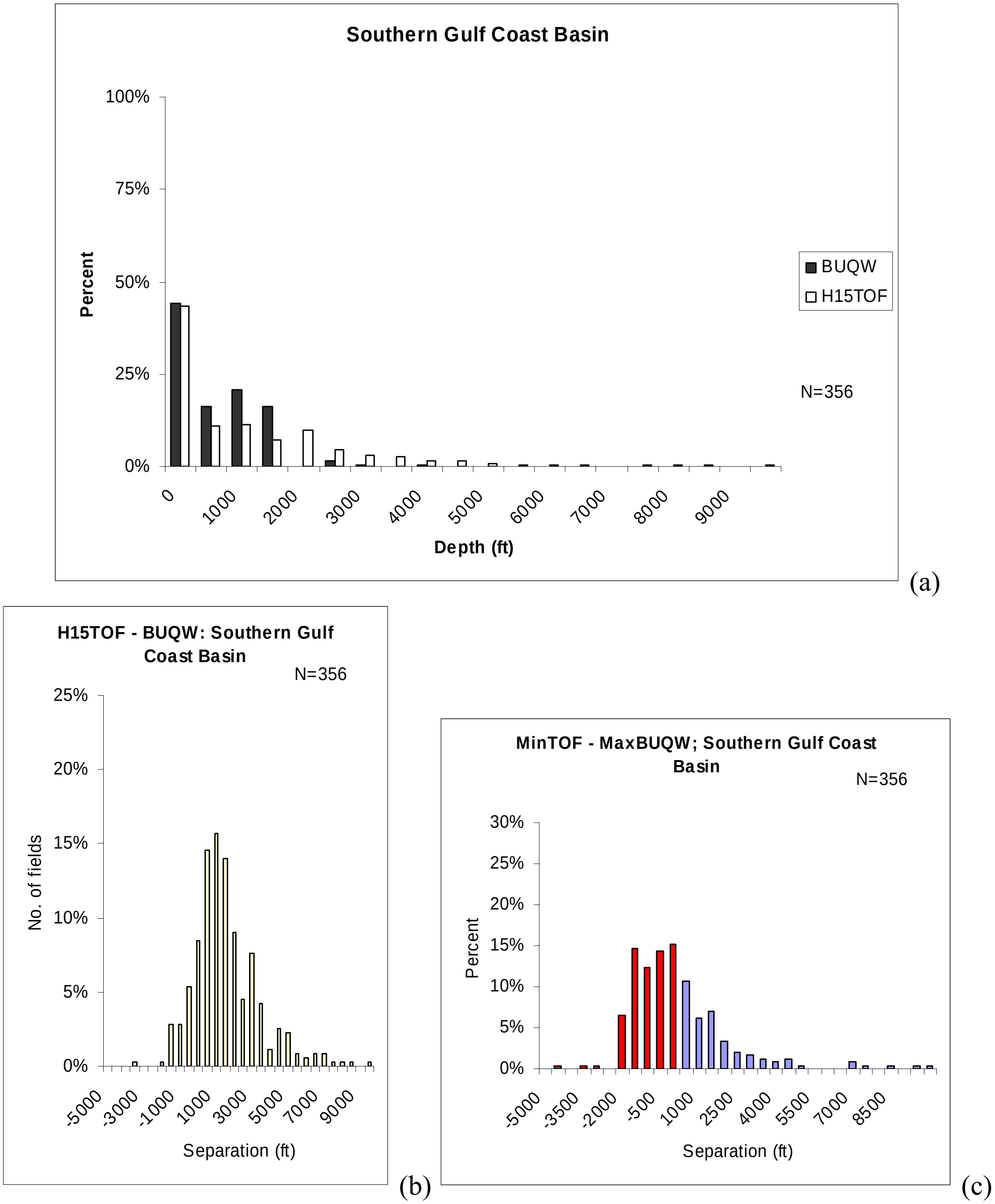

Figure 7.7. Variance of AOR study results (Southern Gulf Coast Basin): (a) distribution of the depth to top of fluids (TOF) and the depth to the base of the usable quality water (BUQW); (b) distribution of field average of individual well separation between TOF and BUQW; (c) distribution of difference between maximum TOF and maximum BUQW across a given field. N=number of fields

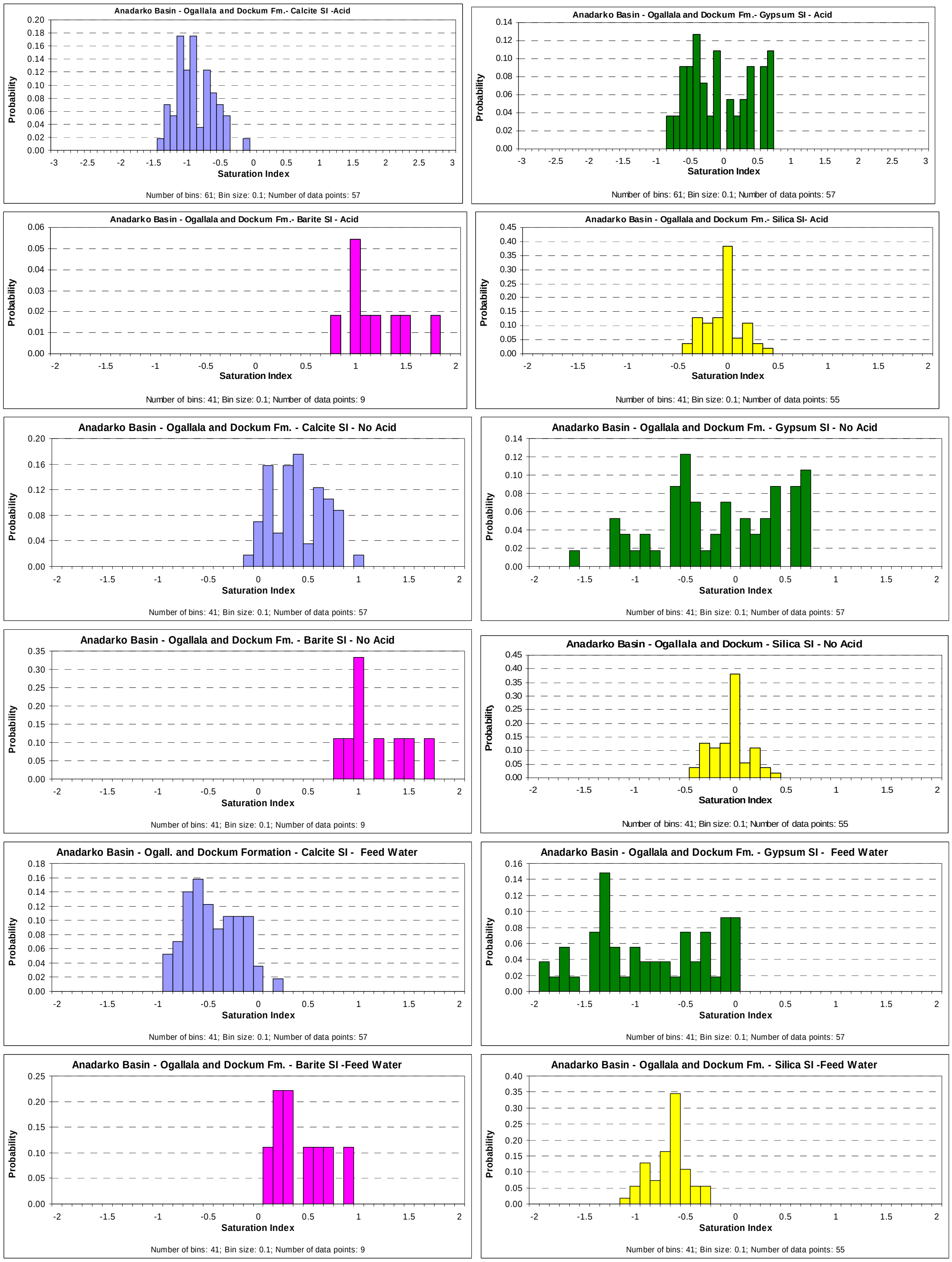
Anadarko Basin - Ogallala and Dockum Fm.- Calcite SI -Acid

Number of bins: 61; Bin size: 0.1; Number of data points: 57

Anadarko Basin - Ogallala and Dockum Fm.- Gypsum SI - Acid

Number of bins: 61; Bin size: 0.1; Number of data points: 57

Anadarko Basin - Ogallala and Dockum Fm.- Barite SI - Acid

Number of bins: 41; Bin size: 0.1; Number of data points: 9

Anadarko Basin - Ogallala and Dockum Fm.- Silica SI- Acid

Number of bins: 41; Bin size: 0.1; Number of data points: 55

Anadarko Basin - Ogallala and Dockum Fm. - Calcite SI - No Acid

Number of bins: 41; Bin size: 0.1; Number of data points: 57

Anadarko Basin - Ogallala and Dockum Fm. - Gypsum SI - No Acid

Number of bins: 41; Bin size: 0.1; Number of data points: 57

Anadarko Basin - Ogallala and Dockum Fm. - Barite SI - No Acid

Number of bins: 41; Bin size: 0.1; Number of data points: 9

Anadarko Basin - Ogallala and Dockum - Silica SI - No Acid

Number of bins: 41; Bin size: 0.1; Number of data points: 55

Anadarko Basin - Ogall. and Dockum Formation - Calcite SI - Feed Water

Number of bins: 41; Bin size: 0.1; Number of data points: 57

Anadarko Basin - Ogallala and Dockum Fm. - Gypsum SI - Feed Water

Number of bins: 41; Bin size: 0.1; Number of data points: 57

Anadarko Basin - Ogallala and Dockum Fm. - Barite SI -Feed Water

Number of bins: 41; Bin size: 0.1; Number of data points: 9

Anadarko Basin - Ogallala and Dockum Fm. - Silica SI -Feed Water

Number of bins: 41; Bin size: 0.1; Number of data points: 55

Figure 7.8. Saturation index of scale-forming minerals for the concentrate with and without acidification and for the feed water (Anadarko Basin)

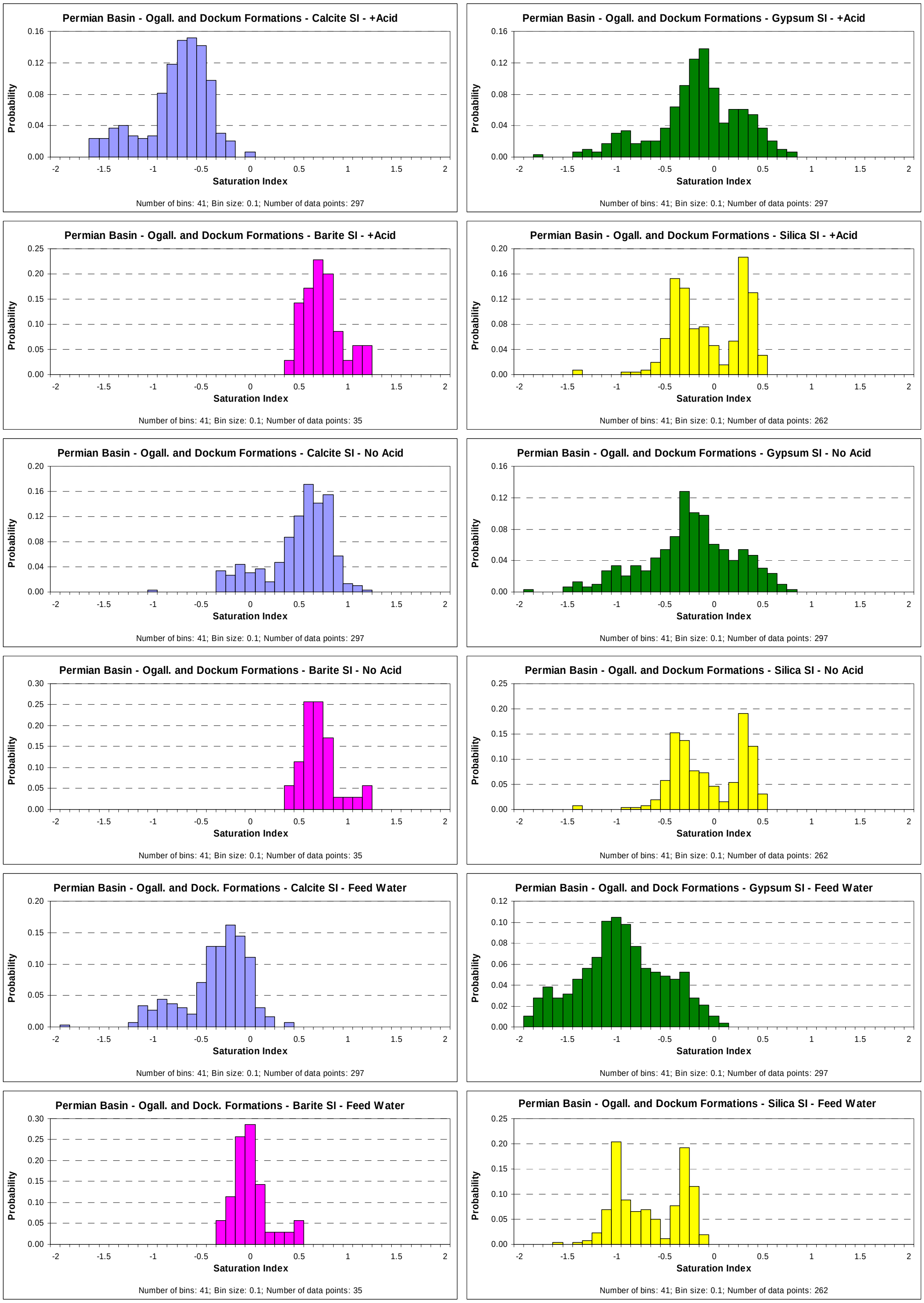
Permian Basin - Ogall. and Dockum Formations - Calcite SI - +Acid

Number of bins: 41; Bin size: 0.1; Number of data points: 297

Permian Basin - Ogall. and Dockum Formations - Gypsum SI - +Acid

Number of bins: 41; Bin size: 0.1; Number of data points: 297

Permian Basin - Ogall. and Dockum Formations - Barite SI - +Acid

Number of bins: 41; Bin size: 0.1; Number of data points: 35

Permian Basin - Ogall. and Dockum Formations - Silica SI - +Acid

Number of bins: 41; Bin size: 0.1; Number of data points: 262

Permian Basin - Ogall. and Dockum Formations - Calcite SI - No Acid

Number of bins: 41; Bin size: 0.1; Number of data points: 297

Permian Basin - Ogall. and Dockum Formations - Gypsum SI - No Acid

Number of bins: 41; Bin size: 0.1; Number of data points: 297

Permian Basin - Ogall. and Dockum Formations - Barite SI - No Acid

Number of bins: 41; Bin size: 0.1; Number of data points: 35

Permian Basin - Ogall. and Dockum Formations - Silica SI - No Acid

Number of bins: 41; Bin size: 0.1; Number of data points: 262

Permian Basin - Ogall. and Dock. Formations - Calcite SI - Feed Water

Number of bins: 41; Bin size: 0.1; Number of data points: 297

Permian Basin - Ogall. and Dock Formations - Gypsum SI - Feed Water

Number of bins: 41; Bin size: 0.1; Number of data points: 297

Permian Basin - Ogall. and Dock. Formations - Barite SI - Feed Water

Number of bins: 41; Bin size: 0.1; Number of data points: 35

Permian Basin - Ogall. and Dockum Formations - Silica SI - Feed Water

Number of bins: 41; Bin size: 0.1; Number of data points: 262

Figure 7.9. Saturation index of scale-forming minerals for the concentrate with and without acidification and for the feed water (Permian Basin)

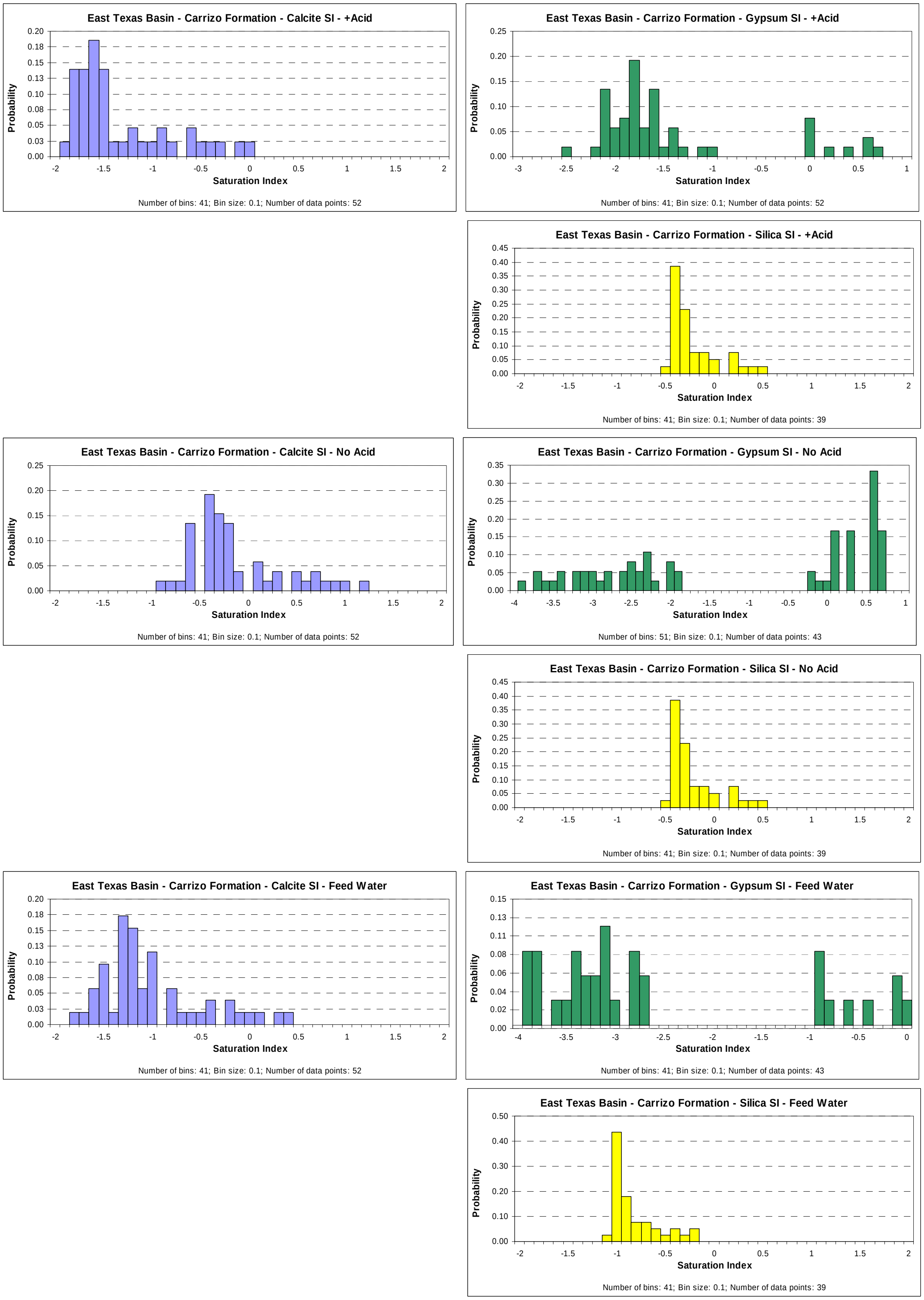

Figure 7.10. Saturation index of scale-forming minerals for the concentrate with and without acidification and for the feed water (East Texas Basin)

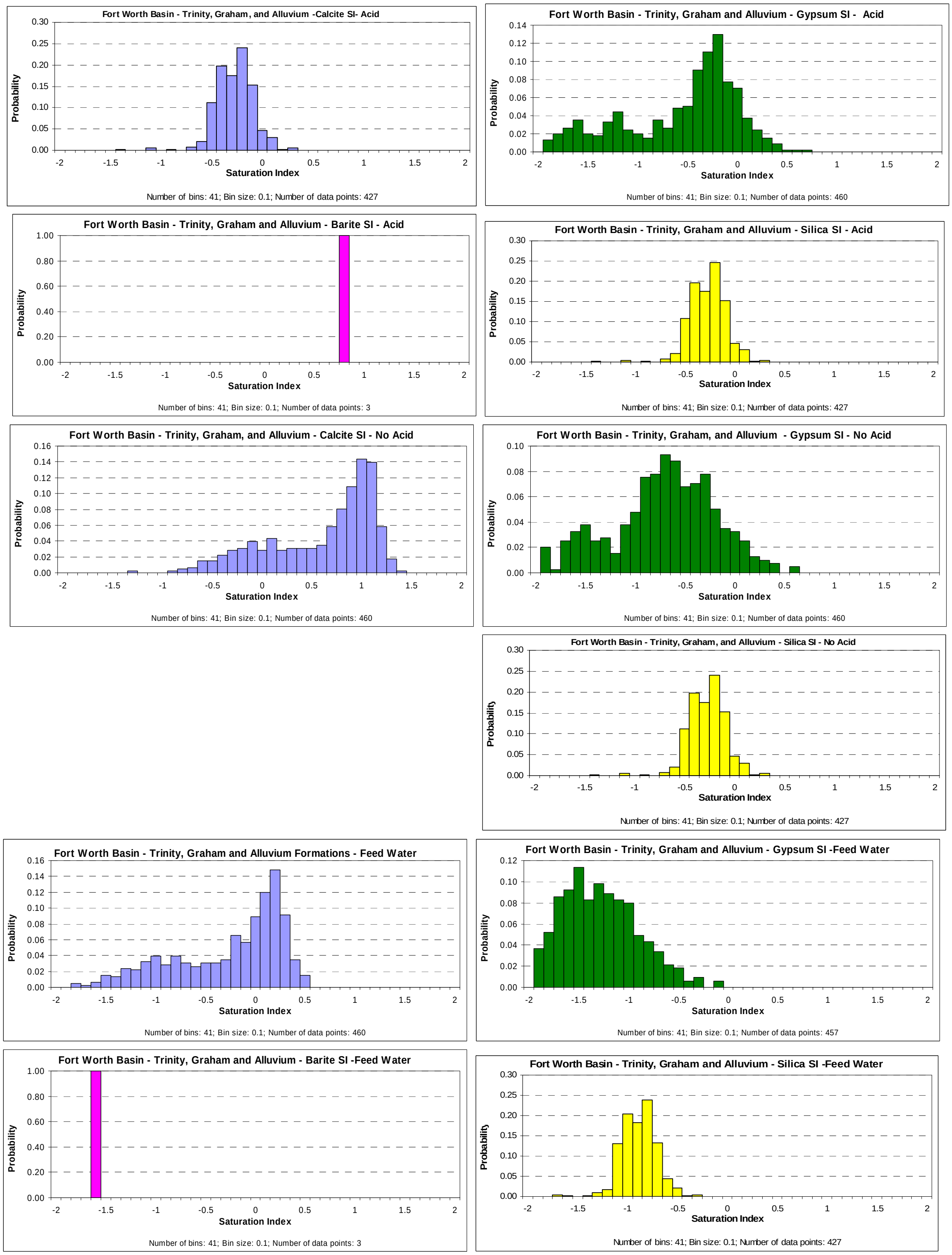

Fort Worth Basin - Trinity, Graham, and Alluvium -Calcite SI- Acid

Number of bins: 41; Bin size: 0.1; Number of data points: 427

Fort Worth Basin - Trinity, Graham and Alluvium - Gypsum SI - Acid

Number of bins: 41; Bin size: 0.1; Number of data points: 460

Fort Worth Basin - Trinity, Graham and Alluvium - Barite SI - Acid

Number of bins: 41; Bin size: 0.1; Number of data points: 3

Fort Worth Basin - Trinity, Graham and Alluvium - Silica SI - Acid

Number of bins: 41; Bin size: 0.1; Number of data points: 427

Fort Worth Basin - Trinity, Graham, and Alluvium - Calcite SI - No Acid

Number of bins: 41; Bin size: 0.1; Number of data points: 460

Fort Worth Basin - Trinity, Graham, and Alluvium - Gypsum SI - No Acid

Number of bins: 41; Bin size: 0.1; Number of data points: 460

Fort Worth Basin - Trinity, Graham, and Alluvium - Silica SI - No Acid

Number of bins: 41; Bin size: 0.1; Number of data points: 427

Fort Worth Basin - Trinity, Graham and Alluvium Formations - Feed Water

Number of bins: 41; Bin size: 0.1; Number of data points: 460

Fort Worth Basin - Trinity, Graham and Alluvium - Gypsum SI -Feed Water

Number of bins: 41; Bin size: 0.1; Number of data points: 457

Fort Worth Basin - Trinity, Graham and Alluvium - Barite SI -Feed Water

Number of bins: 41; Bin size: 0.1; Number of data points: 3

Fort Worth Basin - Trinity, Graham and Alluvium - Silica SI -Feed Water

Number of bins: 41; Bin size: 0.1; Number of data points: 427

Figure 7.11. Saturation index of scale-forming minerals for the concentrate with and without acidification and for the feed water (Fort Worth Basin)

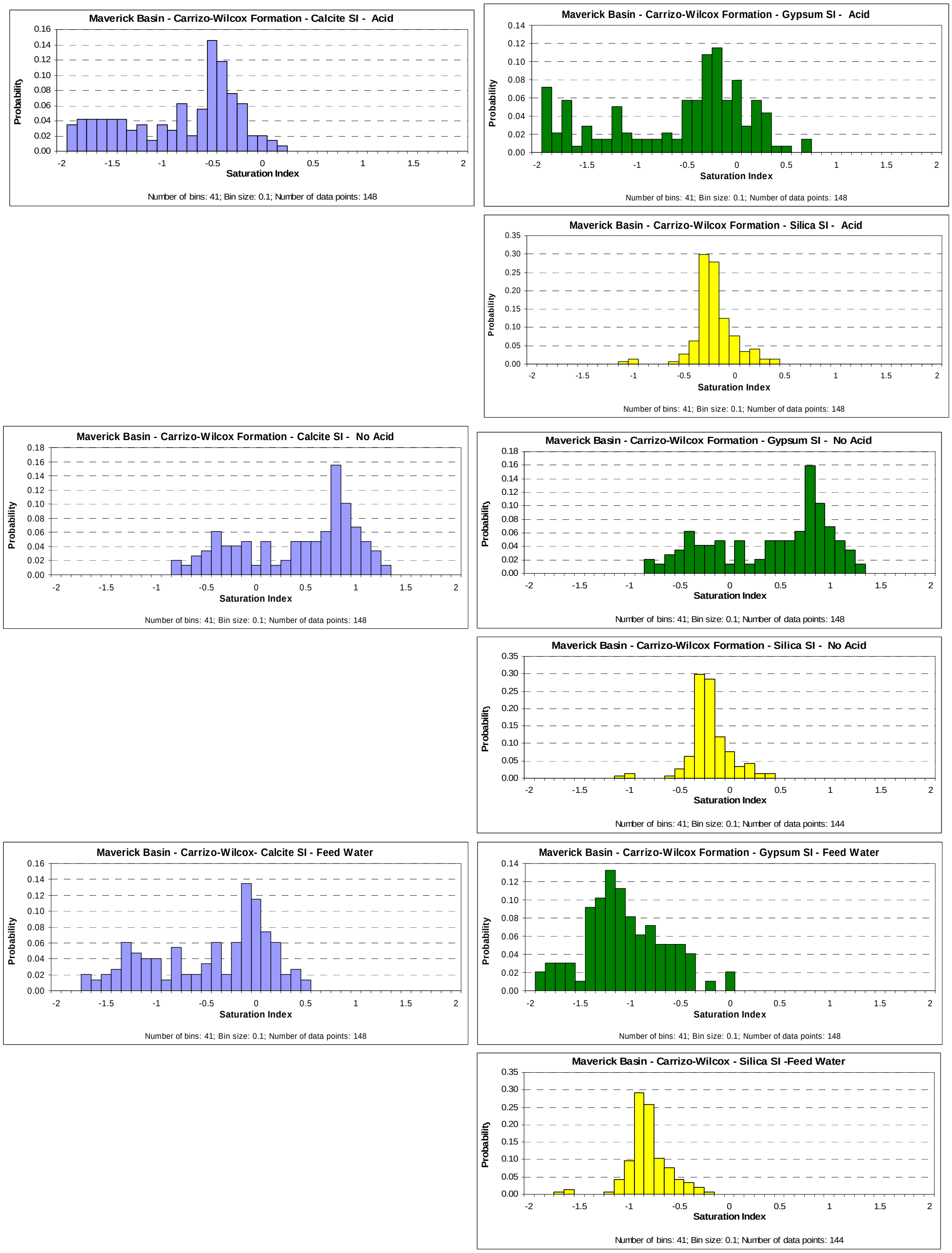

Figure 7.12. Saturation index of scale-forming minerals for the concentrate with and without acidification and for the feed water (Maverick Basin)

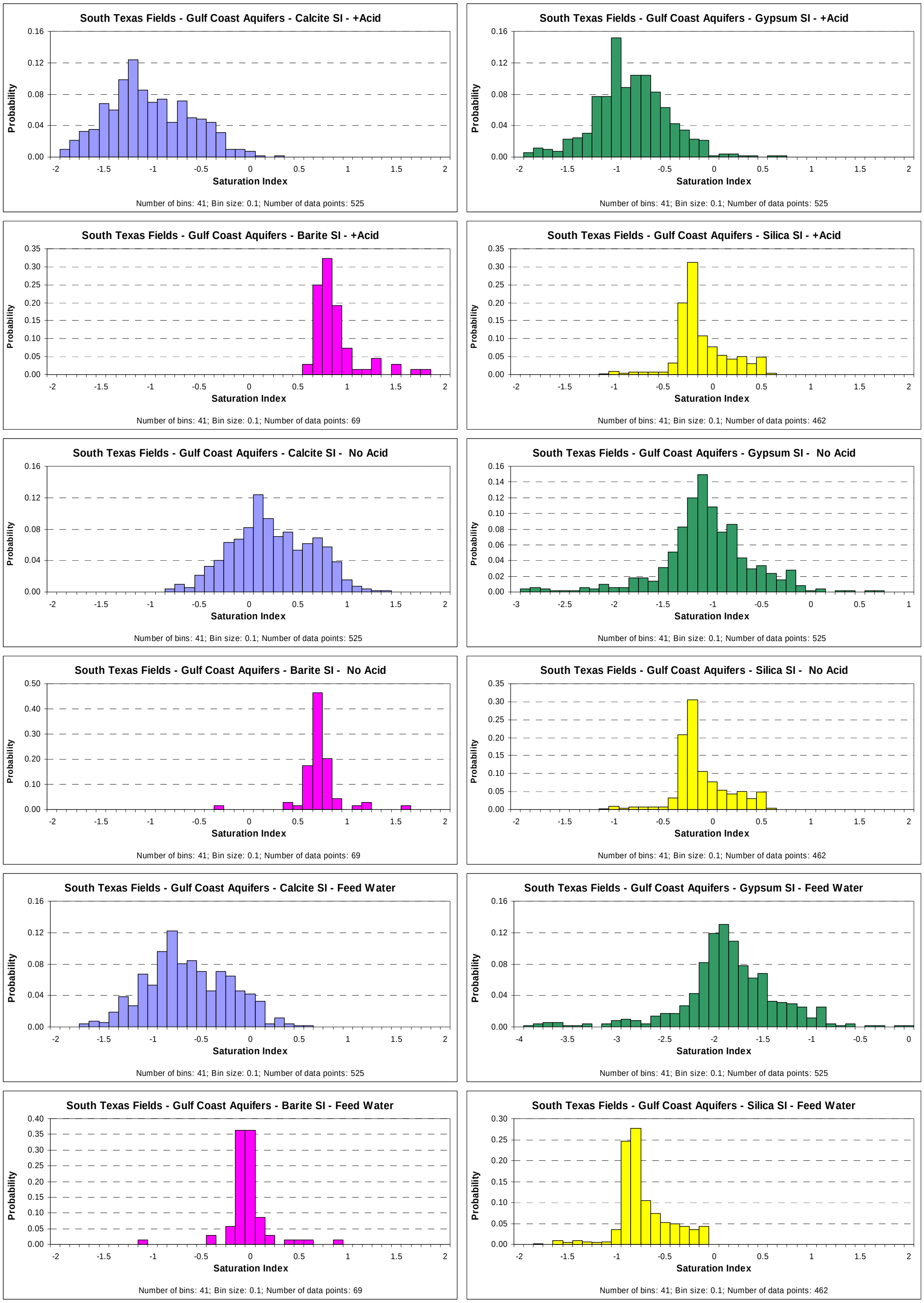

Figure 7.13. Saturation index of scale-forming minerals for the concentrate with and without acidification and for the feed water (Gulf Coast Basin)

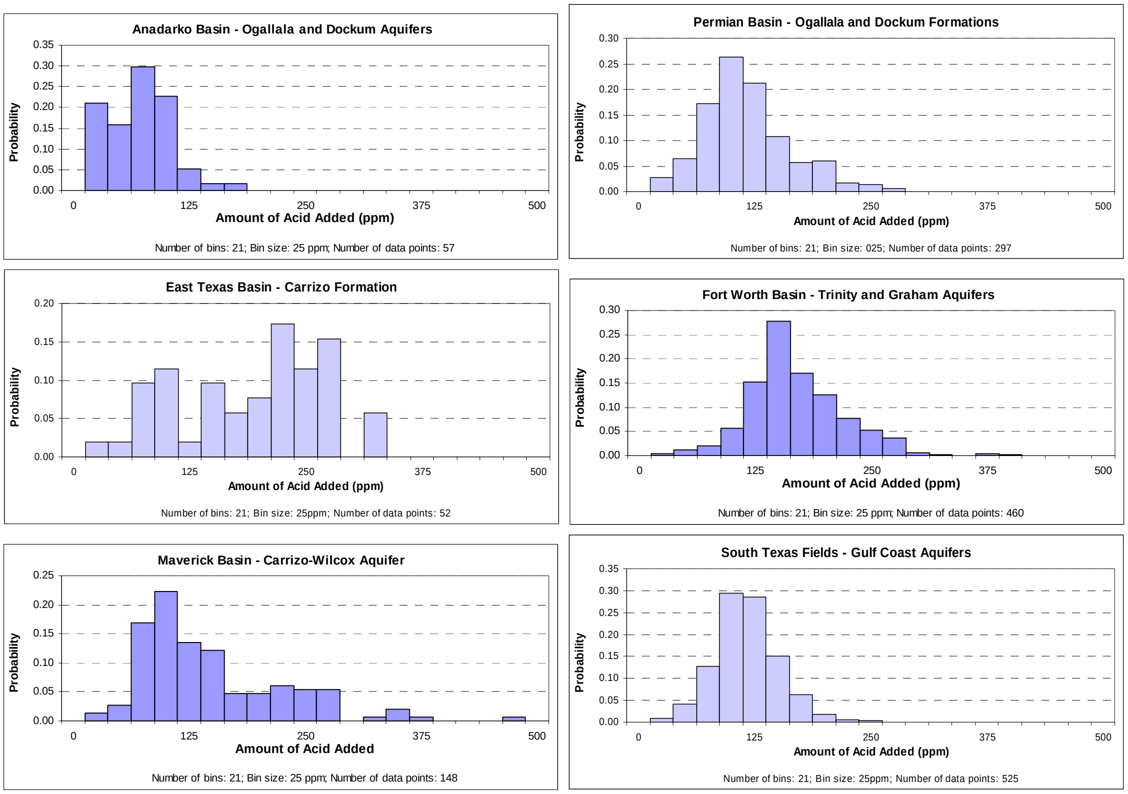

Figure 7.14. Distribution of the amount of sulfuric acid to be added to the feed water to maintain a pH of 6

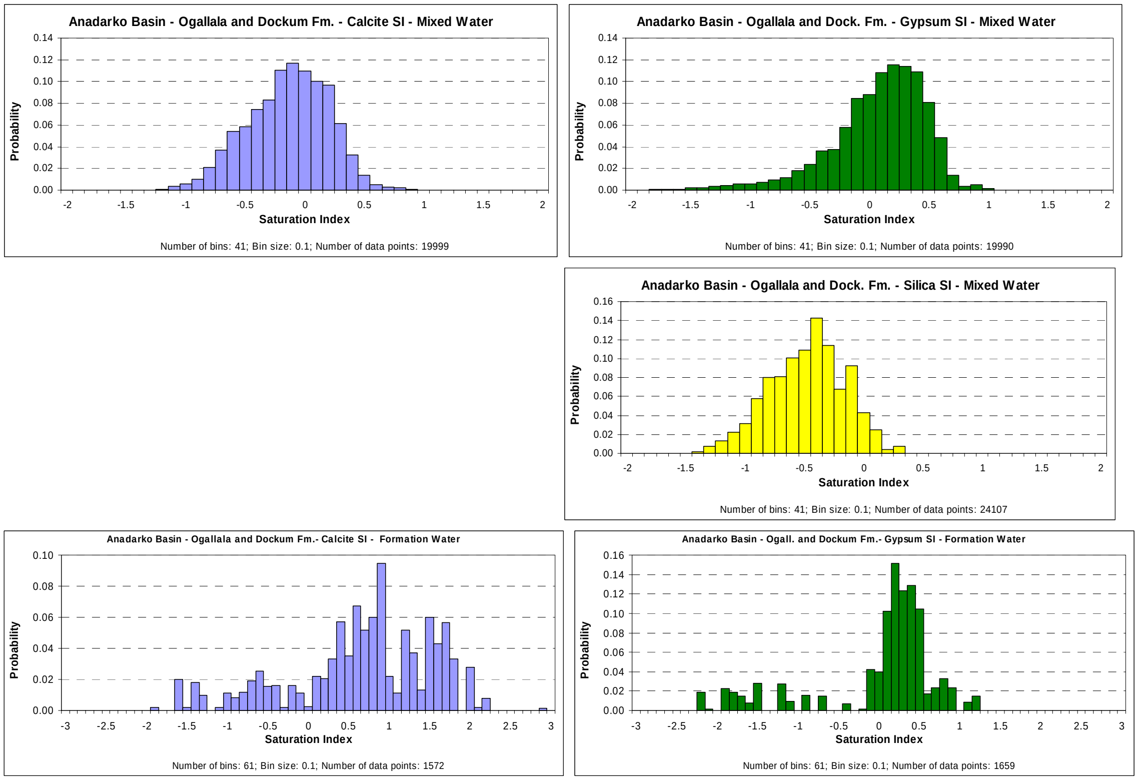

Figure 7.15. Saturation index of scale-forming minerals for the mixed solution (with acidified concentrate) and for the formation water (Anadarko Basin)

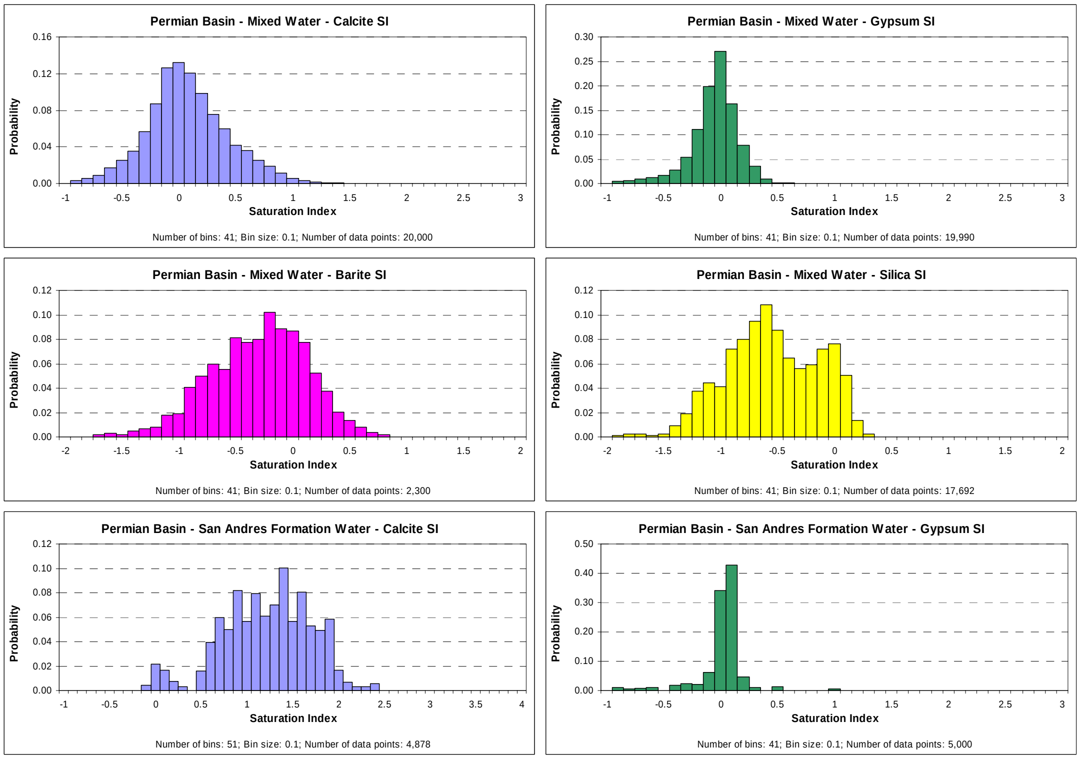

Figure 7.16. Saturation index of scale-forming minerals for the mixed solution (with acidified concentrate) and for the formation water (Permian Basin)

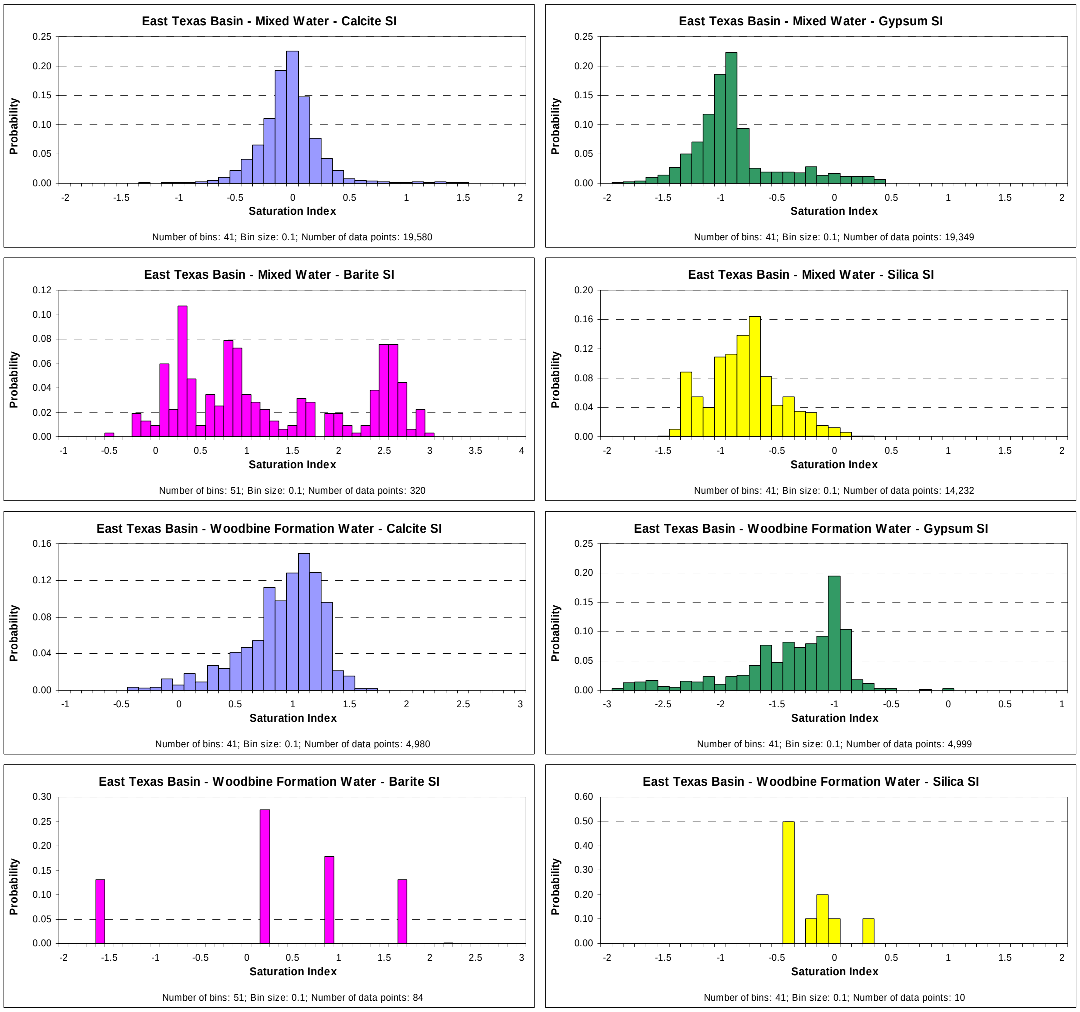

Figure 7.17. Saturation index of scale-forming minerals for the mixed solution (with acidified concentrate) and for the formation water (East Texas Basin)

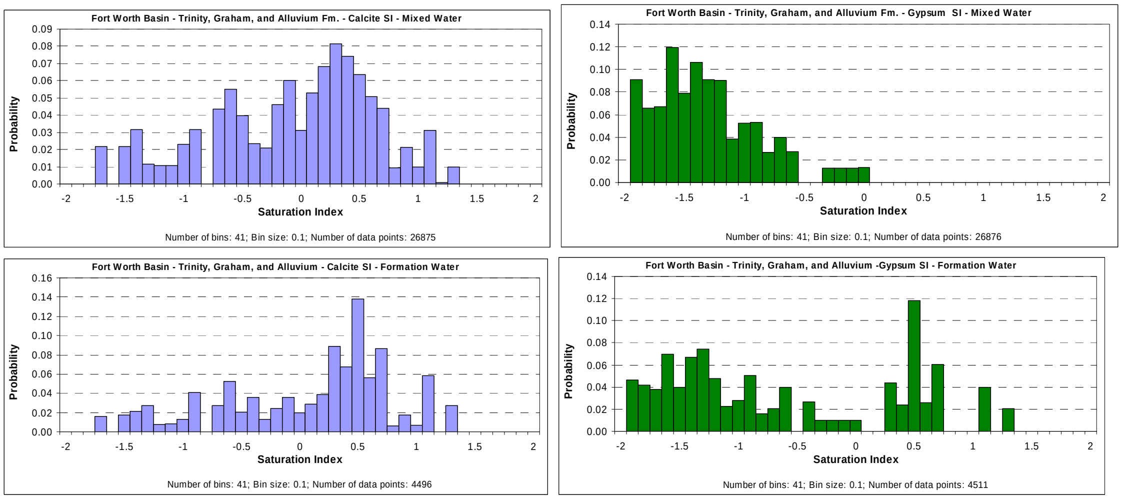

Figure 7.18. Saturation index of scale-forming minerals for the mixed solution (with acidified concentrate) and for the formation water (Fort Worth Basin)

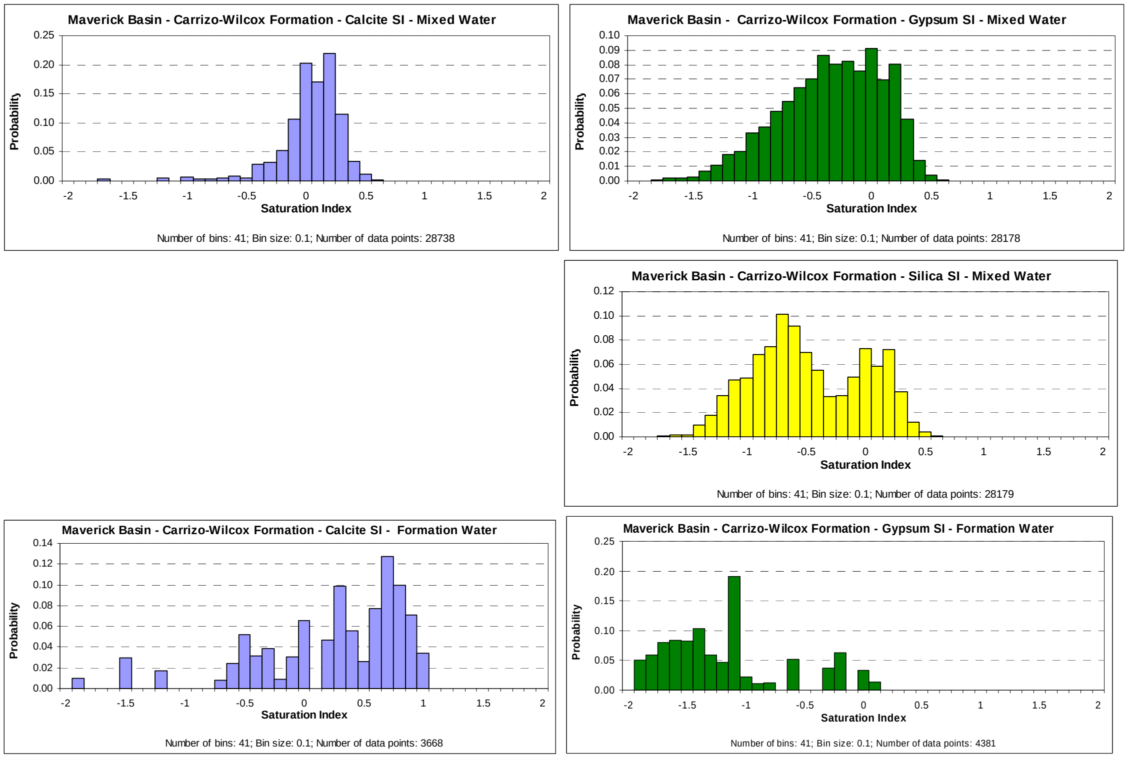

Figure 7.19. Saturation index of scale-forming minerals for the mixed solution (with acidified concentrate) and for the formation water (Maverick Basin)

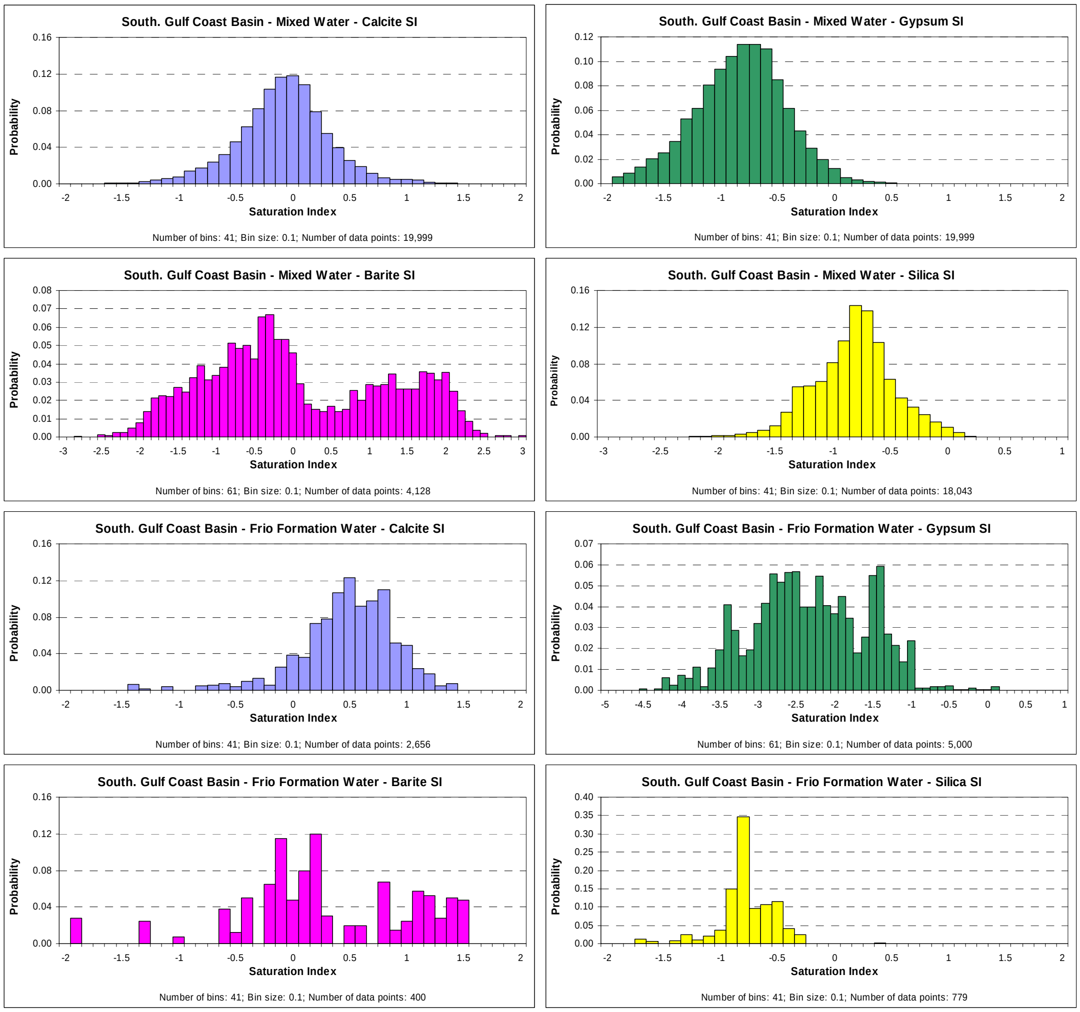

Figure 7.20. Saturation index of scale-forming minerals for the mixed solution (with acidified concentrate) and for the formation water (Southern Gulf Coast Basin)

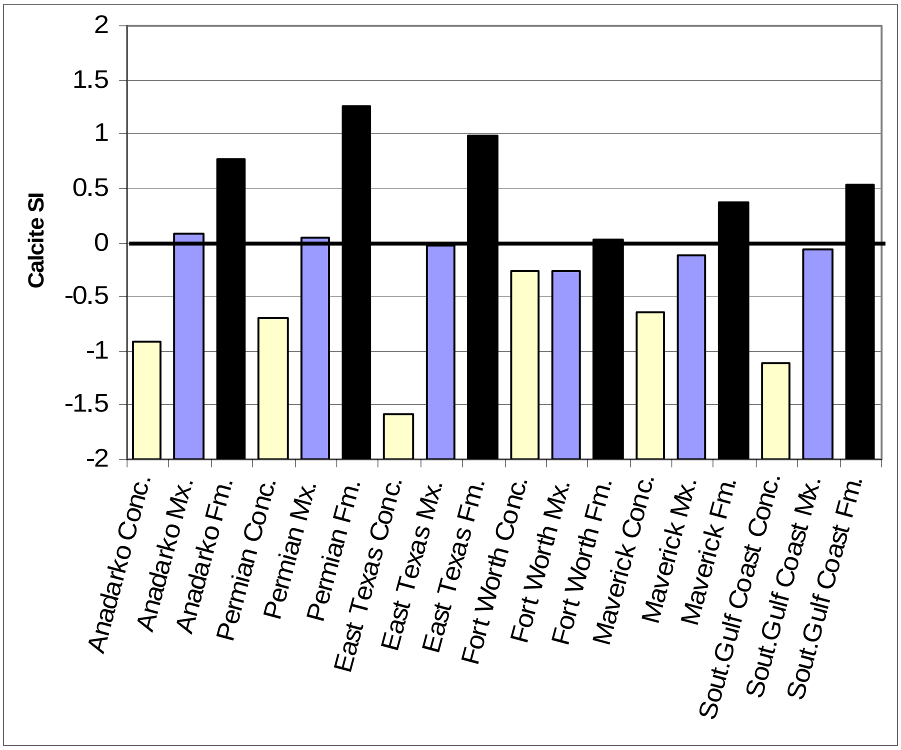

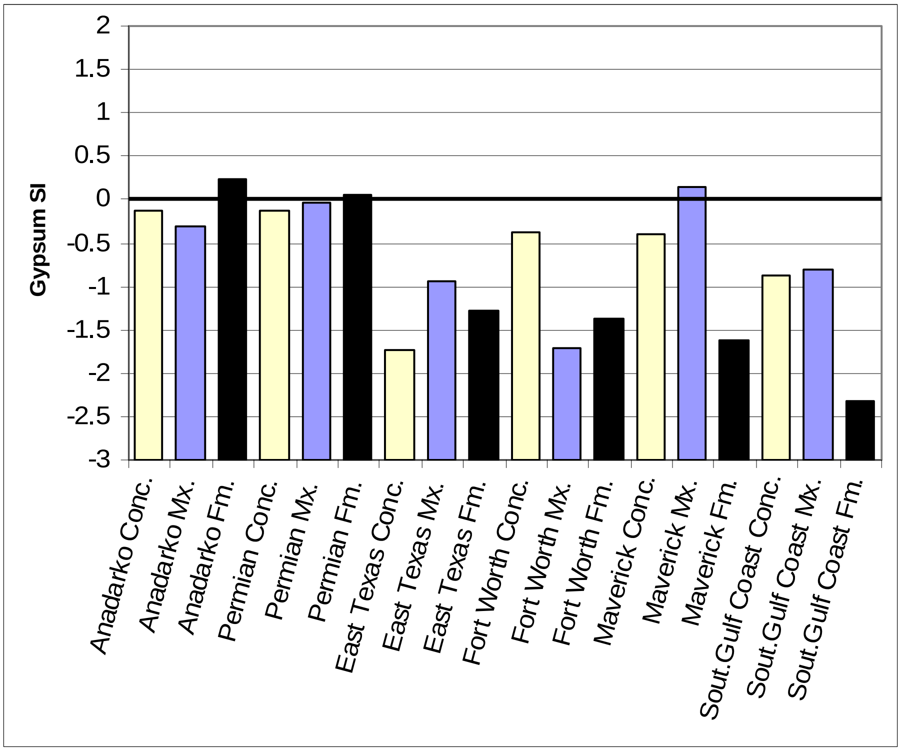

Figure 7.21. Summary of saturation indices for (a) calcite; (b) gypsum; (c) barite; (d) silica for concentrate, formation water and mixing solutions (median values)

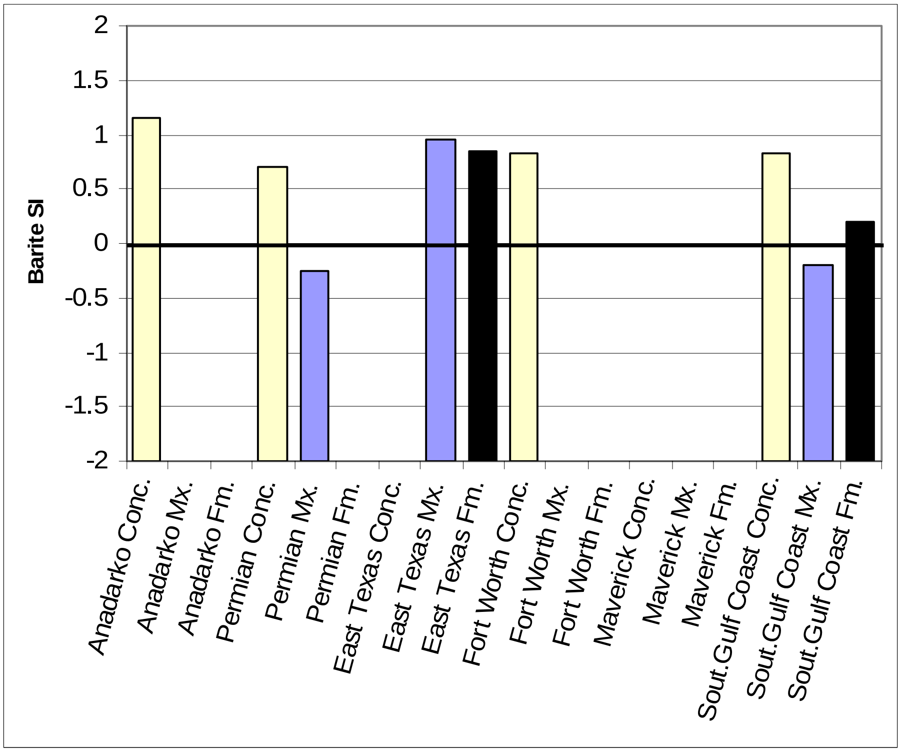

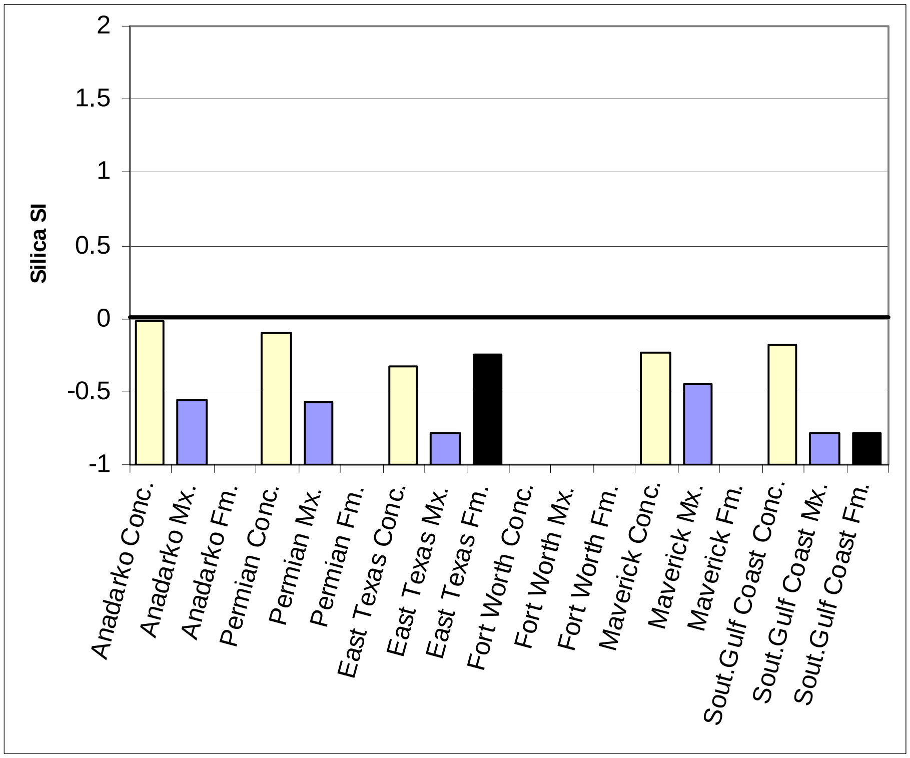

Figure 7.21 (continued). Summary of saturation indices for (a) calcite; (b) gypsum; (c) barite; (d) silica for concentrate, formation water and mixing solutions (median value)

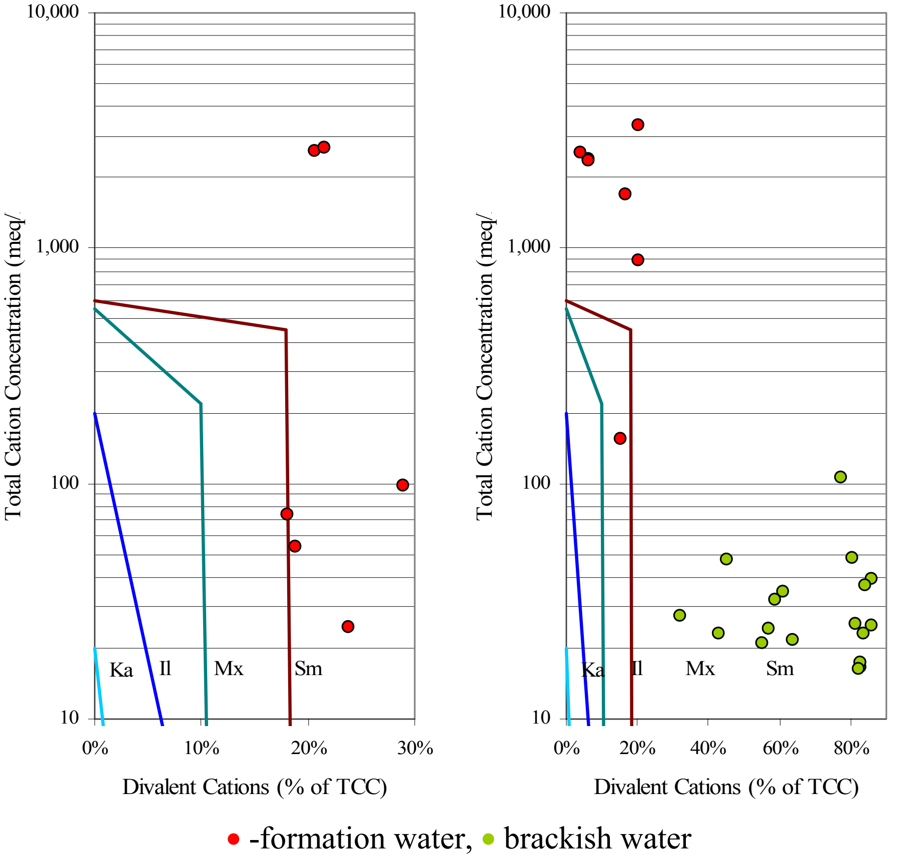

(a) Moore County (b) Hutchinson County

Note: Most of the brackish waters have high divalent cations and fall to the right of the smectite boundary (not shown).

Figure 7.22. Plot of total cation concentration and divalent cations percent for the brackish groundwater and the formation water (Anadarko Basin)

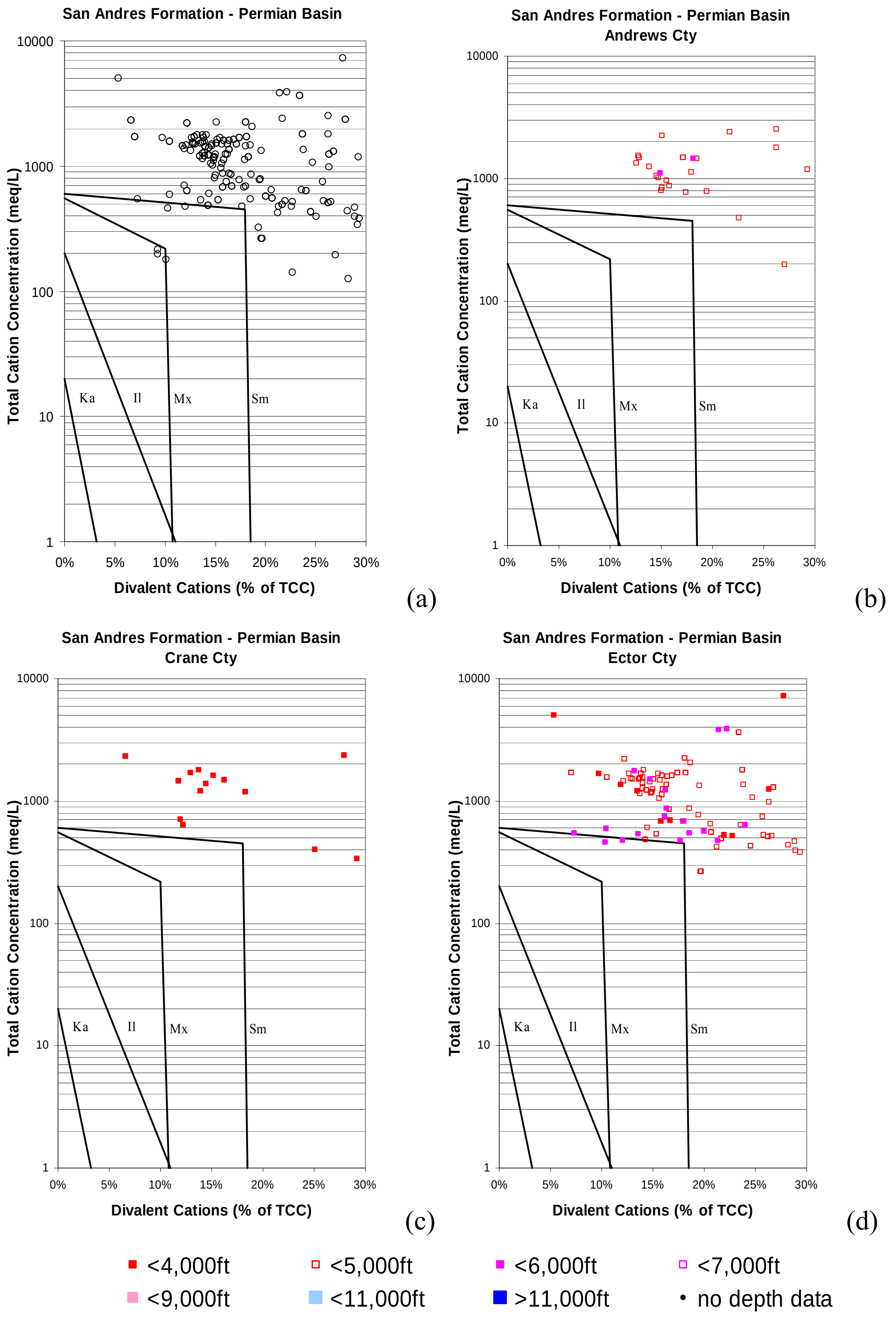

Ka=Kaolinite; Il=Illite; Mx=Mixed layers; Sm=Smectite

Figure 7.23. Plot of total cation concentration and divalent cations percent for the formation water (Permian Basin)

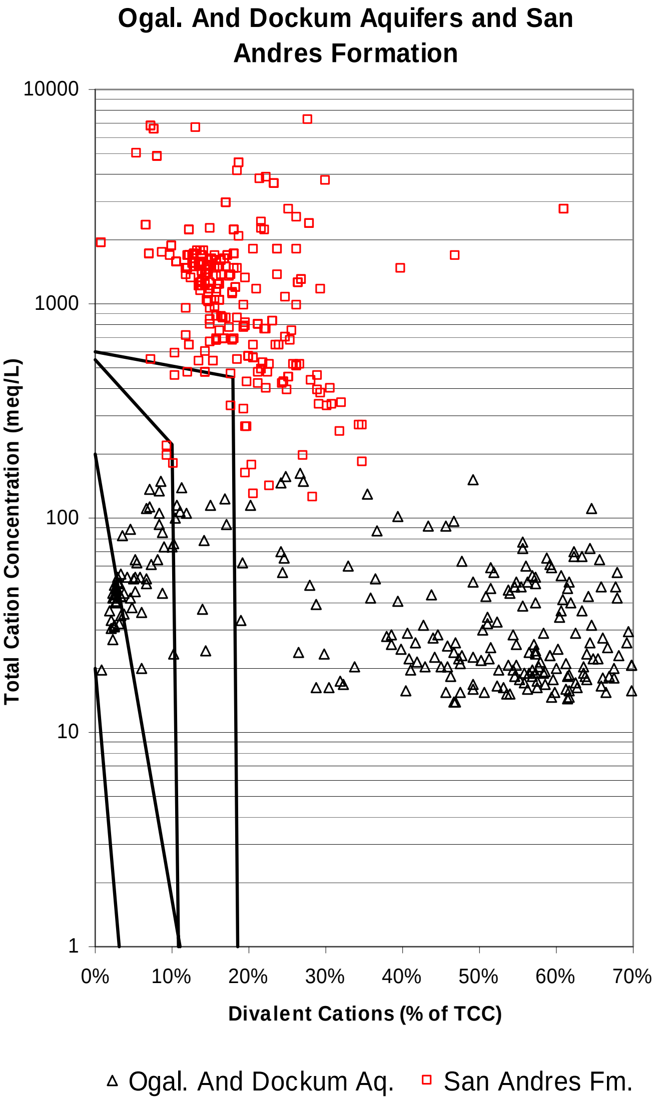

Figure 7.24. Plot of total cation concentration and divalent cations percent for the concentrate and the formation water (Permian Basin)

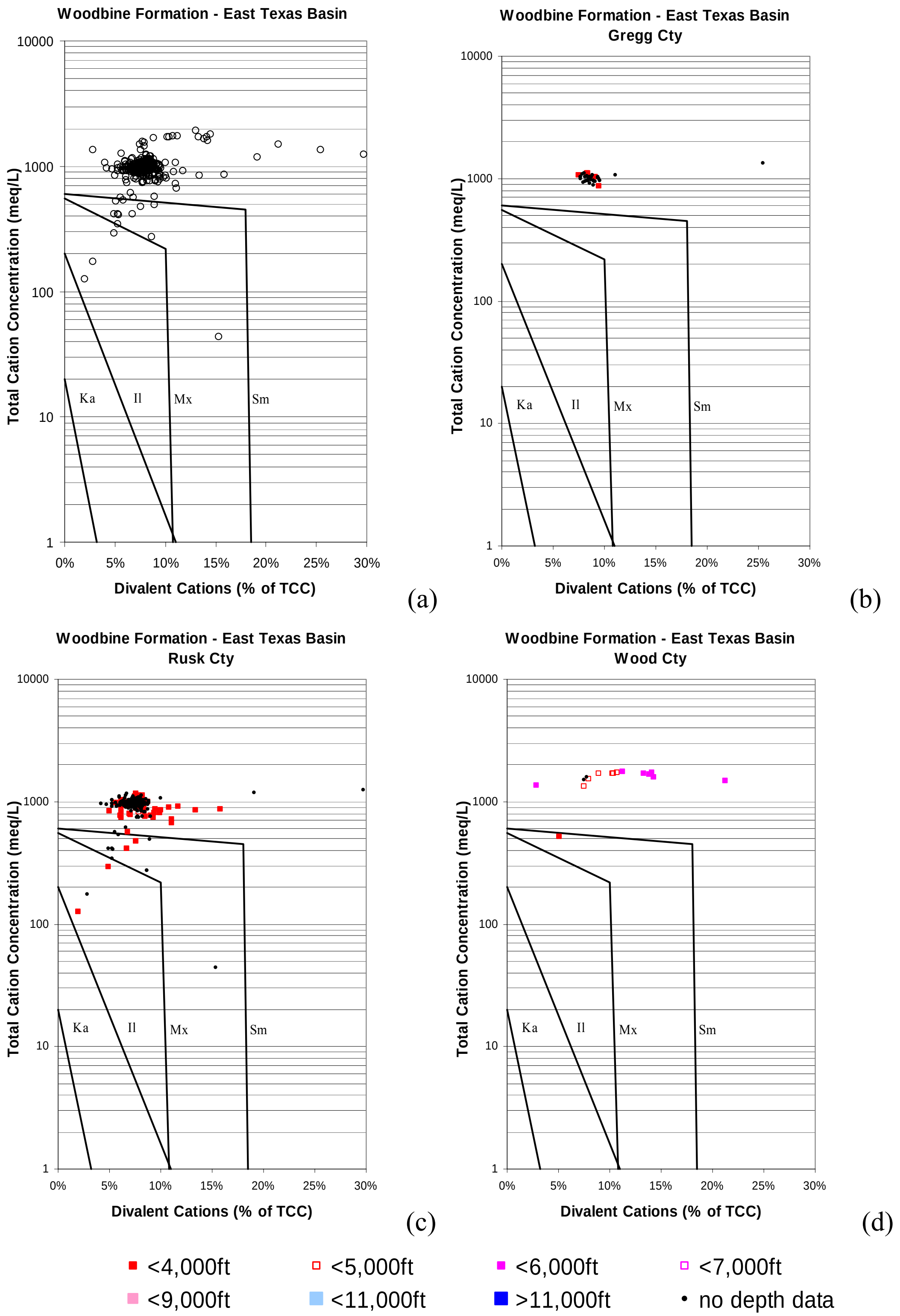

Ka=Kaolinite; Il=Illite; Mx=Mixed layers; Sm=Smectite

Figure 7.25. Plot of total cation concentration and divalent cations percent for the formation water (East Texas Basin)

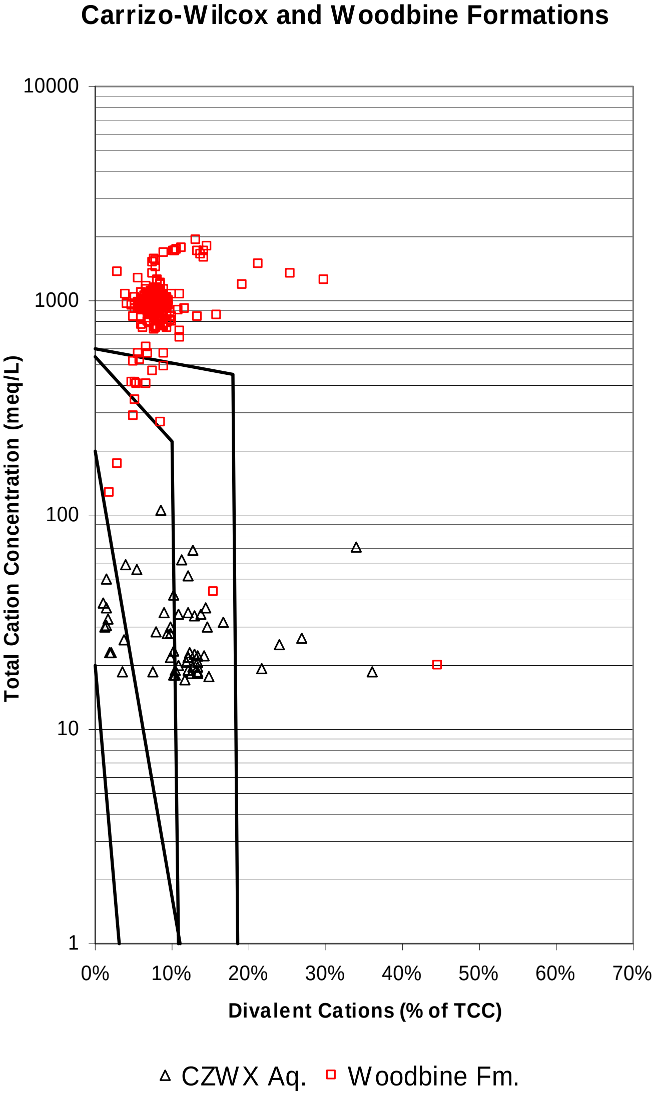

Figure 7.26. Plot of total cation concentration and divalent cations percent for the concentrate and the formation water (East Texas Basin)

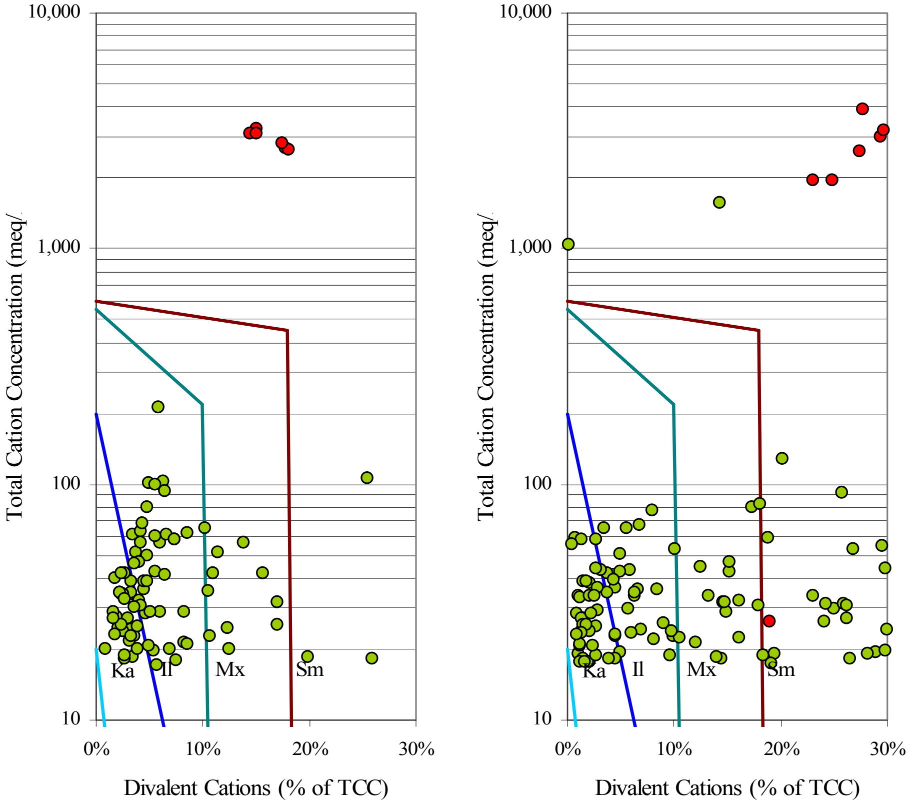

● -formation water, ● brackish water

(a) Stephens County (b) Young County

Figure 7.27. Plot of the total cation concentration and divalent cations percent for the brackish groundwater and the formation water (Fort Worth Basin)

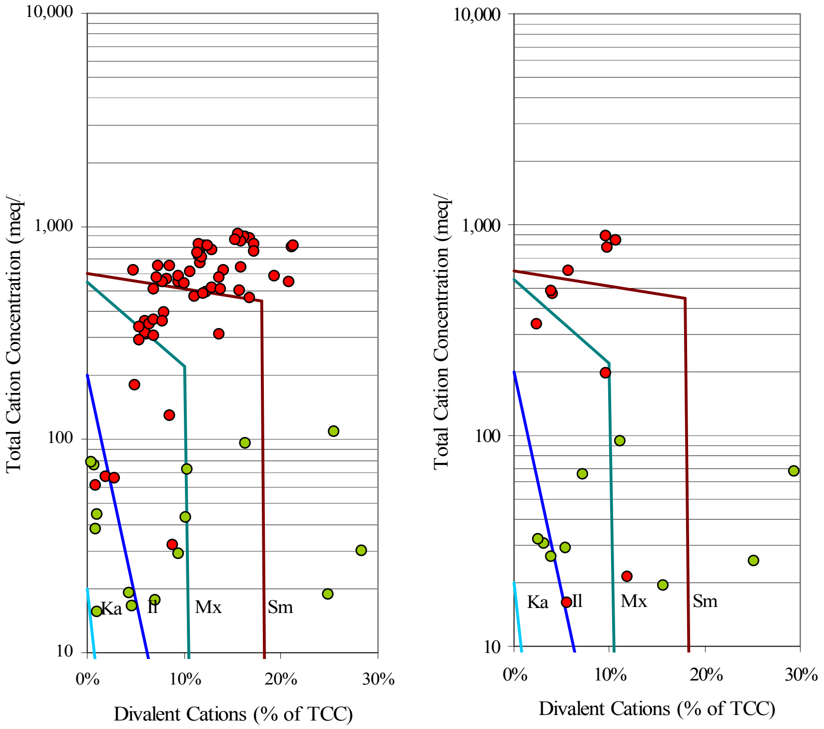

(a). Dimmit County, (b). Zavala County

● -formation water, ● brackish water

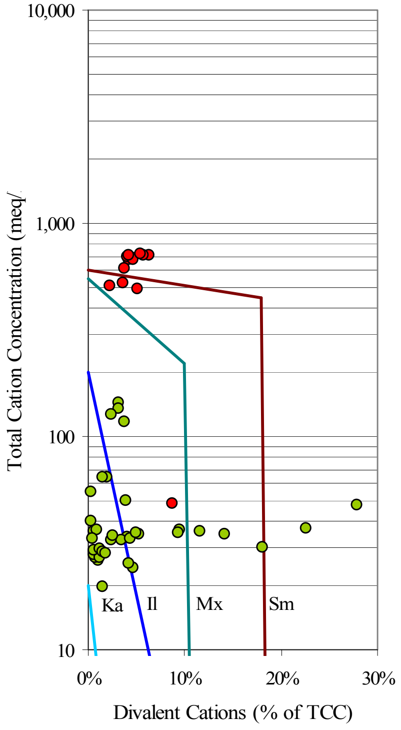

(c)Atascosa County

Note: Most of the brackish waters in Zavala County have high divalent cations and fall to the right of the smectite boundary (not shown).

Figure 7.28. Plot of total cation concentration and divalent cations percent for the brackish groundwater and the formation water (Maverick Basin)

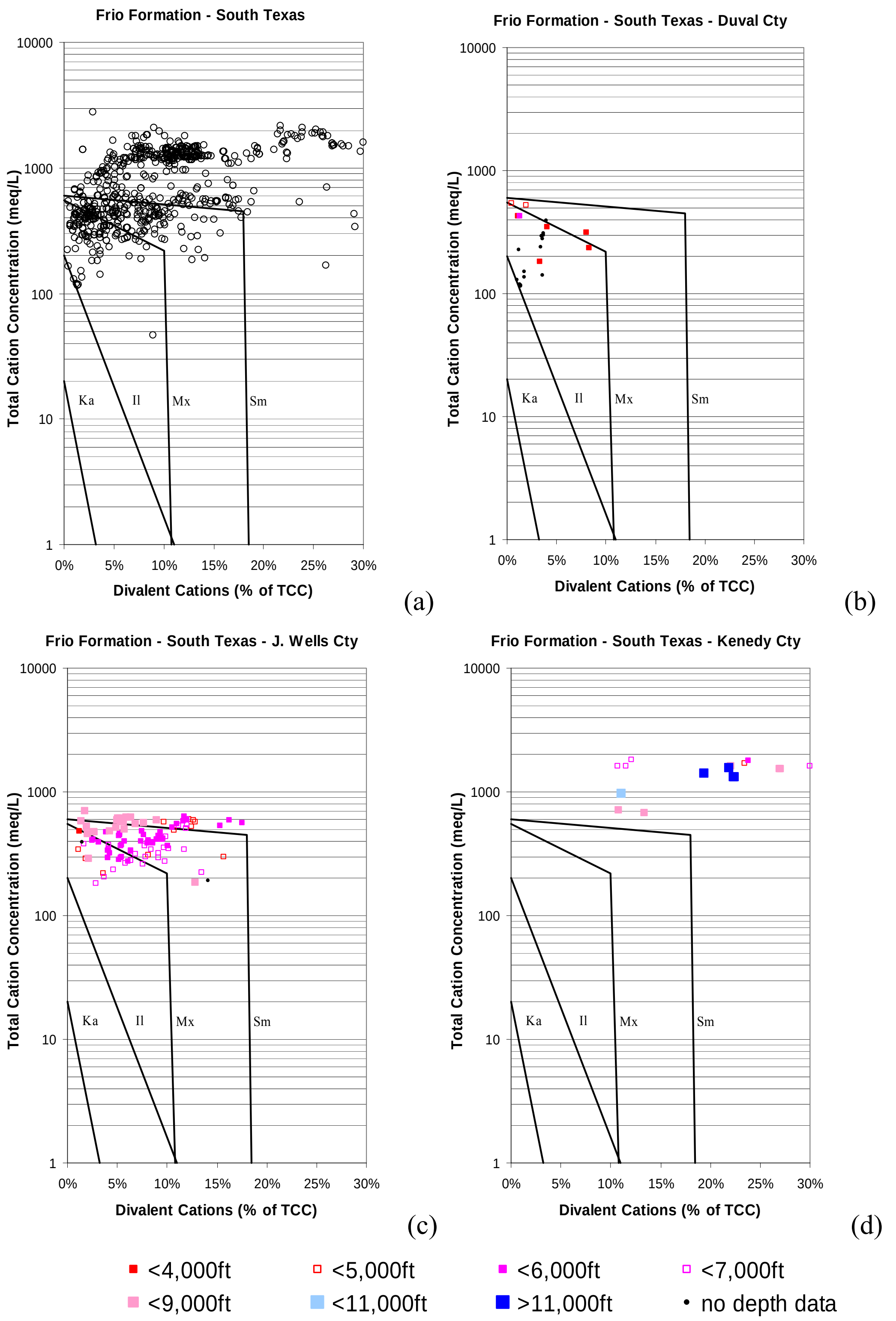

Ka=Kaolinite; Il=Illite; Mx=Mixed layers; Sm=Smectite

Figure 7.29. Plot of total cation concentration and divalent cations percent for the formation water (Southern Gulf Coast Basin)

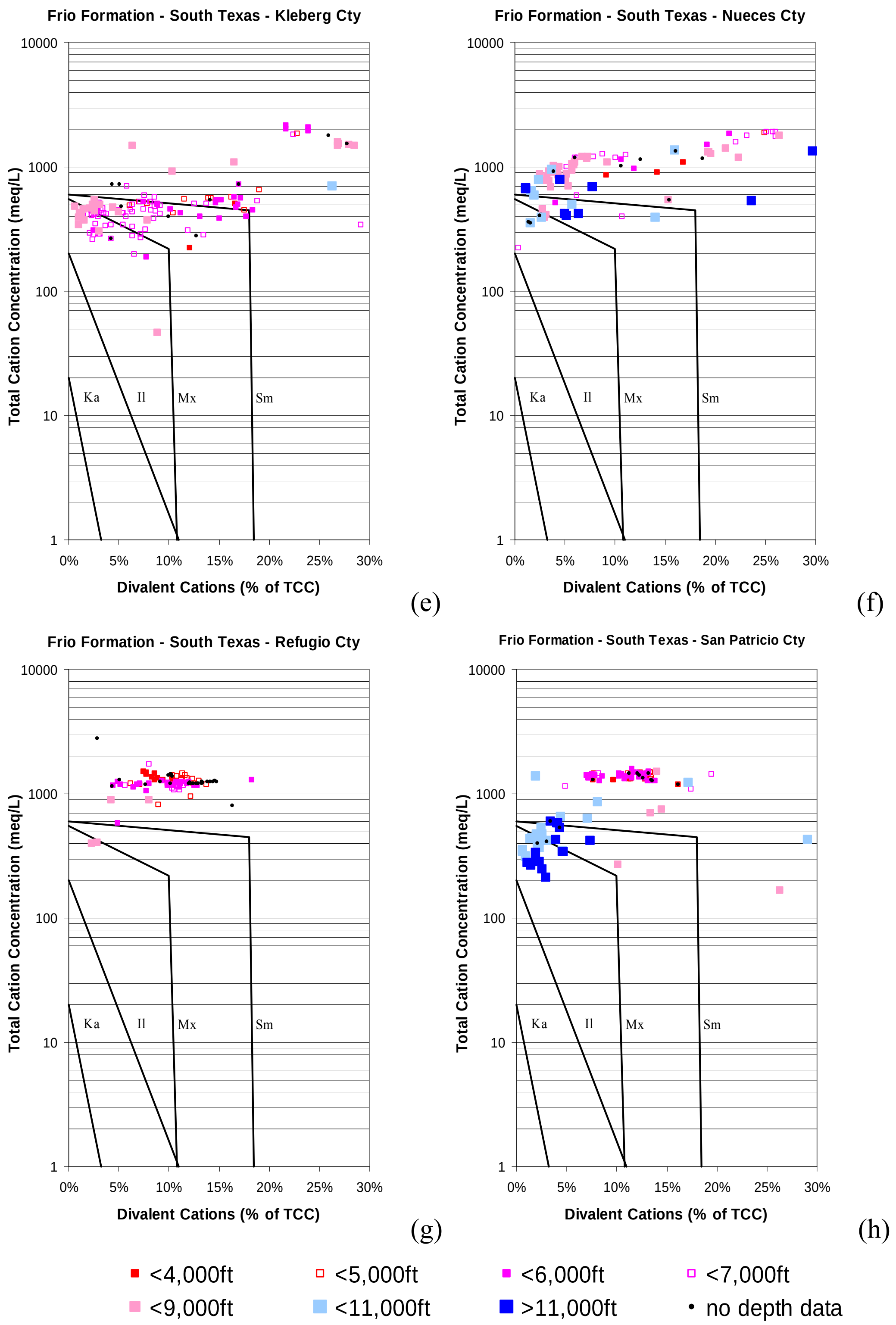

Ka=Kaolinite; Il=Illite; Mx=Mixed layers; Sm=Smectite

Figure 7.29 (continued): Plot of total cation concentration and divalent cations percent for the formation water (Southern Gulf Coast Basin)

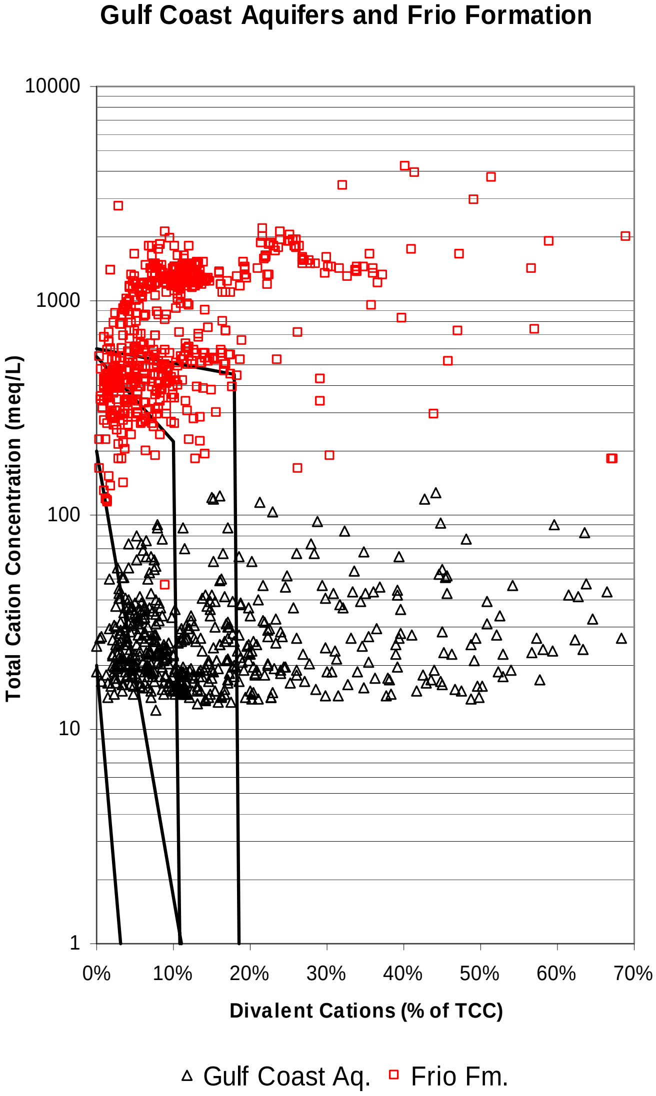

Figure 7.30. Plot of total cation concentration and divalent cations percent for the concentrate and the formation water (Southern Gulf Coast Basin)

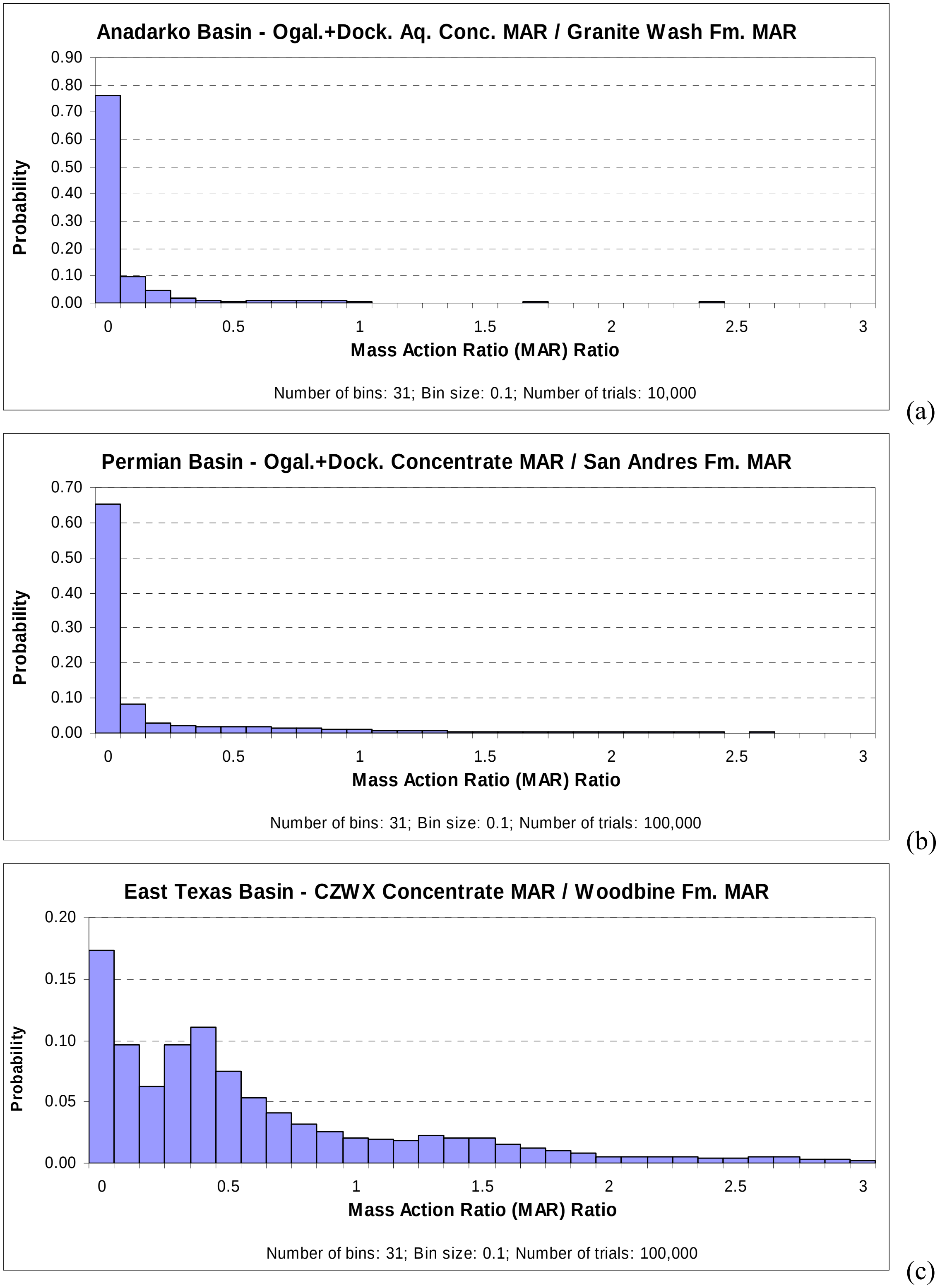

Figure 7.31. MAR ratio distributions

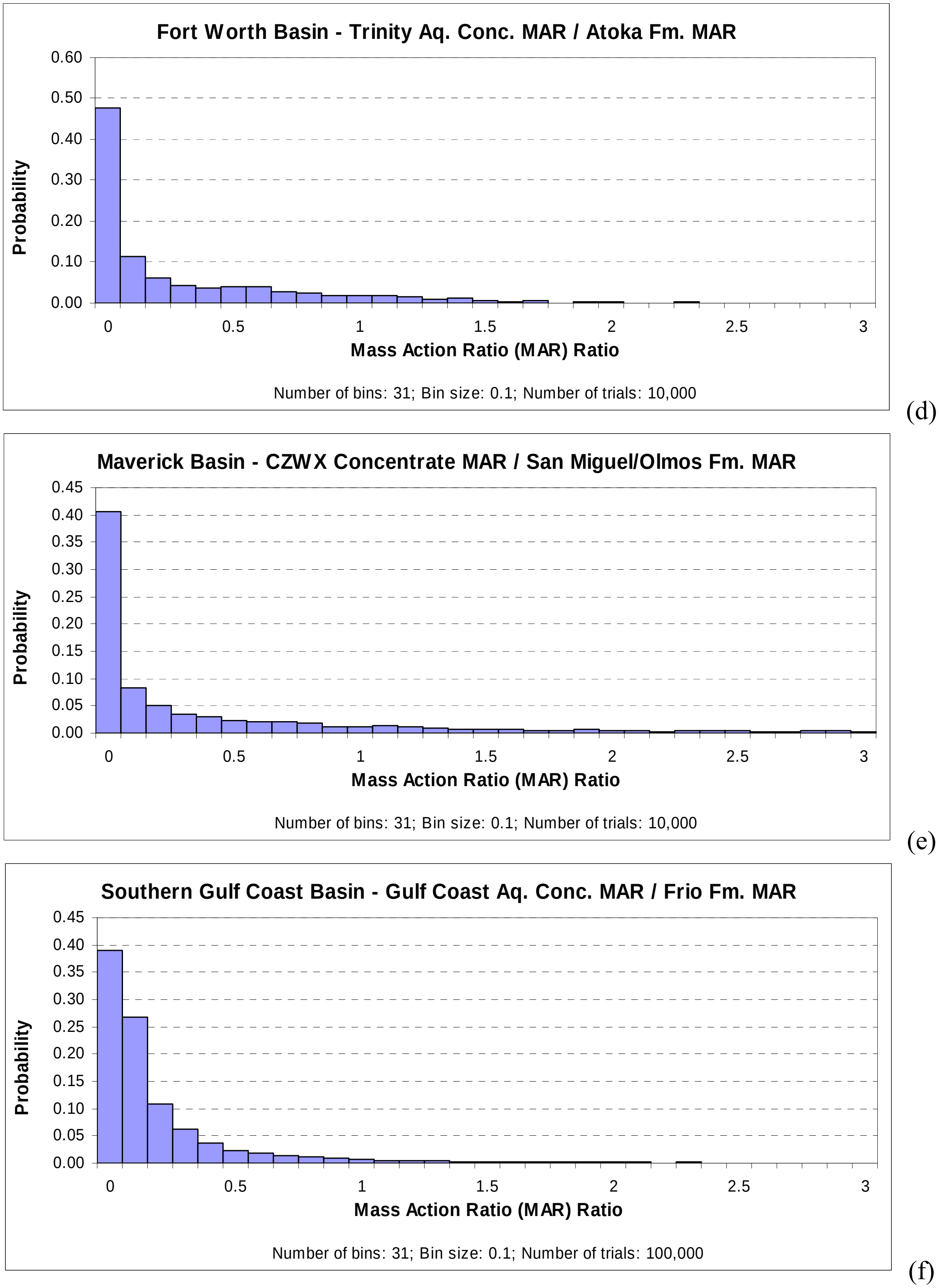

Figure 7.31 (continued): MAR ratio distributions

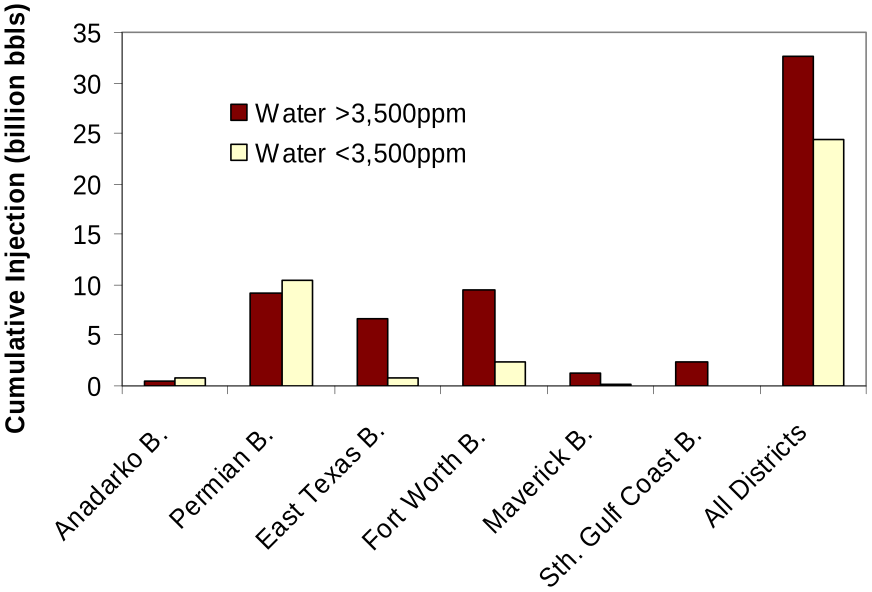

(a)

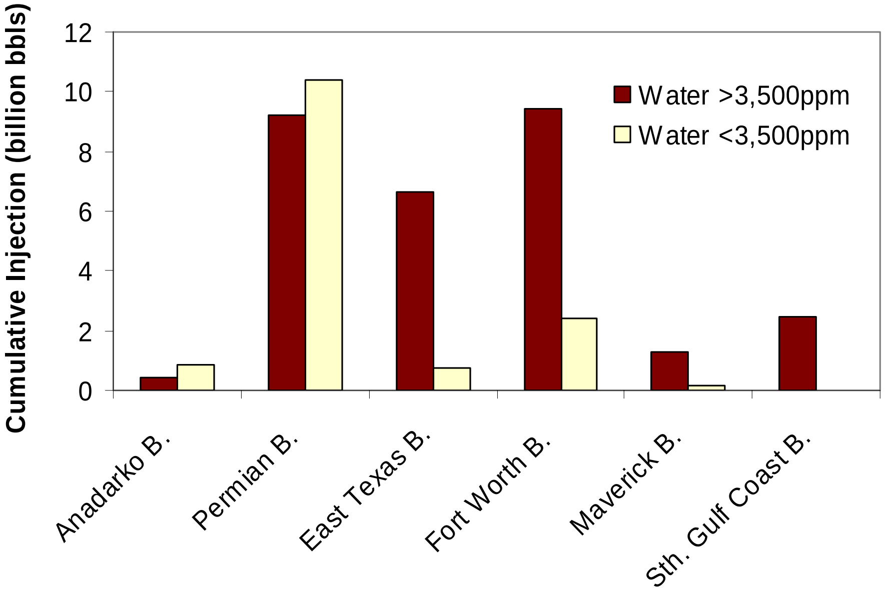

(b)

Figure 7.32. Cumulative volume of injected water up to 1981: (a) from districts including the analysis area and all districts in Texas and (b) only from districts including the analysis areas

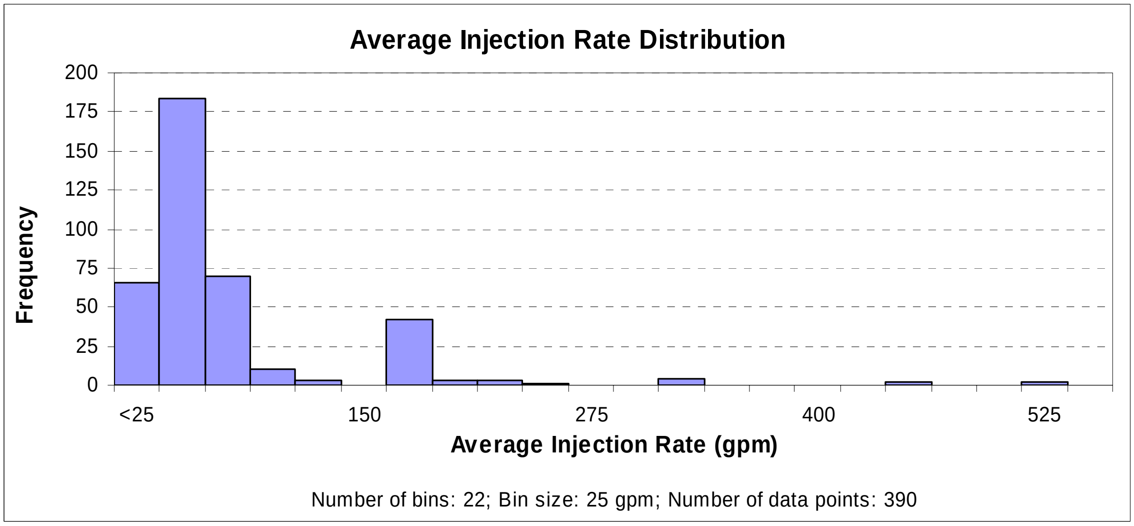

Number of bins: 22; Bin size: 25 gpm; Number of data points: 390

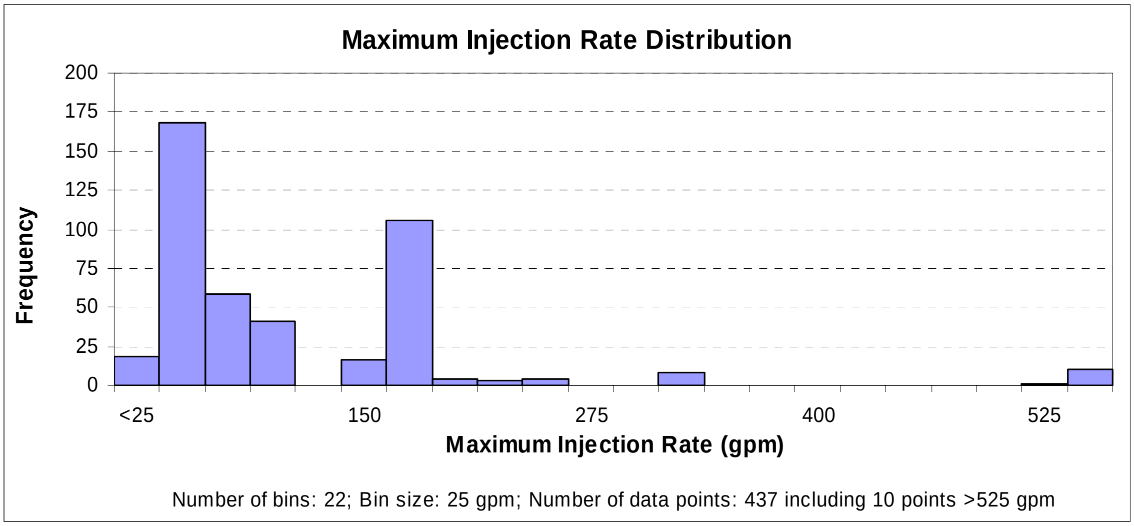

Number of bins: 22; Bin size: 25 gpm; Number of data points: 437 including 10 points >525 gpm

Figure 7.33. Injection rate distribution (from Form H1)

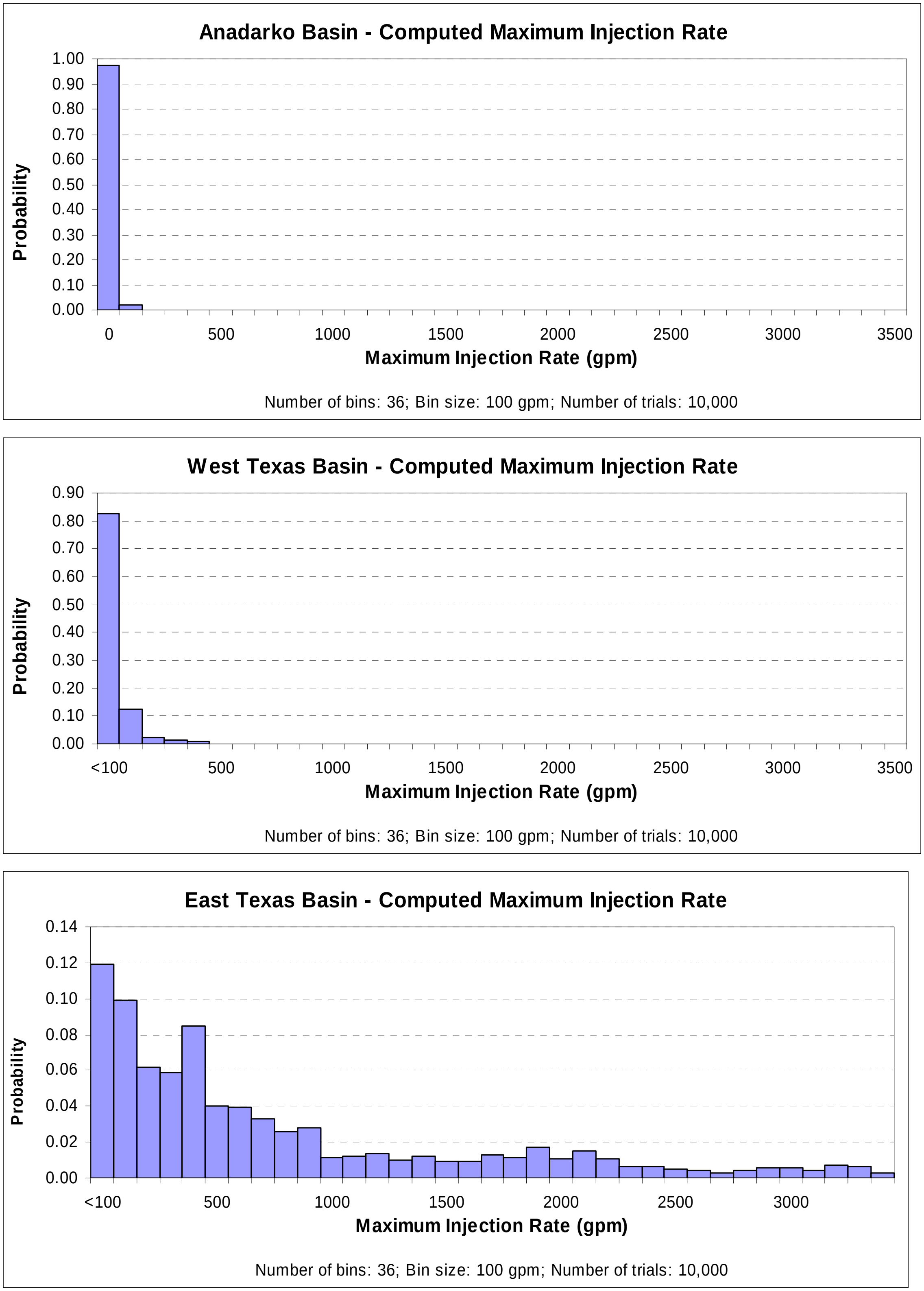
Anadarko Basin - Computed Maximum Injection Rate

Number of bins: 36; Bin size: 100 gpm; Number of trials: 10,000

West Texas Basin - Computed Maximum Injection Rate

Number of bins: 36; Bin size: 100 gpm; Number of trials: 10,000

East Texas Basin - Computed Maximum Injection Rate

Number of bins: 36; Bin size: 100 gpm; Number of trials: 10,000

Figure 7.34. Distribution of computed maximum injection rate (no skin effect)

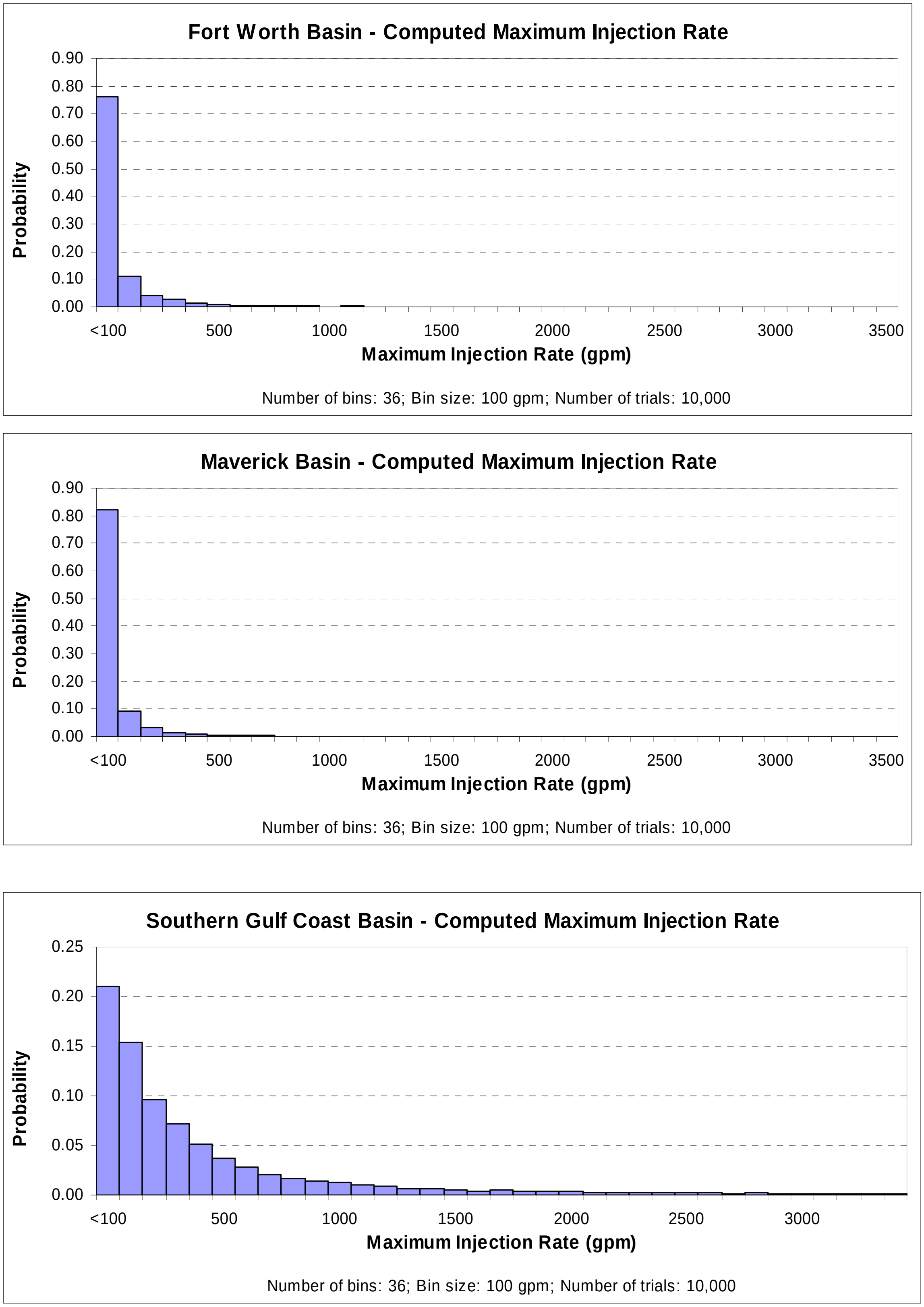

Figure 7.34 (continued). Distribution of computed maximum injection rate (no skin effect)

# 8 Conclusions and Recommendations

Our investigation results are divided into four important topics: (1) formation pressure conditions in depleted oil and gas fields and implications for area-of-review (AOR) variance, (2) potential for scale formation due to mixing of desalination concentrates and formation water using PHREEQC and SOLMINEQ geochemical codes, (3) water sensitivity of fines and clays in the formations of depleted oil and gas fields to injected waters, and (4) injection rate, which we calculated for each site on the basis of local porosity and permeability conditions. Results are summarized in Table 8.1. Analysis areas are given scores on the basis of their suitability for accepting desalination concentrates. Major conclusions of this work are also published in Nicot and Chowdhury (2005).

Formation pressure conditions of the depleted oil and gas fields indicate that a significant number of the wells would qualify for a AOR variance (Table 7.1). A high percentage of wells could potentially receive the AOR because the analysis areas are largely pressure depleted (Figure 7.1 and Table 6.8). For each analysis area (Figure 7.2 to Figure 7.7), we examined distribution of pressure conditions with depth relative to the BUQWs on a well-by-well and field-by-field basis. Large pressure depletion in the Anadarko Basin (Figure 7.1), where 67 percent of the fields could potentially receive the AOR variance is very favorable. In the Permian, East Texas, and Fort Worth Basins (Figure 7.5), between 50 and 60 percent of the fields could potentially receive the AOR variance. The Maverick Basin (Figure 7.6) is an anomaly among the six analysis areas because only 35.5 percent of the fields appear favorable for a AOR variance. In the southern Gulf Coast Basin, about 56 percent of the fields have a separation >500 ft between the top of the fluid in the formation and the BUQW (Figure 7.7).

We used PHREEQC and SOLMINEQ geochemical codes, along with a Monte Carlo statistical approach, to analyze the results of mixing formation water and concentrate. Results are reported in terms of saturation indices (SI) of the scale-prone minerals calcite, gypsum, barite, and silica. Potential feed waters are mainly undersaturated relative to calcite, gypsum, and silica. The barite saturation index for some basins, particularly the Anadarko Basin, suggests that it is supersaturated. However, given the low solubility of barite, the high saturation index may also be due to erroneous temperature field measurements. Acidification of the concentrate drops the calcite saturation index by one order of magnitude, in most cases, bringing it below a value of 0. The other minerals analyzed (gypsum, barite, and silica) show small variations in *SI* due to the changes in the ionic strength with the addition of acid and of sulfate ions (more evident for gypsum and barite). Formation water from all analysis areas shows supersaturation with respect to calcite, and, to a much lesser degree, to gypsum. It is common for calcium carbonate to be supersaturated.

Saturation indices for the mixing solutions fall between those of the formation water and acidified concentrate. SI values of several samples exceed the theoretical threshold for precipitation $SI=0$ for the various combinations of mixing of concentrate/formation water. However, addition of antiscalant products (Section 4.4) will increase the threshold to a value of approximately 2. This value is retained as the saturation index beyond which recurrent scaling problems could occur during the injection. The threshold value of 2 is exceeded only in the East Texas Basin for barite, where the 95th percentile is 2.7. Nonetheless, it is important to note that the SI values obtained from batch modeling are based on the assumption that total mixing between the formation water and the concentrate occurs. In reality, the injected concentrate may simply displace the resident formation water with little mixing.

Water sensitivity is of considerable importance in formation evaluations because clay deflocculation on injection of fresher water can severely reduce permeability of the reservoirs, causing a reduction in injection flow rate. We used water compatibility guidelines for injection water following methods and diagrams developed by Schuerman and Bergersen (1990). Most of the data points for all the basins except for the southern Gulf Coast Basin fall outside the smectite salinity line, suggesting that smectite in the formation is in equilibrium with the formation water. In the southern Gulf Coast Basin, most of the data points reach the illite salinity line. A trail toward the illite salinity line in Rusk County in the East Texas Basin (Figure 7.25) suggests that illite may be the controlling clay in the southern part of this analysis area. Smectite clay is transformed progressively into illite with increasing depth and temperature. These mineralogical changes are highlighted by composition changes of the formation water. It can be concluded from these analyses that water sensitivity in the formations are most likely controlled by smectite except for the southern Gulf Coast, where it may be controlled by mixed-layer clays and illite in deeper sections.

Injected concentrate derived from the overlying brackish water aquifer is unlikely to be at equilibrium with the formation clays in the reservoirs. However, all brackish water samples fall outside the smectite salinity line in the Anadarko Basin (Figure 7.22). Approximately 75 percent of the concentrate data points fall outside the smectite salinity line in the Permian Basin (Figure 7.24). Most of the Carrizo-Wilcox data points fall within the smectite salinity line and only 65 percent outside the illite salinity line. Similarly the Fort Worth Basin analysis area has more than half of the brackish water samples fall inside the smectite salinity line (Figure 7.27). Most of the brackish water samples in the Maverick Basin analysis area fall outside the smectite salinity line (Figure 7.28). The southern Gulf Coast analysis area has 29 and 58 percent of the data points outside the illite and smectite salinity lines, respectively (Figure 7.30). Concentrate injection in the East Texas and Fort Worth Basins could present a challenge if operational solutions are carefully devised. Concentrate injection may not pose a problem in the Maverick or southern Gulf Coast Basins. The Anadarko and Permian Basins should be easily amenable to concentrate injection.

However, even apparently compatible water can generate problems owing to cation stripping. The mass action ratios ($MAR_{i/f}$ = MAR of injected water / MAR of formation water) of the different waters involved can be used to assess this. We have performed statistical analyses using the risk-analysis package Crystal Ball® running under Excel (Crystal Ball, 2001). Results of these analyses (Figure 7.31), when compared with the water compatibility guidelines (Table 5.4), suggest that pretreatment of the waters would be needed for most combinations of concentrate and formation water.

Injectivity variation was modeled by calculating the flow rate that would result from combining formation physical characteristics (porosity, permeability, and compressibility) and pressure requirements (admissible surface pressure, well depth, and head loss). Multiple combinations of these parameters allied with a MonteCarlo analysis (using Crystal Ball®) show that the median injection rate for a single well is about 10 gpm in the Paleozoic basins, while it reaches 278 and 466 gpm in the southern Gulf Coast and East Texas Basins, respectively. It should be noted that the calculation includes all porosity and permeability regardless of their values. The distribution is biased toward the low flow rates; an actual injection well will likely be located where permeability is higher. The rate could also be increased by screening more intervals and performing well stimulation.

Using results from the previous sections, we built a qualitative score table (Table 8.1) that lists high, medium, and low values for four parameters. It grades scaling tendency, water sensitivity, injection rate, and magnitude of pressure depletion. The score relative to scaling for all analysis areas was set at medium because (1) barium scaling could not be ruled out with available data and (2) information is missing for several important scale-forming minerals such as iron compounds. The analysis areas were rated in three groups according to their water sensitivity. The Anadarko and the Permian Basins scored high because most of the concentrate samples fall outside the salinity line, (i.e., injection is sustainable with pretreatment). Fort Worth, Maverick and southern Gulf Coast Basins received a medium score because a significant number of concentrate data points fall on the wrong side the smectite salinity line. The East Texas Basin has very few concentrate samples located beyond the smectite salinity line and may require periodic stimulations. The injection parameter criterion places the analysis areas in two groups: Paleozoic basins (Anadarko, Permian, Fort Worth, and Maverick Basins) with potentially low injection rates and more recent basins (East Texas and southern Gulf Coast Basins) with much higher potential injection rates. All analysis areas rate favorably relative to pressure depletion criteria.

A general observation is that very few problems occur in an injection well owing to water incompatibility. This is because injectate (desalination concentrate) miscibly displaces the formation water. A sharp interface could exist between the injected and resident fluids. However, the interface is somewhat smoothed by diffusion and dispersion. Mixing calculations in this study are done assuming complete mixing (batch runs) and describe one end member of what is actually occurring and the other end member where no mixing occurs at all. Batch modeling represents an upper limit on the amount of precipitation that can occur during the injection process. Exploratory 3D reactive transport modeling, with SHEMAT (Clauser, 2001), which uses PHRQPITZ as its geochemical module, confirmed those observations. Once the front is passed at a given location, no precipitation occurred because the pore space is occupied mainly by injection water, and some of the precipitates even dissolved back into the solution.

Technical challenges of injecting desalination concentrates into oil-producing formations are not unlike those of injecting water from a source different from that of the formation water. The oil industry has a long history of dealing with such issues. This work suggests that injection of desalination concentrates in the formation water will likely not be a problem if the injection water and the formation are appropriately pretreated, as is done routinely by the oil industry in the application of produced waters.

Table 8.1.  Summary of conclusions

| Basin | Score Relative to Scaling | Score Relative to Water Sensitivity | Score Relative to Injection Rate | Score Relative to Pressure Depletion |
|---|---|---|---|---|
| **Anadarko** | | | | |
| | Medium | High | Low | Very High |
| **Permian** | | | | |
| | Medium | High | Low | High |
| **East Texas** | | | | |
| | Medium | Low | High | High |
| **Fort Worth** | | | | |
| | Medium | Medium | Low | High |
| **Maverick** | | | | |
| | Medium | Medium | Low | High |
| **Southern Gulf Coast** | | | | |
| | Medium | Low-Medium | High | High |

# 9 Acknowledgments

This study was indirectly founded by the Desalination and Water Purification Research and Development Program, U.S. Bureau of Reclamation (Agreement No. 03-FC-81-0846) through the Texas Water Development Board (Interagency Contract No. IA 2004-0001-012). In addition to the authors of this document, several people contributed to this project: Katie Kier, Research Assistant at the BEG, collected and analyzed H1 forms and assisted with GIS analysis. Discussions with Mark Holtz, Researcher at the BEG, helped in formulating issues discussed in the report. He also reviewed a preliminary draft. We also thank Robert Mace (project manager) of the Texas Water Development Board for his thorough review of the final draft. Fernando Deleon of the Railroad Commission of Texas was instrumental in delivering a complete data set of the H15 forms. Sylvia Jennette was very diligent and helpful in designing Web pages and producing this report in pdf format. Sigrid Clift was instrumental in getting TIPRO and PTTC involved in the project. Those two organizations were kind enough to either allow presentation at their meetings or post questionnaires on their Web sites. The report was edited by Lana Dieterich. Illustrations were in part prepared by John T. Ames, Paula B. Beard, Jana S. Robinson and Joel L. Lardon, Media Information Techynology Manager.

The views and conclusions contained in this report reflect those of the Bureau of Economic Geology and should not be interpreted as necessarily representing the opinions, either expressed or implied, or official policies of the U.S. Bureau of Reclamation and of the Texas Water Development Board.

# 10 References

Ahmed, M., 2000. Investigation on the use of evaporation ponds for brine disposal in inland desalination plants, MEDRC Series of R&D Reports, MEDRC Project:97-AS-007, The Middle East Desalination Research Center, Muscat, Oman, 73p.

Ashworth, J. B. and Hopkins, J., 1995. Major and minor aquifers of Texas. Texas Water Development Board, Report N$^o$ 345, 68p.

American Water Works Association (AWWA), 2004. Water desalting planning guide for water utilities. John Wiley & Sons, Hoboken, New Jersey. 198p.

API, 2003. Sampling petroleum reservoir fluids. Report RP44, American Petroleum Institute, 49p.

API, 1998. Analysis of oilfield waters. Report RP45, American Petroleum Institute, 49p.

Barrow, K.T., and Asquith, G.B., 1992, Geologic controls on tight-gas production from a strom-dominated shelf: Upper Cretaceous Olmos Formation (Texas), Bulletin of American Association of Petroleum Geologists, Annual Convention Official Program, Calgary, Alberta, Canada, p. 7.

Bass, D. M., Jr., 1987. Properties of reservoir rocks, Chapter 26 in Petroleum engineering handbook by Bradley, H. B., Society of Petroleum Engineers, Richardson, TX.

Beall, A. O., Jr., 1964. Fabric and mineralogy of the Woodbine Formation, East-Central Texas: Ph.D. Dissertation, Stanford University, 172 p.

Bein, A. and Dutton, A. R., 1993, Origin, distribution, and movement of brine in the Permian Basin (U.S.A.): a model for displacement of connate brine: Geological Society of America Bulletin, v. 105, p. 695–707.

Belk, J. K., Ledger, E. B., and Crocker, M. C., 1986. Petrography of volcaniclastic Woodbine Formation, Southwest Arkansas. American Association of Petroleum Geologists Bulletin, September 1986, Vol. 70, Issue 9, pp.1177.

Bloetscher, F., and Ortiz, R. S., 1999. The city of Hollywood's experience with multi-source membrane treatment processes. Florida Water Resources Journal, January 1999, p. 24-25.

Brady, N. C., 1990. The nature and properties of soils, Chap. 7. 10th edition, Macmillan Publishing Company, New York, NY. 621p.

Burnett, D. B. and Veil, J. A., 2004. Decision and risk analysis study of the injection of desalination byproducts into oil and gas producing zones. SPE#86256.

Capuano, .R. M., Kreitler, C. W., and Donnelly A., 1989. Deep well injection: chemical waste disposed and their subsurface reactions. University of Texas at Austin, Bureau of Economic Geology report prepared for U.S. Environmental Protection Agency, 169p.

Clauser, C., 2001. Numerical simulation of reactive flow in hot aquifers, SHEMAT and Processing SHEMAT. C. Clauser (Ed.), Springer. 331p.

Clesceri, L. S., Greenberg, A. E., and Eaton, A. D., 1998. Standard methods for the examination of water and waste water, 20th edition, American Water Works Association, variously paginated.

Collins, A. G., 1975. *Geochemistry of Oilfield Waters*. Elsevier, Amsterdam. 496p.

Collins, A. G., 1987. Properties of produced waters, Chapter 24 in Petroleum Engineering Handbook, Bradley, H.B., Editor-in-chief, Society of Petroleum Engineers, Richardson, TX, 1987.

Core Laboratories Inc., 1972a. A survey of the subsurface saline water of Texas, Vol. 1, Texas Water Development Board, Report 157, 113p.

Core Laboratories Inc., 1972b. A survey of the subsurface saline water of Texas, Vol. 3, Aquifer Rock Properties, Texas Water Development Board, Report 157, 364p.

Cowan, J. C. and Weintritt D. J., 1976. Water-formed deposits. Gulf Publishing Company, Houston, Texas, 596p.

Crystal Ball, 2001. Crystal Ball 200.2 user manual. Decisioneering, Inc. 412p.

Deeds, N., Kelley, V., Fryar, D., Jones, T., Whallon, A. J., and Dean, K. E., 2003. Groundwater availability model for the southern Carrizo-Wilcox aquifer, Final Report, submitted to the Texas Water Development Board, variously paginated.

Domenico, P. A. and Schwartz, F. W., 1990. Physical and chemical hydrogeology. John Wiley and Sons, New York, NY. 824p.

Dunoyer de Segonzac, G., 1970. The transformation of clay minerals during diagenesis and low-grade metamorphism. Sedimentology, 15, p.281-346.

Dutton, A. R. and Orr, E. D., 1986. Hydrogeology and hydrochemical facies of the San Andres Formation, Texas Panhandle and eastern New Mexico: The University of Texas at Austin, Bureau of Economic Geology Report of Investigations No. 157, 58 p.

Dutton, S. P., 1982. Pennsylvanian fan-delta and carbonate deposition, Mobeetie field, Texas Panhandle, American Association of Petroleum Geologists Bulletin, v. 66, no. 4, p. 389-407.

Dutton, S. P., 1990. Mobeetie field, in Beaumont , E. A., and Foster, N. H., compilers, Structural Traps II: traps associated with tectonic faulting: Treatise of petroleum geology, atlas of oil and gas fields: American Association of Petroleum Geologists, p. 127-159.

Dutton, S. P., Clift, S. J., Hamilton, D. S., Hamlin, H. S., Hentz, T. F., Howard, W. .E, Akhter, M. S., and Laubach, S. E., 1993. Major low-permeability-sandstone gas reservoirs in the continental United States. The University of Texas at Austin, Bureau of Economic Geology Report of Investigations No. 211, 221 p.

Dutton, S. P., Kim, E. M., Broadhead, R. F., Breton. C. L., Raatz, W. D., Ruppel, S. C., and Kerans, C., 2004. Play Analysis and Digital Portfolio of Major Oil Reservoirs in the Permian Basin: Application and Transfer of Advanced Geological and Engineering Technologies for Incremental Production Opportunities: Draft Final Report prepared for U. S. Department of Energy under Contract Number DE-FC26-02NT15131by The University of Texas at Austin, Bureau of Economic Geology, 408p.

East Texas Salt Water Disposal Company, 1958. Salt Water Disposal. Industrial and Business Training Bureau Petroleum Extension Service. 131p.

Ewing, T. E., 1991. The tectonic framework of Texas, text accompanying “The tectonic map of Texas”. University of Texas at Austin, Bureau of Economic Geology, 36p.

Finley, R. J., 1984. Geology and engineering characteristics of selected low-permeability gas sandstones: a national survey: The University of Texas at Austin, Bureau of Economic Geology Report of Investigations No. 138, 220p.

Folk, R. L., 1980. Petrology of sedimentary rocks. Hemphill Publishing Company, Austin, Texas. 182p.

Fryar, D., Senger, R., Deeds, N., Pickens, J., Whallon, A., and Dean, K., 2003. Groundwater availability model for the northern Carrizo-Wilcox aquifer. Prepared for the Texas Water Development Board, January 2003, 529p.

Galloway, W.E., 1975, Process framework for describing the morphologic and stratigraphic evolution of deltaic depositional systems, in Brossard, M.L. ed. , Deltas: Models for Exploration: Houston Geological Society, p. 87-98.

Galloway, W. E., 1977. Catahoula Formation of the Texas coastal plain: depositional systems, composition, structural development, ground-water flow history, and uranium distribution. The University of Texas at Austin, Bureau of Economic Geology Report of Investigations No 87.

Galloway, W. E., 1982. Epigenetic zonation and fluid flow history of uranium-bearing fluvial aquifer systems, south Texas uranium province, The University of Texas at Austin, Bureau of Economic Geology Report of Investigations No 119.

Galloway, W. E., Ewing, T. E., Garrett C. M. Jr., Tyler N., and Bebout, D. G., 1983. Atlas of Major Texas Oil Reservoirs. University of Texas at Austin, Bureau of Economic Geology Atlas AT0002, 139p.,

Galloway, W. E., Ganey-Curry, P. E., Li, X., and Buffler, R. T., 2000. Cenozoic depositional history of the Gulf of Mexico basin: American Association of Petroleum Geologists Bulletin 84(11):1743–1774.

Galloway, W. E., Hobday, D. K., and Magara, K., 1982. Frio Formation of the Texas Gulf Coast Basin—depositional systems, structural framework, and hydrocarbon origin, migration, distribution, and exploration potential: The University of Texas at Austin, Bureau of Economic Geology Report of Investigations No 122.

Galloway, W. E., Liu, X., Travis-Neuberger, D., and Xue, L., 1994. References high-resolution correlation cross-sections., paleogene section, Texas Coastal Plain, The University of Texas at Austin, Bureau of Economic Geology.

Garrett, C. M. Jr., Kosters, E. C., Banta, N. J. and White, W. G., 1991. Atlas of Major Texas Gas Reservoirs: Database. University of Texas at Austin, Bureau of Economic Geology Atlas AT0003, 1 diskette.

Glater, J., and Cohen, Y., 2003. Brine disposal from land based membrane desalination plants: a critical assessment, University of California, L.A., Prepared for the Metropolitan Water District of Southern California, 15 p.

Grigsby, J. D., and Kerr, D. R., 1991. Diagenetic variability in middle Frio Formation gas reservoirs (Oligocene), Seeligson and Stratton Fields, South Texas: Gulf Coast Association of Geological Societies Transactions 31, p. 308-319.

Ham, W. E, and Wilson, J. L., 1967. Paleozoic epeirogeny and orogeny in the central United States: American Journal of Science, v. 265, p. 332-407.

Hamilton, D. S., Hardage, B. A., Finley, R. J., Carr, D., Lancaster, D. E., and Elphick, R. Y., 1997. Application of integrated geological, geophysical, and engineering analysis in identifying compartmented reservoirs, Boonsville Field, AAPG International Conference and Exhibition, Vienna, p. 1380.

HDR, 2000. Desalination for Texas Water Supply. Report No 2000483328 prepared for the Texas Water Development Board.

He, S., Oddo, J. E., and Tomson, M. B., 1994. The inhibition of gypsum and barite nucleation in NaCl brines at temperatures from 25°C to 90°C. Applied Geochemistry, 9, p. 561-567.

Heitman H.-G., 1990. Saline water processing. H.-G. Heitman Editor, VCH, Germany. 332p.

Hitchon, B. and Brulotte, M., 1994. Culling criteria for “standard” formation water analyses. *Applied Geochemistry*. V.9, PP 637-645.

Holtz, M. H. and McRae, L. E., 1995. *Identification and assessment of remaining oil resources in the Frio fluvial-deltaic sandstone play, South Texas*. University of Texas at Austin, Bureau of Economic Geology Report of Investigations Report #227, 46 p.

Holtz, M. H. Tyler N., Garrett C. M. Jr., White W. G., and Banta N. J., 1991. Atlas of Major Texas Oil Reservoirs: Database. University of Texas at Austin, Bureau of Economic Geology Atlas AT0004, 1 diskette.

Hovorka, S. D., Romero, M. L., Treviño, R. H., Warne, A. G., Ambrose, W. A., Knox, P. R., and Tremblay, T. A., 2000. Project evaluation: phase II: optimal geological environments for carbon dioxide disposal in brine-bearing formations (aquifers) in the United States: The University of Texas at Austin, Bureau of Economic Geology, final report prepared for U.S. Department of Energy, National Energy Technology Laboratory, under contract no. DE-AC26-98FT40417, 222 p.

Hugman, R. H., Springer, P. S., and Vidas, E. H., 1992. Tight gas field, reservoir, and completion analysis of the United States: Volume I – project summary, volume 2-output tables: topical report nos. GRI-92/0226.1 and 92/0226.2, prepared by Energy and Environmental Analysis, Inc., for the Gas Research Institute, v. 1, 41 p. , plus appendices; v. 2, 516 p.

Johnson, K. S., Amsden, T. W., Denison, R. E., and others, 1988. Southern Mid-Continent Region, in Sloss, L. L., ed., Sedimentary Cover-North American Craton: U. S.: Geological Society of America, v. D-2, p. 307-359.

Kerr, D. R., and Grigsby, J. D., 1991. Recognition and implications of volcanic glass detritus in the fluvial deposits of the Middle Frio Formation, South Texas: Gulf Coast Association of Geological Societies Transactions 31, p. 353-358.

Kharaka, Y. K., Ambats, G., and Thordsen J. J., 1997. Deep well injection of brine from Paradox Valley, Colorado: Potential major precipitation problems remediated by nanofiltration. Water Resources Research, 33(5), p.1013-1020.

Kharaka, Y. K., Gunter, W. D., Aggarwal, P. K., Perkins, E. H., and DeBraal, J. D., 1988. SOLMINEQ88: A computer program for geochemical modeling of water-rock interactions. U.S. Geological Survey Water Resources Investigation Report, 88-4227, 88pp.

King, R. .Y., 2003. Process simplification through the use of antiscalants and antifoulants. Ultrapure Water, September 2003, p.17-20.

Kosters, E. C., Bebout, D. G., Seni, S. J., Garrett, C. M. Jr., Brown, L. F. Jr., Hamlin, H. S., Dutton, S. P., Ruppel, S. C., Finley, R. J., and Tyler, N., 1989. Atlas of Major Texas Gas Reservoirs. University of Texas at Austin, Bureau of Economic Geology Atlas AT0001, 161p.,

Kreitler, C. W., 1989. Hydrogeology of sedimentary basins. Journal of Hydrology, 106, p.29-53.

Kreitler, C. W., Akhter, M. S., Donnelly, A. C. A., Wood, W. T., 1988. Hydrogeology of formations used for deep-well injection. Texas Gulf Coast. UT Bureau of Economic Geology, report prepared for the U.S. Environmental Protection Agency, Contract No. CR812786-01-0, 204p.

Kreitler, C. W., Collins, E. W., Fogg, G. E., Jackson, M., and Seni, S. J., 1987. Hydrogeologic characterization of the saline aquifers, East Texas Basin--implications to nuclear waste storage in East Texas salt domes: The University of Texas at Austin, Bureau of Economic Geology, Contract Report prepared for U.S. Department of Energy under contract no. DE-AC97-80ET46617, Open-File Report OF-ETWI-1987-1, 157 p.

Kreitler, C. W. and Richter, B. C., 1986. Hydrochemical characterization of saline aquifers of the Texas Gulf Coast used for disposal of industrial waste: UT Austin Bureau of Economic Geology, contract report tot the U.S. Environmental Protection Agency, Contract No. R-812785-01-0. 164p.

Land, L. S., 1984. Frio sandstone diagenesis, Texas Gulf Coast: a regional isotopic study, in McDonald, D.A. and Surdam, R.C., eds, Clastic diagenesis: American Association of Petroleum Geologists Memoir 37, p.47-62.

LBG-Guyton Associates, 2003. Brackish groundwater manual for Texas Regional Water Planning Groups, Report prepared for the Texas Water Development Board, 188p.

Lindquist, S. J., 1977. Secondary porosity development and subsequent reduction, overpressured Frio Formation Sandstone (Oligocene), South Texas: Gulf Coast Association of Geological Societies Transactions 27, p. 99-107.

Loucks, R. G., Bebout, D. G., and Galloway, W. E., 1977. Relationship of porosity formation and preservation to sandstone consolidation history – Gulf Coast lower tertiary Frio formation, Bureau of Economic Geology, Geological Circular GC 77-5, P.109-120.

Loucks, R. G., Dodge, M. M., and Galloway, W. E., 1979. Sandstone consolidation analyses to delineate area of high-quality reservoirs suitable for production of geopressured geothermal energy along the Texas Gulf Coast. The University of Texas at Austin, Bureau of Economic Geology, report prepared for the U.S. Department of Energy, Division of Geothermal Energy, under contract no EG-77-5-05-5554, 98p.

Loucks, R. G., Dodge, M. M., and Galloway, W. E., 1986. Controls on porosity and permeability of hydrocarbon reservoirs in Lower Tertiary sandstones along Texas Gulf Coast: The University of Texas at Austin, Bureau of Economic Geology Report of Investigations No. 149, 78 p.

Lozier, J. C., Smith, G., Chapman, J. W., and Gattis, D. E., 1992. Selection, design, and procurement of a demineralization system for a surface water treatment plant. Desalination, 88, p.3-31.

Matty, J. M., and Tomson, M. B, 1988. Effect of multiple precipitation inhibitors on calcium carbonate nucleation. *Applied Geochemistry*, 3, 549-556.

Matty, J. M, Varughese, K., Waggett, G. G., and Tomson M.B., 1985. Control of scale associated with geopressured-geothermal brine production, p.137-147 in Geopressured-Geothermal Energy, Proceedings of the sixth U.S. Gulf Coast geopressured-geothermal energy conference, Ed. M.H. Dorfman and R.A. Morton, Pergamon Press, 1985, 344p.

Mickley, M. C., 2001. Membrane concentrate disposal: practices and regulations, Desalination and Water Purification Research and Development Program Report No. 69, U.S. Department of the Interior, Bureau of Reclamation, Technical Service Center, 252 p.

Mickley, M. C., Hamilton, R., Gallegos, L., and Truesdall, J., 1993. Membrane concentrate disposal, Denver, Colorado, American Water Works Research Foundation and American Water Works Association.

Messner, S., Hart, G., Netzel, J., and Dietrich J. A., 1999. Membrane concentrate reuse by controlled blending. Florida Water Resources Journal, January 1999, p. 23.

Morton R. A. and Land L. S., 1987. Regional variations in formation water chemistry, Frio Formation (Oligocene), Texas Gulf Coast: American Association of Petroleum Geologists Bulletin 71(9): 191–206.

Muecke, T. W., 1978. Formation fines and factors controlling their movement in porous media, *in* Third SPE Symposium on Formation Damage Control, February 15-16, 1978, Lafayette, Louisiana, Society of Petroleum Engineers SPE Paper No. 7007, p.84-91.

Nicot, J.-P. and Chowdhury A.H., 2005. Disposal of brackish water concentrate into depleted oil and gas fields: a Texas study. Desalination, in press.

Nicot, J.-P., Walden, S., Greenlee, L., and Els, J., 2005. Development of a Database for Desalination Facilities in Texas. The University of Texas at Austin, Bureau of Economic Geology. Report prepared for the Texas Water Development Board, Austin, TX under contract No. 2004-483-021.

Palmer, D. P., 1987, A saponite and chlorite-rich clay assemblage in Permian evaporite and red-bed strata, Palo Duro Basin, Texas Panhandle: The University of Texas at Austin, Bureau of Economic Geology Geological Circular 87-03, 21 p.

Pang, S. and Sharma, M. M., 1994. A Model for Predicting Injectivity Decline in Water-Injection Wells, SPE paper 28489 presented at the 1994 SPE Annual Technical Conference and Exhibition, New Orleans.

Parkhurst, D. L. and Appelo, C. A. J., 1999. User's guide to PHREEQC (Version 2) – A computer program for speciation, batch-reaction, one-dimensional transport, and inverse geochemical calculations. U.S. Geological Survey Water-Resources Investigations Report 99-4259. 312p.

Patton. C. C., 1986, Applied water technology. Campbell Petroleum Services, Norman, OK. 364p.

Plummer, L. N., Parkhurst, D. L., Fleming G. W., and Dunkle S. A., 1988. PHRQPITZ – a computer program incorporating Pitzer's equations for calculation of geochemical reactions in brines. U.S. Geological Survey Water Resources Investigation Report, 88-4153, 310pp.

Railroad Commission (RRC), 1982. A survey of secondary and enhanced recovery operations in Texas to 1982. The Railroad Commission of Texas, Oil and Gas Division, Underground Injection Control, Austin and The Texas Petroleum Research Committee, College Station, 608p.

Reynolds, R. R. and Kiker, R. D., 2003. Produced water and associated issues. Oklahoma Geological Survey Open-File Report 6-2003 and Petroleum Technology Transfer Council, 56pp. (http://www.pttc.org/pwm/produced_water.htm).

Rosenbauer, R. J., Bischoff, J. L., and Kharaka, Y. K., 1992. Geochemical effects of deep-well injection of the Paradox Valley brine into Paleozoic carbonate rocks, Colorado, USA. Applied Geochemistry, 7, p.273-286.

Ruppel, S. C., and Cander, H. S.,1988. Effects of facies and diagenesis on reservoir heterogeneity: Emma San Andres Field, West Texas: The University of Texas at Austin, Bureau of Economic Geology Report of Investigations No. 178, 67 p.

Saripalli, K. P., Sharma, M. M., and Bryant, S. L., 2000. Modeling injection well performance during deep-well injection of liquid wastes. Journal of Hydrology, 227, p. 41-55.

Scheuerman, R. F., and Bergersen, B. M., 1990, Injection water salinity, formation pretreatment, and well operations fluid selection guidelines, *in* Society of Professional Engineers SPE Reprint Series No. 29, 225p., SPE Paper No. 18461, p.154-170.

Senger, R. S., Fogg, G. E., and Kreitler, C. W., 1987. Effects of hydrostratigraphy and basin development on hydrodynamics of the Palo Duro Basin, Texas. The University of Texas at Austin, Bureau of Economic Geology, Report of Investigation No 165, 48p.

Simmons, K. A., 1967. A primer on "serpentine plugs" in South Texas, in Ellis, W. G., ed., Contributions to the geology of South Texas: South Texas Geological Society, p. 125-132.

Sharma, M. M. and Yortsos, Y. C., 1986. Permeability impairment due to fines migration in sandstones, *in* Seventh Symposium on Formation Damage Control, February 26-27, 1986, Lafayette, Louisiana, Society of Petroleum Engineers SPE Paper No. 14819, p.91-101.

Smyth, R. C., Nava, R., Sullivan, E. J., and Mace, R. E., 1998. Methodology for determination of Texas oil fields eligible for variance from area of review requirements in underground injection control regulations for Class II injection wells: The University of Texas at Austin, Bureau of Economic Geology, final report prepared for the Railroad Commission of Texas, variously paginated.

Snedden J. W., and Jumper, R. S., 1990. Shelf and shoreface reservoirs, Tom-Walsh-Owen field, Texas, in Barwis, J. H., McPherson, J. G., and Studlick, J. R. J., eds., Sandstone petroleum reservoirs: New York, Springer-Verlag, Casebooks in Earth Sciences, p. 415-436.

Tang, G. and Morrow, N. R., 1997. Temperature, salinity, and oil composition on wetting behavior and oil recovery by waterflooding. SPE Reservoir Engineering, SPE paper #36680, pp.269-276.

Tang, G. and Morrow, N. R., 2002. Injection of dilute brine and crude oil/brine/rock interactions, AGU Geophysical Monograph Series Volume 129, Environmental Mechanics: Water, Mass and Energy Transfer in the Biosphere, edited by Raats, Smiles and Warrick, (July, 2002), pp.171-179.

Texas Water Development Board (TWDB), 2002. Water for Texas. 156p.

Thomas, C. E., Mahoney, C. F., and Winter, G. W., 1987. Water-injection pressure maintenance and waterflood processes, Chapter 44 in Petroleum Engineering Handbook, Bradley, H.B., Editor-in-chief, Society of Petroleum Engineers, Richardson, TX, 1987.

Thomas R. L. and Crowe C. W., 1978. New chemical treatment provides stimulation and clay control in sandstone formations. *in* Third SPE Symposium on Formation Damage Control, February 15-16, 1978, Lafayette, Louisiana, Society of Petroleum Engineers SPE Paper No. 7012, p.113-119.

Thompson, D. M., 1982. Atoka Group (Lower to Middle Pennsylvanian), Northern Fort Worth Basin, Texas: Terrigenous Depositional Systems, Diagenesis and Reservoir

Distribution and Quality, Bureau of Economic Geology, Report of Investigations No. 125,62p.

Tyler, N. and Ambrose, W. A., 1986. Depositional systems and oil and gas plays in the Cretaceous Olmos Formation, South Texas: The University of Texas at Austin, Bureau of Economic Geology Geological Circular 84-2, 31p.

Tyler, N., Ghloston, J. C., Ambrose, W. A.. 1986, Genetic stratigraphy and oil recovery in an Upper Cretaceous Wave-Dominated Deltaic Reservoir, Big Wells (San Miguel) Field, South Texas, Report of Investigations No. 153, Bureau of Economic Geology, 38p.

U.S. Geological Survey, 2002, Produced waters database, http://energy.cr.usgs.gov/prov/prodwat/data2.htm.

Uziemblo, N., and Petersen, H., 1983. Diagenetic components within Woodbine Formation, East Texas: In American Association of Petroleum Geologists Bulletin, March 1983, Vol. 67, Issue 3, pp.562-563.

Wagner, W. O., 1987. Reservoir study of Cretaceous Woodbine fields in the Northern East Texas basin. Unpublished M.A. Thesis, Baylor University, Waco, Texas.

Watson, I. C., 1990, Characterization of desalting concentrates, Desalination, 78, p. 5-9.

Warner, D. L., Koederitz, L., and Laudon, R. C., 1997. Application of an area-of-review (AOR) concept to the East Texas Field and other selected Texas oilfields: University of Missouri-Rolla, Final Report for U.S. Department of Energy Grant No DE-FG22-94MT-94002, 402p.

Warner, D. L., Koederitz, L., Dunn-Norman S., and Laudon, R. C., 1996. Application of an AOR variance methodology to the Permian Basin, Texas: prepared for The American Petroleum Institute, 288p.

Warner, D. L. and Lehr, J. H, 1977. An Introduction to the technology of subsurface wastewater injection. Final Report, Jul 75-Jul 77. (Dec 1977) Missouri Univ.-Rolla.; Robert S. Kerr Environmental Research Lab., Ada, Okla.; Municipal Environmental Research Lab., Cincinnati, Ohio. Report No.: EPA/600/2-77/240 <NTIS> PB-279 207/5, 355p.

Weise, B. R. 1980, Wave dominated delta systems of the Upper Cretaceous San Miguel Formation, Maverick Basin, South Texas, Bureau of Economic Geology, Report of Investigation no. 107, 39p.

Wilbert, M. C., Leitz, F., Abart, E., Boegli, B., and Linton, K., 1998. The desalting and water treatment membrane manual: A guide to membranes fro municipal water treatment. Water Treatment Technology Program Report N°29, 2nd Edition, U.S. Department of the Interior, Bureau of Reclamation, variously paginated.

Woodruff, C. M., Gever, C., and Wuerch D., 1984. Geothermal Gradient Map of Texas, 1/1,000,000. University of Texas at Austin, Bureau of Economic Geology GG8401.

# APPENDIX 1: Unit Conversion Table

**Length**
1 inch = 0.0254 m
1 ft = 0.3048 m

**Volume:**
1 bbl = 42 gallons = 159 liters = 0.159 $m^3$
1 gallon = 3.785 liters = $3.785 \times 10^{-3}$ $m^3$
1 acre-ft = 325,851.4 gallons = 1,233,482 liters = 1,233.5 $m^3$
1 cubic foot = 0.02832 $m^3$

**Flow rate:**
1 gpm = 0.0631 liter/s = $6.31 \times 10^{-5}$ $m^3/s$
1 bbl/day = 0.0292 gpm = $0.184 \times 10^{-5}$ $m^3/s$
1 MGD = 694.4 gpm = 43.8 liter/s = 0.0438 $m^3/s$

**Pressure**
1 psi = 0.068948 bar = 6894.757 Pa

**Permeability**
1 md = $1 \times 10^{-15}$ $m^2$

**Temperature**
T in $^oF$ is so that T in $^oC = 5/9(T-32)$

# APPENDIX 2: Stakeholder Communication

Early in the project, at the end of 2003, the BEG put together a roadmap for communicating with oil and gas operators, including arranging a presentation at the TIPRO (Texas Independent Producers and Royalty Owners) meeting in January 2004, coordinating with PTTC (Texas Petroleum Technology Transfer Council) and TIPRO staff on how to contact operators, and setting up a Website directed at answering specific operator concerns and collecting their comments.

In order to gain feedback from the oil and gas industry, BEG gave a short presentation on the concept of the project at the TIPRO midwinter policy meeting in January 2004 in Fort Worth, TX (Figure A2.1). As a follow-up to the meeting, the presentation, a companion text file, and a questionnaire (Table A2.1 and Figure A2.2) were posted on Website of the PTTC (http://www.energyconnect.com/pttc/), as well as on the BEG Website. PTTC sent an email to its 1,200 members, giving information on the project and encouraging them to fill out the on-line questionnaire.

Table A2.1: Text of the stakeholder questionnaire posted on the Web

The Texas Water Development Board and the Bureau of Economic Geology are soliciting input from the industry relative to the acceptance of desalination concentrates in Class II injection wells. The following questionnaire is meant to gauge the industry interest in the project. For additional information, view the slides, and accompanying text, presented at the TIPRO Mid-Winter Policy Meeting in Fort Worth, TX, in January 2004.

**Question 1**: Assuming that the concentrate is delivered to your injection wellhead, there are no compatibility issues and no adverse effects to the formation and adjacent aquifers, and assuming that the entire process is margin neutral at minimum, how likely would you be to accept the concentrate for injection?

Very likely / Somewhat likely / Neither likely or unlikely / Somewhat unlikely / Very unlikely

**Question 2**: If you agree to taking the concentrate under the conditions outlined in Question 1, what volume would you most likely be willing to accept?

Less than 100 gpm (~3,500 barrels/day)
From 100 to 299 gpm (~3,500 and ~10,000 barrels/day)
From 300 and 699 gpm (~10,000 and 20,000 barrels/day)
700 gpm or more (20,000 barrels/day +)
Do not know

**Question 3**: How much would you be likely to charge per 1,000 gallons of concentrate?

**Question 4**: What, if any, concerns might you have in accepting desalination concentrates?

**Question 5**: Additional comments

Optional Information:
Name:
Company:
Address:
Phone:
Email:

Figure A2.1: Slides of presentation made at the January TIPRO meeting in Fort Worth.

## Please, Pass the Salt: Can the Oil Industry Benefit from Desalination Wastes?

**TIPRO Mid-Winter Policy Meeting**
**Fort Worth, Texas**
**January 13, 2004**

**Jean-Philippe Nicot, P.E.**
**Bureau of Economic Geology**
**The University of Texas at Austin**

**Work done in collaboration with the Texas Water Development Board and funded by the U.S. Bureau of Reclamations**

1

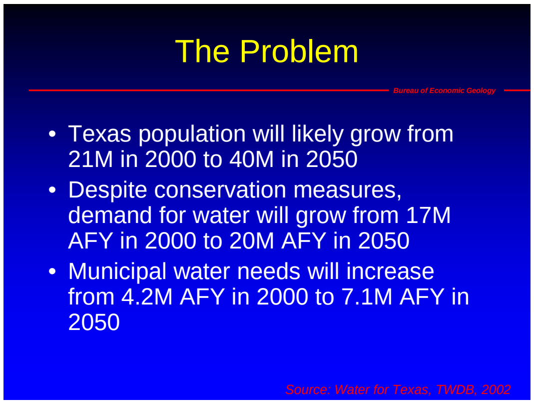

## The Problem

*Bureau of Economic Geology*

- Texas population will likely grow from 21M in 2000 to 40M in 2050
- Despite conservation measures, demand for water will grow from 17M AFY in 2000 to 20M AFY in 2050
- Municipal water needs will increase from 4.2M AFY in 2000 to 7.1M AFY in 2050

*Source: Water for Texas, TWDB, 2002*

2

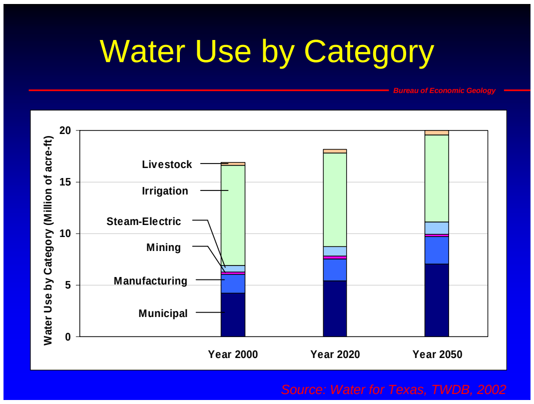

## Water Use by Category

*Bureau of Economic Geology*

*Source: Water for Texas, TWDB, 2002*

3

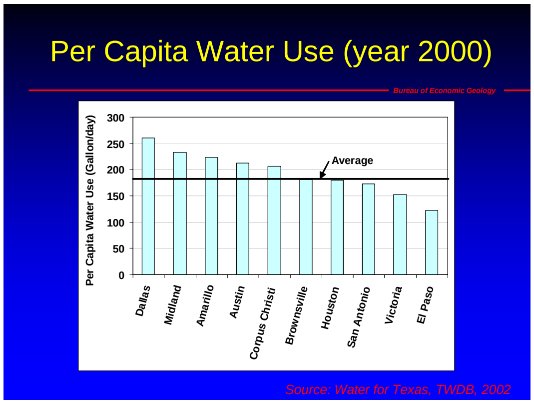

## Per Capita Water Use (year 2000)

*Bureau of Economic Geology*

*Source: Water for Texas, TWDB, 2002*

4

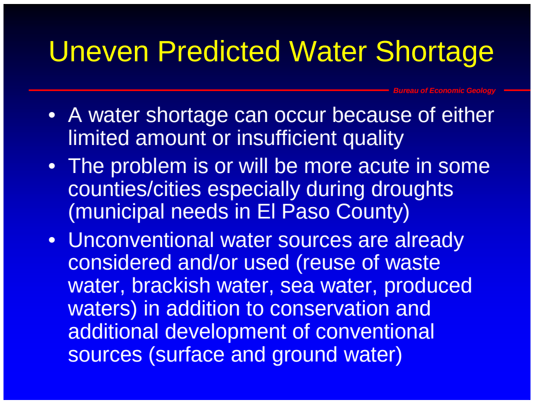

## Uneven Predicted Water Shortage

*Bureau of Economic Geology*

- A water shortage can occur because of either limited amount or insufficient quality
- The problem is or will be more acute in some counties/cities especially during droughts (municipal needs in El Paso County)
- Unconventional water sources are already considered and/or used (reuse of waste water, brackish water, sea water, produced waters) in addition to conservation and additional development of conventional sources (surface and ground water)

5

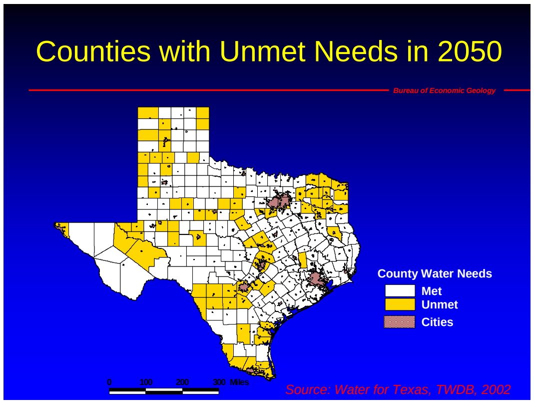

## Counties with Unmet Needs in 2050

*Bureau of Economic Geology*

*Source: Water for Texas, TWDB, 2002*

6

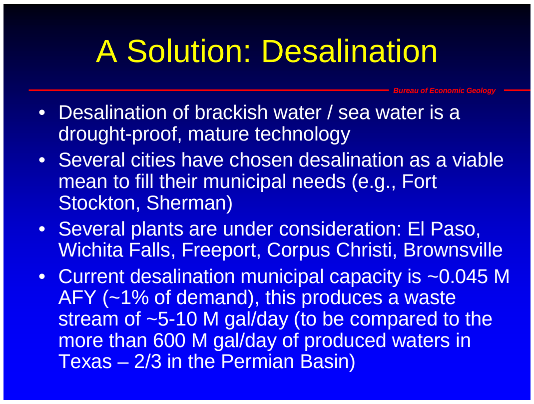

## A Solution: Desalination

Bureau of Economic Geology

- Desalination of brackish water / sea water is a drought-proof, mature technology
- Several cities have chosen desalination as a viable mean to fill their municipal needs (e.g., Fort Stockton, Sherman)
- Several plants are under consideration: El Paso, Wichita Falls, Freeport, Corpus Christi, Brownsville
- Current desalination municipal capacity is ~0.045 M AFY (~1% of demand), this produces a waste stream of ~5-10 M gal/day (to be compared to the more than 600 M gal/day of produced waters in Texas – 2/3 in the Permian Basin)

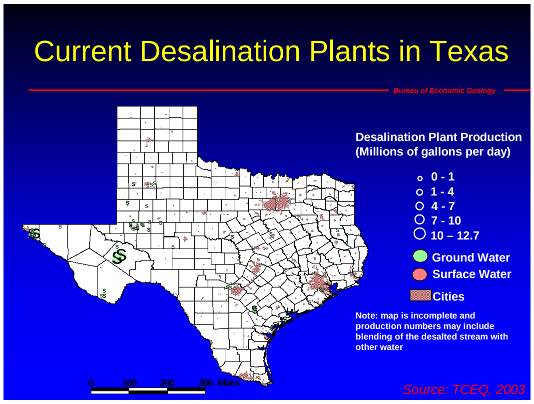

## Current Desalination Plants in Texas

Bureau of Economic Geology

Note: map is incomplete and production numbers may include blending of the desalted stream with other water

Source: TCEQ, 2003

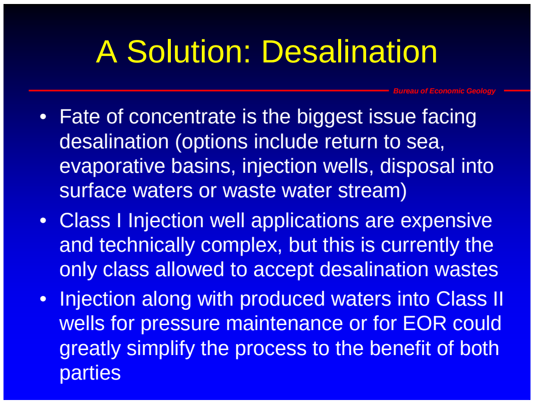

## A Solution: Desalination

Bureau of Economic Geology

- Fate of concentrate is the biggest issue facing desalination (options include return to sea, evaporative basins, injection wells, disposal into surface waters or waste water stream)
- Class I Injection well applications are expensive and technically complex, but this is currently the only class allowed to accept desalination wastes
- Injection along with produced waters into Class II wells for pressure maintenance or for EOR could greatly simplify the process to the benefit of both parties

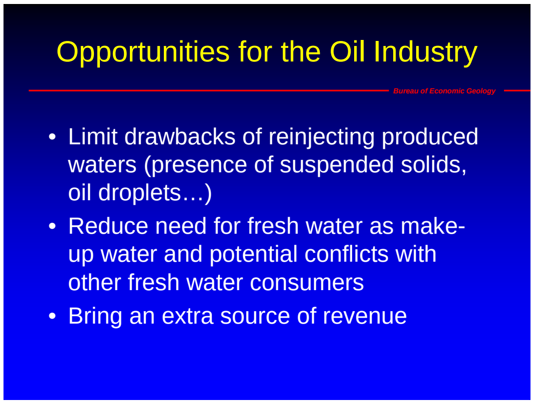

## Opportunities for the Oil Industry

Bureau of Economic Geology

- Limit drawbacks of reinjecting produced waters (presence of suspended solids, oil droplets…)
- Reduce need for fresh water as make-up water and potential conflicts with other fresh water consumers
- Bring an extra source of revenue

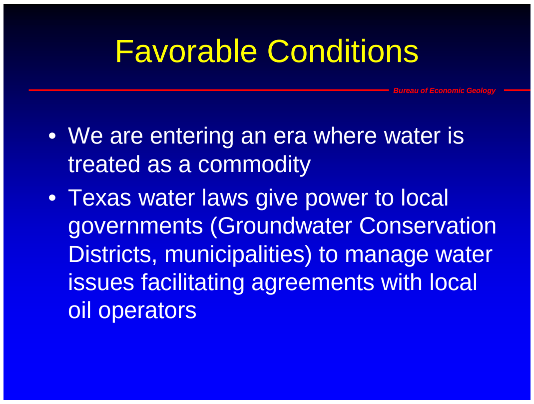

## Favorable Conditions

Bureau of Economic Geology

- We are entering an era where water is treated as a commodity
- Texas water laws give power to local governments (Groundwater Conservation Districts, municipalities) to manage water issues facilitating agreements with local oil operators

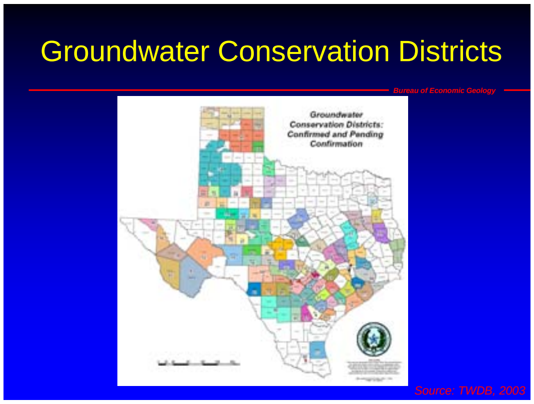

## Groundwater Conservation Districts

Bureau of Economic Geology

Source: TWDB, 2003

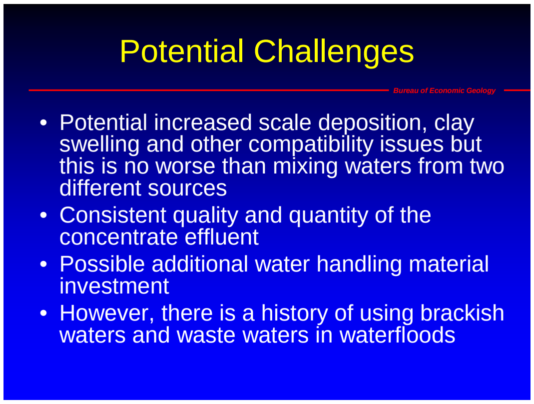

## Potential Challenges

Bureau of Economic Geology

- Potential increased scale deposition, clay swelling and other compatibility issues but this is no worse than mixing waters from two different sources
- Consistent quality and quantity of the concentrate effluent
- Possible additional water handling material investment
- However, there is a history of using brackish waters and waste waters in waterfloods

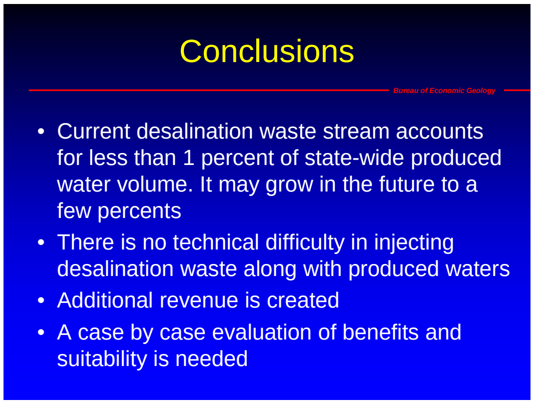

## Conclusions

Bureau of Economic Geology

- Current desalination waste stream accounts for less than 1 percent of state-wide produced water volume. It may grow in the future to a few percents
- There is no technical difficulty in injecting desalination waste along with produced waters
- Additional revenue is created
- A case by case evaluation of benefits and suitability is needed

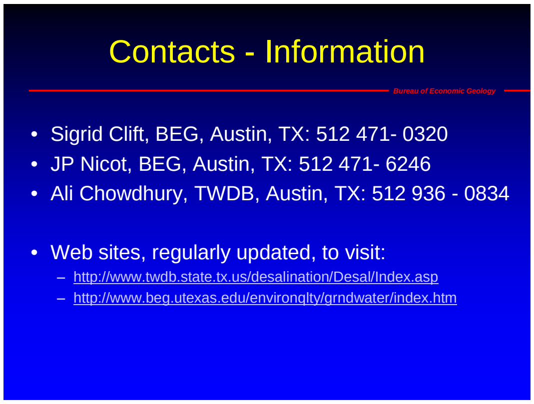

## Contacts - Information

Bureau of Economic Geology

- Sigrid Clift, BEG, Austin, TX: 512 471- 0320
- JP Nicot, BEG, Austin, TX: 512 471- 6246
- Ali Chowdhury, TWDB, Austin, TX: 512 936 - 0834

- Web sites, regularly updated, to visit:
  - http://www.twdb.state.tx.us/desalination/Desal/Index.asp
  - http://www.beg.utexas.edu/environqlty/grndwater/index.htm

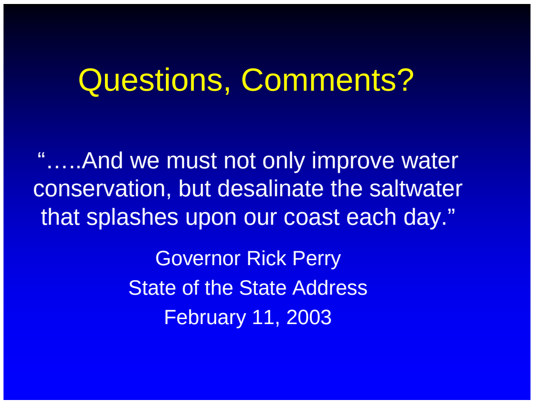

## Questions, Comments?

"…..And we must not only improve water conservation, but desalinate the saltwater that splashes upon our coast each day."

Governor Rick Perry
State of the State Address
February 11, 2003

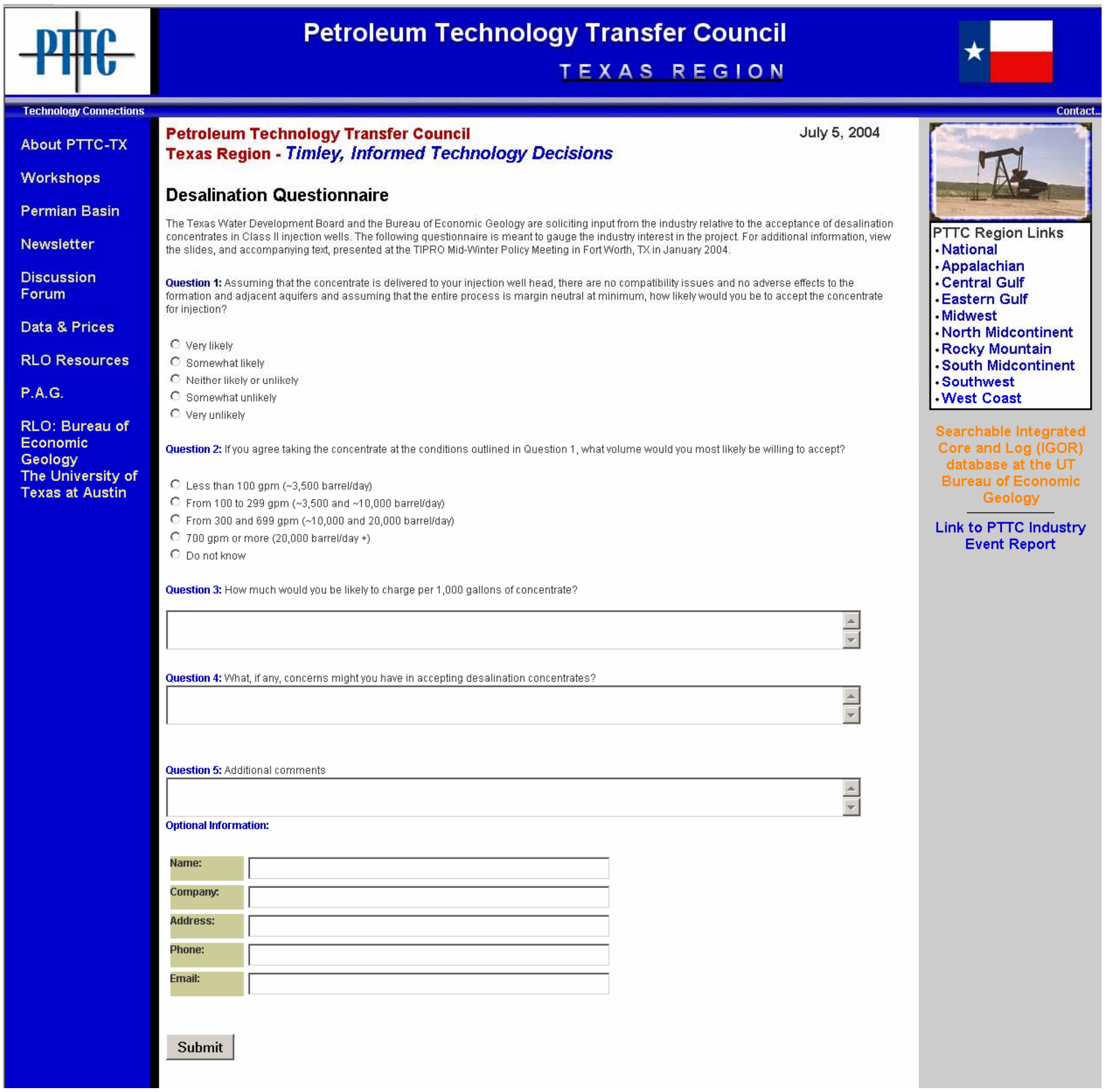

**Petroleum Technology Transfer Council**
**Texas Region - *Timley, Informed Technology Decisions***

July 5, 2004

**Desalination Questionnaire**

The Texas Water Development Board and the Bureau of Economic Geology are soliciting input from the industry relative to the acceptance of desalination concentrates in Class II injection wells. The following questionnaire is meant to gauge the industry interest in the project. For additional information, view the slides, and accompanying text, presented at the TIPRO Mid-Winter Policy Meeting in Fort Worth, TX in January 2004.

**Question 1:** Assuming that the concentrate is delivered to your injection well head, there are no compatibility issues and no adverse effects to the formation and adjacent aquifers and assuming that the entire process is margin neutral at minimum, how likely would you be to accept the concentrate for injection?

○ Very likely
○ Somewhat likely
○ Neither likely or unlikely
○ Somewhat unlikely
○ Very unlikely

**Question 2:** If you agree taking the concentrate at the conditions outlined in Question 1, what volume would you most likely be willing to accept?

○ Less than 100 gpm (~3,500 barrel/day)
○ From 100 to 299 gpm (~3,500 and ~10,000 barrel/day)
○ From 300 and 699 gpm (~10,000 and 20,000 barrel/day)
○ 700 gpm or more (20,000 barrel/day +)
○ Do not know

**Question 3:** How much would you be likely to charge per 1,000 gallons of concentrate?

**Question 4:** What, if any, concerns might you have in accepting desalination concentrates?

**Question 5:** Additional comments

**Optional Information:**

| | |
|---|---|
| Name: | |
| Company: | |
| Address: | |
| Phone: | |
| Email: | |

Figure A2.2: Screen capture of the questionnaire posted on the Web

# APPENDIX 3: Chemical Analyses

Because chemical analyses are used in geochemical runs, it is important to ensure their consistency. Data used in this study come from different sources of variable quality. Internal consistency of the water analyses was checked by making sure that the sum of the ions is close to the TDS value and that the sample is charge-balanced. The following steps were taken for each chemical data set as applicable:

- retain latest analysis if several
- recompute TDS from sum of ions and compare with given TDS. TDS given in older databases or older samples in newer databases is often lower than sum of ions. This is because, in past decades, TDS was often measured as the weight of the residue after total water evaporation. In the process about half of the bicarbonate is converted into gas during calcite precipitation. This results in a true TDS higher than the reported TDS. The formula is:

  $Ca + 2HCO_3^- ==> CaCO_3 + H_2O + CO_2$

  However, some more recent analytical techniques report the true TDS.
- delete analyses with an electrical balance outside permissible range
- delete analyses showing “red flags” as showed in Table A3.1.
- retain only those samples with a TDS > 1,000 mg/L and < 10,000 mg/L
- if no temperature is given, use the median of the given temperatures.

The approach follows the general rules of the Quality Assurance tests from the American Water Works Association “Standard Methods” reference (Clesceri et al., 1998). Other criteria are discussed in Hitchon and Brulotte (1994) and Collins (1975, Chapters 2 and 3).

Table A3.1. Selection of consistent chemical analyses

| Criteria | Action if met | Rationale |
|---|---|---|
| TDS=Σ(ions) | suspicion | Nonanalysis of Na. Na could be backcalculated from TDS. This would yield a perfect charge balance |
| Σ(ions+)= Σ(ions-) | suspicion | nonanalysis of Na |
| TDS>>Σ(ions) or TDS<<Σ(ions) | deletion | Incomplete analysis |
| Σ(ions+)>> Σ(ions-) or Σ(ions+)<<Σ(ions-) | deletion | Incomplete analysis |
| Ph<4 or Ph>9 | deletion | Likely contamination by acid wash or cement wash |
| K>Na | deletion | Likely contamination by KCl mud in oil wells |
| K missing | suspicion | Incomplete analysis or K grouped with Na |
| Mg>Ca | deletion | Signifies loss of $CO_2$ and calcite precipitation |
| OH or $CO_3$ reported | suspicion | Equivalent to a high pH |
| High Fe | suspicion | Pipe or other material corrosion |
| Ba missing | | |
| High $NO_3$ | deletion | Surface contamination for oil wells, probably located in an otherwise fresh water zone |

# APPENDIX 4: Formation Water Sampling

Given the complexity of sampling formation water, samples collected may not always accurately reflect the chemistry of the formation. Formation water sampling can be made at different locations on the production line following different procedures. Reliability of the different sampling techniques according to the USGS (USGS, 2002) is shown in Table A4.1. Those sampling methods are discussed in API (2003) and API (1998). Only analyses with a grade of A or B were used in this study. The best analyses are those samples taken during production (not too soon because of influence of drilling mud and later test materials). Fluids recovered during tests can also be usable. All other modes of sampling are only marginally useful. There are two main problems during sampling: loss of dissolved gas ($CH_4$, $CO_2$, $H_2S$, $O_2$) and carbonate precipitation. Those losses occur mainly because of change in temperature/pressure and lack of data for T/P conditions of analysis. The pH of the formation will change because of oxidation of reduced species and release of dissolved gas. We assume that all pH values were determined in the lab at 20°C and that no $CO_2$ loss occurred.

Table A4.1. Grading of formation water sampling methods

| **Location** | **Possible Problems** | **USGS Grade** |
|---|---|---|
| Production | | B |
| Well head | | B |
| Bomb | | C |
| Drill Stem Test (DST) | Improper sampling | C |
| Formation Test | | C |
| Production Test | | C |
| Bailer | Evaporation | D |
| Swab | Contamination | D |
| Bleeder | | E |
| Heater/Treater | Gas venting, multiple wells, corrosion | E |
| Open Hole | Gas venting, mixing with condensed water | E |
| Separator | Gas venting, multiple wells, corrosion | E |
| Tank | Gas venting, evaporation, corrosion | E |
| Unknown | | F |